Key Factors Affecting Distribution and Orientation of Fibres in Steel Fibre Reinforced Concrete and Subsequent Effects on Mechanical Properties

By

Olubisi A. Ige
B. Eng. (Honours), MSc

JANUARY 2017

A thesis submitted in partial fulfilment of the requirements for the award of the degree of Doctor of philosophy in Civil Engineering of the University of Portsmouth

School of Civil Engineering and Surveying
University of Portsmouth

DECLARATION

I declare that whilst registered as a candidate for the above degree, I have not been registered for any other research award. The results and conclusions embodied in this thesis are original and the work of the named candidate and have not been submitted for any other academic award except for publications.

Name: Olubisi A. Ige

Signature: _____

Date:

Word count: 52,807

ABSTRACT

Use of fibres to reinforce brittle materials for better performance in buildings and for construction purposes has been employed since time immemorial. Inclusion of steel fibres in concrete therefore, has always improved the post-cracking strength and concrete ductility to a large extent. Nevertheless, there is no doubt that it has become imperative to have more understanding of the internal workings of steel fibre reinforced concrete to fully exploit its potential in practice.

In this PhD study, investigation of distribution and orientation of steel fibres within steel fibre reinforced concrete, studying how the positioning of steel fibres in SFRC (steel fibre reinforced concrete) matrix affects the post-cracking strength and other properties that enhance concrete ductility is reported. Variables selected for this study were those considered to influence how steel fibres and concrete matrix associate together during mixing. Hooked-end steel fibres with 50 mm and 60 mm length, of varying diameter resulting in different aspect ratio (ratio of length to diameter of fibre) of 45, 65 and 80, and dosages of 0 kg/m^3, 25 kg/m^3, 40 kg/m^3, 50 kg/m^3 and 60 kg/m^3 were employed with maximum sizes of coarse aggregate of 10 mm and 20 mm. The same mix proportions of concrete were used throughout the investigation.

Workability of the fresh mix was carried out through slump test, flexural performance was assessed through beam and slab tests at 28 day while compressive strength was also measured using cubes. Subsequently, cores were extracted from these panels and X-ray computed tomography was employed for imaging the cores while Insight Toolkit Software was used to analyse the position of fibres in hardened concrete.

The experimental results show that the strength performance of steel fibre reinforced concrete improved drastically when compared to plain concrete without fibres. Remarkable improvements were observed at larger dosages of steel fibres, and with fibres with highest aspect ratio of 80 noted to give the best results which suggests that aspect ratio of fibre is critical to SFRC performance. It was found that fibre effects on compressive strength is slightly pronounced, with optimum compressive strength of 68 MPa noticed at fibre dosage of 50 kg/m^3 and with fibre of 80 l/d ratio with 20 mm aggregate mixture which is about increase of 8 MPa when compared with plain concrete. Also, in SFRC beams, there were up to 83% increase in maximum stress reached when compared to unreinforced concrete. Moreover, it was found that the results of X-ray CT image analysis by The Insight Toolkit software correlate well with the outcome of mechanical performance of steel fibre reinforced concrete.

The slab test results show that mixtures containing 10 mm maximum aggregate size sustain higher load than those of 20 mm counterparts. Harmonization of beam and slab

results using yield line analysis revealed that the values of theoretical and experimental failure loads are reasonably close for slabs containing 20 mm maximum aggregate size while the analysis does not agree perfectly with slabs containing 10 mm maximum aggregate size. The 3D rendering images of SFRC cores show that steel fibres are generally positioned horizontally in the slabs which can be seen to be more pronounced in 10 mm maximum aggregate mixes resulting in their ability to sustain higher failure loads.

The study has revealed a clear relationship between the geometry of steel fibre and maximum aggregate size, establishing the fibre-aggregate interaction effects on post-cracking capacity of SFRC. Finally, the study has quantitatively measured the distribution and orientation of steel fibre within the concrete matrix while the correlation between the internal mechanism and the mechanical properties of SFRC has been established.

Dissemination

Prior to completion of this Thesis, parts of the results have been published:

Ige, O., Barnett, S., Chiverton A., Nassif, A., & Williams J. (2017). *Effects of steel fibre-aggregate interaction on mechanical behaviour of steel fibre reinforced concrete.* Advances in Applied Ceramics: Structural, Functional and Bioceramics. Vol. 116, pp. 193-198.

Chiverton J., Ige O., Barnett S., & Parry T. (2017). *Multiscale Shannon's Entropy Modelling of Orientation and Distance in Steel Fibre Micro-Tomography Data*. IEEE Transactions on Image Processing. PP (99):1-1. DOI 10.1109/TIP 2017.2722234.

Ige, O., Barnett, S., Nassif, A., & Williams J. (2016). *Influence of fibre aspect ratio and aggregate size on flexural performance of steel fibre reinforced concrete.* Proceedings of 9th RILEM International Symposium on Fibre Reinforced Concrete, Vancouver, Canada, (2016, 18-22nd September), pp. 545-556.

Ige, O., Barnett, S., Nassif, A., & Williams J. (2016). *Distribution and orientation of steel fibres in steel fibre reinforced concrete.* Proceedings of the International Conference on Advances in Civil, Structural and Construction Engineering, Rome, Italy, (2016, 18-20th August), pp. 43-47.

Ige, O., Barnett, S., Nassif, A., & Williams J. (2016). *Effect of Steel Fibre Distribution and Orientation on Post-Cracking Ductility of Steel Fibre Reinforced Concrete.* Paper presented at 3rd Young Researchers' Forum, Innovation in Construction Materials, Department of Civil and Environmental Engineering, Imperial College, London, UK, (2016, 12th April).

Ige, O. A., Barnett, S., Nassif, A. Y., & Williams, J. B. (2015, 26-28th August 2015). *Effect of steel fibres on compressive and flexural strength of steel fibre reinforced concrete.* Paper presented at the Cement & concrete science conference, Aberdeen, Scotland, UK.

Papers in preparation

Ige, O., Barnett, S., Chiverton A., Nassif, A., & Williams J. *Flexural and post-cracking performance of steel fibre reinforced concrete beams and panels*.

Prize won on Thesis Competition

1. Three minutes thesis competition - First prize at Faculty of Technology Research Conference, 2014.
2. PhD Student Paper Competition – 'Highly commended paper' prize at Faculty of Technology Research Conference, 2017.

DEDICATION

This Thesis is dedicated to my wife, **Felicia Olayinka Ige** for being a strong support and source of encouragement to me. Her unconditional love, sacrifice and prayers all the way made the completion of this programme possible.

I also dedicate this Thesis to my late parents, **Samuel Osuola and Lydia Omoronike Ige**, for training and putting in me, what I needed to succeed in life in the way of the Lord, sleep on till we meet to part no more!

ACKNOWLEDGEMENT

First and foremost, I give all glory, adoration and honour unto the giver of wisdom, most high and all-knowing God for sustaining me from the beginning to the end of this programme. To my Lord and my Saviour, Jesus Christ and my Comforter, Holy Spirit, I am grateful.

I would like to express my sincere gratitude to my first supervisor, Dr Stephanie Barnett for initiating this research project when my initial project could not continue due to materials and logistics problem. Her constant guidance, wise counsels, constructive suggestions and quick and timely responses during the period of investigation has made possible the completion of this project. I equally appreciate my second and third supervisors, Dr Ayman Nassif and Dr John Williams for their unflinching support, helpful ideas and for being there for me at all times.

I would also like to thank Dr John Chiverton of School of Engineering, University of Portsmouth who carried out the processing of X-ray CT images by software application, Bekaert (Dramix) for supplying all the steel fibres used in this research work, the technical staff of School of Civil Engineering and Surveying, University of Portsmouth and Mr Chris Fox of Central Engineering Stores, University of Nottingham for their assistance in data collection.

I extend my appreciation to Dr Muhammad Ali with whom I got engaged as a demonstrator in soil and material courses, all the staff and all my friends and colleagues in the Research Centre, all in School of Civil Engineering and Surveying, University of Portsmouth, and members of Victory Chapel International, Portsmouth, you all have been source of inspiration to me.

The financial support I received from Tertiary Education Trust Fund, Nigeria and the opportunity given to me to study this PhD programme by Osun State Polytechnic, Iree are gratefully acknowledged.

Finally, I wish to express my profound gratitude to my wife Felicia, children, Faith, Emmanuel and Treasure for their understanding, encouragement, forbearance and most especially, their prayers during the period of study, I sincerely appreciate.

TABLE OF CONTENTS

LIST OF TABLES

LIST OF FIGURES

LIST OF ABBREVIATIONS

ACI	American Concrete Institute
AR	Aspect Ratio
ASTM	American Society for Testing Materials
BS	British Standard
BS EN	European Standard adopted by British Standard Institution
	CMOD crack mouth opening displacement
FRC	Fibre reinforced Concrete
ITK	Insight ToolKit (Type of software)
JSCE	Japan Society of Civil Engineers
L	Fibre Length
l/d	Fibre Aspect Ratio
LVDT	Linear Variable Displacement Transducer
PC	Portland cement
RILEM	International Union of Laboratories and Experts in Construction Materials, Systems and Structures
SFRC	Steel Fibre Reinforced Concrete
UHPFRC	Ultra-High Performance Fibre Reinforced Concrete
X-Ray CT	X-ray Computed Tomography
XμT	X-ray Microtomography

LIST OF EQUATIONS

LIST OF APPENDICES

CHAPTER 1

INTRODUCTION

1.1 Introduction

Concrete remains the most widely used man-made material in the world. In actual fact, our world is continuously being built up by concrete from ancient age to present time, from cities to communities and in every continent of the globe. There cannot be any sustainable development without the contribution of this composite material which has been known for many years and has metamorphosed from very crude to highly technical material through the ages. The economic importance, being the cheapest bulk building material, the relative strength acquired at different level of usage and its availability everywhere coupled with the general usefulness of concrete material has made it much sought after with many research going on for its improvement on daily basis (Caggiano et al., 2012). However, notwithstanding its usages and popularity within the building and construction industries, the tensile strength of concrete is very low when compared to its compressive strength and has an undesirable, brittle nature mode of failure. García-Taengua et al. (2014) reported that the challenge of strain and crack of concrete is fundamental issue for the durability of concrete structures. This is a crucial challenge the engineers, the researchers and all the construction and building industry players have to deal with and find a lasting solution to.

The introduction of conventional reinforcement bars to complement the weakness of concrete in 19th century was a celebrated idea which made it possible for the combined efforts of concrete and reinforcement bar termed ‘reinforced concrete’ to achieve more structural applications in construction and building industries. The steel reinforcement bars are responsible for carrying the tensile forces while the concrete is to withstand the compressive, which make the combination a complementary arrangement. However, the reinforced bars are stationary within a particular region of

concrete matrix and cannot be everywhere in the matrix, thereby making the task of preventing cracks and eventual structural failure a difficult one. Despite the evolution of reinforced concrete, the tensile failure strain of the concrete is significantly lower than the yield strain of the steel reinforcement, therefore concrete cracks before any significant load is transferred to the steel (The Concrete Society, 2007).

Concrete has continued to undergo persistent development with various types of concrete developed through the ages while research has been nonstop to further improve the properties of concrete. There have been usages of admixtures and pozzolans in concrete, prestressed concrete, light weight concrete, high strength concrete, high performance concrete, ultra-high performance concrete, self-compacting concrete and lots of others. The various concretes are specially developed to meet one specific need or other and achieve a particular improvement in the properties of concrete. Some of the concretes have been developed to have the density increased with decrease in permeability while others were made to produce high strength either early enough or in the life time of the concrete and lots more. In all these, little has been achieved in concrete ductility whereas, there have been continuous intentions to improve the structural integrity of concrete to serve better the end users in the civil engineering, construction and building industries.

Meanwhile, the challenges of sudden collapse of concrete which is catastrophic in nature as a result of brittle character of concrete continued to be an issue to the engineers and the researchers, notwithstanding the major milestones already achieved in the improvement of concrete properties. Added to the challenges is the subjection of concrete structures to more loadings as a result of increase in the world population, advancement in technology, increase in natural disaster and terrorist attack through blast and explosions of different enormity. Additional impact and fatigue to concrete structures have continued to be experienced in progressive manner which have further challenged the engineers and researchers to find an enduring solution to the brittleness of concrete, by means of transforming it to a tough and ductile material. Then, came the initiation of the modern era of research and development that brought much excitement of discovery when Romualdi, Batson and Mendel published the

papers on steel fibre reinforced concrete in the early 1960s (Zollo, 1997). Since the discovery, researches have been stimulated in this direction attracting both the academic and industry players in building on the foundation already laid to keep improving the properties of the concrete.

The emerging results of the discovery of early 1960s about steel fibres in concrete have stimulated and they are still attracting research all over the world, however, most of the early findings and assumptions are being corrected as at the latest research findings. Example of this was the declaration that even the publication of paper by Romualdi and Batson which stimulated the research into and practical applications of fibre in cement and concrete were incorrect in some respects (Hannant, 2002). For instance, the positioning of fibres within concrete matrix was believed to be evenly distributed in the publication (Roumaldi & Batson, 1963). This assumption that steel fibres are evenly and randomly distributed all over the concrete matrix may not be so with the new research findings. All of these contradictions and assumptions must be investigated and be established by thorough investigations to bridge the gap between past findings and recent development in the steel fibre phenomenon in concrete.

1.2 Aims and objectives

The aim of this research is to investigate the key factors (length, aspect ratio and dosage of steel fibres, and aggregate size) affecting distribution and orientation of steel fibres within steel fibre reinforced concrete (SFRC) matrix and the influence of fibre positioning on the mechanical properties which include compressive strength, flexural strength, flexural toughness/energy absorption and the residual flexural strength, by which ductility through the post-cracking strength of the fibre reinforced concrete is examined.

To achieve the aim of this project, the following objectives were set:

- To determine the influence of sizes of coarse aggregate on the orientation of the steel fibres within the concrete matrix and the effects on SFRC mechanical performance
- To investigate how various quantities of steel fibre in SFRC can affect their distribution and orientation within SFRC and post-cracking ductility of the concrete
- To investigate the influence of the length and aspect ratio of steel fibres on the mechanical performance including post cracking strength and the properties relating to ductility of concrete
- To examine the internal positioning of steel fibres in the hardened steel fibre reinforced concrete using X-ray Computed Tomography scan and Insight Toolkit (ITK) software for analysis
- To study the correlation between distribution and orientation of steel fibres and mechanical properties of steel fibres reinforced concrete.

1.3 Background of the study

1.3.1 Problem statement

There is no doubt that demand for a better and high strength concrete has continued to grow for use in construction industries in recent years and that the inclusion of steel fibres in concrete is a breakthrough in this regard. However, most studies have concentrated on the strength properties of the resulting hardened SFRC or the general influence of fibres on concrete with research results showing relationship between post-cracking strength and fibre volume, type, geometry and with varying specimen geometry and binder formulation.

However, the experimental results on study of distribution and orientation of steel fibres in steel fibre reinforced concrete investigating the internal arrangement of fibres to corroborate the laboratory experimental details to determine the effects on

maximum output of the resulting concrete are considered few by literatures available on the subject.

Proper and full understanding of the material is necessary to fully exploit the full potential of steel fibre reinforced concrete in practice; this research will investigate and evaluate the distribution and orientation of fibres within the concrete matrix by both extensive laboratory experiments and with sophisticated equipment, X-ray computed tomography (X-ray CT) to monitor the internal positioning and use one result to corroborate the other so as to maximise the contribution of fibres to the post-cracking ability of steel fibre reinforced concrete for more structural application.

1.3.2 Research significance

The research will contribute to the current knowledge on steel fibre reinforced concrete and improve the understanding of the composite material for better application in civil engineering, construction and building industries. The outcome of this research will have impact on academic community by stimulating a future research trend in the field of concrete materials in general and particularly in the direction of internal mechanism of fibres in concrete and relation to structural behaviour of SFRC.

National and international communities will also benefit from the outcome of these research findings. Presently, design of fibre reinforced concrete structural element is not covered by Eurocodes, while the existing codes for conventional reinforced concrete cannot be adopted for SFRC because of the post cracking nature of response of fibres in concrete matrix (Soutsos et al., 2012). This has been a hindrance to the designers who cannot fully rely on scientific journal papers or committee report or guidelines for their designs. Therefore, a research like this shedding more light into fibre positioning and the internal mechanism and how it affects the structural behaviour would be part of recommendation leading to advice to policy makers for future design codes to optimise steel fibre reinforced concrete. There are numerous developing countries that will adopt the design codes for SFRC for their usage as well.

The outcome of this research which will come up with better understanding of the material behaviour will benefit the infrastructural advancement of the nation whereby the application of the material would be drastically expanded beyond what it is being used for at present. The technology of SFRC will also be extensively applied to structures of national importance like military intelligence structures and the prevention against terrorist attack.

1.4 PARAMETER AND GENERAL OUTLINE OF THE STUDY

This section describes the particular areas in which the operations of the research would be involved and how the investigation has been organised. It also outlines how the thesis has been structured to sequentially reveal the significant contribution of this research from the introductory stage to the findings and finally, to the recommendations.

1.4.1 Scope of the research

This thesis consists of three major areas of study. These are laboratory experimental investigation of steel fibre reinforced concrete and mechanical properties, the imaging technique of hardened SFRC by the use of X–ray computed tomography to scan the internal distribution and orientation of fibres with the employment of Insight toolkit software for the analysis of scanned results to show the 3D view of the samples and the investigation of the correlation between the imaging results of distribution and orientation with the mechanical properties of steel fibres reinforced concrete.

1.4.1.1 Laboratory experimental *programme*

The laboratory investigations were carried out utilising the normal conventional constituent materials of concrete, Portland cement, water, the fine and coarse aggregates with addition of steel fibres of different geometry, varying sizes of coarse aggregate and dosages of steel fibres. All the variables have been carefully selected and

studied well as those that would affect the distribution and orientation of steel fibres within the concrete matrix. The same concrete mix proportion that was found after a series of trial mixes was used for all the samples made. The specimens used for this research work are cubes, prisms and slabs while the relevant standards were judiciously employed.

The mechanical properties of SFRC targeted are those properties relating to flexural behaviour and ductility of SFRC like flexural strength, flexural toughness and residual strength factor.

1.4.1.2 Imaging technique

The imaging technique adopted to investigate the positioning of steel fibres in the interior of hardened SFRC is X-ray computed tomography which is a non-destructive technique for visualizing features in the interior of opaque solid objects like concrete. The technology makes use of high-resolution X-ray that has ability to resolve details as small as a few microns in size no matter how high the density of the material may be.

Cores were taken from the slab specimens after testing and analysed by X-ray CT for detailed investigation of the effects of the chosen variables on fibre distribution and orientation and the subsequent effects on mechanical performance of the material. The data from scanned results were analysed by the library insight toolkit software with the ability to transform the volumetric images from X-ray CT scan into segmented images to show the position and orientation of steel fibres in 3D.

1.4.1.3 Correlation between X-ray CT data and mechanical performance

The outcome of the analysis showing the internal positioning of steel fibres within the matrix of hardened SFRC, the distribution and orientation were compared with the mechanical performance results. The processes embarked in this research made it possible to investigate the correlation between the two results and used as a tool for validation and confirmation.

1.4.2 Thesis structure

This thesis consists of seven chapters including this introductory chapter which relates the background of the study and the aim and the objectives of the study. There follows two chapters on literature review, a chapter on the core laboratory experimental methods, a chapter on results analysis with discussion, a chapter on image technique and analysis, and the last chapter on conclusions and recommendations.

Chapters 2 and 3 are reviews of the literature on fibres in general, steel fibres and steel fibre reinforced concrete. Chapter 2 is a comprehensive review of the general concept of fibres, its development and functions in concrete. Chapter 3 on the other hand essentially reviews the current literature on SFRC that is relevant to the study.

Chapter 4 reports research methodology presenting how laboratory-based experimental investigation, imaging technique and imaging analysis on steel fibre reinforced concrete will achieve the aim and objectives of this research. It also deals with how the various variables were selected for the study, materials and the experimental techniques utilised during the laboratory investigation which include mixing, production, and moulding of fresh and mechanical testing of hardened SFRC and reports the manufacture of cubes, prisms and slabs used for the study of distribution and orientation of steel fibres in SFRC.

Chapter 5 comprehensively presents the various results obtained from the series of tests with discussion on the implications of the outcome on steel fibre reinforced concrete performance.

Chapter 6 is dedicated to the report on imaging technique on cores samples for investigation of internal positioning of fibres in SFRC using X-ray Computed Tomography. The analyses of the scanned results by Insight Toolkit Software are also reported in this chapter.

Chapter 7 finally summarises the various conclusions, the corroboratory aspect of X-ray CT scan on laboratory experimental results was also discussed in this chapter. The most significant contributions and findings of this research, recommendations for

future research work and improvement on the current understanding of steel fibre reinforced concrete were also provided.

CHAPTER 2

OVERVIEW AND BASIC CONCEPT OF FIBRES

2.1 Introduction

This chapter discusses comprehensively the broad view and the fundamental concepts of fibres used for construction purposes. The discussion here includes the historical development of concrete, reinforced concrete and fibre reinforced concrete as construction materials, and various methods earlier invented to improve the brittle properties of concrete. The crack mechanism of concrete and the bridging of cracks with the aid of steel fibres, different types of steel fibres and their applications are also discussed.

2.2 Historical development of fibres in concrete

2.2.1 Background

The word concrete has been in existence for over 5000 years, from the time of the Egyptian pyramids to the time of Roman builders and to the present day concrete development. It was recorded that Egyptians used mud and straw with gypsum and lime to make mortars about 3000 BC, (ConcreteNetwork.com, n.d.). The straw used in these mortars was a form of fibre to add stability to the then construction. In another study (Jackson et al., 2013), it was discovered recently that the ancient Romans concrete is both stronger and greener than today's concrete. A sample of Roman concrete taken from a harbour which has withstood an aggressive seawater harsh condition for over 2,000 years was investigated. The researchers found out the Romans used a naturally occurring material, volcanic ash, lime and sea water which then produced calcium aluminium silicate hydrate (C-A-S-H) as the binding material. It was reported that the process adopted by the Romans in creating concrete releases less carbon dioxide when compared to today's method but takes a much longer time to

harden. Though, as reported, it was Romans who first made concrete with a hydraulic cement but as the interest in the material continued, the industrial revolution in the second half of eighteenth century culminated to the present day Portland cement in1824 which has remained a major constituent of concrete to date (Illston & Dinwoodie, 1994).

Concrete which is a composite mixture made from Portland cement, aggregate and water can be manufactured differently depending on how the constituents have been selected or varied in the mixture. There have been other types of cement used in concrete, aimed at achieving a peculiar purpose in the mixture for construction processes while there can also be addition of admixtures that are added in the process of manufacturing concrete to change its properties either at fresh, early age or at hardened state to a particular advantage. Concrete is therefore made popular because of higher strength it possesses when compared to natural soils and materials. It can withstand considerable amount of compressive forces or loads and can be said to be strong in compression. However, concrete is weak in tension and cannot withstand a significant tensile stress or load, it easily fractures when sustaining a tensile load and the failure mode is sudden. This is because of the effects of tensile loading on components of concrete which separates the cement particles acting as binding substance from the aggregates it is binding together thereby resulting in crack propagation in the internal structure of concrete. Fracture is a problem that society has been battling with for as long as there have been man-made structures with the problem being worse today than in previous century because of our more complex technological society (Anderson, 2005).

In order to improve the properties of concrete as a major building and construction material, especially in the strength aspect and its brittle nature, to avoid the catastrophic failure being experienced in structures and to be able to improve the performance in various applications, the concrete technology has been undergoing rapid development since its discovery. There have been various technologies employed in the usage of concrete before and after the industrial revolution that have brought about great improvement and wide variety of usability of concrete. Veenendaal et al.

(2011) reported that the Roman architect and engineer Vitruvius, in the construction of cofferdams, explains a method of creating two retaining walls that are filled with clay in woven reed baskets. Many of the early engineers and architects in their wisdom worked out how the weakness of concrete in tension could be managed effectively and succeeded in doing so. Many admixtures were also tried with concrete mixes in order to secure a presentable construction material in concrete.

Every structure is built on expectations that it will serve the purpose for which it was built. This is the main reason why fractures are always avoided from both designing and building of structure. The concept of designing to avoid fracture or failure is not a new one, it has been pointed out that the fact that many structures of ancient Egypt and Roman empire are still standing today is as a result of good design and ability of the architects and engineers to successfully manage the construction, even at the time of non-usage of metals as load-bearing members prior to Industrial Revolution, (Anderson, 2005). According to Anderson, the pre-Industrial Revolution structures were designed to be loaded in compression having in mind that brick and mortar are relatively brittle and would be unreliable to carry tensile loads. An example of such a structure is as shown in Figure 2.1.

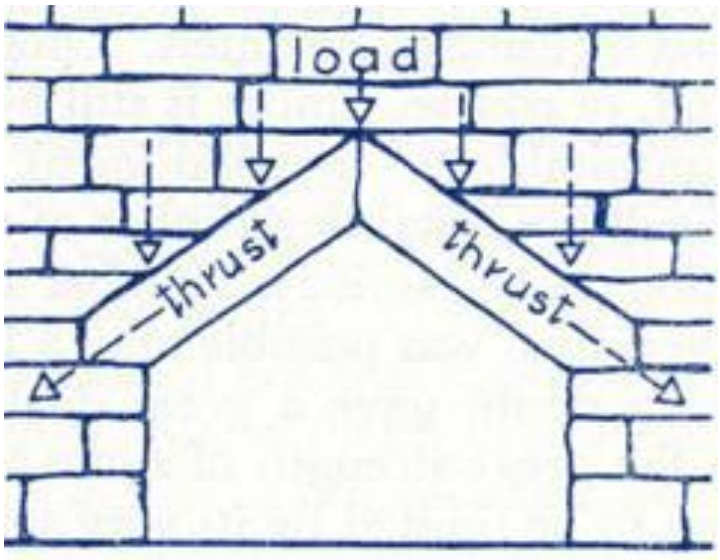

Figure 2.1: Arches from early design

(Claydon, 2015)

2.2.2 Conventional reinforced concrete

The shortcomings of concrete which has been considered as weak in tension and as a brittle material are generally thought to be overcome with inclusion of reinforcement bars within its matrix. The mass production of iron and steel came with the industrial revolution as reported earlier by Anderson (2005) stating that the availability of relatively ductile construction materials removed the earlier restriction on design. It then became finally practicable building structures that carried tensile stresses. Initially however, there was no knowledge of reinforcing principles as understood today, satisfactory methods of calculation were only developed towards the end of the 19th century, (Claydon, 2015). The researcher further stated that an early example of reinforced concrete was displayed in the Paris international Exhibition of 1855, the rowing boat designed by a French contractor, Josef Lambot and made of hydraulic lime concrete reinforced with a skeleton of iron rods. This was also reiterated by (Condit, 1968), that Lambot only poured concrete reinforced with a grid of thin iron rods to increase the cohesion of the concrete and hence its total strength, that there is no evidence that he, or anyone else for more than twenty years, understood the actual role of the metal which is mainly to impart a workable tensile strength to a material which behaves like stone and possesses this property only to a negligible degree. However, the innovation that came in the decade of 1870's and thirty years following brought about typical evolution of a pioneer stage of technical development through the medium of increasing scientific insight into the properties of this newly found composite material.

The discovery and advancement of 'reinforced concrete' was an exceptional step-up in the history of building and construction processes in the later part of the 19th century. Reinforced concrete is the term used to describe a concrete in which reinforcement bars which are mainly steel have been incorporated into brittle concrete matrix to strengthen the material especially in the area most likely to be subjected to tensile load. Social, economic and technological development at this time created the environment for modern high-rise buildings to emerge in North American cities and Europe (Condit, 1968; Kayvani, 2014). The development of reinforced concrete

therefore was a timely technological advancement at the time when structures were needed to withstand the tensile loads in preparation for the civilization age. As discussed by Thomas and Jennings (n.d.), in order to allow concrete to support or withstand tensile or bending loads, steel rods are put inside the concrete in the area that are expected to be in tension, so that when load is applied, the concrete supports the compressive stress and the steel bars support the tensile stress while steel reinforcement is also rendering helps to concrete in resisting the tensile forces associated with drying shrinkage.

Meanwhile, the change from brick and mortar structures loaded in compression to steel structures in tension did not come absolutely free from problems, knowing fully the structures are subjected to different forces including compression, bending, tension, shear and torsion. Occasionally, a steel structure would fail unexpectedly at even stresses well below the designed tensile strength, (Anderson, 2005). Many reasons may be responsible for failure of reinforced concrete structures ranging from misplaced reinforcement bars or error in size, materials used, excessive loading, and internal effects such as early thermal shrinkage during curing, deficiency in shear resistance, manufacturing procedures and bonding problems. In its technical report, The Concrete Society (2007) stated that the major structural application of steel reinforcing bars is to carry the tensile force once the concrete has cracked or by prestressing the concrete to remain largely in compression under load apart from or in addition to providing sufficient area of steel to carry the tensile stresses at the ultimate load that is to be applied to the member. However, the concrete cracks before any appreciable load is transferred to the steel as a result of significant difference between tensile failure strain of the concrete and the yield strain of the steel reinforcement. The report further stated that, sometimes in the event of concrete cracks, it is impossible to accurately predict the crack widths in some applications where a normal amount of steel is provided to prevent uncontrolled crack development or failure in the event of accidental overload.

2.2.3 Crack mechanism of concrete.

The most significant problem associated with concrete is cracking. It can also be said that all other problems in connection to concrete originate from or begin by cracking. Even if the eventual failure of concrete is as a result of cracking, development of cracks on a structure may not necessarily mean that the structure has failed. It should be noted that not all cracks are structural, some are surface cracking caused by the faster rate of evaporation of the surface moisture. Cracking can be as a result of one or a combination of factors such as drying shrinkage, thermal contraction, subgrade settlement, and applied loads. It may be impossible to prevent cracking but it can be significantly reduced or controlled when the causes are taken into account and preventative steps are taken, (Concrete Foundations Association, 2005).

It has been reported that very fine cracks at the interface between coarse aggregate and cement paste exist, even prior to application of the load on concrete which may be due to the inherent differences in mechanical properties between the coarse aggregate and the hydrated cement paste, coupled with shrinkage or thermal movement (Neville, 1995) . Concrete being a composite material has its properties depending on the properties of the components it is made of and the interaction among them. Giaccio and Zerbino (1998) reported that the interfacial transition zones between the cement paste and aggregate particles are the weakest link of the composite material, playing a very important role in the process of concrete failure, stating that crack propagation usually starts at the matrix-aggregate interfaces, and the cracks grow through the matrix. Furthermore, the study suggested that coarse aggregates normally arrest crack growth thereby causing meandering and branching of cracks while some particles are fractured in the process, this process depending on the characteristics of the aggregates, especially surface texture and shape, and on strength differences between aggregates and matrix. In another study, the position of Giaccio and Zerbino (1998) on interfacial transition zones and the influence of coarse aggregate was reiterated. Guo et al. (2007) added that texture of coarse aggregate in concrete matrix will decide greatly the compressive strength and the failure mode of the concrete, reporting that there were two fracture modes; first one is the cracks along

with the interface zone between the matrix and coarse aggregate, and the other is the crack tips penetrating through the coarse aggregate to the above matrix. Also, from the same study, it was found that incorporating ground granulated blast-furnace slag into the concrete matrix weakened the bond strength of interface transition zones between coarse aggregate and matrix because more coarse aggregates on fractured profile of concrete with ground granulated blast-furnace slag were debonded during the cyclic loading. The plausible reason for this as suggested by the researchers is that the grain size of ground granulated blast-furnace slag in the study was similar to those of Portland cement while the elastic modulus of ground granulated blast-furnace slag grain was lower than those of cement grain.

In another development, it was found that failure of concrete in compression can be considered as a sequence of a two-stage crack mechanism. In the first phase, micro-cracks open at random but within the specimen oriented in the direction of loading or stress application where the randomness of the cracking is related to the heterogeneity of the material and to the existence of weak points and hard points of interface zone thereby leading to formation of small columns within the specimen. The second phase involves the amalgamation of micro-cracks to form macro-cracks, still oriented parallel to the direction of loading and by bonding small columns of different sizes and slopes within the specimen, oblique cracks appear which then merge to bring about failure (Rossi et al., 1996). Micro-cracks have not been universally defined in terms of size, but an upper limit of 0.1 mm has been suggested by Slate and Hover's study (as cited in Neville, 1995, p. 298) which is the smallest size that can be detected by the naked eye. Domone and Illston (2010) also reported that non-linear stress – strain behaviour of concrete in compression is mainly due to the increasing contribution of micro-cracking to the strain with increasing load, citing Glucklich, (1965) study where four stages of cracking behaviour were identified as up to 30% maximum stress, 30 – 50% maximum stress, 50-75% maximum stress and above 75% ultimate stress. As reported, the cracking pattern transforms from stable pre-existing transition zone crack where the stress-strain curve remains approximately linear to the stage where the crack begins to increase in length, width and number causing non-linearity and then the cracks start to

spread into the matrix and become unstable and finally, resulting to spontaneous and unstable crack growth which becomes increasingly frequent, leading to very high strain and eventually, complete breakdown. Figure 2.2 shows the crack path which usually originates from aggregate - paste interface zone (the weakest area of concrete) and later moves through the concrete, as the load on the concrete increases, it grows and becomes extensive until it results in complete breakdown.

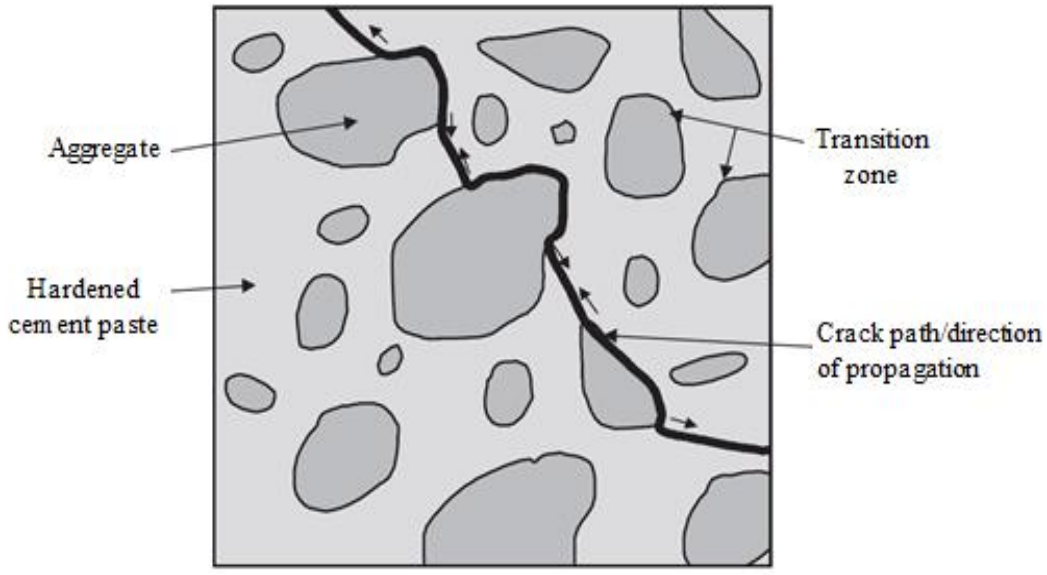

Figure 2.2: Cracking pattern in normal-strength concrete
(Domone & *Illston*, 2010)

Concrete structural cracking and eventual failure can occur when a structure is overloaded beyond the point which the structure can sustain. However, failure does occur sometimes at less than design load when it is exposed to a large number of stress cycles referred to fatigue failure, (Li et al., 2007). Some other studies have been carried out on flexural fatigue of concrete (Graeff et al., 2012; Guo et al., 2007; Kolluru et al., 2000) investigating crack propagation, fatigue resistance and cracking mechanism and flexural fatigue performance of concrete used in various applications. The findings suggested that concrete performance is greatly reduced when cyclic loads are induced which causes high level of propagation of macro-cracks from micro-cracks leading to

the brittle failures of the materials. It was also found by Kolluru et al. (2000) that crack growth due to constant fatigue loading comprises of two stages; firstly, a deceleration stage where there is a decrease in crack growth rate with increasing crack length and the second stage, an acceleration stage where the rate of crack growth increases at a steady rate.

2.3 Functions of steel fibres in concrete

2.3.1 Origin and development of fibres in construction materials

It is relatively difficult to exactly state when and where the concept of fibre reinforcement started. The inclusion of fibres as reinforcement for brittle matrix materials is not a recent phenomenon; it has been since time immemorial such as horsehair in mortar and straw in bricks. Almost every publication on fibre-reinforced cement and concrete opens by just a reminder that man has formed useful composites by combining brittle materials with more ductile fibres for millennia and that since Biblical times as recorded in Exodus, over 3500 years ago, brittle building materials such as sun-baked clay bricks were reinforced with horsehair and straw, (Brandt, 2008; Domone & Illston, 2010). Another study tracing the origin of fibres in construction processes reported that usage of fibres in brittle materials has a long history going back at least 3500 years when bricks reinforced with straw were used to build the 57 m high hill of Aqua Quf near Baghdad (Hannant, 2003) . The researcher however stated that in more recent times, asbestos fibres have been used as reinforcing materials in cement products for about 100 years and cellulose fibres for at least 60 years. It was also reported that large scale commercial use of asbestos fibres in a cement paste matrix actually began with the invention of the Hatscheck process in 1898 with asbestos cement construction products widely used throughout the world until the health hazards associated with asbestos fibres came to light and alternative fibres were introduced, (American Concrete Institute, 2002). It was later after the Hatscheck technology was invented for production of plates for roofing, pipes and other

construction elements that glass fibres were proposed for reinforcement of cement paste and mortar by Biryukovichs, as reported by Brandt (2008), though there were issues with the non-resistance and durability of ordinary glass fibres in highly alkaline Portland cement paste.

Slater et al. (2012) reported that at present, four primary fibre types are being used in concrete and for construction purposes; natural, synthetic, glass and steel, stating natural fibres such as sisal, coconut, jute, sugar cane, bamboo, and flax are the oldest type of fibre reinforcement in building construction and that they are popular reinforcement option in developing countries because of their low cost and local origins. Figures 2.3 and 2.4 show the examples of sisal natural fibre as a plant and in processed form respectively.

Figure 2.3: Natural fibre, sisal plant
(FAO, 2016)

The sisal natural fibre in a raw form as plant as shown in Figure 2.3 cannot be used directly in construction materials but subjected to few stages of processing to produce what is shown in Figure 2.4 .

Figure 2.4: Natural fibre, processed sisal
(Miller Waste Mills, 2016)

There have been various usages of natural fibres in both clay bricks and concrete. The natural fibres mostly used can be categorised into three classes, the plant or vegetable origin fibres which include jute, sisal, bamboo, elephant grass, cotton and others, the animal fibres comprising of silk, wool, hair, and others like animal skin and the third class is the naturally available mineral fibre, asbestos. Castro and Naaman (1981) claimed that natural organic fibres, exist in reasonably large quantities in many countries of the world and if properly exploited, they can represent continuously renewable resources, stating that the best used natural fibres such as sisal or jute have been limited mostly to the production of fabrics, ropes, and the like. Jute natural fibre is as shown in Figure 2.5.

Figure 2.5: Natural fibres, jute
(FAO, 2016)

Shah (1981) reported that the natural fibres may be economical and since they are lighter in weight, they may be chemically inert than the man-made fibres. The researcher in addition also reported that these natural fibres however produce lower bond and a lower modulus of elasticity than the metallic fibres and when they are used in proportions similar to the other types of fibres, they do not improve concrete strength properties as much. Natural fibres abound in large quantities in developing countries, for example in Nigeria; there are research works where the performance of natural fibres in concrete have been investigated exploiting the advantage of the economical and abundant availability of materials such as Kenaf fibre (Hibiscus cannabinus L.), akwara, palm nut fibre and bamboo strips, (Akubueze et al., 2014; Okafor, 1988; Salau et al., 2012; Udoeyo et al., 2011; Uzomaka, 1976).

In modern times, other fibres have been developed as well which are different from glass, natural or steel fibres. Synthetic fibres are petrochemical based polymers and those which are used as fibres in synthetic fibre reinforced concrete may include polypropylene, polyethylene, nylon and polyester fibres. Synthetic fibres are man-made, and available in a variety of formulations. The twentieth century interest in

synthetic fibres as a component of construction material was first reported in 1965 in Goldfein's study (as cited by ACI, 2002). It was also reported that synthetic monofilament fibres were used in blast resistant structures for U.S. Army corps of Engineers and that synthetic fibres are said to be melted when the crystalline portions of the polymers that they are made of are converted on heating from a solid to a glassy or liquid state since fibres melt, oxidize or decompose at a particular temperature. It has also been suggested that synthetic fibres have some advantages when compared to steel or other fibres in that they are corrosion-resistant and exhibit high energy absorption capacity, (Oh et al., 2007).

The use of asbestos fibres as reinforcing materials in concrete was the first modern fibre reinforced concrete known which was introduced in about 1900 with the development of the Hatscheck process (Hannant, 2003; Mindess, 2007) . The world consumption of asbestos fibres rose to high level up to 3 million Tonnes as claimed by Shah (1981) since they are naturally available and have the required thermal, mechanical and chemical resistance but due to the health hazard associated with asbestos, there was a serious decline in the usage. Hence, an urgent replacement for asbestos was lunched, that will be a suitable substitute. This search was the advances that produced the current materials in use as reinforcing fibres in concrete which include glass fibres, organic man-made fibres such as polypropylene and polyethylene fibres (as shown in Figure 2.6) as well as steel fibres that have now been popularly used for the past 40 years.

Figure 2.6: Synthetic fibres, polypropylene type

The research performed by Romualdi and Batson and Romualdi and Mendel in the early 1960s brought the turning point and represented the first substantial steps towards development of steel fibre reinforced concrete technology, which attracted the attention of academic and industry research scientists around the world, (Portland Cement Association, 1991; Zollo, 1997). It was claimed by Zollo (1997) that the discovery was welcomed with excitement regarding the promise that fibre reinforced concrete held for future development of the composite materials but many however never imagined the magnitude of the impact fibre reinforced concrete would have on research, technological advancement and commercial development communities world-wide as we have today. The use of steel fibre reinforced concrete has outweighed that of any other fibre reinforced concrete as it is more widely used throughout the world, although polymer fibres are catching up, (Domone & Illston, 2010). Today, steel fibre reinforced concrete is very widely used for both structural and non-structural purposes, unlike when it first started and used only for non-structural

applications, according to a study by Mindess (2007). Steel fibres are being used in wide variety applications world-wide with ever growing researches on how to improve the properties and advance the technological effectiveness of this composite material.

2.3.2 General concept of fibres in concrete

The undesirable brittle characteristics of concrete which make it unreliable when it comes to withstanding tensile loading and its weak strain capacity are the major problems of concrete. In trying to improve the weaknesses, materials that can mix with concrete matrix are included to reinforce it in various directions. These materials are fibres, which are of different sizes and lengths, but generally short, discontinuous and found all through the concrete matrix. When fibres have been incorporated into the concrete, its tensile strength is then increased by delaying the growth of cracks, and to increase the toughness by transmitting stress across a cracked section so that much larger deformation is possible beyond the peak stress than without fibre reinforcement (Neville & Brooks, 1987) thereby modifying the brittle characteristics to a ductile one.

From structural point of view, most researchers agreed that the main objective of inclusion of fibres is to attempt to modify the properties of concrete by improving the mechanical properties including compressive, tensile and shear strengths, flexural toughness, post-cracking strength and fracture energy (Balendran et al., 2002; Bencardino et al., 2013; Kang et al., 2011; Michels et al., 2003). In another study, it has been suggested that inclusion of any kind of short fibre in a concrete matrix will not significantly alter the load at which cracking occurs in hardened concrete, but the benefits of fibres in hardened concrete relate to the post-cracking state, (Hannant, 2003) . The researcher however listed the five main objectives of inclusion of fibres in concrete matrix as

(a) To improve the or plastic cracking characteristics of the material in the fresh state or up to about 6 hours after casting.

(b) To improve the tensile or flexural strength.

(c) To improve the impact strength and toughness.

(d) To control cracking and the mode of failure by means of post-cracking ductility.

(e) To improve durability.

2.3.3 Definition of steel fibre reinforced concrete

There have been many and different definitions proposed by literatures dealing with steel fibre reinforced concrete (SFRC) which would be appropriate if synchronised. Zhang et al. (2013) defined SFRC as a multi-phase composite material in which short steel fibres are distributed in random directions in conventional reinforced concrete. Although, the researchers were investigating combined effects of steel fibres with or without conventional reinforcement in concrete and therefore related the definition to reinforced concrete instead of ordinary concrete matrix. In another study by Van Chanh (2004), fibre reinforced concrete was defined as a composite material made with Portland cement, aggregate, and incorporating discrete discontinuous fibres. Zollo (1997) in his study, citing ACI 116R, Cement and Concrete Terminology, defined fibre reinforced concrete (FRC) as concrete containing dispersed randomly oriented fibres. In another term, Cengiz and Turanli (2004) simply defined SFRC as concrete containing discontinuous discrete steel fibres as a reinforcement. In a report by ACI Committee on fibre reinforced concrete, (American Concrete Institute, 2002), steel fibre reinforced concrete was defined as concrete made of hydraulic cements containing fine or fine and coarse aggregate and discontinuous discrete steel fibres. Bekaert NV (2013) at a technical presentation defined steel fibre reinforced concrete as normal concrete in which thin steel fibres are evenly spread throughout the mass in order to obtain multi-directional reinforcement.

There are terms used from the above authors and bodies that must be considered and fine-tuned so as not to have a confusing understanding of what actually SFRC is. Firstly, steel fibres can be included in a conventional reinforced concrete as a combined effort while the inclusion in concrete without conventional reinforcement is also SFRC, this is even the ideal situation where a normal concrete is reinforced with steel fibres only.

Another term used in which diverging views can be expressed is that of even distribution of steel fibres within the concrete matrix. This has not been the case from recent researches, however, steel fibres can spread throughout the concrete matrix. Also, going by the definition of concrete by Neville and Brooks (1987), that concrete in the broadest sense, is any product or mass made by the use of a cementing medium, different definition of concrete as mentioned by authors should also be left as a normal concrete which each researcher can confine to the study being carried on.

Therefore, having looked at various definitions and with the aim of synchronising to arrive at the modest definition of steel fibre reinforced concrete (SFRC), it can be defined as;

'A concrete which contains thin short discrete steel fibres that are spread throughout the mass in order to obtain multi-directional reinforcement with main objective of modifying the properties of concrete'

The above definition is that which would be considered in this research work while the concrete is that which contains fine and coarse aggregates with Portland cement as a cementing medium.

2.3.4 Types of steel fibres

Steel fibres that are used in concrete as reinforcing materials have been defined as short, discrete lengths of steel having an aspect ratio (ratio of length to diameter) from about 20 to 100, with any of several cross-sections, and that are sufficiently small to be randomly dispersed in an unhardened concrete mixture using usual mixing procedures, (American Concrete Institute, 2002). Though, as earlier mentioned, there are numerous types of fibres used in and for construction purposes from natural to artificial, the artificial type of fibres and most especially, the steel types have been most used of all the commercially available fibres because of their effectiveness. The steel fibres however are in turn of different types available for commercial use which depends on how they were manufactured. There are many processes by which steel

fibres are produced leading to why they are supplied in many different shapes, sizes and in tensile strengths. From literature, (American Concrete Institute, 2002; Henager, 1981; Shah, 1981; The Concrete Society, 2007), four classes of steel fibres according to the method of manufacture have been identified, as follows:

Group I	Cold-drawn wire
Group II	Cut sheet
Group III	Melt-extracted
Group IV	Others/shaved cold drawn wire.

From the manufacturing routes, round steel fibres are produced by cutting or chopping the wire with a typical diameter between 0.25 and 0.76 mm. Flat, straight or sheet steel fibres having typical cross sections in the range of 0.15 to 0.64 mm in thickness and 0.25 to 2.03 mm in width are produced by shearing sheets or flattening wire. Crimped and deformed steel fibres have been produced with full length crimping or bent or enlarged at the ends only. Fibres have also been produced from hot melt extraction process. This method uses a rotating wheel that contacts a molten metal surface, lifts off liquid metal, and rapidly solidifies it into irregular surface fibres. Fibres can be produced as well from cold drawn wire that have been shaved down in order to make steel wool while the remaining wires have a circular segment cross-section that may be crimped to produce deformed fibres. Figures 2.7, 2.8 and 2.9 show various steel fibres available for use.

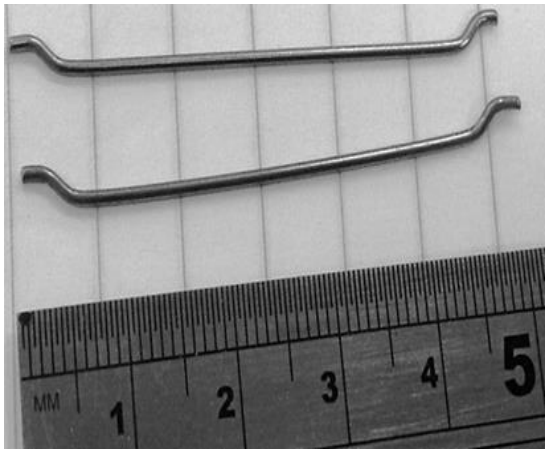

Figure 2.7: Hooked end steel fibres

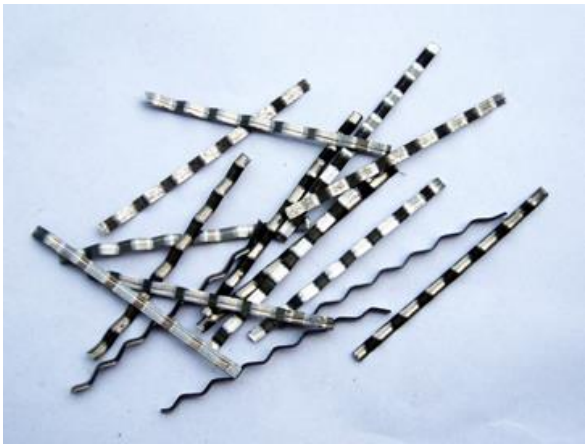

Figure 2.8: Crimped steel fibres
(Tradekorea.com, 2008)

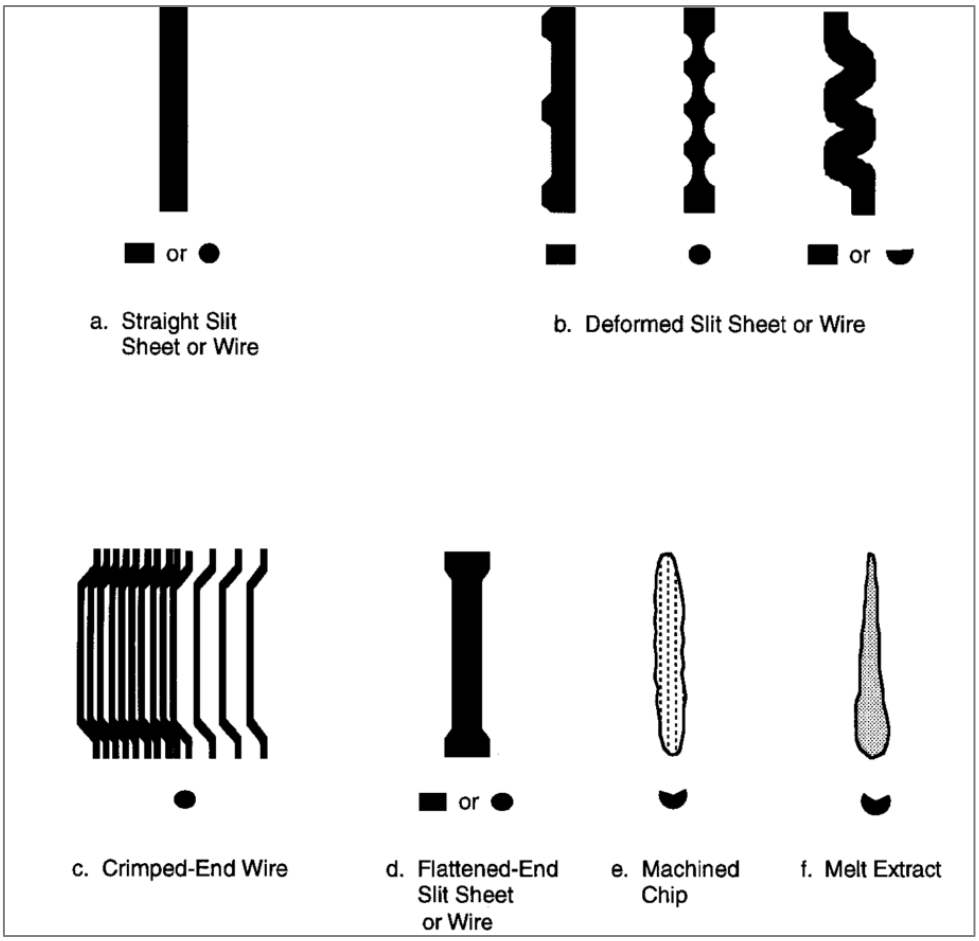

Figure 2.9: Various steel fibres geometries
(American Concrete Institute, 2002)

There have been investigations carried out in the recent past where the effects of different types and geometry of steel fibres on the post-cracking strength of steel fibre reinforced concrete were studied. Pająk and Ponikiewski (2013) studied the flexural behaviour of self-compacting concrete reinforced with two different types of steel fibres with comparable but different shape; hooked end and straight. In another study, effect of steel fibres on mechanical properties of concrete investigating two types of fibres as well; hooked end and corrugated steel fibres, (Holschemacher et al., 2010). Working on effects of fibre geometry on the flexural behaviour of SFRC, Soulioti et al. (2011) investigated waved or wavy profile and hooked end steel fibres. Other researchers, Sable and Rathi (2012) studied the effects of hooked end, crimped and straight type of steel fibres on mechanical properties of self-compacting concrete while Soutsos et al. (2012) did not only investigate the hooked end, wavy profile, flattened ends types of steel fibres but also worked on the synthetic type of fibres commonly used in reinforcing concrete as well. In all this research, hooked end type of steel fibres were found to show the best result in post cracking strength and ductility of steel fibre reinforced concrete exhibiting higher values of toughness and residual strength as compared to all other types of fibres.

Therefore, in this research work, hooked end steel fibres have been adopted to be used throughout the investigation being the type that presents higher ductility properties. The geometry and dosage were varied though, since the distribution and orientation of the fibres can be affected by the variables chosen.

2.3.5 Application and benefits of steel fibre reinforced concrete

Steel fibre reinforced concrete has been used extensively in almost every part of the world for a wide variety of applications in building and civil engineering works of non-structural and structural, new constructions and repair of older ones and in ground-supported industrial slabs. Also, there are numerous benefits and advantages of SFRC over the conventional mode of concrete reinforcement.

2.3.5.1 Applications

Sorelli et al. (2006) reported that usage of SFRC in the last decades has significantly increased in industrial pavement, roads, parking areas, and airport runways as an effective alternative to conventional reinforcement providing help in the area of structural behaviour because of heavy concentration of industrial machinery induced loads causing intensive cracking and excessive deformation of pavements.

Ground supported slabs

Steel fibres are used for ground-supported industrial floor slabs as the easy and fast installation of the slab reduces the total time of construction, (The Concrete Society, 2007). It has been reported that Twintec industrial flooring laid the UK's biggest ever SFRC flooring project, of about 250,000 m^2 of joint-less ground-bearing SFRC floor slabs constructed in Scotland, where the choice of steel fibres as reinforcement provided a joint-less and very versatile surface that is suitable for modern heavily trafficked and heavily loaded distribution warehouses (Eddy, 2008). Figure 2.10 shows the internal floor slab (a) and external floor slab (b) of the UK's biggest SFRC floor slab at Tesco, Livingston, Scotland, UK.

Figure 2.10: Tesco Livingston, UK's biggest SFRC floor slab: (a) internal slab, (b) external slab (Darryl Eddy, 2008)

Dobbins (2012) has reported that SFRC joint-less designs are ideally suited to construction of both ground bearing and pile-supported external yards, itemising the benefits as including;

(a) Elimination of sawn induced contraction joints leading to reduced joint maintenance cost and time and improved ride quality.
(b) Substantially reduced construction time on site.
(c) Improved toughness and durability.

Floor on piles and suspended slabs

Besides those pavements that are on ground which are statically indeterminate structures in which steel fibres effectively increase the ultimate load, (Sorelli et al., 2006), SFRC is currently being used for pile-supported ground floor slabs where steel fibres are used to replace some or all the conventional reinforcement. Illston and Dinwoodie (1994) reported that traditionally the design has been to provide a double layer of steel mesh where large sheets of mesh are laid on spacers to ensure that the layers are positioned at the correct depth and concrete then poured over the mesh. It was further stated that replacement with steel fibres provides several advantages including elimination of all handling and placing cost/time, reinforcement is distributed throughout the full thickness of the slab and that steel fibre reinforced concrete can be used more easily in conjunction with composite floor construction. Some pile-supported slabs without any conventional reinforcement have also been constructed with success. Example of floor on piles is shown in figure 2.11.

Figure 2.11: Floor on piles

(Bekaert NV, 2013)

It has also been reported, (The Concrete Society, 2007) that steel fibres have been used as reinforcement for elevated suspended slabs that are fully supported by columns where all the conventional flexural and shear reinforcement for slabs were fully replaced by steel fibres.

Hard standings, airport pavement, railways and roads

Steel fibre reinforced concrete is being used largely in hard standings, railways, in roads and airport pavements, in overlays to repair the existing pavement as well as in new construction. American Concrete Institute (2002) reported that many cast-in-place SFRC applications involving twenty-two airport pavements had been completed in the United States as early as 1983 while SFRC has been used for many other projects, including bridge deck overlays. It was also reported that the U.S. Army Construction Engineering Research Laboratory performed controlled testing of SFRC runway slabs subjected to C5A airplane wheel loadings in 1971, the analysis of the test data indicated that SFRC slabs need to be only about one half the thickness of plain concrete slabs for the same wheel loads. Figure 2.12 is an example of where steel fibre reinforced concrete has been used in airfield construction.

Figure 2.12: Aircraft hard-standing

(The Concrete Society, 2007)

Portland Cement Association (1991) reported that a number of highway and bridge deck applications have been undertaken using steel fibre reinforced concrete with considerable success, stating SFRC has been used as top layer of a two-course floor, a full-depth floor, or an overlay on an existing floor while some of these floor must withstand potentially damaging concentrated and dynamic loads. It was also reported that SFRC was used for replacement of 260m of the track bed slab in the Thames link tunnels in London, steel fibres being selected in preference to traditional bar reinforcement so that the thickness of the slab could be reduced, allowing a larger loading gauge for the railway, (The Concrete Society, 2007).

Mine and tunnel linings

Steel fibres are being used in form of dry and wet sprayed concrete also known as steel fibrous shotcrete in mining, tunnel linings, for rock slope stabilization, in dam

construction, for repair of deteriorated surfaces and in thin shell dome construction, (Henager, 1981). It was also reported by the same author that inclusion of steel fibres in shotcrete improves many of the properties of the basic material like toughness, impact resistance, shear strength, flexural strength, durability factor, and the fatigue endurance limit. Steel fibres have been used to replace the traditional fabric reinforcement in tunnelling with enhanced ductility properties and great reduction of the amount of material lost due to rebound. Figure 2.13 is a typical example of tunnel with permanent shotcrete linings in a metro station in Sweden.

Figure 2.13: Stockholm Metro with permanent shotcrete linings

(The Concrete Society, 2007)

Hydraulic structures and underwater concrete

Steel fibre reinforced concrete is equally used to make precast storage tank, fluid tight structures, septic tanks reinforced with only steel fibres, and for some precast units such as pipes and manholes. It has been reported that steel fibre reinforced concrete

has been used in hydraulic structures, and has enhanced the resistance to cavitation and erosion damage caused by high velocity water flow. It was further stated that steel fibre reinforced concrete has been used in the construction and repair of spillways, sluiceways, and stilling basins where both laboratory test and applications have indicated that SFRC will last about three times longer than plain concrete subjected to high-velocity water flow (Portland Cement Association, 1991). Figure 2.14 is a typical underground concrete structure.

Figure 2.14: Underwater concrete

(Bekaert NV, 2013)

Lightly loaded foundations and combined reinforcement

Steel fibres are commonly used in concrete today as reinforcement with or without the conventional reinforcement. There are diverse civil engineering project where steel fibre reinforced concrete is being used without the conventional reinforcement like in lightly loaded or individual houses foundations, while it is also used in a combined

system of reinforcement with the conventional rebar where the conventional rebar can be greatly reduced with the combined reinforced structure resulting in higher life span (improved durability). A typical combined reinforcement is shown in figure 2.15 where SFRC has been used to eliminate the whole top reinforcement in a track slab construction in New Zealand (Bekaert NV, 2013). Top reinforcement could have been needed in the first instance probably because of the nature of the load the slab will be sustaining being a track railway slab.

Figure 2.15: Track slab of combined reinforcement
(Bekaert NV, 2013)

2.3.5.2 Benefits of steel fibre reinforced concrete

The benefits of using steel fibres to replace or to combine with conventional reinforcement bars in concrete are numerous, ranging from economical to technical or structural advantages. Boulekbache et al. (2010) listed some structural benefits of using fibres in cementitious system as including provision of effective reinforcement against shear failure when vertical stirrups are replaced by steel fibres in concrete and taking up of internal stresses through their tension resistance and ensuring the transfer

of the loads. Other advantages of steel fibres over conventional rebar as listed by (Bekaert NV, 2013) for both technical and economical include:

- Multidirectional reinforcement
- Elimination of damages at edges and corner due to the spalling forces
- High impact resistance
- Post fire durability superior to rebar
- Increase in productivity
- Quick and easy installation

2.3.6 Concluding remarks

This chapter reviewed the fundamental concepts of fibres used for construction purposes, especially, steel fibres as used in concrete. The functions of steel fibres within the concrete matrix, the current applications, and benefits of steel fibre reinforced concrete were also discussed.

Concrete has been in existence for over 5000 years and had passed through series of development from very crude form to the present day concrete. The inclusion of fibres as reinforcement for brittle matrix materials is not a recent phenomenon as straws were used by Egyptians to make mortar over 3500 years ago. This is because, concrete is a brittle material, relatively strong in compression but weak in tension.

The mass production of iron and steel which came with industrial revolution brought about the advancement of 'reinforced concrete' in the later part of 19th century. The main structural application of steel reinforcing bars is to carry the tensile force once the concrete has cracked. However, the concrete cracks before any appreciable load is transferred to the steel as a result of significant difference between tensile failure strain of the concrete and the yield strain of the steel reinforcement. For this reason, the fibres are majorly being included in concrete matrix to arrest the propagation of cracks from micro to macro cracks.

It was reported in this chapter that four primary fibres are in use for construction purposes; natural, synthetic, glass and steel. In the present advancement of fibre

reinforced concrete though, the use of steel fibre reinforced concrete has outweighed that of any other fibre reinforced concrete as it is more widely used throughout the world. Also, different types of steel fibres that are available for commercial use have been identified. However, in various research works and literatures considered in this study, hooked end type of steel fibres were found to show the best result in post cracking strength and ductility of steel fibre reinforced concrete. Therefore, in this research work, hooked end steel fibre was adopted for the investigation.

Most researchers agreed that the main objective of inclusion of fibres is to attempt to modify the properties of concrete by improving the mechanical properties including compressive, tensile and shear strengths, flexural toughness, post-cracking strength and fracture energy. Structurally, fibres in concrete increase its tensile strength by delaying the growth of cracks, and to increase the toughness by transmitting stress across a cracked section thereby modifying the brittle characteristics to a ductile one.

Steel fibre reinforced concrete has been used for a wide variety applications in building and civil engineering works which include ground supported slabs, hard standing, airport pavements, mine and tunnel linings, hydraulic structures and underwater concrete, lightly loaded foundations and combined reinforcement. Some of the benefits of steel fibre reinforced concrete include provision of multidirectional reinforcement, high impact resistance, post fire durability, increase in productivity amongst the rest.

CHAPTER 3

REVIEW OF LITERATURE ON STEEL FIBRE REINFORCED CONCRETE

3.1 Introduction

This part of the study reviews the findings of the previous research works carried out on steel fibre reinforced concrete. The materials used in the review are mainly published works found relevant to this investigation which are useful in pointing out the direction to adopt for this research and clearly revealing the gap in knowledge which this research will fill for the advancement and full exploitation of SFRC in practice. The review also assists in the choice of variables and the effectiveness of method of investigation adopted in this research work.

3.2 Mechanical properties of steel fibre reinforced concrete

A number of studies have been carried out on the mechanical properties of steel fibre reinforced concrete since when the current knowledge on the composite material was stimulated in the early 60's. The effects of inclusion of steel fibres on both fresh and the resulting hardened concrete material have been investigated. There has been research on the reinforcing mechanism of steel fibres within the concrete matrix and the workability, compressive strength and post-cracking ductility have been reported. Mode of testing and test specimens have also been reported. All these are reviewed in this section.

3.2.1 Workability of fresh steel fibre reinforced concrete

The workability of the fresh concrete is a key attribute that determines the quality of a potential hardened form of the concrete. The term workability describes the capability of fresh material to be well handled and flow into the formwork or around the particular area of the structure where it is required. It was reported that workability has always been traditionally the combination of two properties, fluidity and compactability which has now been replaced by the term consistence in some current standards, including those in Europe (Domone & Illston, 2010). Therefore, to guarantee uniform distribution of steel fibres in the concrete, it is necessary to control concrete fluidity, concrete composition and fibre addition to the concrete.

In a study conducted to determine combined effect of water/cement ratio, steel fibre tensile strength and volume fraction of fibre on mechanical behaviour of steel fibre reinforced concrete, Köksal et al. (2013) reported that the addition of steel fibres into concrete has negative influence on the workability. The study further established by employing Vebe test that steel fibres decrease workability of fresh concrete stating that Vebe time increases with increasing steel fibre volume fraction for each water/cement ratio while on the other hand, the unit weight of the fresh concrete increases with the increasing of steel fibre content which can be attributed to the specific gravity of steel fibres. In a related development, Soulioti et al. (2011) investigated the slump properties as well as the air content of fresh unreinforced and fibre reinforced concrete mixtures in order to study the effect of fibre inclusion on the workability of the obtained systems. It was observed that the addition of steel fibres in the concrete reduced the slump compared to the plain concrete which is in agreement with the report of Köksal et al. (2013), and the air content increases with increasing fibre volume fraction with high fibre volume fraction presenting higher air content than mixtures with low fibre volume fraction. It was also observed that the properties of SFRC in its freshly mixed state are influenced by the aspect ratio of the fibres, fibre geometry, fibre volume fraction and matrix proportions.

On the other hand, a study on flowability of fibre reinforced concrete and its effect on the mechanical properties of the material (Boulekbache et al., 2010) observed that flowability of fibre reinforced concrete, which is in effect, the ease of placing the material has a direct impact on the orientation of fibres inside the concrete matrix and this consequently affects the structural efficiency of the hardened concrete once it is loaded. Furthermore, the researchers stated that the distribution of fibres is modified according to the rheology of the cement matrix, which makes fibres in a fluid concrete having a lower yield stress to exhibit great mobility within the concrete matrix aiding the fibres to move and orient easily under the effect of a light external vibration. And on the contrary, homogeneous distribution of fibres becomes impossible to achieve when the fibres are in a stiff concrete, which is a concrete with higher yield stress, where there is a risk of fibre balls being formed leading to limitation of fibres' movement within the concrete matrix.

Meanwhile, The Concrete Society (2007) has defined 'ball up' or 'balling' as a terminology which describes the formation of large clumps of entangled fibres that may occur during the mixing process. Balling affects the workability of freshly mixed steel fibre reinforced concrete and the distribution as well as orientation of steel fibres in the concrete matrix. Mohammadi et al. (2008) conducted tests such as compaction factor, inverted slump cone time and Vebe time on plain and steel fibre reinforced concrete containing different fibre volume fractions with each volume fraction containing fibres of mixed aspect ratio and reported that introduction of steel fibres resulted in an apparent increase in the stiffness of the mix with workability decreasing uniformly with the increase in fibre content. Also, it was reported that the fibre aspect ratio has significant influence on the workability of the fresh mix as lower aspect ratio resulted in higher compaction factors or lower inverted slump cone time and Vebe time consequently making the tendency of fibres clumping together markedly reduced when compared to concrete with fibres of higher aspect ratio. In agreement to this, the American Concrete Institute (2002) reported that a collection of long thin fibres with aspect ratio greater than 100 will, if shaken together, tend to interlock to form a mat, or ball, which is quite difficult to separate by vibration alone while short fibres

with an aspect ratio less than 50 are not able to interlock and can be easily dispersed by vibration, but adding that while balling of fibres must be avoided, a high aspect ratio is desired for many improved mechanical properties in the hardened state.

3.2.2 Compressive strength

According to British Standards Institute (2009c), compressive strength of test specimens of hardened concrete are determined using cube, cylinder or core meeting the specified requirements, whereby the specimens are loaded to failure in a compression testing machine.

Ordinarily, the strength of plain concrete in compression is perceived to be very high when compared to its strength in tension and the main purpose of adding steel fibres to concrete is not to improve its strength in compression but in tension. Thus, the reports from the numerous research works that have been carried out to date have generally indicated that inclusion of steel fibres in concrete has little effect on compressive strength of SFRC. Some researchers have reported significant improvement in compressive strength of SFRC while others have reported decrease in compressive strength of SFRC where plain concrete exhibited a higher strength than SFRC in compression. However, the majority concluded that the effect of steel fibres in concrete are insignificant in compressive strength of the composite material (Akcay & Tasdemir, 2012; Bayramov et al., 2004).

Ezeldin and Balaguru (1992) in a study on normal and high strength fibre reinforced concrete under compression investigated the influence of steel fibres and their parameters on steel fibre reinforced concrete. Steel fibre reinforced concrete consisting of 30 kg/m^3, 45 kg/m^3 and 60 kg/m^3 of steel fibres in concrete and three equivalent aspect ratios of 60, 75 and 100 were experimented to produce stress-strain behaviour of steel fibre reinforced concrete with compressive strength ranging from 35 MPa to 85 MPa while steel fibre effects on peak stress and corresponding strain were investigated. Typical experimental curves from the study are shown in Figures 3.1 and 3.2.

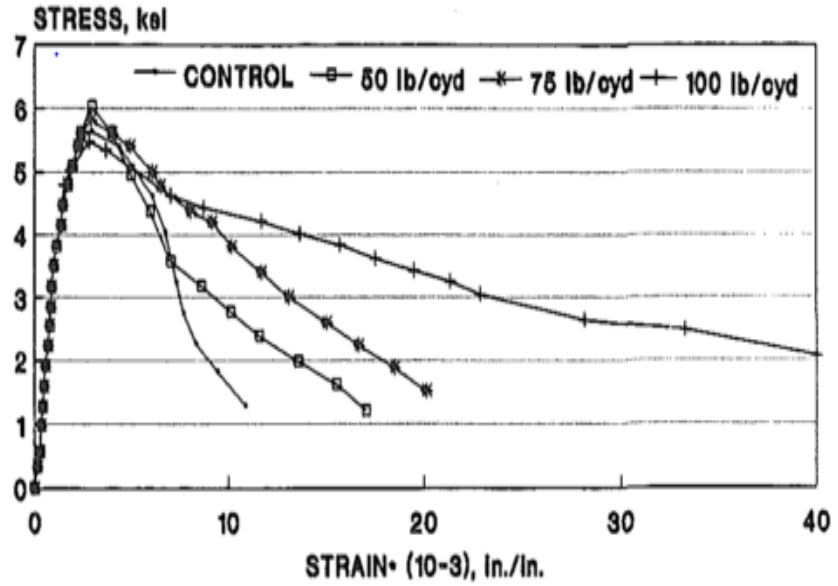

Figure 3.1: Influence of steel fibres in compressive strength; stress-strain curves SFRC of aspect ratio 60 (**1 ksi = 6.9 MPa; 1 in = 25.4 mm; 1 lb/cu yd = 0.59 kg/m3**).

(Ezeldin & Balaguru, 1992)

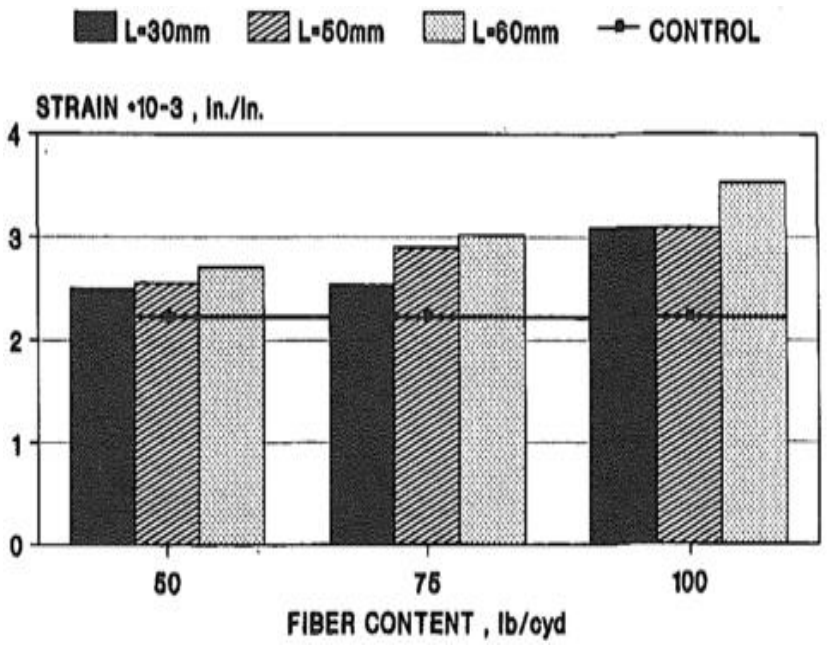

Figure 3.2: Steel fibre and compressive strength; steel fibre effects at peak stress (**1 ksi = 6.9 MPa; 1 in = 25.4 mm; 1 lb/cu yd = 0.59 kg/m3**)

(Ezeldin & Balaguru, 1992)

The study concluded that the addition of steel fibres to concrete is slightly effective in the strain capacity corresponding to the peak stress as indicated in figure 3.1 (b), while this is more pronounced when using higher fibre dosage and longer fibre length. However, the addition of steel fibres to concrete only produced a marginal increase in the compressive strength of the composite.

Soutsos et al. (2012) conducted research on the compressive strength of fibre reinforced concrete made with steel and synthetic fibres using cubes of size 100 mm and 150 mm. The researchers found that the 28-day mean compressive strength of plain concrete was 32.5 MPa while the incorporation of steel fibres increased the compressive strength by about 4 and 5 MPa for the fibre dosage rates of 30 kg/m^3 and 50 kg/m^3 respectively. The increase in the compressive strength of synthetic fibres were reported to be lower, which was about 2 to 3 MPa for dosage rates of 4.5 to 5.3 kg/m^3. These findings are in agreement with other studies carried out by many researchers as well. Balendran et al. (2002) reported that the density and compressive strength of fibre reinforced concrete are about the same as those of the plain counterparts when 1% by volume of steel fibre (78.5 kg/m^3) in concrete were investigated. Gao et al. (1997), American Concrete Institute (2002) and Portland Cement Association (1991) have also reported that addition of steel fibres in concrete has little effect on compressive strength of conventional SFRC with fibre dosage ranging from 0.5% to 2.0% by volume.

However, some other researchers have also reported a decrease in compressive strength of SFRC when compared with the plain concrete. In a study investigating the influence of steel fibres on the compressive strength of ordinary concrete, self-compacting concrete and high performance concrete performed on cylindrical specimens with 40 kg/m^3 dosage of hooked end steel fibres in all the concretes, it was reported that the presence of steel fibres in concrete reduced slightly the compressive strength by about 7% for ordinary fibre reinforced concrete, 6% for fibre reinforced self-compacting concrete and 10% for high-strength fibre reinforced concrete (Boulekbache et al., 2010). In a related study, the influence of the fibre geometry and volume fraction on the compressive strength has been investigated using 150 mm x

150 mm x 150 mm cubic specimens with two geometries of steel fibres, waved and hooked ends and three different volume fractions, 0.5%, 1% and 1.5% by concrete volume. It was observed that for both geometries, the addition of fibres in the concrete mix at fractions of 0.5% and 1.5% steel fibre volume slightly increased the compressive strength, and on the contrary, the compressive strength of the concrete with 1% volume fraction of steel fibres was lower than that of the plain concrete specimens (Soulioti et al., 2011). It was suggested by the researchers that incorporation of steel fibres into the concrete makes consolidation of the mixture more difficult to achieve leading to an increase of the entrapped air. In agreement with (Boulekbache et al., 2010) and (Soulioti et al., 2011), Bencardino et al. (2008) carried out compressive strength tests at 28 days using both 150 mm cubes and 150 mm x 300 mm cylinders. It was recorded that the compressive strength value was affected by the shape of the test specimen, that at 1% fibre volume, the cubes registered a significant increase in strength compared to the plain concrete, whereas only marginal increase in strength was recorded for the cylinders over that of the plain concrete specimens. However, at 1.6% and 3% fibre volume dosages, the cubes gave almost the same comprehensive strength as the plain concrete, while the cylinder specimens recorded a significant reduction in strength of about 12% when compared to that of plain concrete. The researchers attributed the variation to fibre orientation within the concrete matrix. Nevertheless, the differences in compressive results reported in literature may be due to compaction effects mentioned previously. The compressive strength is expected to rise and then decline with increasing fibre dosage which can also be noticed from the workability measurement as the mixtures become more difficult to get compacted.

3.2.3 Flexural properties of SFRC

The inclusion of steel fibres in concrete has been generally accepted to improve or increase the tensile or flexural strength of the concrete, improve the impact strength and toughness of the concrete and also reduce the brittle failure mode by reducing the propagation of cracks within the concrete matrix by arresting the formation of macro

cracks from micro-cracks thereby forming a more ductile material. Hannant (2003) reported that the addition of any type of short fibre in a three-dimensional random fibre distribution at practical fibre volume in a concrete matrix will not significantly alter the load at which cracking occurs in hardened concrete and that the main advantage of the inclusion of fibres in hardened concrete is in relation to the post-cracking state. This is a state of material whereby the fibre reinforcement within the material guarantees the sustaining of bearing capacity of the material after cracking, most time leading to a strain hardening. Therefore, the parameters through which the post-cracking ductility is achieved in steel fibre reinforced concrete are considered in this section.

3.2.3.1 Effect of fibres in crack and fracture behaviour of SFRC

The two different ways a steel fibre embedded in fibre reinforced concrete can fail have been described as either breaking in two or by being pulled out of the cement or concrete matrix depending on the particular SFRC application (Illston & Dinwoodie, 1994).

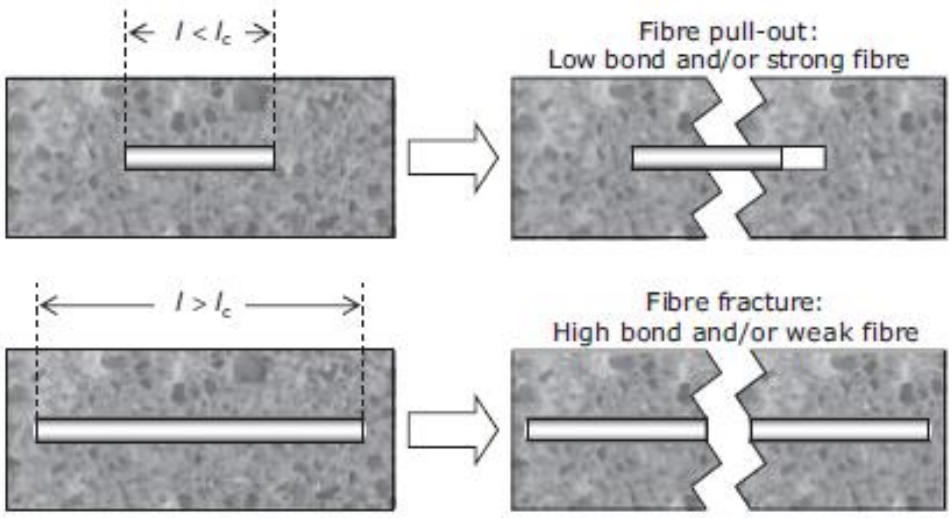

Figure 3.3: Critical fibre length at failure

(Illston & Dinwoodie, 1994)

As illustrated in Figure 3.3, the critical length of fibre, l_c is the minimum length of fibre required such that on failure of the matrix, the full strength of the fibre is mobilised whereby the fibre will break rather than pull out of the matrix. Fibre length, *l* is expressed in terms of critical length when fibre reinforced concrete behaviour is to be analysed. Furthermore, it was explained that another key parameter determining the type of post-cracking behaviour that will occur in SFRC is critical fibre volume fraction. This is the fibre volume fraction that is just sufficient to carry the stress transferred to the fibres at the point of crack of the matrix. This follows that when the fibre volume fraction is above the critical value, the composite failure stress will be higher than the first crack stress and after the first crack has formed, if the load on the composite is increased, stress would be transferred back to the matrix owing to the fibre-matrix bond while further increases in stress will cause further matrix cracking until a network of closely-spaced cracks is formed.

A study was conducted on cracking behaviour of steel fibre reinforced slabs with traditional reinforcement with two types of hooked end of length 35 mm and 60 mm with varying dosages of 20 kg/m^3 and 40 kg/m^3 and polypropylene fibre types as well (Pujadas et al., 2012). It was observed that the fibres with 60 mm length and higher aspect ratio allow them to withstand higher tensile stresses and likewise, the transfer length which is the length necessary to develop its maximum strength capacity by means of a bond stress transfer mechanisms has an influence over the anchorage capability of the fibres thereby making them more active in bridging the cracks when the cracks are bigger, providing a more stable post-cracking response. Graeff et al. (2012) has also reported that the crack behaviour for un-failed specimens follows a pattern where the matrix itself also contributes to preventing the propagation of micro-cracks, making both fibres and concrete matrix responsible for initial crack control at micro level.

In another study, Zollo (1997) has reported that the crack arrest mechanism of SFRC and the manner in which aggregate fillers absorb energy and arrest micro-cracks in concrete are similar. The matrix itself continues to conduct the load while on the ascending, which is the strain hardening or the descending, strain softening portions of

material's load/deflection response while further loading on the composite system is either absorbed or transferred to part of lesser fracture toughness. The researcher further stated that the number of fibres in a unit volume of matrix material is directly related to the statistical probability of a crack encountering fibres. Figure 3.4 as cited from Anderson's work by the researcher was given to demonstrate how fibres act to absorb energy and control crack growth, which was described from the phenomenon moving from left to right of the schematic diagram, which are fibre rupture, fibre pull-out, fibre bridging system by tension and debonding at the fibre/matrix interface respectively.

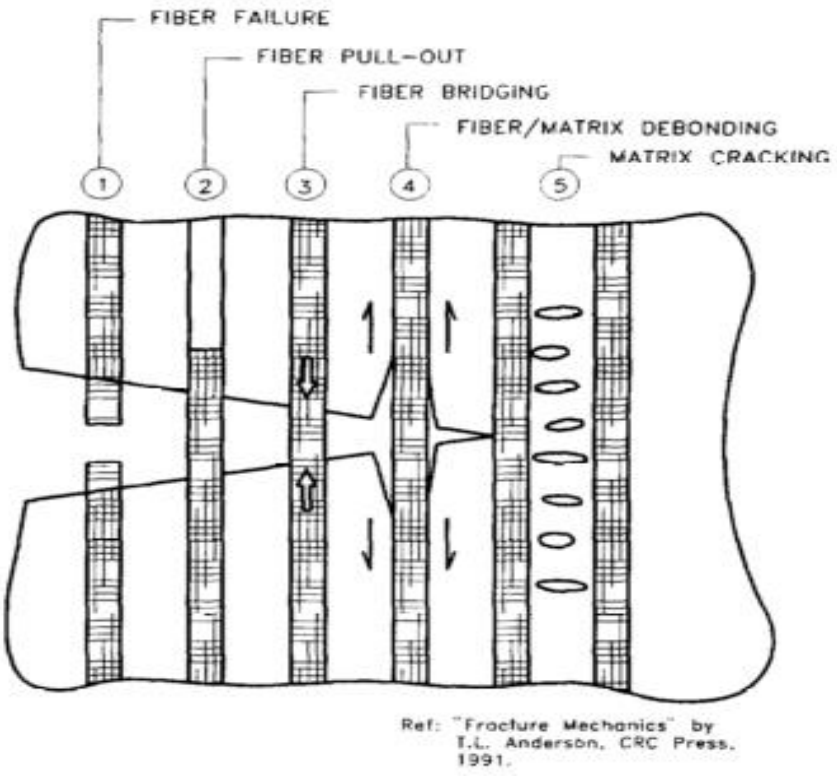

Figure 3.4: Fibre/matrix cracking mechanisms

(Zollo, 1997)

3.2.3.2 Flexural Strength

The flexural tensile strength also expressed as modulus of rupture is an alternative method that has been prescribed for measuring the direct tensile strength of concrete by the standards. This is because it is difficult to test concrete in direct uniaxial tension without the gripping devices of the specimen that might induce additional stresses which can cause a premature failure occurring at the end attachment (Neville, 1995) . The tensile behaviour or bending behaviour of steel fibre reinforced concrete is determined from the load-crack mouth opening displacement curve (CMOD) or load-deflection curve obtained by applying a centre-point load (three-point bending test) on a simply supported notched prism (British Standards Institute, 2005). Two strength values are commonly associated with flexural strength however; first crack strength where the load-CMOD curve depart from linearity, and ultimate flexural strength (Portland Cement Association, 1991).

Many of the previous studies on steel fibre reinforced concrete have noted that the influence of steel fibres on the flexural strength of concrete is significant. American Concrete Institute (2002) reported that the effects of steel fibres on flexural strength of steel fibre reinforced concrete is considerably greater than in the case of tensile or compressive strengths. This agrees with most researchers that have carried out studies in fibre reinforcement in concrete. The transformation of concrete from brittle to ductile material as a result of inclusion of steel fibres in concrete matrix is demonstrated mainly in the flexural behaviour of the hardened composite material.

Balendran et al. (2002) conducted a study on effectiveness of steel fibre inclusion on mechanical performance of concrete, especially in the improvement on strength and ductility of the resulting composite with regard to concrete types and specimen sizes. It was found that the flexural strength of notched beams subjected to three-point bending tests showed that there was increase in flexural strength due to addition of 1% by volume of steel fibres in normal weight concrete up to a maximum of 43% while a maximum strength increase for light weight concrete of 260% was recorded. From these results, it was concluded that the influence of steel fibres on the flexural strength

was more pronounced in the light weight concrete which is more brittle than the normal weight concrete. The flexural strength considered in this research work is the ultimate flexural strength which is calculated from the maximum load recorded as specified by EN 14488-3 (British Standards Institute, 2006b)

In another related study, Yazıcı et al. (2007) investigated the effect of steel fibres on the flexural strength of the hardened steel fibre reinforced concrete exploring the influence of fibre geometry, the aspect ratio (l/d) and the volume fraction of steel fibres in concrete. Hooked end steel fibres with three different aspect ratios of 45, 60 and 80 and three volume fractions of 0.5%, 1%, and 1.5% by volume of concrete were employed. The researchers found that the flexural strengths of steel fibre reinforced concrete are higher by about 3 to 81% than the control mixture. Also, when the results of flexural strengths were compared with those of split tensile and compressive strengths in the same study, it was observed that flexural strength results were higher which is in agreement to the report of American Concrete Institute (2002). Moreover, it was observed that the increase in the flexural strength of SFRC is significantly pronounced with increasing aspect ratio and volume fraction. Research works carried out by other researchers (Bencardino et al., 2013; Gao et al., 1997; Pająk & Ponikiewski, 2013; Soulioti et al., 2011), all obtained similar pattern of results closely related to results obtained by Yazıcı and Arel (2013). Pająk and Ponikiewski (2013) in their investigation compared the flexural behaviour of normal and self-compacting concretes reinforced with straight and hooked end steel fibres, varying the dosages of steel fibres in concrete matrix. They concluded that both concretes exhibit similar flexural behaviour when steel fibres were added and that the types of steel fibres affects the flexural behaviour of the tested beams, while like the flexural results obtained by almost all the research works considered, the best performances were recorded at higher dosages and higher aspect ratio of steel fibres.

Gao et al. (1997) in their study gave typical flexural load-deflection curves of steel fibre reinforced, high strength, lightweight concrete as presented in Figure 3.5, showing two fibre volume fractions of 1% and 2% and aspect ratios of 70 and 58. The curves as presented in the figure show that the load-deflection curve for steel fibre reinforced,

high-strength, lightweight concrete are similar to the steel fibre reinforced concrete and represent the outcome of most studies on flexural strength of steel fibre reinforced concrete.

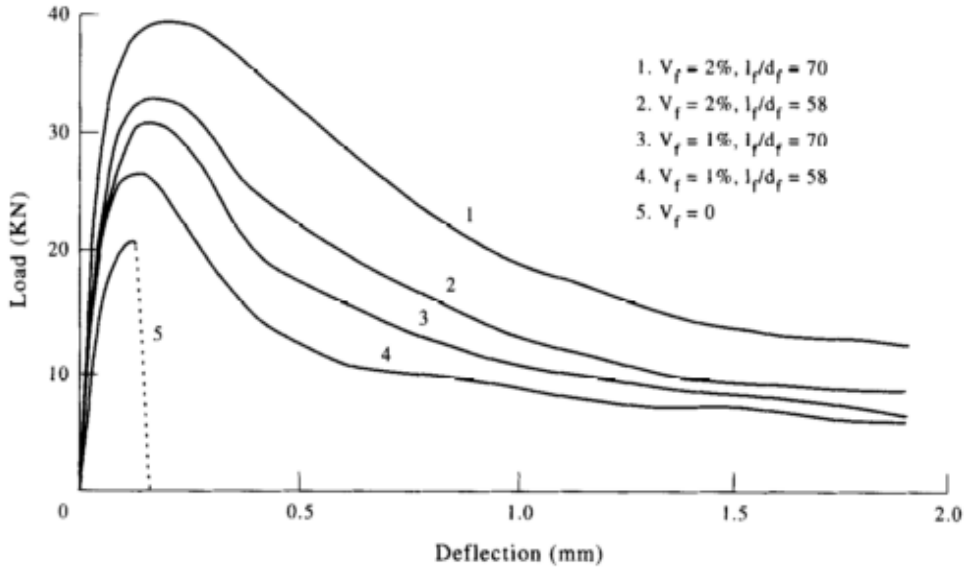

Figure 3.5: Typical load-deflection of SFRC, high-strength, and lightweight concrete (Gao et al., 1997)

American Concrete Institute (2002) also presented a range of load versus deflection curves for plain concrete and fibre reinforced concrete as shown in fig 3.6. The plain unreinforced concrete exhibits brittle nature of failure by which a sudden failure occurs the moment it reaches the first cracking value and this is without any warning signs. On the contrary, SFRC might fail in one of the type 1, 2 or 3 as shown in Figure 3.6 depending on the dosage, length and aspect ratio of the steel fibres in the mixture. The type 1 shows a closely related pattern of failure to the unreinforced matrix which after the first crack can no longer sustain the external load. This is possible when the dosage of steel fibres in concrete matrix is not sufficient or the fibre length are short and difficult to bridge the micro-cracks from developing to macro-cracks. Type 2 exhibits more effectiveness in post-cracking performance than type 1, showing more ductility

and resistance to cracking but unable to sustain increase in applied load after cracking while type 3 shows more strain hardening, resisting and bridging the cracks which enable the sustainability of further increase in applied load even after the initial crack.

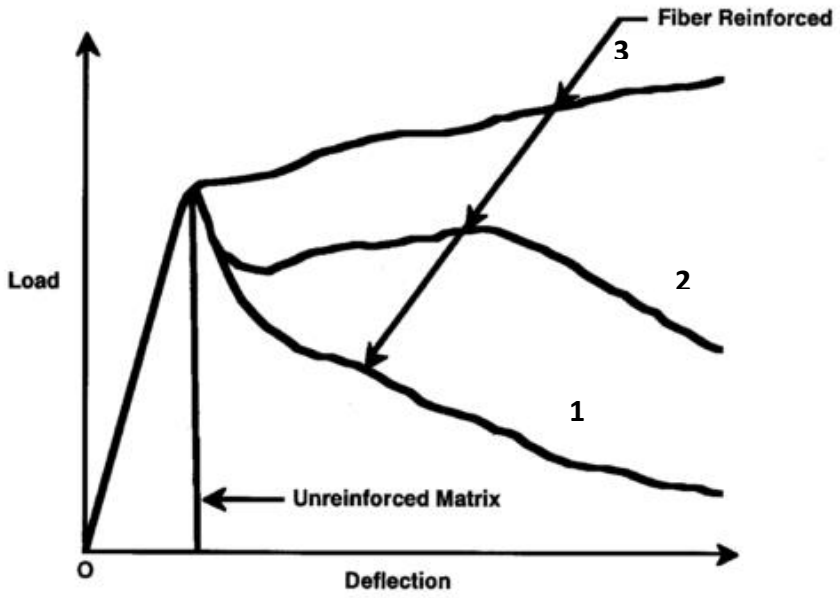

Figure 3.6: Range of flexural behaviour for plain and steel fibre reinforced concrete (American Concrete Institute, 2002)

3.2.3.3 Flexural toughness/energy absorption

According to Portland Cement Association (1991), toughness is defined as the total energy absorbed in breaking a specimen which can be quantified by measuring the area under the load-deflection curve obtained from a flexural test. Increased toughness has been identified as the greatest advantages of using steel fibre reinforced concrete, and that toughness index is the measure of the amount of energy required to deflect the 100 mm beam in the modulus of rupture (flexural) test (Ramakrishnan et al., 1998). Zollo (1997) reported that though, there have been criticism from one or two directions, attempts to quantify the toughness of fibre reinforced concrete using

energy concepts related to the area under a stress/strain diagram have been numerous.

The flexural toughness of the round panel specimens (550 mm in diameter) used for the study by Barnett et al. (2010) was determined by the area under the load-deflection curve up to a deflection of 40 mm. It was found that the flexural toughness of the mixture containing 4% of fibres of 13 mm length was higher but by only 5% than that of 2% fibre mixture whereas there was a significant increase in flexural strength. It was reported that the load carrying capacity of the panels reduced more quickly with increasing deflection for the higher fibre dosage for this little improvement to be obtained. According to Ding et al. (2009), micro fibres are mainly used to reduce the shrinkage cracks while the long ones are needed to retain some degree of structural integrity and post-crack resistance by bridging the crack even with significant deflection, affecting toughness of the matrix. The result of flexural toughness from the study carried out by Barnett et al. (2010) might not be unconnected with the length of steel fibres used which was short fibre used in ultra-high performance fibre reinforced concrete, which is a specialised type of concrete.

In a related study on flexural performance of fibre reinforced concrete by Soutsos et al. (2012), the differences in flexural toughness of concretes made with fibres of different shapes, types, lengths and dosages were quantified. The flexural toughness according to the researchers is the term used to quantify the energy absorbing capability of concrete and is dependent on the dimensions of the specimen since these will influence the total flexural load it can carry. The findings of the study showed clearly that there was a substantial increase in flexural toughness of concrete when fibres were added to the concrete matrix. It was however found that there was a significant difference in the flexural toughness of specimens with equal dosage but of different fibres and lengths, while the flexural toughness of mixture containing hooked end steel fibres of 60 mm length had the highest value of 80 J, the mixture with wavy profile fibre and shorter length of 50 mm gave the lowest value of 45 J resulting in existence of flexural toughness differences of 35 J.

In another research conducted by Taylor et al. (1997) on strength and toughness measurements on steel fibre reinforced normal and high strength concrete, toughness evaluation was carried out using notched beams that were loaded centrally and the mid span crack mouth opening displacement (CMOD) was measured and used in a closed loop testing mode to achieve complete load/displacement curves. In this investigation, toughness measurements were determined using the load-CMOD as can also be found in British Standards Institute (2005) rather than the load-deflection curves, though the toughness indices did not extend sufficiently far to capture the enhanced toughness due to fibre reinforcement.

Toughness of steel fibre reinforced concrete has been described as the characteristic that most clearly distinguishes it from concrete without steel fibres and the preferred technique for determining toughness of SFRC is by flexural loading, (American Concrete Institute, 2002). The report further stated the different methods to specify and test the toughness levels appropriate to different application through flexural toughness indices, as prescribed by some standards such as JSCE SF-4 and ASTM C1018, the schematic illustration of the method and calculations shown in figure 3.6 as presented in the report is according to ASTM C1018 method.

3.2.3.3.1 Testing of flexural toughness properties of specimens

Balendran et al. (2002) reporting on the same ASTM C1018 method stated that the flexural toughness indices I_5, I_{10} and I_{20} are calculated as ratios of the area under the load-deflection curve up to 3, 5.5 and 10.5 times the first crack deflection, divided by the area up to the first crack deflection, respectively as shown in figure 3.7. The report further stated that for an elastic brittle material, all indices should be 1, but for an elastic-ideal plastic material, I_5, I_{10} and I_{20} should equal to 5, 10 and 20 respectively, and however concluded that flexural toughness indices become smaller when the specimen size increases, making fibre effectiveness on toughness decreases for large specimen for steel fibre reinforced normal weight concrete.

The term toughness is often referred to as energy absorption, or sometimes as fracture energy. British Standards Institute (2006a) for instance recommends the procedures for determining energy absorption capacity of fibre reinforced slab which is reported as the area under the load-deflection curve between 0 and 25 mm deflection.

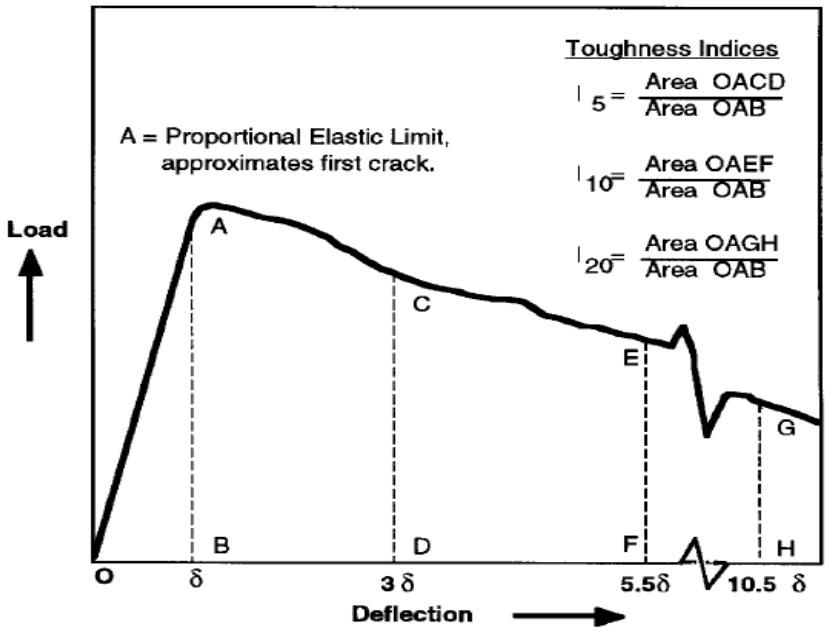

Figure 3.7: Flexural toughness parameters according to ASTM C1018

(American Concrete Institute, 2002)

3.2.3.4 Residual flexural strength

Steel fibre reinforced concrete has been described as a composite material that is characterised by an enhanced post-cracking residual strength due to the reinforcing mechanism of fibres in bridging the crack surfaces, and since the reinforcing mechanism are mainly activated after cracking of the concrete matrix, there is need for residual post-cracking flexural strength, which represents an important design parameter for fibre reinforced structures (Di Prisco et al., 2009). In addition, The Concrete Society (2007) reported that residual flexural strength of steel fibre reinforced concrete after cracking depends on the fibre type and dosage, while stating that it can be determined experimentally since it cannot be calculated reliably in terms of the properties of the plain concrete matrix and the steel fibres. Furthermore, it was

stated that standard test methods that are available for the determination of residual strength in bending, and tension and its toughness while standard flexural test procedures have been proposed by some international organisations including RILEM, the Japanese Concrete Institute (JCI), ASTM and the European Federation of Producers and Applicators of Specialist Products for Structures (EFNARC).

3.2.3.4.1 Testing of residual strength properties of specimens

RILEM beam test method has now been covered by BS EN 14651: 2005, British Standards Institute (2005) which recommends a method of measuring the flexural tensile strength (limit of proportionality, residual) for steel fibre reinforced concrete. The standard specifies the size of the notched beam specimens as width and depth of 150 mm and a length, L between 550 mm and 700 mm while the steel fibres intended for the experiment must not be longer than 60 mm. The flexural residual strength is then calculated from the relationship between the applied load and crack mouth opening displacement (CMOD), and the LOP is defined as highest load (F_L) up to CMOD of 0.05 mm as illustrated in figure 3.8. According to the standard, British Standards Institute (2005), residual tensile strength f_{Rj} is given by the expression:

$$f_{Rj} = \frac{3F_j l}{2\mathrm{b}h_{sp}^2} \qquad 3.1$$

where

f_{Rj} is the residual tensile strength corresponding with CMOD = $CMOD_j$ (j = 1,2,3,4).

F_j is the load corresponding with CMOD = $CMOD_j$ as in figure 3.8.

l is the span

b is the width if the specimen

h_{sp} is depth of the beam above the notch = 125 mm

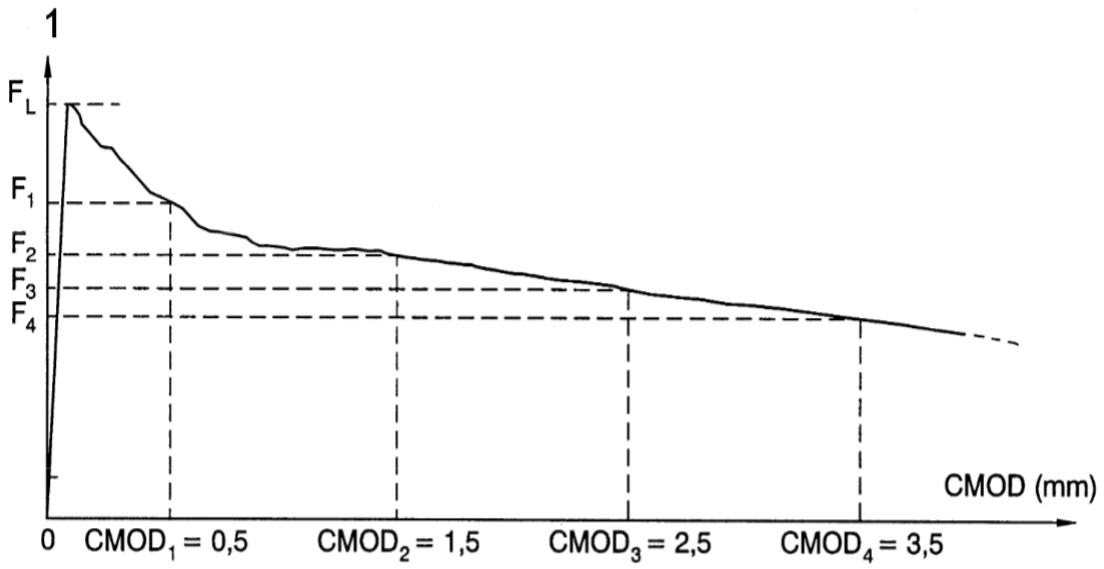

Figure 3.8: Load-CMOD graph for SFRC

(British Standards Institute, 2005)

Gopalaratnam and Gettu (1995) in a study conducted on the characterization of flexural toughness in fibre reinforced concretes reported that in addition to energy based dimensionless indices of flexural toughness, the dimensionless residual strength indices; $R_{5,10}$ and $R_{10,20}$ are also required which are computed as $20(I_{10} - I_5)$ and $10(I_{20} - I_{10})$, respectively, stating that residual strength indices are intended to represent the average strength retained between 3 δ and 5.5 δ, and between 5.5 δ and 10.5 δ respectively, relative to the first crack strength. Meanwhile, (Barros et al., 2005) in another study on post-cracking behaviour of steel fibre reinforced concrete, compared the concept of residual flexural tensile strength with another flexural parameter recommended by RILEM TC162-TDF referred to as equivalent flexural tensile strength which corresponds to flexural toughness factor originally proposed by Japanese Society of Civil Engineers (JSCE). The study made use of hooked end steel fibres of 60 mm length, varying aspect ratios of 65 and 80, and different steel fibre dosages in concrete matrix while the post-cracking behaviour was assessed by carrying out three-point notched beam test. From the findings of the study, it was reported that a strong correlation between equivalent and residual flexural tensile strength parameters occurred in the series reinforced with the two utilised types of fibres, values of both

strengths are higher for the specimens reinforced with fibres of aspect ratio 80 than that of aspect ratio 65 and that both equivalent and residual flexural tensile strength parameters increased with dosages.

3.3 Different effects of steel fibres on concrete

Short discrete steel fibres are introduced into the concrete matrix in order to prevent or control the initiation and propagation of cracks both at initial stage of production of concrete or at hardened state which substantially improves many of engineering properties of concrete. However, there are different degrees by which the improved structural integrity of steel fibre reinforced concrete is achieved. The parameters and the scale of extent by which the composite is influenced have been investigated by previous studies.

3.3.1 Properties of steel fibres

Different types of steel fibres have been looked at in the previous chapter arriving at hooked end steel fibres as the type of steel fibre favoured by many of the studies considered as giving the best post-cracking strength. However, there are other properties that have been found to affect the resulting fibre reinforced concrete. American Concrete Institute (2002) and The Concrete Society (2007) have both reported that the important reinforcing properties of steel fibres considered to have strongest influence on the performance of a steel fibre in concrete are the fibre strength, stiffness, bond and anchorage mechanisms which is the ability of the fibres to bond with the concrete. It was further stated that steel fibres have a relatively high strength and elastic modulus and are protected from corrosion by the alkaline environment of the cementitious matrix.

Naaman (2003) in a study investigating the steel fibres with optimal properties for reinforcement of cement composites stated that apart from classification of fibres according to material such as natural organic or man-made and physical/chemical

properties such as density or chemical stability, there is a classification according to the mechanical properties of steel fibres such as tensile strength, stiffness, ductility etc. Furthermore, it was also suggested from both analysis and experimental test results that, since steel fibre as a reinforcement are supposed to induce an increase in strength to the matrix, steel fibres must possess some properties as shown in figure 3.9 which include tensile strength, bond strength and elastic modulus outstandingly higher than that of concrete.

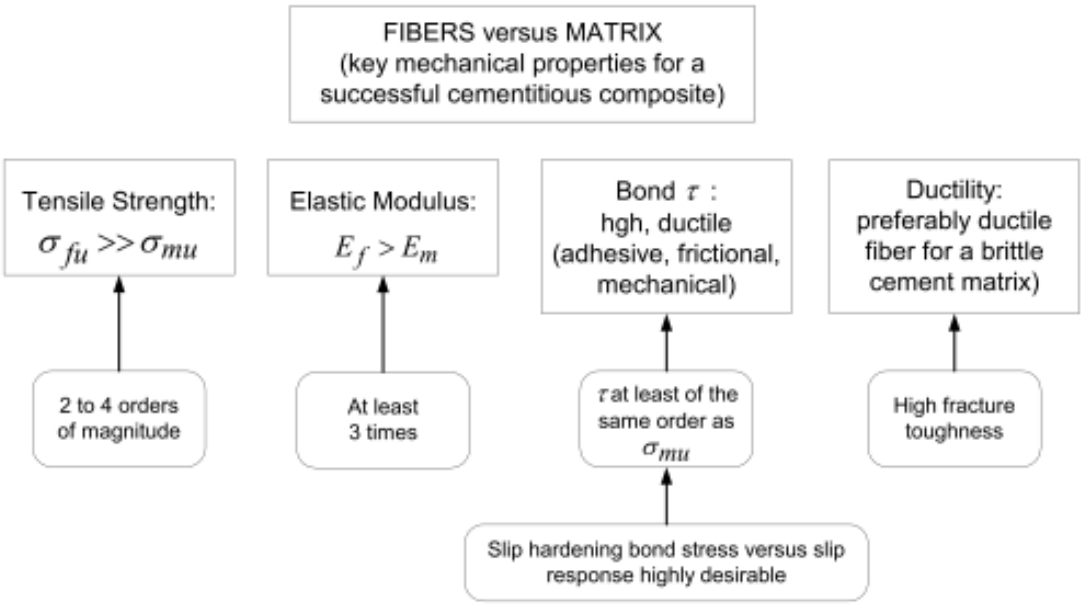

Figure 3.9: Desirable properties of fibre against concrete matrix

(Naaman, 2003)

3.3.2 Dosage of steel fibres in concrete

The effects of dosage of fibres (otherwise referred to as fibre content) in the concrete matrix on the mechanical properties of steel fibre reinforced concrete have been conducted by many researchers because of the outstanding influence on the transformation of the resulting composite from brittle to ductile material. Eddy (2012) has reported that high dosage of steel fibres distributed in right order into fresh concrete will control and re-distribute the stresses that occur during the shrinkage of

concrete and bridge the cracks that appear in hardened concrete thereby providing a degree of post-cracking load transfer which also helps to prevent micro–cracks from developing into macro cracks, which means, with fibre dosage rates of between 30 and 50kg/m^3, steel fibre reinforced concrete typically shows partial ductile behaviour.

Investigation on the effect of volume fraction of steel fibres on the mechanical properties of high performance alkali-activated slag/silica fume mortars has been carried out where four different volume fractions of 0.5 %, 1.0 %, 1.5 % and 2.0 % and two different lengths of steel fibres, 6 mm and 13 mm were employed while a plain concrete was used as a control mixture. It was found that the mechanical performance, especially in terms of flexural strength and toughness of mixture with steel fibres were significantly better than that of the control mixture without steel fibres. Also, the test results of the findings showed a drastic improvement of the mechanical performance at higher fibre dosages with longer fibre resulting in better performance which was also pronounced at higher fibre dosages. Figure 3.10 shows a typical result from the study, of load-displacement curves with a particular steel fibre and different dosages in concrete mixture, (Aydın & Baradan, 2013).

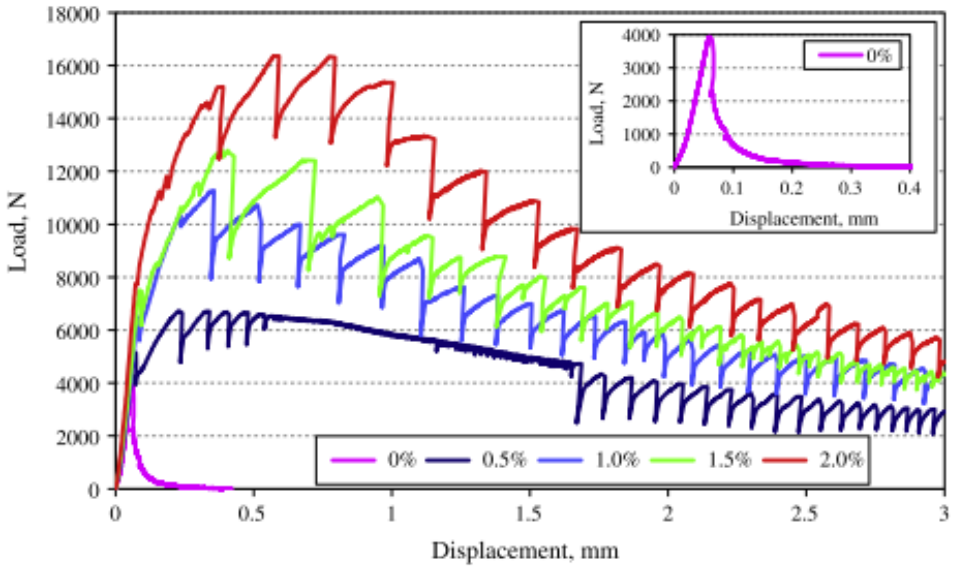

Figure 3.10: Load-displacement curves of concrete mixture of different fibre dosages (Aydın & Baradan, 2013)

Meanwhile, results from previous studies have also shown reduction in workability of the fresh concrete with increase in steel fibre dosages in concrete matrix, however, all the studies concluded that increase in the volume fraction of the fibres in the concrete mixture increased the post-cracking strength, and specifically, it increased the first-peak strength, the peak strength, the residual strength, and especially, the flexural toughness of the composite material, (Michels et al., 2013; Soulioti et al., 2011; Yazıcı et al., 2007). All other research works considered on steel fibre dosage in concrete concluded in agreement with the findings of Aydın and Baradan (2013) on the importance of fibre dosage in ductility behaviour of steel fibre reinforced concrete and how the effects of any other parameters became well pronounced at higher dosages of steel fibres in concrete, (Alani et al., 2013; Kazemi & Lubell, 2012; Yazıcı & Arel, 2013).

3.3.3 Geometry of steel fibres

Geometry of steel fibres relates to the shape, length, surfaces and the diameter of the fibre. Usually, when referring to a particular type of steel fibre, shape and surfaces are already defined and the geometry can be referred to as fibre dimension which specifically relates to its length and diameter, and hence the fibre aspect ratio. Aspect ratio as defined in the previous chapter is the ratio of the length to diameter of a fibre. In general, the most common steel fibre length is said to vary from 12.7 mm to 63.5 mm and the diameters are in range of 0.45 mm to 1. O mm, (Soulioti et al., 2011). Figure 3.11 shows a typical hooked end steel fibre that is glued for easy dispersion during mixing.

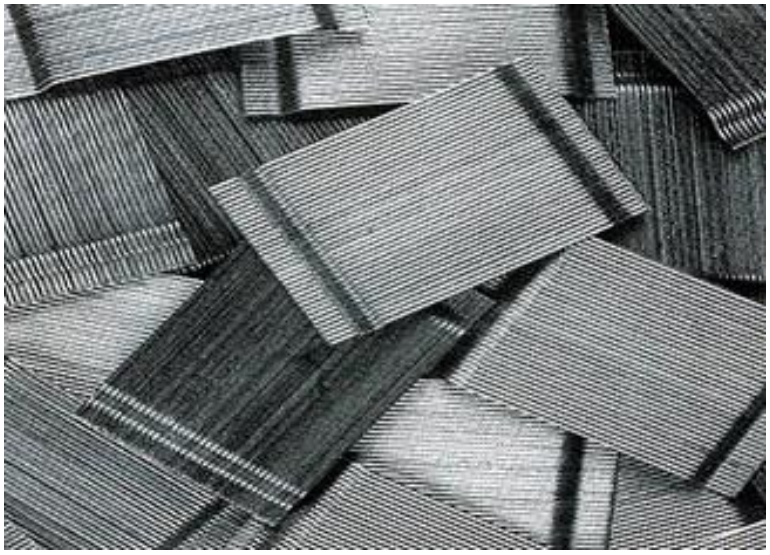

Figure 3.11: Typical glued high strength hooked end steel fibres

The aspect ratio of steel fibre has been identified as one of the key factors that influence the mechanical properties of steel fibre reinforced concrete, Portland Cement Association (1991) reported that bond between matrix and fibre increases as the length of the fibre increases, hence, the longer the fibre the stronger the strength of the composite which makes it desirable to have a fibre length sufficient to induce enough stress in the fibre for a tensile failure to occur. However, this is usually difficult to attain since fibres with aspect ratios greater than 100 are not workable and not able to disperse freely resulting in balling effects.

Other studies have investigated the effects of length and often, the aspect ratio of steel fibres on the resulting composite materials and have concluded that the fibres with high aspect ratio decreased the workability of concrete mixtures while split tensile strength of the test specimen increases with the increasing aspect ratio and flexural strength of SFRC was significantly improved with increasing l/d ratio as well, longer fibres showing a better results where the same fibre type (hooked end steel fibres) and dosage but different aspect ratio were employed, (Sable & Rathi, 2012; Yazıcı et al., 2007). Meanwhile, Vallarasu Manoharan and Anandan (2014) investigating steel fibre reinforcing characteristics on concrete has observed that longer fibres have tendency

to get aligned along the direction of the beam axis thereby affecting the orientation of fibres in the concrete matrix.

3.4 Orientation and distribution of steel fibres in concrete

Orientation and distribution of steel fibres within the concrete matrix is critical for the best performance of the composite material and therefore, the understanding and good knowledge of the positioning of steel fibres in concrete and how it affects the mechanical properties of the concrete will greatly help in the development of structural design procedures that will fully promote steel fibre reinforced concrete as a material that exhibits its strength after concrete cracks. Therefore, to optimize the maximum contribution of steel fibres for controlling crack width, it is important to evaluate the distribution and orientation of the fibres with respect to the crack plain, because fibres are more effective when aligned mainly in the direction of the principal stresses, (Abrishambaf et al., 2014). Figure 3.12 illustrates the right alignment of fibre in concrete matrix at right angle to the crack formation, in which fibres are able to bridge the cracks as they form, whereas, the fibres become less effective when in parallel position to the direction of crack propagation.

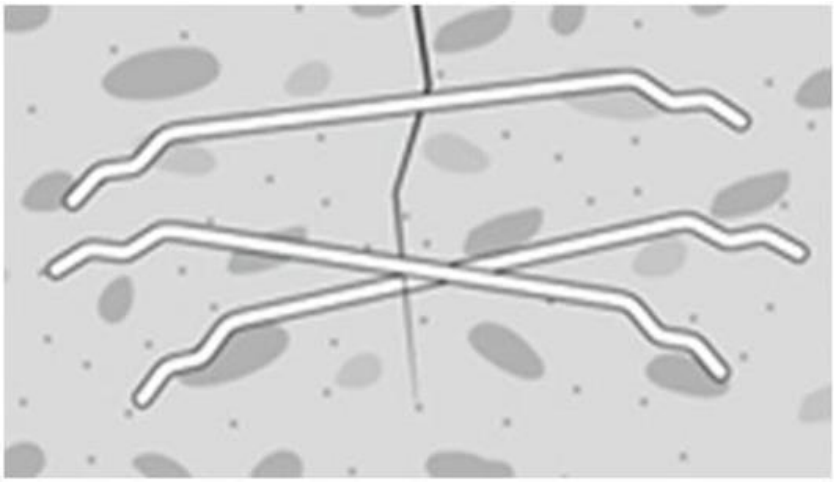

Figure 3.12: Fibre alignment in concrete matrix

In a study conducted by Barnett et al. (2010), steel fibre of 13 mm length and dosages of 2% and 4% by volume, thickness of panel of 25 mm and 50 mm and three patterns of panel casting, from centre, randomly and from edge were employed as variables. The researchers investigated the effect of fibre distribution and orientation on flexural strength of ultra-high performance fibre reinforced concrete using electrical resistivity measurement and confirmed by X-ray computed tomography imaging. In the study, how pouring specimens in different ways could influence the orientation and hence the flexural strength of the panels used for the experiments was determined. It was reported that panels poured from the centre were found to have the highest strength since fibres tend to align perpendicular to the flow of the concrete. The study also affirmed that fibre orientation has a significant effect on the flexural strength and other mechanical properties of UHPFRC in particular and fibre reinforced concrete in general, suggesting that fibre orientation and distribution should be considered during structural design of steel fibre concrete materials.

In another study conducted by Wang and Wang (2013), the static and dynamic mechanical properties of steel fibre reinforced lightweight aggregate concrete were examined. It was reported that the toughening mechanism of fibres in the concrete, especially on the impact resistance, comes mainly from large amount of energy absorbed in de-bonding, stretching and pulling out of steel fibres, and as such occurs and acts after the cracks emerge in concrete. Furthermore, it was reported that when concrete cracks, the randomly oriented fibres arrest a micro cracking mechanism and limit crack propagation, the direct advantage of which is to improve the strength and ductility of the concrete.

Michels et al. (2013) in a related study, investigated post-cracking behaviour of steel fibre reinforced concrete (SFRC) and reported that crucial impact factors are the fibres' dispersion in the cement matrix and orientation in direction of the applied stress. The study further stated that the numerical dispersion of the fibres through the concrete volume and the fibre alignment in the matrix are both governed by several influence factors during production, such as concrete consistency at fresh state, formwork dimensions, casting direction, compacting technique and concrete composition. Also,

stated as part of the findings of the study was the fact that a perfect fibre alignment in stress direction offers the highest fibre efficiency resulting in higher post-cracking strength than for a random orientation. These results corroborated earlier research findings of Barnett et al. (2010).

3.4.1 Workability, fibre distribution and post-cracking behaviour of SFRC

The relationships between workability or the performance of steel fibre reinforced concrete at fresh state and the distribution of steel fibres in the hardened concrete with the effects on the mechanical properties, especially, post-cracking behaviour of the composite material have been investigated. In a study where the correlation between fibre distribution, workability and mechanical properties of steel fibre reinforced concrete were analysed, Ferrara and Meda (2006) aimed to optimise the fresh and hardened state properties of steel fibre reinforced concrete to assess the reliability in a series production of precast SFRC roof elements, recognising that a homogeneous distribution of randomly oriented fibres is a crucial point in guaranteeing a suitable structural performance. The researchers employed steel fibres of length 30 mm and aspect ratio 45 at 30 kg/m^3, 50 kg/m^3 and 70 kg/m^3 dosages with slabs of different thickness as test specimens while concrete mix design without the effects of vibration (a self-compacting concrete), the main cause of fibre segregation was compared with vibration-compacted steel fibre reinforced concrete in the investigation. X-ray analysis was also carried out on the cores from the test specimens. It was found that usage of viscosity enhancing admixture was effective in producing a rheologically stable fresh concrete resulting in homogeneity of fibre distribution along the casting direction. In addition, when the mechanical properties of the two materials were compared, it was observed that despite a lower compressive strength, the concrete mix designed that needed no vibration, self-compacting steel fibre reinforced concrete has almost the same first cracking strength as SFRC and a better performance in toughness properties due to better bond between fibre and concrete matrix and

more uniform distribution of fibres within the concrete because the concrete mass was less influenced by casting processes of vibration leading to fibre-concrete segregation.

In another related study, Abrishambaf et al. (2013) investigated the experimental connectivity of distribution and orientation of fibres (noted to be affected by flowability of concrete) to the post-cracking behaviour of steel fibre reinforced self-compacting concrete of hooked-end steel fibres (length of 33 mm, aspect ratio 60) using panels that were cast from the centre point and cylindrical specimens extracted from the panels. The cylindrical specimens were notched either parallel or perpendicular to the direction of concrete flow and the post-cracking behaviour of the materials assessed by both splitting tensile tests and uniaxial tensile tests while on the other end, high resolution digital camera and ImageJ software used for fibre orientation and distribution detection. The findings of the study showed that the wall effect are negligible since the casting process adopted was from the centre and the flow velocity is uniform and diffuses outwards radially from casting point showing also that fibres have a tendency to orient perpendicular to the concrete flow direction. Furthermore, in the case of orientation and distribution influence on cylindrical specimens, it was reported that in the series with crack plane parallel to the concrete flow direction, there was significant higher post-cracking parameters than the other case with a perpendicular crack plain to concrete flow direction as a result of the earlier case possessing higher number of effective fibre intersecting the parallel crack plain than the later which registered less fibres in the orthogonal crack plain.

3.4.2 Distribution and orientation of fibres and specimen dimensions

The influence of specimens' dimension or the formwork wall on the distribution and orientation of fibres in concrete matrix has been investigated. The wall effects introduced by the formworks has been identified by Pujadas et al. (2014) to influence the way fibres are distributed and orientated within the concrete matrix. In the study to investigate the influence of wall effects of the formwork in the orientation pattern of plastic fibres caused by the geometry of slabs of three different widths with concrete

of same mix proportion required to cast all the specimens. X-ray computed tomography and a post-processing software was used in the analysis of the image data and the effects of different slab dimension was experimentally evaluated using post-cracking results. The results of the study suggest that fibres tend to be oriented parallel to the walls or surfaces of the formwork, though there was also the influence of the flow in fibre orientation in area far from the wall which shows that for free flow, alignment of fibres is usually perpendicular to the flow direction, suggesting that at the wall, there was a slight redistribution by the wall confinement effect as the transverse dimension of the slab is reduced.

Another study on fibre distribution and orientations in concrete engaging electrical resistivity and mechanical tests was carried out by Lataste et al. (2011). In this study, round panels of two different thicknesses, 2.5 cm and 5 cm were employed with different fibre dosages. It was found that though, the fibres tending to align perpendicular to the flow of the fresh concrete (i.e. align perpendicular to the radius of the panel) was confirmed, for all the panels irrespective of the thickness, the average angle between the fibres and the radius of the round panels is lower close to the base of the specimen which suggests that fibres tend to lie more parallel to the radius at the base of the panel. Also from the results, it was observed that tests carried out on the fibre distribution highlight the larger influence of thickness on physical and mechanical properties of concrete compared to the influence of fibre dosage.

3.4.3 Other studies on effect of fibre distribution and orientation

There have been other investigations carried out on various effects of distribution and orientation of fibres in concrete applying different methods of analysis. One of such studies is the investigation carried out on flexural behaviour of ultra-high performance cementitious composites where the effects of fibre distribution and orientation was considered by Kang and Kim (2012). In the study, straight steel fibres of 13 mm length and 0.2 mm diameter were incorporated into concrete placed either parallel to the longitudinal direction of the beam specimen or transversely to the longitudinal

direction of the specimen measuring 100 mm by 100 mm by 400 mm while a three-point bending test, finite element analyses and image analysis process were performed. Results show that there is no noticeable difference in first cracking load between the two placing direction cases, however, significant differences existed for the maximum load with the concrete placed parallel to the longitudinal direction of the specimen having a greater value than that placed transversely to the longitudinal direction of the specimen by about 30%. This result as reported by the researchers is an indication that post-cracking behaviour is considerably sensitive to how concrete is placed which also reflected in the image analysis results showing the concrete placed parallel to the longitudinal direction of the specimen as having more uniformly dispersed fibres, aligning more parallel in the direction of cut plain and having higher number of fibre per unit area as compared to the other transversely placed concrete.

3.5 Aggregate size effects on steel fibre reinforced concrete

The importance of aggregate in any kind of concrete cannot be overemphasized as larger percentage of the volume of concrete is occupied by aggregate, both fine and coarse. Therefore, being a substantial member of the composite, especially the coarse aggregate, its effects need to be considered in investigating steel fibre arrangement within the concrete. From the previous studies, it has been reported that fracture resistance of high-strength concrete decreases and the brittleness increases with age of concrete as a result of increase in the strength of the hardened cement paste and the aggregate-matrix interface which is due to hardening processes (Gettu et al., 1998). It has also been reported by Zhou et al. (1995) investigating fracture properties of high-strength concrete with varying coarse aggregate sizes and types that the compressive strength and fracture energy of the concrete increase as the size of aggregate increases with 20 mm crushed limestone producing higher compressive strength than 10 mm crushed limestone and gravel which is in agreement to another study carried out by Elices and Rocco (2008) that fracture energy seems to increase as aggregate size increases.

In studies of fibre reinforced concrete, aggregate size effect in steel fibre reinforced concrete has been observed to be a factor to consider when considering the post-elastic property changes of the composite material while the behaviour of steel fibre in flowing concrete are affected by their length, shape and their interaction with coarse aggregate particles which might in turn alter their orientation in concrete (Barnett et al., 2010; Soulioti et al., 2011).

Research works on study of size effects of coarse aggregates on steel fibre reinforced concrete have been evaluated to be few. Limited studies that have investigated effects of aggregates on the mechanical performance of steel fibre reinforced concrete have only succeeded in examining different types of aggregates such as natural and lightweight aggregates and steel fibre concrete (Düzgün et al., 2005; Wang & Wang, 2013), while others have investigated the contents of both fine and coarse aggregates in the composition of steel fibre reinforced concrete such as Kim et al. (2012) that researched on the effect of sand:coarse aggregate ratio on bond strength of steel fibre reinforced concrete. Nevertheless, in a study of steel fibre reinforced concrete containing large coarse aggregate, Huang and Zhao (1995) investigated the mechanical properties of using coarse aggregate (crushed limestone) of maximum sizes 20 mm and 40 mm in steel fibre reinforced concrete and with three types of steel fibres of lengths 25 mm, 35 mm and 45 mm. The results of the study concluded that the effect of the aggregate size on compressive strength of the composite is negligible whereas, at the same dosage of steel fibres, tensile strength decreases with the increase in the size of medium crushed stone from 20 mm to 40 mm while a slight reduction was noticed in the same trend in the case of flexural strength.

3.6 Gap in Knowledge and the contribution of this research

It is apparent from the review of literatures in steel fibre reinforced concrete that there is crucial need to shed more light into the internal mechanism of how fibres associate and interact with concrete matrix. This will greatly improve the knowledge and

therefore the design of the composite material for maximum utilization in construction industry.

Notwithstanding, many studies on steel fibre reinforced concrete have presented research results showing relationship between post-cracking strength and fibre volume, type, geometry, and with varying specimen geometry and binder formulation. Most of the research mainly focused on strength development while a good number of research combined steel fibres and other variables like binder formulation and different concrete mix design which made the conclusions a bit lumped together which affects the clarity of the outcome. Though, the benefits of fibre reinforced concrete are well known, however, there must be improvement through which a clearer investigation to identify specific factors that will be responsible for full exploitation of the mechanisms of fibre reinforced concrete in practice. This research work will fill this gap.

Also, the experimental results on monitoring of distribution and orientation of steel fibres in steel fibre reinforced concrete and the effects on maximum output of the resulting concrete are considered few. There is a need for this monitoring especially on relationship between the internal arrangement and positioning of steel fibres and the strength and ductility of the composite material. In achieving this feat, a better understanding leading to full utilisation of the potential of SFRC in practice will be realistic.

This research will therefore address all the above-mentioned gap in knowledge. The clear identification of main factors responsible for how internal arrangement of steel fibres within concrete matrix are formed through fibre-matrix interaction leading to optimum post-cracking strength will be studied. These shall be accomplished by both mechanical experiment and exploring X-ray CT with a software application and hence, investigation of correlation between these two resulting in clear conclusions.

CHAPTER 4

RESEARCH METHODOLOGY; MATERIALS AND EXPERIMENTAL TECHNIQUES

4.1 Introduction

In this chapter, the structure of the research is discussed, the main focus being the concept of the research and how it is designed to achieve the aim and objectives earlier stated. This chapter also describes the variables selected for the research work and materials which make up the constituents of the concrete mixtures, mixing proportion and pattern of mixing, casting and curing procedures of steel fibre reinforced concrete as well as plain concrete. Techniques adopted in testing steel fibre reinforced concrete both at fresh and hardened states ranging from workability test to flexural properties are also described in this chapter.

4.2 Basic concept of the research

Steel fibre reinforced concrete as described in chapter two of this project is becoming more popular in construction industries and in academic community with different ideas that will improve the mechanical behaviour of the material as a construction material coming to play. Although, there have been a lot of improvement on the usage of the composite material when compared to when it all started about 5 decades ago as a result of benefits from research which has made the application of the material more expansive, there is still more understanding needed to maximise the full potential of the mechanism of steel fibres in concrete. Perhaps, with better and full understanding of the material, design codes taking into consideration the post-cracking effects of steel fibre reinforced concrete will be facilitated.

Therefore, the concept of this research is to comprehensively undertake a systematic investigation of steel fibre reinforced concrete, employing the strategy of monitoring the material from the manufacturing stage, at fresh state to the hardened form, studying how the selected constituents and interaction between them affect both mechanical properties and the structural behaviour in response to the internal workings of the material. The outcome of the research is intended to reveal a better 'know-how' that will bring about a greater understanding of steel fibre reinforced concrete by both academic and industry based player for maximum utility of the composite material.

4.3 Research design

The research has been designed in a way to investigate the effects of distribution and orientation of steel fibres within the concrete matrix on the steel fibre reinforced concrete. This was accomplished by employing extensive laboratory experiments and X-Ray Computed Tomography (X Ray CT) technology to study the internal arrangement of steel fibres within the matrix at hardened state. The laboratory experimental results producing the mechanical properties at different stages of test on the composite material were then made to be validated by the results of image analysis of X Ray CT. The study also involved the application of an open source medical image processing C++ libraries, the Insight Toolkit (ITK) used to process the volumetric images acquired from CT scan. Figure 4.1 gives a diagrammatic representation of design of the research.

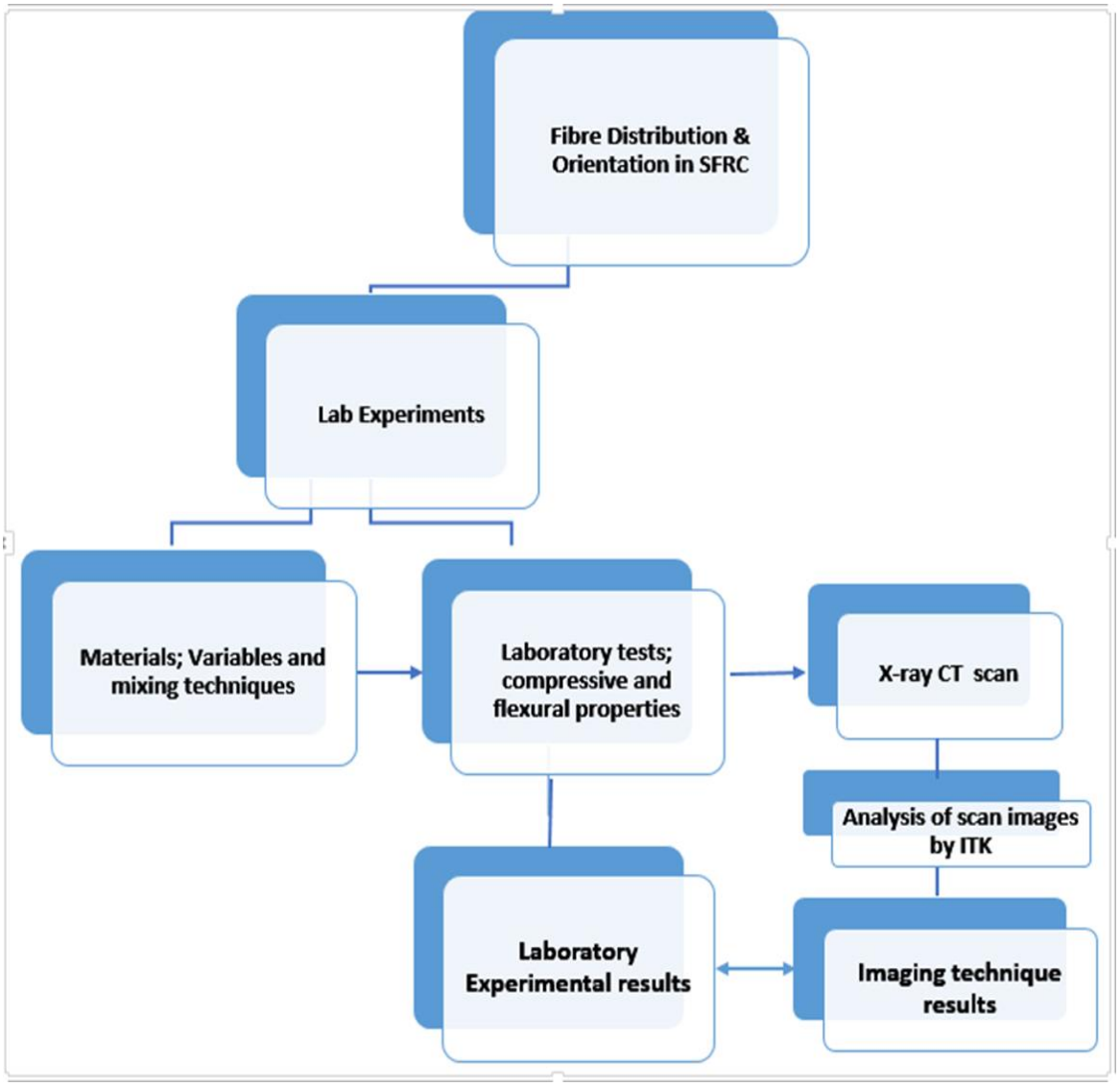

Figure 4.1: Diagrammatic representation of research design

4.3.1 Laboratory experimental investigation

The first set of experimental campaign on the planned investigation commenced in the concrete laboratory (School of Civil Engineering and Surveying, University of Portsmouth). After the preliminary consideration of the constituting materials of SFRC and the subsequent selection of variables for the study, the laboratory experiments were carried out to investigate the influence of the variables on the various properties of concrete, especially the flexural properties. The experimental procedures were

carried out under a control environment so as to produce a good result and as recommended in the Standards and in the literature review.

4.4 Variables for the research

In this research work, the investigation has been centred on the variables identified by the understanding of cementitious material or concrete, and through research articles. The literatures consulted also gave the direction to which the research should follow to get the best outcome that will maximise the mechanism of steel fibre reinforced concrete. General consideration for the selection of the variables were based on the variables that would influence how steel fibres and concrete matrix associate together during mixing, affecting the positioning of steel fibres within the steel fibre reinforced concrete. Care was taken also in the method of controlling and changing the variables to secure a clear, proper and perfect comparison in the outcome of the tests carried out on the experimental samples.

4.4.1 Maximum size of coarse aggregate

Since concrete is a composite, its properties will also depend on the interaction between the components it is made of. Therefore, maximum aggregate sizes were varied in this research to investigate how the coarse aggregate sizes affect the distribution and orientation of steel fibres within the concrete matrix. This was chosen specifically because it is expected that fibres will interact significantly with aggregate particles, especially larger particles. Two maximum sizes of coarse aggregate were selected for the study; 10 mm and 20 mm maximum coarse aggregate sizes. These sizes of coarse aggregate were investigated to see how they affect the mixing pattern and interaction of steel fibres and concrete matrix. The same fine aggregate was used throughout the study.

4.4.2 Length of steel fibres

Another factor that could be responsible for how steel fibres are positioned in the concrete matrix is the length of the fibres. This variable is very important when considering the post-cracking tendency of steel fibre in concrete as well. Two fibre lengths of 50 mm and 60 mm have been considered in this research, investigating the effects of the length in the interaction ability of the steel fibres with other components of the concrete and how this is demonstrated in fibres' distribution and orientation and hence, the result in mechanical properties of steel fibre reinforced concrete. Details of steel fibres employed in this research work are given in Table 4.3 in section 4.5.4.

4.4.3 Aspect ratio of steel fibres

Aspect ratio of steel fibre as earlier defined in previous chapter is the ratio of length to diameter of the steel fibre. It shows how thin/slim or thick a steel fibre is which can also affect the interaction with other components of the concrete. For this study, steel fibres of aspect ratio 45, 65 and 80 were employed for the investigation. The research was also able to study the different aspect ratio but of the same length of a particular set of steel fibre (details in Table 4.3) with length 60 mm and different aspect ratio of 65 and 80 respectively.

4.4.4 Dosage of steel fibre in concrete

Dosage of steel fibres in concrete were investigated in the research work to study how the various quantities of steel fibres in the concrete influence the interaction of steel fibres with the concrete matrix and the effects this would have on the distribution and orientation of the fibres in the matrix and hence, the effect on mechanical properties of the resulting steel fibre reinforced concrete. The dosages selected for this research were 0 kg/m^3, 25 kg/m^3, 40 kg/m^3, 50 kg/m^3 and 60 kg/m^3, where concrete with 0 kg/m^3 dosage of steel fibres represented the control variable, the plain concrete. The dosages were in mass.

4.5 Materials

All materials used in this research were commercially available and used to produce a normal concrete. The materials, the main constituents of the concrete for the investigation were made consistent, maintaining the same source throughout the period of the research.

4.5.1 Cement

Portland cement CEM I, type 52.5R supplied by Lafarge Cement was used throughout this study. The cement also known as Snowcrete white cement, a quality assured cement which complies with all requirements according to EN 197-1 (British Standards Institute, 2011) for Portland Cement as supplied by the technical, compliance and evaluation department of the manufacturer in the Declaration of Performance certificate (Jensen, 2013). The essential characteristics of the declared performance are shown in Table 4.1

White cement is a cement made from especially pure non-iron containing raw materials so as to have the tetracalcium aluminoferrite content ($Ca_4Al_2Fe_2O_{10}$) very low, (Cemex Mortars, 2016). The chemical composition of the cement was determined using XRF analysis method, prepared by pulverising in a Tungsten Carbide TEMA mill after which pellets were made and later analysed using a Rigaku ZSX Primus II x-ray fluorescent spectrometer. The chemical compositions are as presented in Table 4.2. The same cement was used for all the mixes.

Table 4.1: Performance characteristics of CEM I 52.5R

Essential characteristics	Performance	Requirements in EN 197-1
2 day strength	36 – 44 MPa	≥ 30 MPa
28 days strength	66 – 76 MPa	≥ 52.5 MPa
Initial setting time	110 – 160 min	≥ 45 min
Loss on ignition	≤ 2 %	≤ 5.0 %
Insoluble residue	≤ 0.3 %	≤ 5.0 %
Sulphate content SO3	1.8 – 2.3 %	≤ 3.5 %
Chloride	≤ 0.04 %	≤ 0.10 %
Alkali content	≤ 0.3%	None
Water soluble chromate	≤ 2 mg/kg	≤ 2 mg/kg
Y – Reflection, (DIN 5033)	85 – 89.5 %	None
Specific density	3090 – 3190 kg/m3	None

Table 4.2 : Chemical composition of Snowcrete white cement

Oxide	Composition (%)
SiO_2	20.30
CaO	73.70
Al_2O_3	1.89
Fe_2O_3	0.41
MgO	0.45
SO_2	2.49
Alkali ($Na_2O + K_2O$)	0.23

4.5.2 Fine aggregate

The fine aggregate used for the entire research was a natural sand obtained from Travis Perkins Limited, a sea-won aggregate dredged from the English Channel south of the Isle of Wight of flint rock type. The aggregates were oven dried using a ventilated oven controlled at 110°C prior to use and allowed to fully cool down before mixing. The 24 hours water absorption test was carried out on the aggregates which resulted in 2.5 % by mass and the free water was then adjusted accordingly. Unlike the coarse aggregate, sand as the fine aggregate of the concrete mixture was not selected as one of the variables. The particle size analysis of the sand used was determined by dry sieve analysis as recommended by British Standards Institute (1990), the particle size distribution is as shown in Figure 4.2.

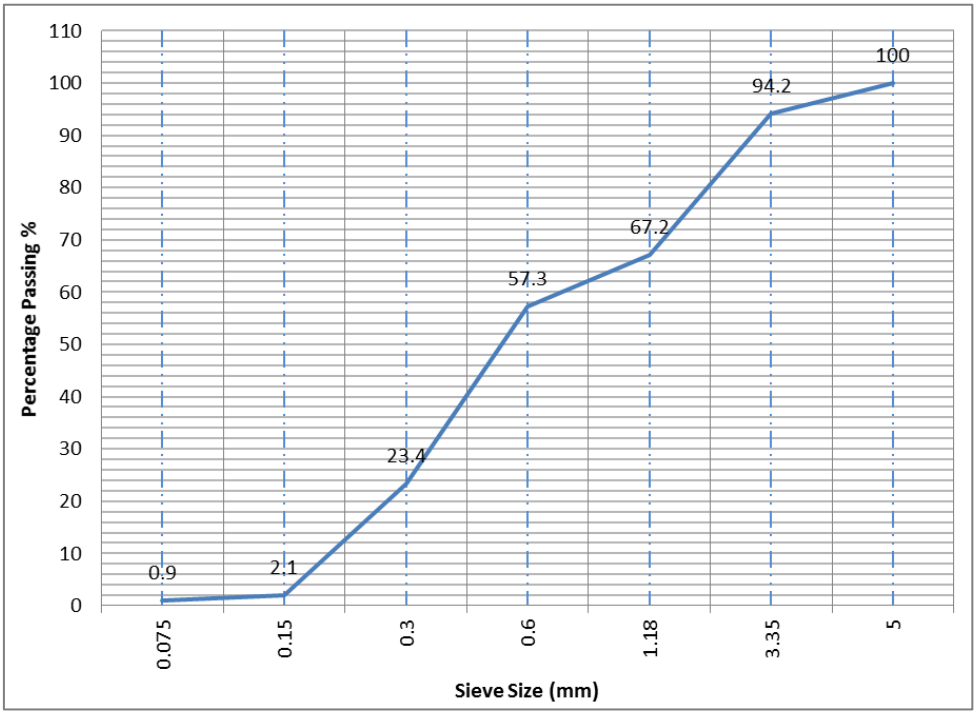

Figure 4.2: Particle size distribution of fine aggregate

4.5.3 Coarse aggregate

The coarse aggregate plays a significant role in influencing the interaction of the components of concrete, hence the selection of the sizes of coarse aggregate as one of the variables being considered in this research project. The coarse aggregate of two sizes, 10 mm and 20 mm maximum aggregate sizes were used. Coarse aggregate which was a natural material, gravel, a local marine rounded and angular flint was supplied by Travis Perkins Limited as well. Figure 4.3 shows the physical view of the two sizes of gravel used for this research project.

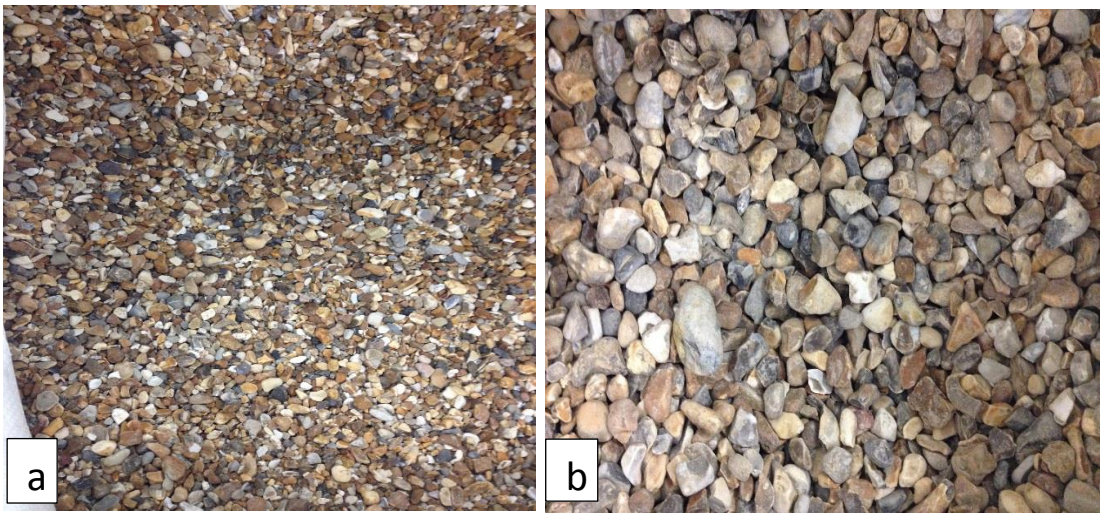

Figure 4.3: Gravel used as coarse aggregate with (a) 10 mm and (b) 20 mm size variables

Particles size distribution of the two sizes of gravel used in concrete mixes, 10 mm and 20 mm are presented in Figure 4.4 (a) and (b) respectively.

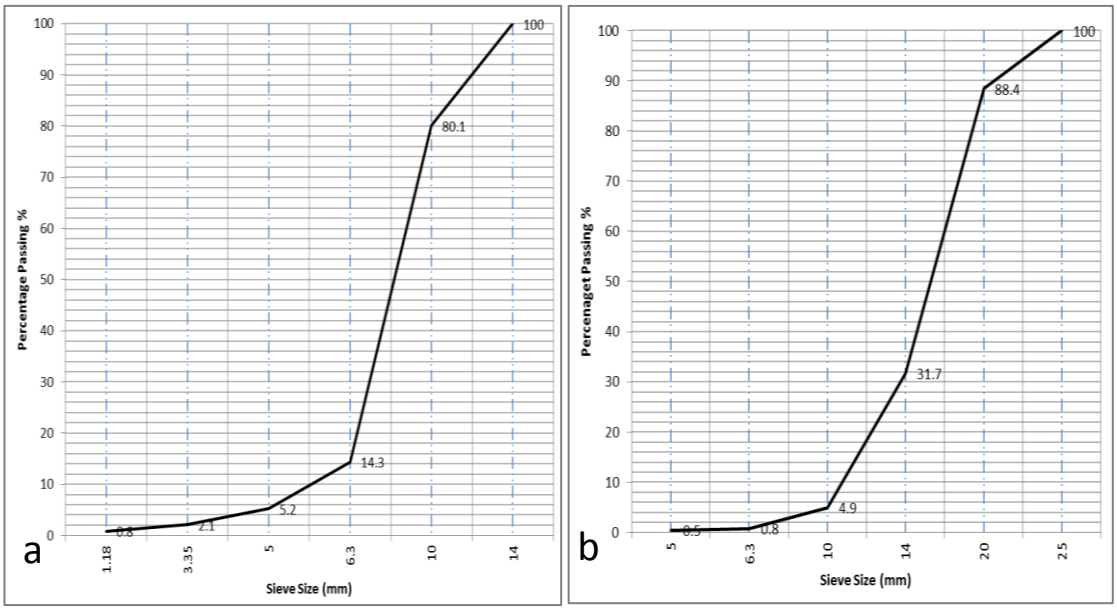

Figure 4.4 Particle size distribution of coarse aggregate of size (a) 10 mm and (b) 20 mm

4.5.4 Steel fibres

The hooked end type of steel fibres were used for all the experiments carried out in this research. The steel fibres branded as Dramix were supplied by Bekaert, a manufacturing company of steel fibre reinforcement while the steel fibres were all of series 3D. The tensile strength of the steel fibres varies from 1115 MPa to 1225 MPa, all the steel fibres were of young's modulus of 210,000 MPa and tolerance of 7.5% average. The steel fibres were either supplied loose or glued for better dispersion. The details of the three types of steel fibres used in this research are as presented in Table 4.3.

Three different steel fibres that were employed in the investigation were of length 50 mm with diameter 1.05, length 60 mm with diameter 0.90 mm, and length 60 mm with diameter 0.75 mm translating to aspect ratio 45, 65 and 80 respectively. The aspect ratio which is the ratio of length to diameter of the steel fibre and the length of the steel fibres can be designated as 45/50, 65/60 and 80/60 making three categories of steel fibres studied as variables in this research project.

Table 4.3: Steel fibre properties

Fibre Series		TYPE I	TYPE II	TYPE III
Material properties	Tensile Strength	1115 MPa	1160 MPa	1225 MPa
	Young's Modulus	±210000 MPa	±210000 MPa	±210000 MPa
Geometry	Hook Shape (3D)			
	Length	50 mm	60 mm	60 mm
	Diameter	1.05 mm	0.90 mm	0.75 mm
	Aspect ratio (l/d)	45	65	80
Fibre network		2802 Fibres/kg	3183 Fibres/kg	4584 Fibres/kg

4.5.5 Water

The water used throughout the research was that which was in compliance with the specification according to BS EN 1008, (British Standards Institute, 2002) which recommends a potable water as a suitable one for use in concrete. Tap water was used for the mixing purposes. Water plays a significant role in the manufacture of concrete as it is responsible for the hydration of cementitious materials to form paste which in turn exhibit how workable a freshly mixed concrete would be and how strong the bond within the aggregate components and fibres form into a whole hardened concrete.

4.5.6 Superplasticiser

A high range water reducing admixture of polycarboxylate polymers which complies with BS EN 934 – 2, (British Standards Institute, 2009a) and supplied by Fosroc Limited, U.K, Fosroc Auracast 200 was used in all the concrete mixes of the research project. The same dosage was used throughout since it was found to give sufficient workability

for good compaction for all other variables. The typical dosage as recommended by the manufacturer for the use in concrete is 0.3 to 1.2 litres/100 kg of cementitious content, though trial mixes with same materials was advised to establish the optimum dosage of Fosroc Auracast 200 in concrete. Table 4.4 gives the properties of the superplasticiser used for the mixes as supplied by Fosroc Limited.

Table 4.4: Properties of Auracast 200 superplasticising admixture

Specification	Properties
Nature	Liquid
Colour	Dark Straw
Specific gravity	1.050 – 1.070
pH	4 +/- 1
Chloride content	< 0.1%
Na_2O equivalent	< 0.5
Freezing point	Sensitive to freezing
Air entrainment	Typically less than 2%

4.6 Concrete production

Concrete was produced with the components that make up concrete for the experimental investigation and because many mixes had to be made with constant and variable materials, it was ensured that the materials used were kept as regular as possible until the end of the experimental work so as to have a uniform basis of mixing. The concrete was mixed for both plain concrete (concrete with normal ingredients without steel fibres) and steel fibre reinforced concrete with same mix proportions and procedure.

4.6.1 Mixing proportions

In consideration of the research aims of this study, and with careful study of previous research works, mix proportions were worked out. Thereafter, there were several trial mixes to see the particular range of material proportion that would give a robust mix that would be uniformly suitable for all the mixes including those with steel fibres. The result was the mix proportion used for all the plain and steel fibre reinforced concretes engaged in this research work as shown in Table 4.5. The same mix proportion was used throughout the study to allow for uniformity and proper comparison. The water/cement ratio used for this study was 0.5. Each mix as shown in Table 4.5 was repeatedly varied between the variables selected for the research, while three replicates were made for each experimental specimen from each mixture.

Table 4.5: Mix proportion of both plain and steel fibre reinforced concrete

Mix Title		M Pl	M SF25	M SF40	M SF50	M SF60
Cement, CEM 1	(kg/m^3)	310	310	310	310	310
Sand	(kg/m^3)	786	786	786	786	786
Gravel	(kg/m^3)	1179	1179	1179	1179	1179
Free water	(kg/m^3)	155	155	155	155	155
Superplasticiser	(kg/m^3)	1	1	1	1	1
Steel fibre dosage	(kg/m^3)	0	25	40	50	60
	(% by volume)	0	0.31	0.51	0.64	0.76

From Table 4.5, M Pl represents the plain unreinforced concrete, M SF25, M SF40, M SF50, M SF60 are steel fibre reinforced concrete mixtures of different fibre dosages, 25 kg/m^3 to 60 kg/m^3.

4.6.2 Mix preparation and technique

The materials used in concrete mixes were all prepared before the mixing. The material were weighed using appropriate digital balance to the nearest gram. Mixing of concrete was accomplished using a pan mixer of 0.05 m^3 capacity as shown in Figure 4.5 (a and b) where Figure 4.5b shows mixing in progress and inclusion of steel fibres to the concrete through spaces provided in the cover of the pan mixer.

Figure 4.5: Pan mixer used for concrete mixing with (b) showing mixing in progress

The technique for mixing adopted in this research was a particular procedure for all mixes so as to achieve a uniform dispersion of fibres in the mix and to avoid balling effects. Gravel, sand and cement were placed into the mixer and dry mixed for three minutes, then water was added in the space of one minute immediately followed by superplasticiser and allowed to mix for another three minutes until when the mix was showing appearance of wetness. The fibres were added last and then a further one to two minutes mixing period was allowed to have the material sufficiently mixed. Figure 4.6 is a schematic diagram showing the mixing time sequence of the mixing procedure.

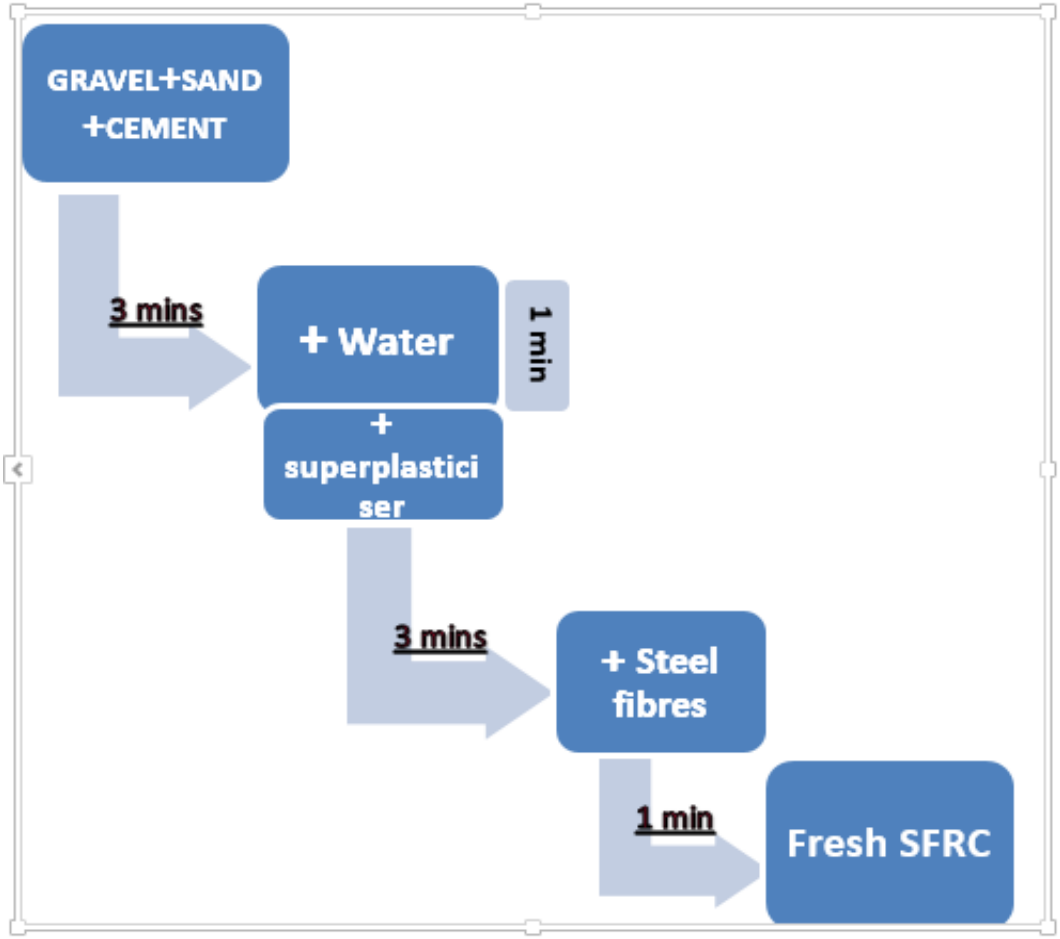

Figure 4.6: Concrete mixing with time sequence

The mixing period for each mix was between nine and ten minutes to ensure the fresh steel fibre reinforced concrete was homogeneous and without balling as shown in Figure 4.7. The control experiments were mixed following the same pattern except without inclusion of steel fibres and the process completed within a shorter time.

Figure 4.7: Homogenous fresh steel fibre reinforced concrete after mixing

4.6.3 Casting and compaction of specimens

The workability of each mix was measured through slump test and findings were recorded. The workability of plain and steel fibre reinforced concretes were assessed using slump test technique. The slump test for the research work was carried out in accordance with BS EN 12350-2, (British Standards Institute, 2009b) with the apparatus as shown in figure 4.8.

Figure 4.8: The slump test apparatus

(directindustry.com, 2016)

The apparatus used were the steel slump cone of base diameter 200 mm, top diameter 100 mm and height of 300 mm placed on a rigid, flat, impermeable plate while the cone was filled with fresh concrete in three layers and each layer compacted by the compacting rod of circular cross-section, straight and made of steel of diameter 16 mm. Each layer was compacted by 25 strokes of the compacting rod. Other apparatus used included scoop for placing the concrete into the slump cone and a ruler graduated from 0 to 300 mm, the zero mark which was at the extreme end of the ruler as stipulated by the standard. The mould was then carefully removed from the concrete by raising it in a vertical direction and leaving the heap of the concrete. Only the true slump of all the concretes was measured.

4.6.3.1 First phase: Casting of cubes and beams

In the first series of experiments, the freshly mixed plain concrete and steel fibre reinforced concrete were cast into 100 mm cubes and beam specimens of 150 mm by 150 mm by 600 mm for each mix of three replicate samples. Figures 4.9 shows the

cubes and beams casting. 100 mm cube specimens were cast to measure the compressive strength while beam specimens were cast to measure the flexural properties.

Figure 4.9: Casting of cube and beam specimens

The casting was done as natural as possible so as not to influence the distribution or orientation of the steel fibres during the casting. In the casting of beam specimens, the procedure for filling the beam mould as recommended in BS EN 14651, British Standards Institute (2005) was strictly followed, as shown in Figure 4.10 where the filling of the mould was in order of size of increment 1 twice that of increment 2.

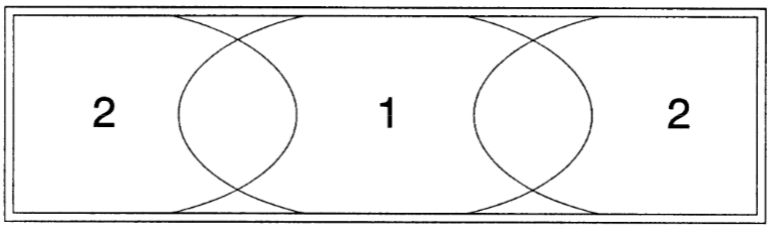

Figure 4.10: Procedure for filling the beam mould

Compaction of beam specimens was accomplished using external vibrating table. The almost filled up moulds were placed on the vibration table and topped up and levelled off while the vibration was on. The compaction was done for a short period of about one minute to avoid segregation of the fibres in the matrix.

4.6.3.2 Curing of cubes and beams

After casting, all samples were removed from their moulds after 24 hours. Curing of the cube and beam specimens was carried out by storing them in a water tank. The water inside the tank was a lime saturated one which was thermostatically controlled at 20±2°C. Figure 4.11 shows the curing tank used for curing all the cube and beam specimens in this research project. The specimens were kept in the curing tank until testing at 28 days.

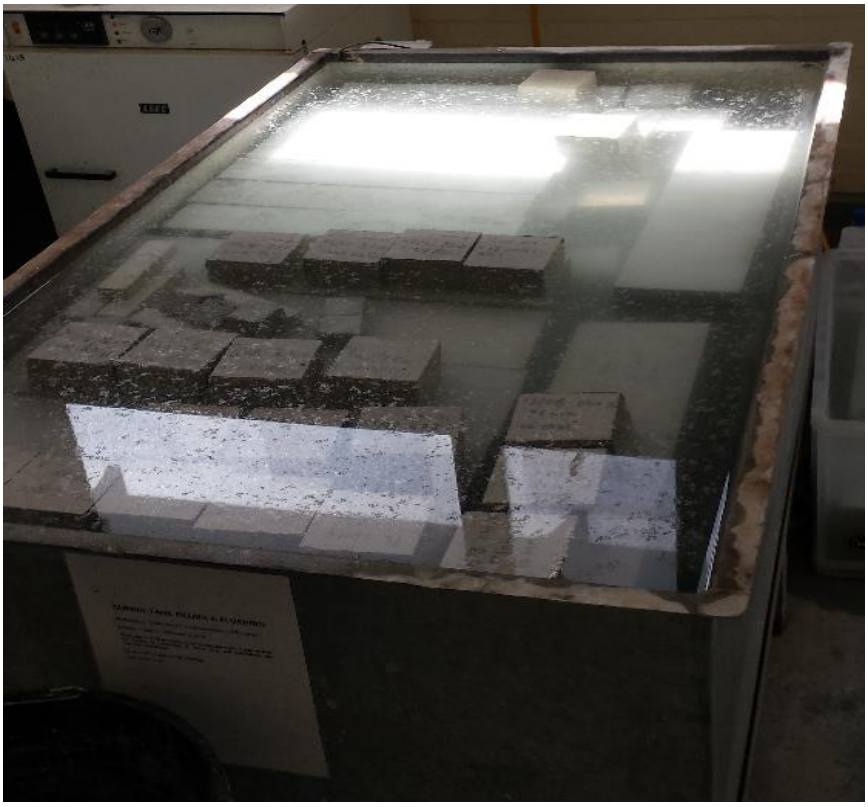

Figure 4.11: Thermostatically controlled curing tank

4.6.3.3 Second phase: Casting of slabs

In a second series of experiments, concrete square slabs of 600 mm by 600 mm by 100 mm were cast, maintaining the same concrete mix proportions and variables apart from the fibre dosages being fixed at 50 kg/m³ for flexural testing. The slab specimens were in three replicates as well. Casting of slab specimen is as shown in Figure 4.12.

Figure 4.12: Casting of slab specimens

4.6.3.4 Curing of slab specimens

Curing of plain concrete and steel fibre reinforced concrete square panels after demoulding at 24 hours was accomplished by covering them with polythene sheet and kept in moist condition through regular spraying with water until testing at 28 days. This method was adopted considering the sizes of the specimens while a suitable moist condition was achieved. Figure 4.13 shows the slab specimens at curing stage.

Figure 4.13: Curing of square panels

4.7 Test set up and procedure

This section gives the details of the methodology followed and the apparatus used in testing both fresh and hardened concrete of the concrete mixes. Both plain concrete and steel fibre reinforced concrete were subjected to the same procedure.

4.7.1 Measurement of workability

The workability check of all the concrete mixes was carried out according to BS EN 12350 Part 2, (British Standards Institute, 2009c). Slump test was carried out on both plain and steel fibre reinforced fresh concretes. The mould used for slump test was as shown in previous section of this chapter in section 4.5.3. The filling of slump mould with steel fibre reinforced concrete was done by scooping the material from the pan mixer randomly and without any pattern so as not to influence the quantity of steel fibres in a particular test. The slump for each mix was determined by recording the difference between the height of the mould and that of the highest point of the slumped test specimen as shown in Figure 4.14.

Figure 4.14: Measuring of workability of SFRC by slump test

4.7.2 Measurement of density

100 mm cube specimens were used to measure the density of each mix of both plain concrete and that of steel fibre reinforced concrete. The determination of density of the specimens was by determining the mass of cube specimen in water and in air

according to BS EN 12390-7 (British Standards Institute, 2009d). The density, (ρ) is given by the equation;

$$\rho = \frac{W_A}{W_A - W_W} x1000 \qquad 4.1$$

Where W_A is the mass in air, g

W_W is the mass in water, g

ρ is the density, kg/m^3

4.7.3 Compressive strength measurement

Compressive strength tests were carried out on 100 mm X 100 mm X 100 mm cubes in accordance with BS EN 12390 Part 3 (British Standards Institute, 2009c). Initially, during casting, the mould's inner surface was first sprayed with a non-reactive oily material before placing concrete so as to make it easier for removing the concrete after 24 hours. The specimens were in three replicates for each mix.

The testing machine employed for carrying out all the compressive strength tests was ADR–Autotest machine with 2000 kN maximum capacity, ELE compression testing machine. The machine which has a digital display attached to it from which the force can be read also has a control system with ability to apply automatic loading on the specimens. A loading rate of 0.3 MPa/s was used for all compressive tests carried out in this research work. Figure 4.15 shows the compression test machine during the test of one of the cubes.

Figure 4.15: The 2000 KN Autotest compression test machine during cube test

4.7.4 Measurement of flexural properties

Flexural tests are mostly considered as the best practical way of classifying the strength and the ductility of steel fibre reinforced concrete. In the phase one of this research work, prism specimens of size 150 mm x 150 mm x 600 mm were used in determining the flexural properties of plain and steel fibre reinforced concretes in the first instance. Thereafter in phase two, was the manufacture of concrete slab of 600 mm x 600 mm x 100 mm for flexural testing. The flexural properties assessed during the investigation included the flexural strength, the flexural toughness/Energy absorption, residual flexural strength and load carrying capacity of the slab. All the test specimens were in triplicates.

The testing machine used was a computer controlled closed-loop servo hydraulic Zwick/Roell Z250 equipment with maximum capacity of 250 kN as shown in Figure 4.16. The machine located in structures laboratory of School of Civil Engineering ans Surveying, University of Portsmouth, has the capacity to load the specimens at a constant deflection rate in closed-loop control.

Figure 4.16: The 250 kN Zwick/Roell machine for measuring flexural properties

4.7.4.1 Beam testing

The beam specimens were tested according to BS EN 14651, British Standards Institute (2005) under the three-point loading as shown in Figure 4.17 with notches introduced in the middle section to a depth of 25 mm by a diamond saw before testing. A crack mouth opening displacement (CMOD) gauge was positioned in the notch to control the test at the CMOD rates specified by the standard. Loading of specimens was at a speed of 0.2 mm/min and with a pre-load of 100 N.

Figure 4.17: Measuring flexural strength under 3–point loading

4.7.4.2 Slab testing

The square concrete slabs were also tested at 28 days as specified by BS EN 14488-5, (British Standards Institute, 2006a). The test was accomplished using the Zwick/Roell 250 KN Universal Testing Machine with a rigid steel square loading block having a contact surface of 100 mm x 100 mm and thickness of 25 mm, which was positioned at the centre of the upper face of the concrete slab. Figure 4.18 is a schematic representation of the test set-up for the square slab showing the support and the loading system.

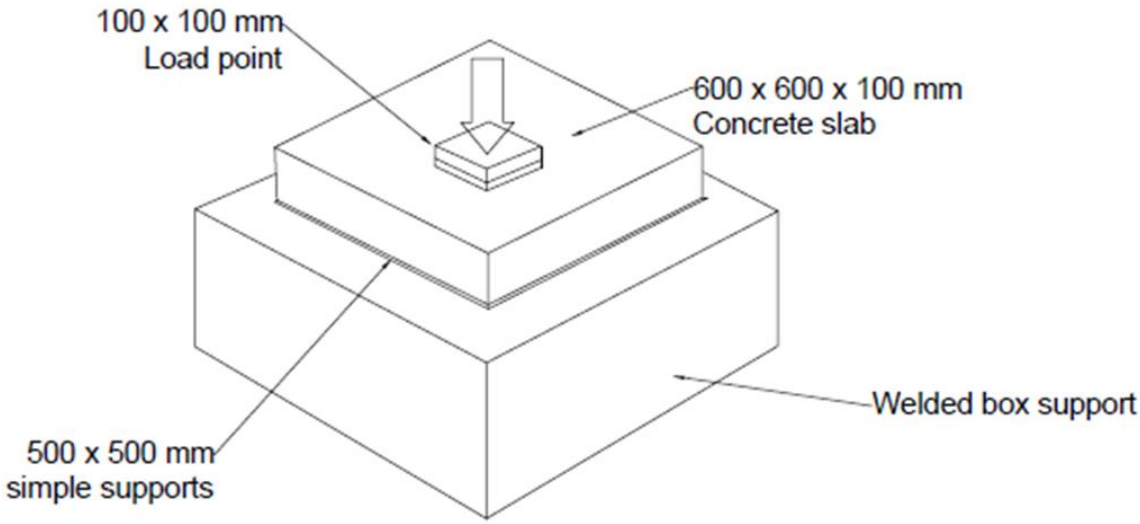

Figure 4.18: Schematic representation of slab testing

The testing machine was a displacement controlled, while a linear variable displacement transducer (LVDT) was positioned beneath the centre of the specimen to record the deflection. Figure 4.19 shows the arrangement of the LVDT and the rigid support before the slab was placed for testing.

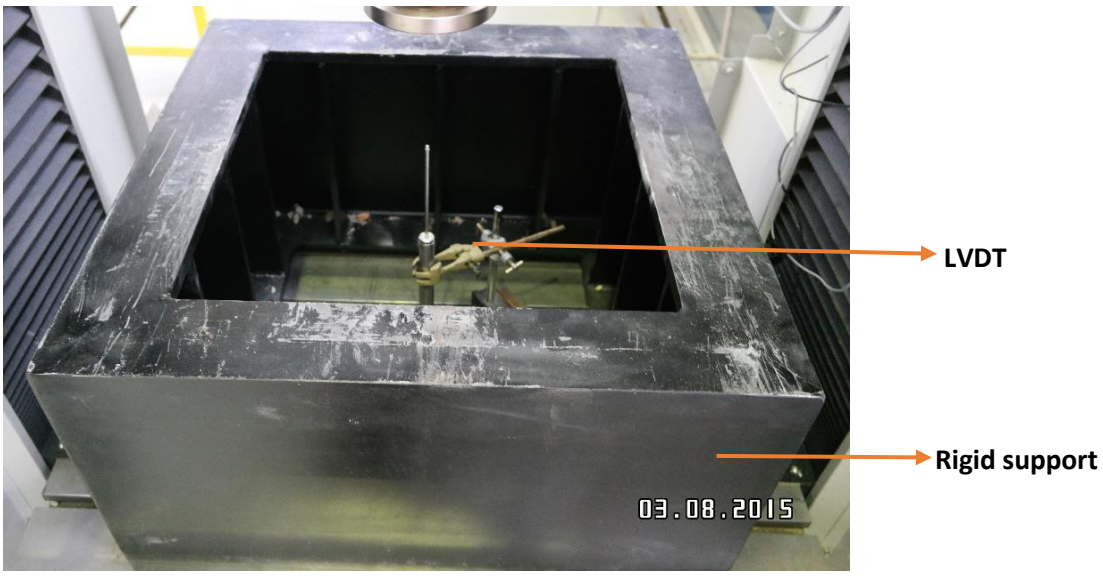

Figure 4.19: Rigid support and LVDT set-up

The loading of the specimen was at a constant rate of 1 mm/min with a pre-load of 500 N. The slab was supported by a rigid square support with internal dimension of 500 mm x 500 mm as shown in Figure 4.20.

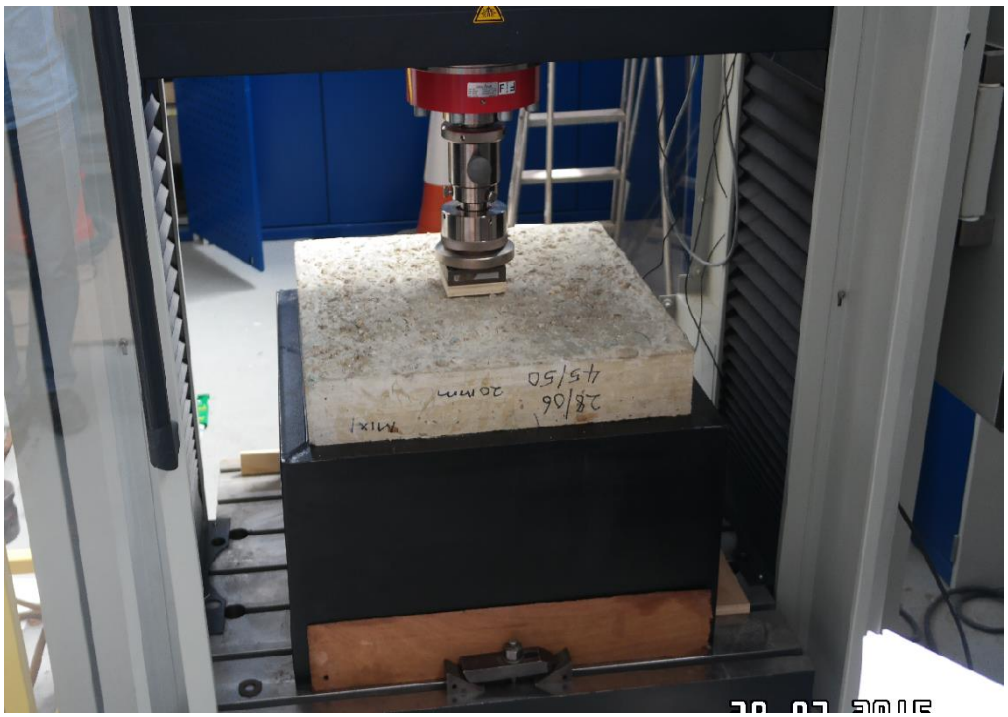

Figure 4.20: Testing of square concrete slab

4.7.4.3 Cores extraction for imaging technique

In order to carry out the detailed investigation of the effects of the chosen variables on fibre distribution and orientation and the subsequent effects on flexural performance of the material, cores were extracted from the panels after 28 days flexural test. Core specimens of 100mm diameter and 100 mm height as shown in Figure 4.21 were subjected to X-ray computed tomography scanning for detailed investigation of distribution and orientation of fibres within hardened SFRC. Two core samples were extracted from each tested SFRC slab.

Figure 4.21: A typical core sample extracted from tested SFRC slab

4.7.4.4 X-ray CT imaging technique

X-ray computed tomography (CT) imaging was carried out on the core samples at University of Nottingham using a 350 kV X-ray source, high energy X-rays that are required to penetrate the high density hardened concrete cores to obtain the high resolution images needed for analysing the positioning of steel fibres within the concrete. In this process, a flat fan-shaped beam was directed at the core sample which was rotated slowly in the beam through 360. The attenuated beam was then captured by a detector consisting of a single line array of over 3000 light sensitive diodes. The rotation and vertical movement of the core sample were made possible by a manipulator on which the concrete core was positioned and after each scan which took around 7 minutes to perform, the manipulator moved the core up or down in order to complete the next scan. Each scan produced an image which corresponded to a 'horizontal slice' through the concrete core while each core of 100 mm produced 90 slices. This process is the same as described by *Barnett et al. (2010)* with a schematic illustration of X-ray imaging technique as described in the journal article shown in Figure 4.22.

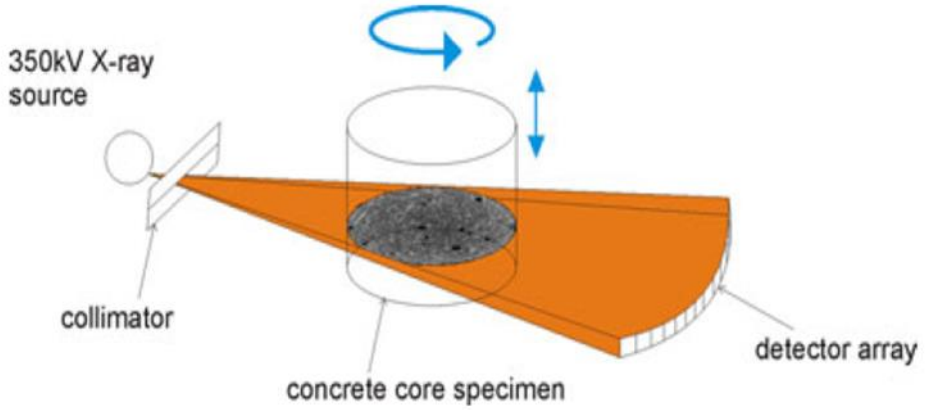

Figure 4.22: Schematic representation of X-ray imaging technique

(Barnett et al., 2010)

CHAPTER 5

EXPERIMENTAL RESULTS AND DISCUSSION

5.1 Introduction

This chapter presents the results of tested specimens of the project, the analysis and the comprehensive discussion of the results. The result presentation, analysis and discussion are divided into four key stages; test on fresh concrete, cube test comprising of density and compressive strengths, flexural properties of plain and steel fibre reinforced concrete beams and the tests carried out on slabs. The main focus of this chapter was on results relating to investigation of the mechanical properties of plain and steel fibre reinforced concretes.

5.2 Test on fresh steel fibre reinforced concrete

Fresh steel fibre concrete and plain concrete were tested after mixing had been accomplished by pan mixer employing the procedure as explained in section 4.6.3 and the actual test in 4.7.1. The main test carried out on the fresh concrete was slump test.

5.2.1 Slump test results

The values of slump tests carried out on fresh plain concrete and steel fibre reinforced concrete with varying fibre dosages, aspect ratio/length and two maximum sizes of coarse aggregate for the workability check are given in Table 5.1. The slump values vary widely between 15 mm and 140 mm. Plain concrete of both aggregate sizes used giving slump values within 60 mm to 120 mm. From the results of the slump, it can be deduced that there was decrease in slump values as dosages of fibres increased in concrete, which was not unconnected with effect of 'fibre balling' noticeable at higher fibre dosages in the concrete.

It can also be seen from the results that mixes with maximum coarse aggregate size of 20 mm generally show higher slump values than mixes with 10 mm maximum aggregate size while the mixes of fibre length of 60 mm and aspect ratio (l/d) 65 and 80 with 10 mm maximum aggregate size gave the least slump values of 15 mm and 18 mm respectively at 60 kg/m³ dosage.

Table 5.1: Slump values of plain concrete and SFRC

Fibre type AR/Length	Fibre dosage kg/m³	Slump, mm	
		10 mm max aggregate size	20 mm max aggregate size
Plain concrete	0	62	120
45/50	25	115	95
	40	53	125
	50	27	88
	60	36	53
65/60	25	55	140
	40	36	70
	50	32	55
	60	15	88
80/60	25	105	115
	40	34	135
	50	32	80
	60	18	65

In general, the inclusion of steel fibres in concrete had a negative effect on the workability of the concrete mixture as checked by the slump test, reducing the workability. The results obtained are in agreement with the results of previous studies on workability of steel fibre reinforced concrete (Sebaibi et al., 2014; Soulioti et al., 2011; Taylor et al., 1997).

5.3 Preliminary test on hardened concrete; cube tests

The cubes that were made from both plain and steel fibre reinforced concrete were tested at 28 day as the initial set of tests on the hardened plain and steel fibre concrete.

5.3.1 Determination of density

The 100 mm cubes were used to check the density of the plain and fibre reinforced concrete by the method described in section 4.7.2 and the average results of three replicate cubes presented in Figure 5.1. The results varied from the average density of plain concrete of 10 mm maximum aggregate size which had the least value of 2377 kg/m^3 to the average density of concrete mixture of 20 mm maximum aggregate size containing steel fibre 45/50 at 50 kg/m^3 fibre dosage with highest value of 2455 kg/m^3. The effects of short period of compaction permitted at casting of concrete to guard against segregation or settlement of steel fibres in the mixture must have been the cause of low density recorded, especially for specimens containing 10 mm maximum aggregate size. The values of theoretical density calculated are in the ranges of 2470 kg/m^3, 2480 kg/m^3, 2490 kg/m^3, and 2500 kg/m^3 for mixtures containing steel fibre dosages of 25 kg/m^3, 40 kg/m^3, 50 kg/m^3 and 60 kg/m^3 respectively. These values are higher when compared to the experimental values which are in the range of 2377 kg/m^3 to 2455 kg/m^3. The decline in the values of experimental densities could have been the result of air content of the mixture.

On the other hand, it was clear from the results that increase in fibre dosage of the mixture actually increased its density. The increase in density as fibre dosage increases in the mixture can be connected to the relatively high specific gravity of steel fibre when compared to other constituents of the concrete. Steel fibre has a specific gravity of about 7.9 compared to that of coarse aggregate ranging between 2.4 and 2.6 and that of cement which is 3.15 (British Standard Institute, 2009b; Neville, 1995; Rana, 2013).

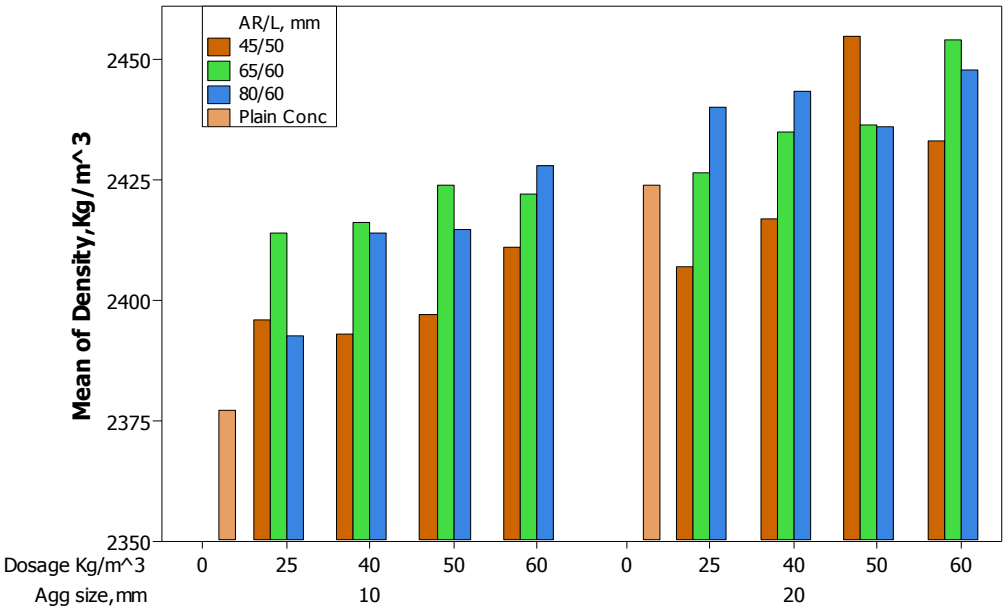

Figure 5.1: Density test results of plain and SFRC

It can also be deduced that mixtures of 20 mm maximum aggregate size have higher values of density than their 10 mm maximum aggregate size counterparts. This was initially noticed from the plain concrete without fibres where there was a difference of 47 kg/m^3 in the density values of 10 mm maximum aggregate size and that of 20 mm maximum aggregate size. The same trend is observed in all the mixtures as higher values of density were recorded for 20 mm maximum aggregate concrete compared to 10 mm maximum aggregate concrete as clearly seen in Figure 5.2 which is a boxplot of summarised values of density as against the dosages of steel fibres and maximum aggregate sizes. The trend of the results in the density of the cubes can be seen also in the workability results where 20 mm maximum aggregate size concrete had higher values of slump in general.

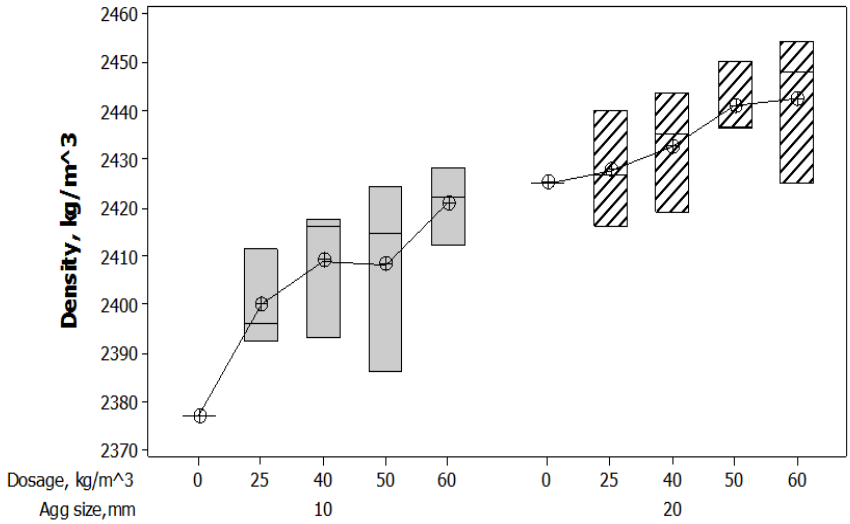

Figure 5.2: Summary values of density vs dosage and aggregate size

5.3.2 Compressive strength test results

The 28 day compressive strength results conducted on 100 mm cubes showing the influence of steel fibres and maximum coarse aggregate sizes are presented in Figures 5.3 and 5.4. It can be deduced from these relationship that there is not a significant increase in the compressive strength of tested cubes initiated by increasing the fibre dosages in the mixture. However, the results generally show a slight improvement in the compressive strength of the mixes by the addition of steel fibres in most cases while reduction in compressive strength are noticed in few cases after the addition of fibres.

The mean strength of SFRC varies between 57.7 to 64.9 MPa and 58.1 to 68.1 MPa for 10 and 20 mm aggregate sizes respectively while plain concrete had 59.2 MPa for 10 mm maximum aggregate size and 59.7 MPa for 20 mm maximum aggregate size. The maximum increase in compressive strength brought about by the inclusion of steel fibres in 10 mm maximum aggregate size mixtures is about 5 MPa, translating to about 9% increase while that of 20 mm maximum aggregate size mixtures recorded the maximum increase of about 8 MPa, which is 14 % increase. The results obtained are closely related to the results from previous studies on compressive strength of steel

fibre reinforced concrete (Mohammadi et al., 2008; Oh, 1992; Soutsos et al., 2012), as discussed in their various studies in pages 959, 2824 and 706 respectively.

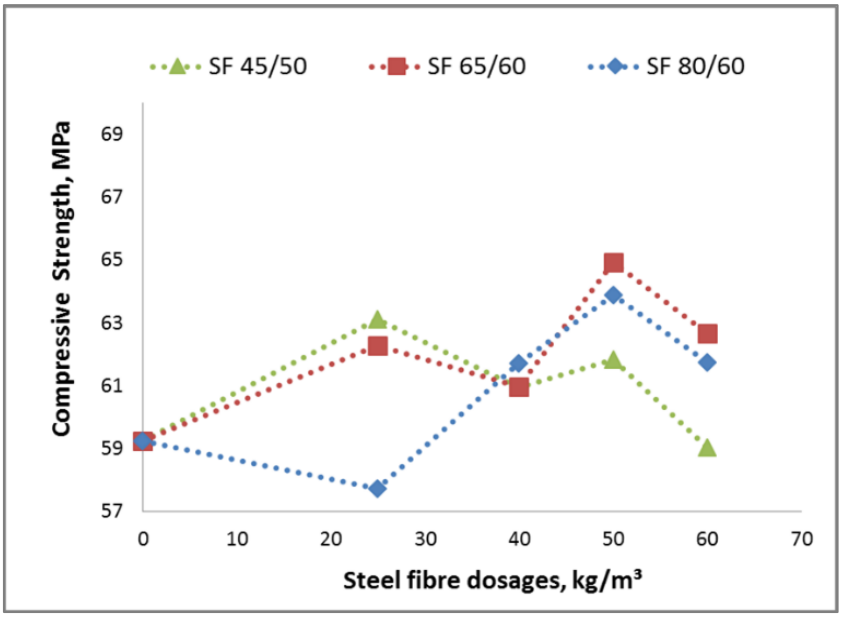

Figure 5.3: Relationship between compressive strength and dosages of different fibres with 10 mm aggregate size

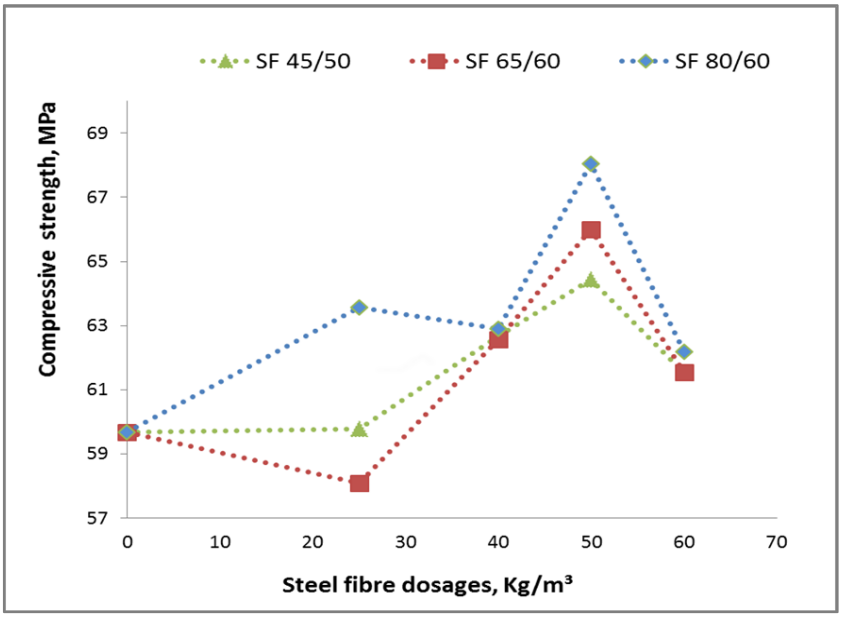

Figure 5.4: Relationship between compressive strength and dosages of different fibres with 20 mm aggregate size

The compressive strength of SFRC as shown in the results generally increases with increase in fibre dosage until optimum compressive strength was achieved at 50 kg/m³ fibre dosage for both maximum coarse aggregate sizes after which it declined. The steel fibre 80 l/d and 65 l/d gave the optimum strength at 50 kg/m3 dosage at 20 mm and 10 mm coarse aggregate sizes respectively. By this indication, it can be deduced that this trend of compressive strength ascending and then declining with increasing fibre dosage is due to compaction effects on the mixtures as earlier mentioned. The highest dosage of steel fibre in this research work which is at 60 kg/m^3 in concrete made the compaction of the mixture more difficult to be accomplished, this resulted in much lower strengths as seen in all the mixes irrespective of maximum coarse aggregate sizes in the concrete mixture.

Also, the lower strengths obtained at the 60 kg/m^3 can be attributed to consequences of low workability of fresh mixture achieved at higher fibre dosage. Since error bars were not added to Figures 5.3 and 5.4 for clarity, Figure 5.5 summarises the compressive strength development of both plain and SFRC with the dosages showing the median, upper quartile and lower quartile as well as upper and lower whisker where applicable.

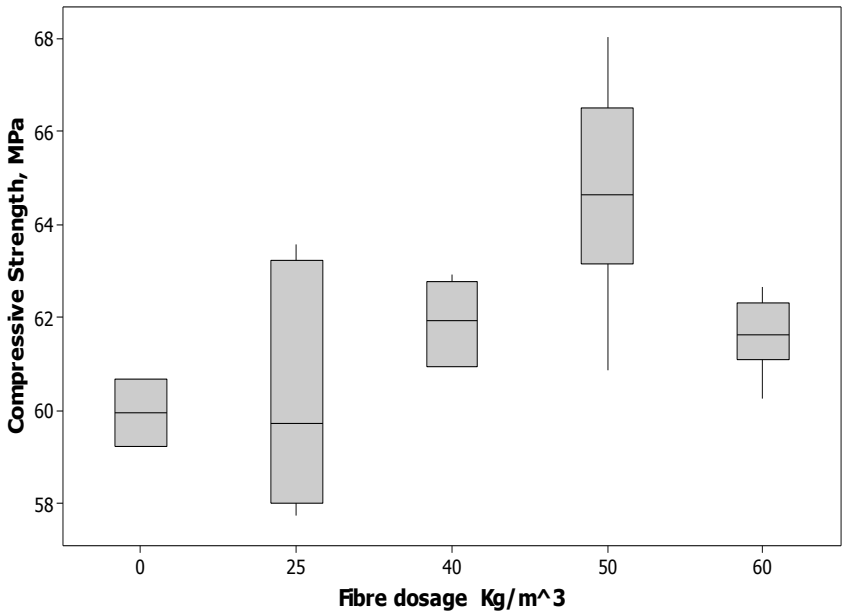

Figure 5.5: Box plot of Compressive strength of plain and steel fibre reinforced concrete

5.4 Flexural behaviour of concrete beams

Plain and steel fibre reinforced concrete beam specimens of size 150 mm by 150 mm by 600 mm were manufactured in three replicates for each mix so that series of tests are performed on them to assess the effects of inclusion of steel fibres and other selected variables on flexural performance of these specimens, as described in Section 4.7.4. Flexural strength, flexural toughness, maximum load sustained and residual flexural strength are the tests carried out in the investigation of the flexural behaviour of the beam specimens.

5.4.1 Flexural strength of beams

Detailed results of the flexural tests on the beams cast in this research work are given in Figures 5.6 – 5.11. The results are represented in typical curves while all the curves showing the three replicate specimens are shown in Appendix A of this report. Each type of concrete mixture is denoted according to its constituents, the type of steel fibre which is 'aspect ratio/corresponding length of the fibre' and the maximum coarse aggregate size. For example, 45/50 + 10 mm refers to the concrete mix which contains steel fibres with aspect ratio (l/d) of 45 and length 50 mm in a concrete mix of 10 mm maximum coarse aggregate size.

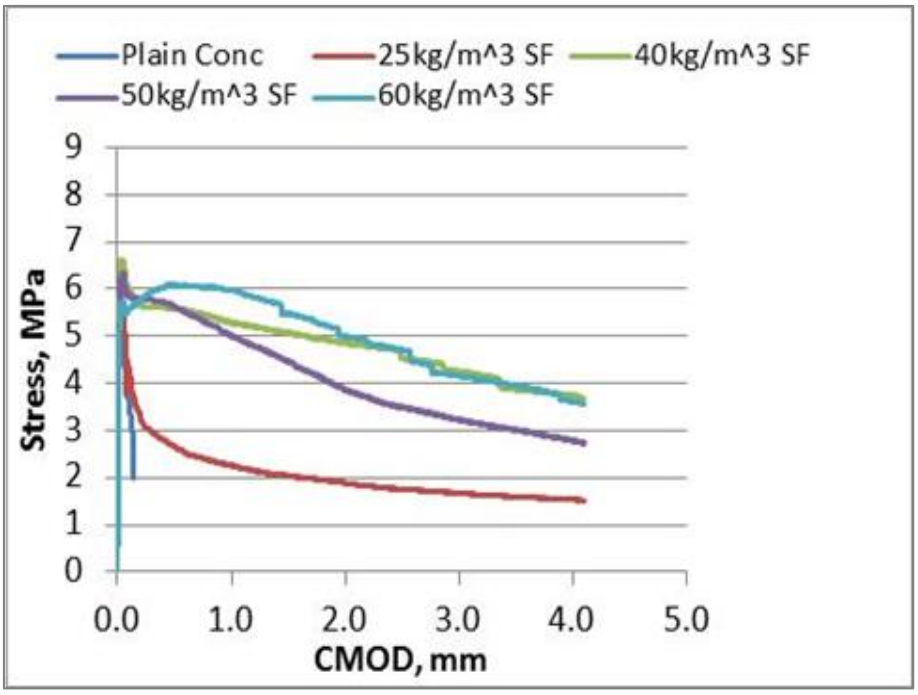

Figure 5.6: Flexural performance of plain and SFRC (45/50 + 10 mm) concrete beams

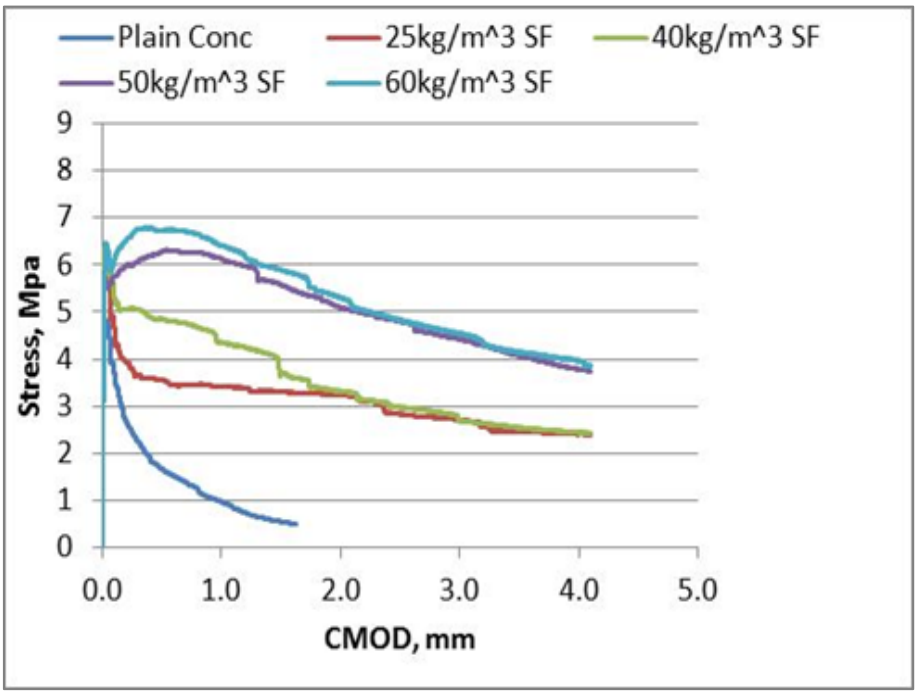

Figure 5.7: Flexural performance of plain and SFRC (45/50 + 20 mm) concrete beams

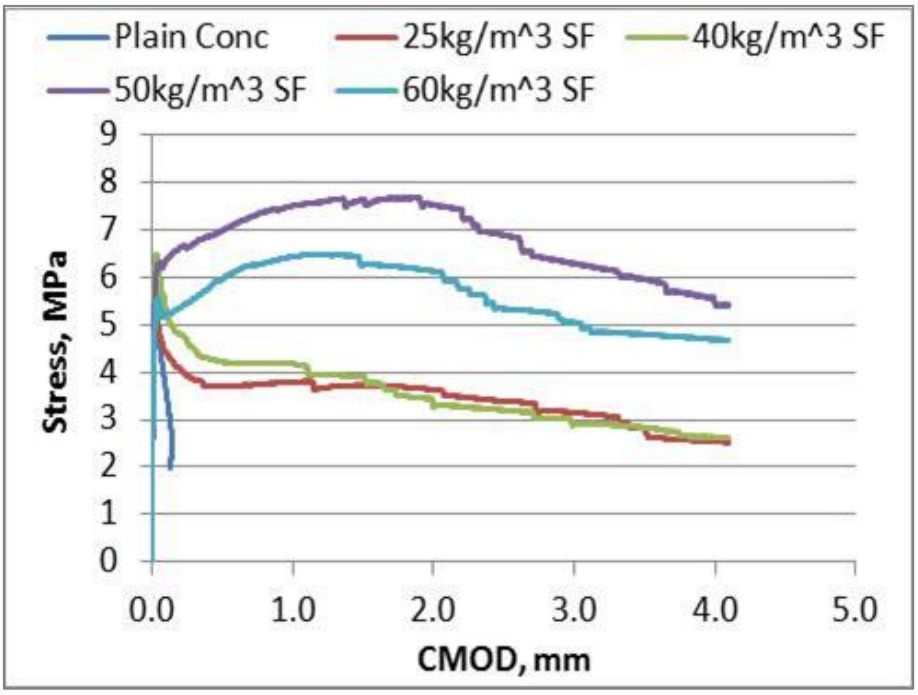

Figure 5.8: Flexural performance of plain and SFRC (65/60 + 10 mm) concrete beams

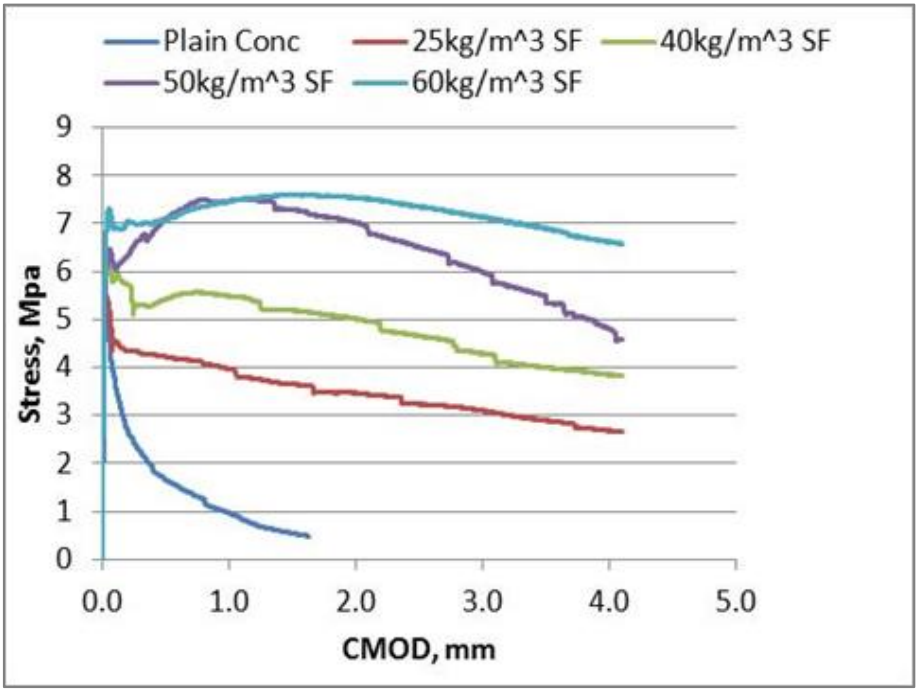

Figure 5.9: Flexural performance of plain and SFRC (65/60 + 20 mm) concrete beams

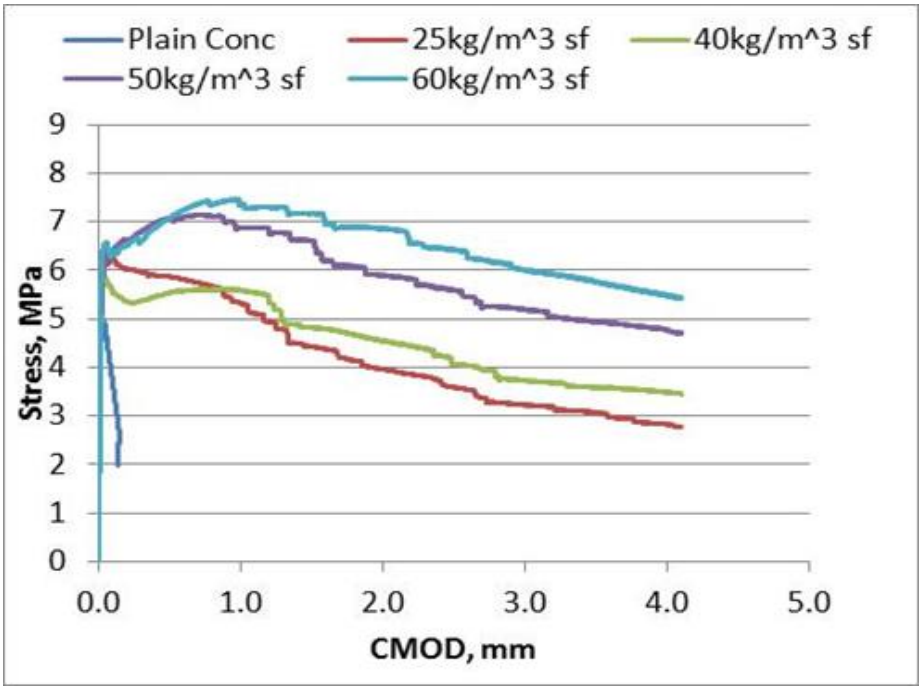

Figure 5.10: Flexural performance of plain and SFRC (80/60 + 10 mm) concrete beams

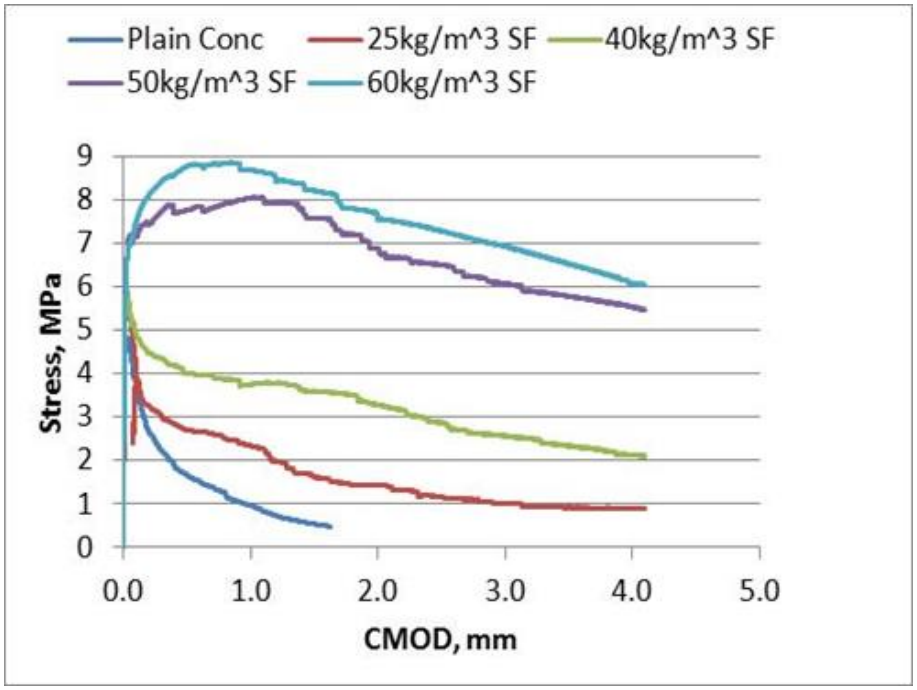

Figure 5.11: Flexural performance of plain and SFRC (80/60 + 20 mm) concrete beams

The results as shown in Figures 5.6- 5.11 are the typical flexural stress versus CMOD relationship of the notched beams determined by three-point bending tests. The results showing the flexural tests on all the three replicates are presented in Appendix A of this Thesis as discussed earlier. The results show the effects of fibre geometry, 10 mm and 20 mm maximum aggregate size in the mixes, various dosages of steel fibres in concrete and in comparison with plain concrete. In considering the results of the three replicates, a substantial scatter could be noticed in the post-cracking region of specimens with higher dosage of fibres. The scatter was generally small for the specimens with low dosage of steel fibres, for the plain concrete and for the specimens containing 45/50 types of fibres. It has been observed from previous studies that the relatively high scatter experienced in steel fibre reinforced concrete test results may be due to irregular distribution of fibres inside the specimens as a result of mixing procedures and casting method utilised (Caggiano et al., 2012; Habel & Gauvreau, 2008). The scatter was observed to be highest in mixes containing 80/60.

The results of flexural strength (defined as ultimate flexural strength in section 3.2.3.3) reveal that addition of steel fibres to concrete remarkably improves the strength of steel fibre reinforced concrete when compared to plain concrete as there were up to 83% and 54% increase in maximum stress reached for concrete with maximum coarse aggregate sizes of 20 and 10 mm respectively. The important factors affecting the performance of steel fibre reinforced concrete are revealed in the results shown. The significance of fibre length can be clearly recognised from the presented results as the shorter fibre length of 50 mm in Figures 5.6 and 5.7 exhibited the least flexural strength when compared to results from other beam containing steel fibre of length 60 mm. This trend is seen in both maximum coarse aggregate sizes and in all dosages of fibres. The improvement in flexural strength from plain concrete to the highest strength recorded for mixes containing fibre length 50 mm is about 40%. The post cracking tendency of the steel fibre reinforced concrete beams is also affected by the fibre length, most of the results from beams containing steel fibres of 50 mm length had the first cracking value as the highest flexural value achieved, whereas, results from beams containing steel fibres of 60 mm length show better post-cracking capability.

Another important factor as revealed in the test results of flexural stress versus CMOD presented in Figures 5.6-5.11 is the influence of fibre dosage on flexural performance and post-cracking potential of steel fibre reinforced concrete materials. It is evident from all the mixes that flexural strength improved drastically with increasing fibre dosage. The steel fibre reinforced concrete beams having higher dosages, for example, 50 kg/m³ and 60 kg/m³ dosages in Figures 5.8-5.11 exhibited strain hardening behaviour with stresses increasing even after first crack. It can be deduced that the right dosage of steel fibres in concrete contributed to a better distribution of fibres within the matrix aiding the composite material to fulfil its aim of steel fibres providing multi-directional reinforcement within the matrix.

It could also be noticed that effectiveness of steel fibre reinforced concrete is dependent on fibre aspect ratio as the best result in flexural behaviour is with the highest aspect ratio of 80 as seen from the results presented in Figures 5.11 of aspect ratio 80. The thinner fibres significantly improved the flexural strength of SFRC and the matrix with the fibres l/d 80 resulted in better post-cracking strength which is in line with earlier studies by Gopalaratnam and Gettu (1995); Yazıcı et al. (2007). This is due to the fact that fibre with aspect ratio 80 has the highest presence in every mixture according to the fibre properties in Table 4.3, section 4.5.4. The fibre dosage was by mass, resulting in different numbers of steel fibres in a mixture depending on their diameter and length. Fibre aspect ratio 80 having 0.75 mm diameter, had the highest number in the beam specimens.

It can be seen as well that in all the mixes presented in the typical curves as presented in Figures 5.6-5.11, mixes with 20 mm maximum coarse aggregate size seem to perform slightly better than the ones of 10 mm maximum coarse aggregate size. This can only be noticed particularly when considering the typical curves of the replicates. This is an indication that fibre length - coarse aggregate maximum size relationship is a factor to consider when selecting materials for fibre reinforced concrete as long fibres of 60 mm and 10 mm maximum coarse aggregate size in Figure 5.10 could not perform optimally when compared to the same fibres with 20 mm maximum coarse aggregate size in Figure 5.11. The reasons being that, ‘balling effect’ might freely occur when the matrix

interacting with fibre in the concrete is not sufficiently sized, which could be affecting the distribution and even the orientation of the fibres.

Figure 5.12 shows typical mixes of both 10 mm and 20 mm maximum aggregate sizes 50 kg/m^3 as summarised for ease of comparison. It can be seen from the Figure that plain concrete failed exhibiting brittle failure while other fibre reinforced concrete can be seen exhibiting ductility behaviour.

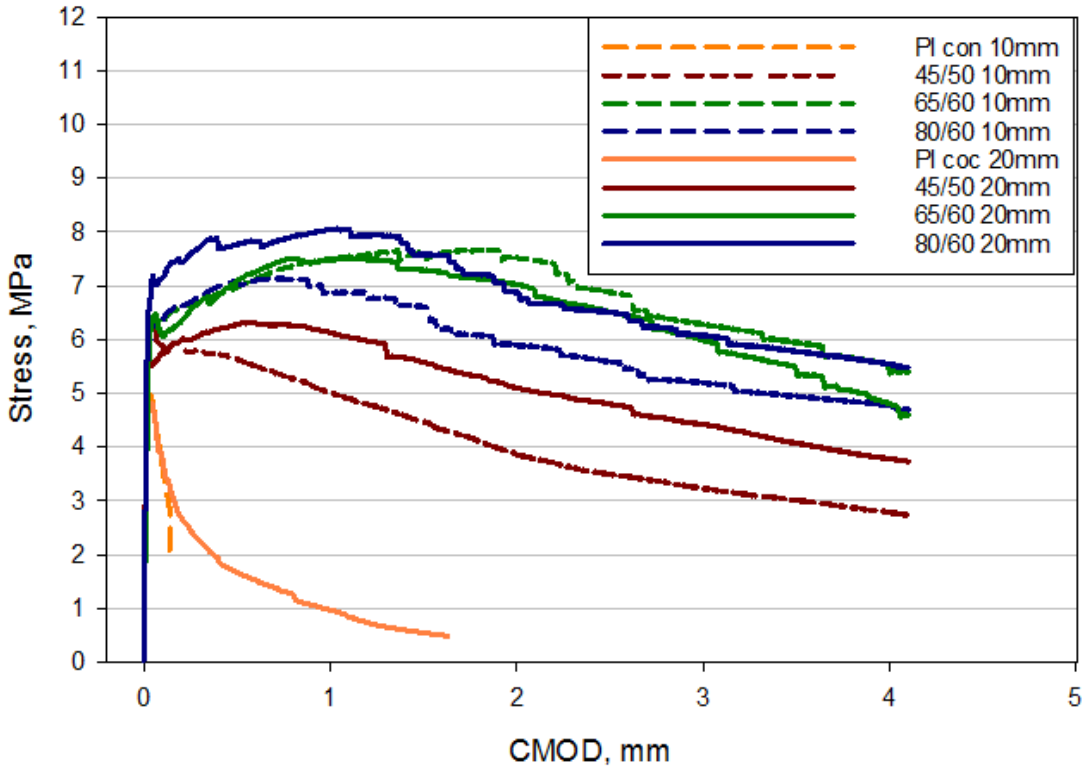

Figure 5.12: Flexural behaviour of plain and SFRC at 50 kg/m^3

The results represented in Figures 5.6 to 5.12 above are typical curves of beams flexural tests. However, the bar chart showing the average response of maximum stress of the three specimens at 50 kg/m^3 dosage of steel fibres is presented in Figure 5.13. The results as shown in the mean values of maximum stress are slightly different from those presented in the typical values in relation to better performance of 20 mm maximum aggregate size.

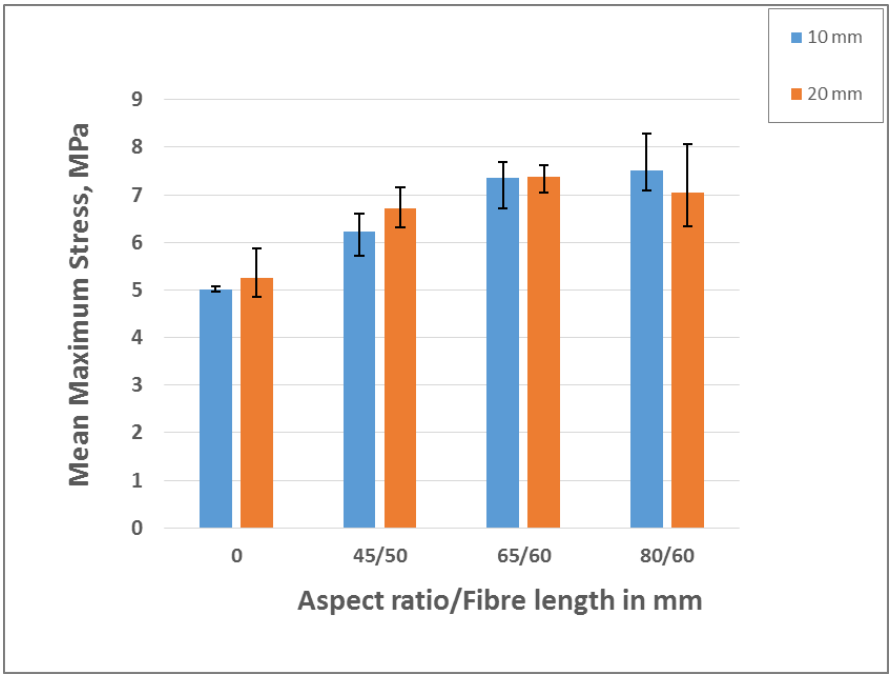

Figure 5.13: Mean maximum stress of plain and steel fibre reinforced concrete beams

The flexural behaviour of steel fibre reinforced concrete beams as represented by maximum stress of the beams as shown in Figure 5.13 revealed that concrete mixtures of both 10 mm and 20 mm maximum aggregate size performed relatively side by side with best performance recorded for mixture containing steel fibre of higher length of 60 mm.

5.4.2 Flexural toughness and residual strength of SFRC beams

Flexural toughness of steel fibre reinforced concrete beam specimens as defined in chapter 3 was computed as the area under the load – CMOD curve obtained from a flexural test of the beams while the residual flexural strength is a concept as also described in chapter 3 as a means of characterising the flexural toughness and evaluate the post-cracking response of steel fibre reinforced concrete material. The flexural toughness average values of three specimens of steel fibre reinforced concrete beams are presented in Figure 5.14. The influence of steel fibre inclusion in concrete is more significant in flexural toughness and residual strength of the composite as the ductility parameter of the material is appropriately measured.

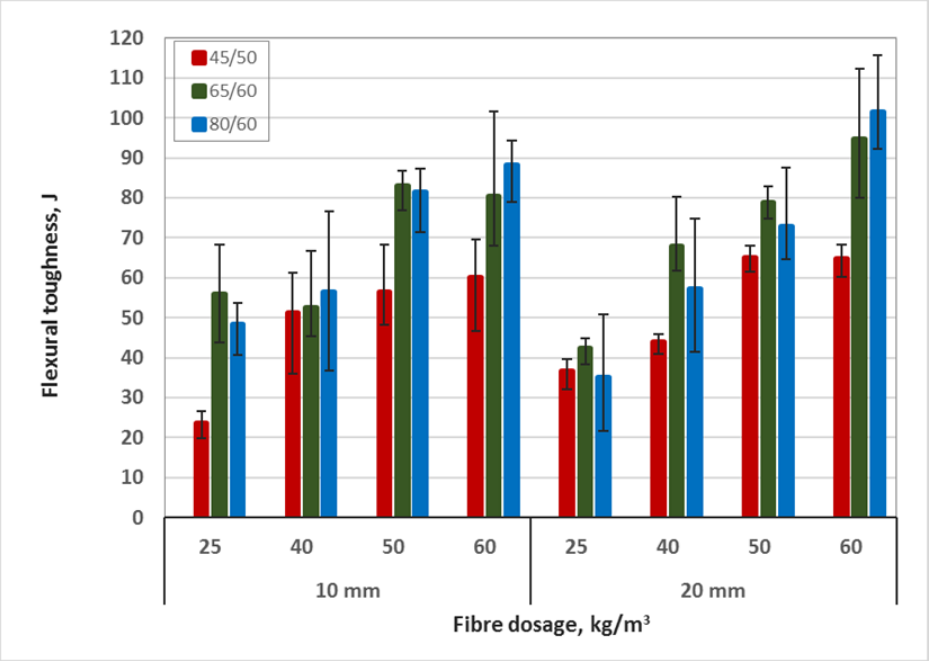

Figure 5.14: Flexural toughness (mean) of SFRC beams at different dosages of steel fibres. 10 mm and 20 mm denote maximum aggregate sizes

The flexural toughness values of plain concrete beams in both 10 mm and 20 mm maximum aggregate sizes are very low due to their brittle nature, hence the failure is sudden and the area under the load – CMOD curve is insignificant as revealed in Figure 5. 15 later in this analysis, and therefore not included in Figure 5.14 and its analysis.

From the presented results in Figure 5.14, it clearly shows that the flexural toughness of steel fibre reinforced concrete increased substantially as the dosage increased irrespective of the fibre geometry (length and aspect ratio) and maximum aggregate size. It has also been observed from the results in Figure 5.14 that mixes of 20 mm maximum coarse aggregate size generally yield a slightly higher flexural toughness compared to mixes of 10 mm maximum coarse aggregate size. The geometry of steel fibre especially the length and aspect ratio have been equally and distinctly identified from the results to affect the flexural toughness of the beams, concrete mixture containing steel fibres of 60 mm length are in the highest range of toughness value

while mixture with steel fibres of 80 aspect ratio performed best in strain hardening and hence, giving the overall best results.

The same trend that has been noticed in the values of the flexural toughness was the same regarding the flexural strength results in the case of influence of dosage, aspect ratio and length of steel fibres on the performance of steel fibre reinforced concrete, but more clearly pronounced in the flexural toughness results, especially in the post-cracking region of the curve. The mixes of 10 mm maximum coarse aggregate size with steel fibre 45/50 (aspect ratio of 45 with 50 mm length) at 25 kg/m^3 dosage of steel fibre in concrete had the lowest performance in flexural toughness with value of about 23 J, while the highest value of about 100 J was obtained from mixes of 20 mm maximum coarse aggregate size with steel fibre 80/60 at 60 kg/m^3 dosage. Consequently, there existed the differences of about 78 J between the lowest and highest value of flexural toughness which translated to 332 % increment. Besides, the highest value of flexural toughness in 10 mm maximum aggregate size mixes is about 88 J obtained from the mix containing steel fibre 80/60 at 60 kg/m^3 dosage, hence, there existed differences of flexural toughness values of about 13 J, translating to an increase of 15 % between the highest values recorded in 10 mm aggregate and that of 20 mm maximum aggregate with mixes containing same steel fibres of 80/60 at the same dosage 60 kg/m^3 but of different coarse aggregate sizes.

Also, the second best performance in all the beams tested for flexural toughness was recorded against the mixes of 20 mm maximum coarse aggregate size at dosage 60 kg/m^3 containing steel fibres 65/60. This, by indication means that beams with the same dosages of steel fibres, same maximum coarse aggregate sizes of 20 mm, and containing steel fibres of the same length of 60 mm have demonstrated both best and second best performances of flexural toughness in the test carried out on beam specimens. However, the only differences in these two mixtures are the aspect ratio, while the concrete mix of steel fibre of aspect ratio 80 had the best result, the concrete mix containing steel fibres of aspect ratio 65 recorded as having the second best result. Hence, there were differences of almost 7 J between the two mixes as a result of differences in the thickness of the fibres in the concrete mixes. This results apparently

identified aspect ratio as a factor influencing post-cracking performance of steel fibre reinforced concrete.

Figure 5.15 shows the trend of flexural toughness of typically, all the concrete mixtures. 'Agg size, mm' represents mixture with either 10 mm or 20 mm maximum aggregate size, 'pl' represents plain concrete while steel fibre designate remains as earlier defined. The results presented give the summarised details of the variables and their performance as compared to one another. The flexural toughness of plain concrete (without steel fibres) is captured in this Figure.

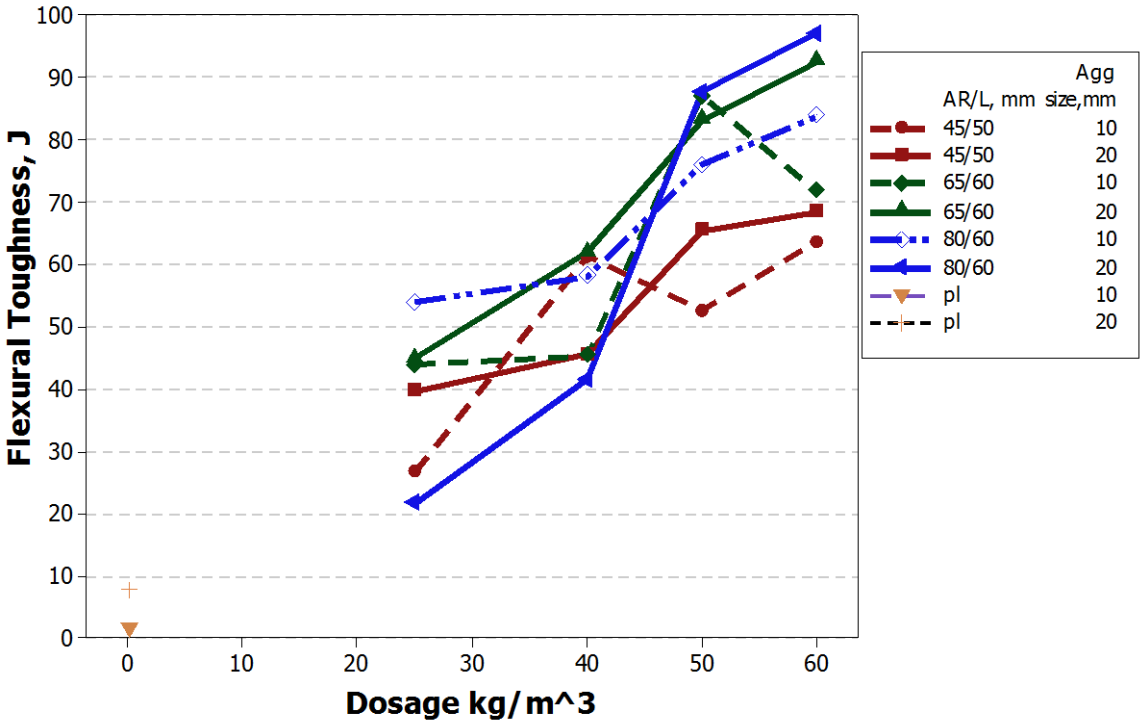

Figure 5.15: Flexural toughness performance trend of SFRC beams

By comparison of the ductility performance of each typical concrete mixture as shown in Figure 5.15, it has been revealed that fibre geometry and aggregate size is a deciding factor in guaranteeing a good performance in steel fibre reinforced concrete. This can be suggested to have an important link to how steel fibres and other concrete

components interact between one another and hence, how the fibres are distributed and orientated within the concrete matrix. Steel fibres 80/60 and 65/60 that have both shown best and second best performance are in 20 mm maximum coarse aggregate mixes respectively.

The unreinforced plain concretes have mean flexural toughness values of about only 2 J and 5 J for 10 mm maximum aggregate and 20 mm maximum aggregate mixes respectively. The results of flexural toughness in this research work has complemented the earlier researches on steel fibre reinforced concretes that the effects of including steel fibres are most felt in the post-cracking potentiality of steel fibre reinforced concrete (Alani et al., 2013; Gopalaratnam & Gettu, 1995; Soutsos et al., 2012). It shows that addition of steel fibres to concrete remarkably and drastically improves the flexural toughness when compared to plain concrete as there were up to 1810% and 5257% increase in the highest toughness reached for concrete mixes containing fibre 80/60 with maximum course aggregate sizes of 20 and 10 mm respectively. This has shown far more improvement than that obtained for flexural strength test of the same specimens.

It can also be seen from results showing the toughness trend in Figure 5.15 that all the beams with different mixture follow the same pattern, increase in toughness values as the fibre dosage increases except for mixture 65/60 + 10 mm that declined sharply from 50 kg/m^3 to 60 kg/m^3 dosage. This actually revealed the consequences of poor or unsatisfactory workability of the mixture at the fresh state, which also reflected on the lower density of the mixture, having a recurring effects on the hardened concrete as the mix, 65/60 + 10 mm had the least slump of 15 mm and a lower density of 2422 kg/m^3.

The good performances of the specimens at high dosages of steel fibres observed from the results has a significant influence on mechanical properties of steel fibre reinforced concrete, especially ductility parameters. The more the steel fibres in the concrete, the more the enhancement of energy absorption and post-cracking ability to carry the imposed load. The lowest values of flexural toughness recorded at 25 kg/m^3 and with

mixes containing steel fibres 45/50 could be due to two facts; firstly, the length of fibres which makes the fibres to get pulled out easily and resulting in not being able to bridge the initial cracks as expected. The second factor is the numbers of fibres that are readily available to do the 'bridging' of the crack. Again, considering the fibre networking through which theoretical calculation of number of fibres in each specimen is done revealed that fibre 45/50 type of fibre has the least number per each specimen. Since the dosage is low, this also affected the number of fibres in the mix, and hence the adequate distribution within the matrix. The outstanding performance of fibre reinforced concrete at higher dosage of steel fibres was made possible because there were more steel fibres in the matrix to bridge the crack at micro-crack level and stop the propagation into macro-crack.

In order to further examine the post cracking strength behaviour of the beam specimens, the residual flexural strength (F_{Rj}) of steel fibre reinforced concrete beams, an important parameter characterising the post-cracking behaviour of the composite material is determined as described in Section 3.2.4.4 of this research work. Figures 5.16 and 5.17 present the mean of results of three replicates of fibre reinforced concrete beams for the residual flexural strengths at CMOD 0.5 (F_{R1}) and CMOD 3.5 (F_{R4}) respectively. These two figures represent the lower and upper limits characteristic residual strengths.

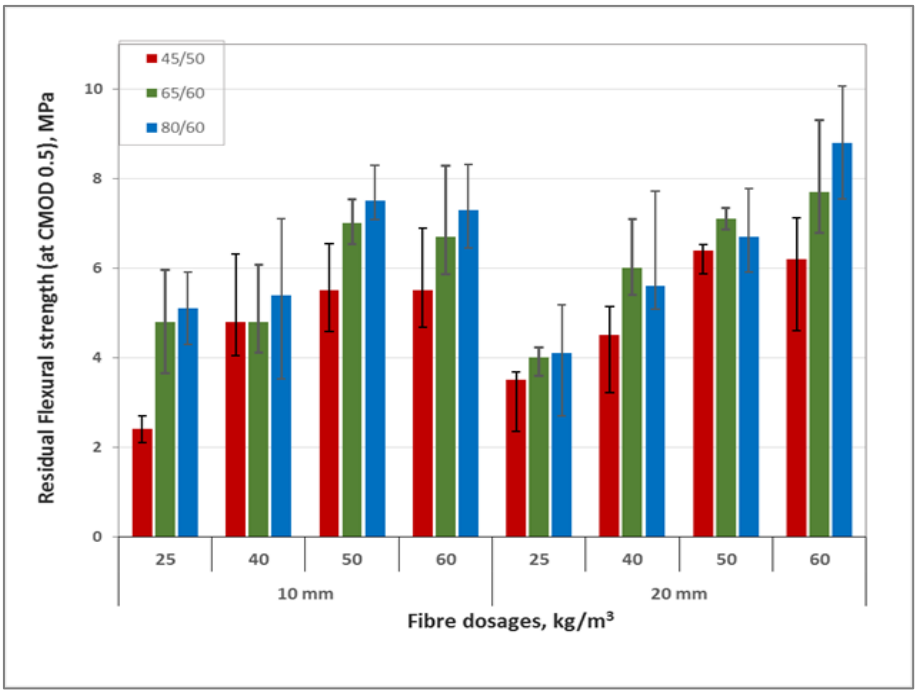

Figure 5.16: Mean of residual flexural strength (F_{R1}) at CMOD 0.5 of fibre types and dosages. Maximum aggregate sizes were represented by 10 mm and 20 mm

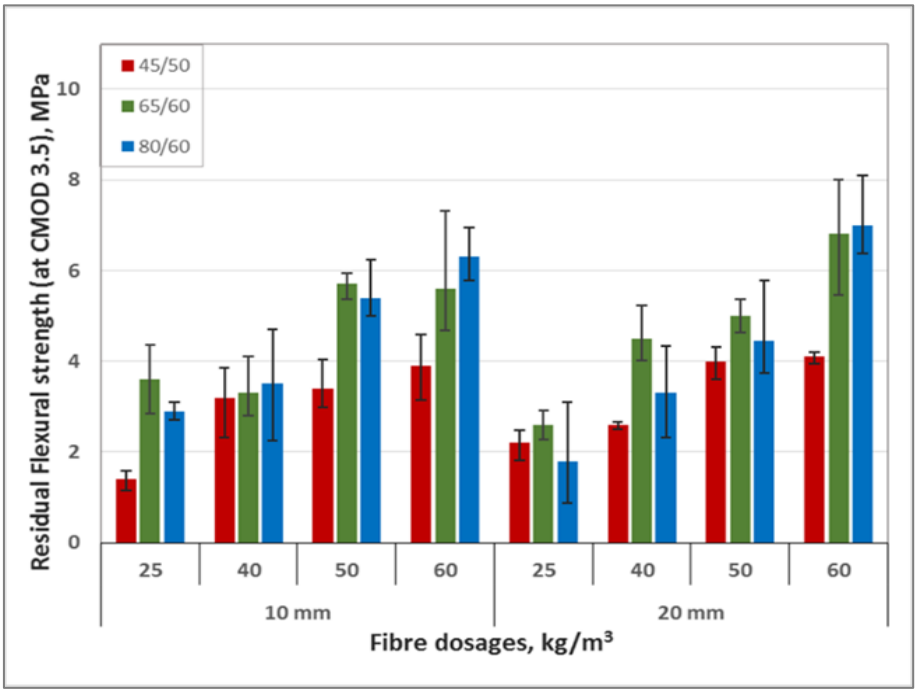

Figure 5.17: Mean of residual flexural strength (F_{R4}) at CMOD 3.5 of fibre types and dosages. Maximum aggregate sizes were represented by 10 mm and 20 mm

The results of residual flexural strengths at CMOD 0.5 (F_{R1}) and CMOD 3.5 (F_{R4}) were selected from all the computed CMOD values, that is, CMOD 0.5, CMOD 1.5, CMOD 2.5 and CMOD 3.5 for the characterisation analysis as suggested by Vandewalle et al. (2003) in RILEM report (final recommendation), that the two parameters denote the minimum guaranteed characteristic residual strengths at CMOD values of 0.5 and 3.5 mm, respectively. In the presented Figures 5.16 and 5.17, no value was recorded for the tested plain (unreinforced) concrete beams as there were no sufficient CMOD values because the beams failed exhibiting brittle nature and most of the plain concrete beams failed and breaking into two before the CMOD could attain 0.5 mm.

The results in Figures 5.16 and 5.17 can be seen to reflect the same trend as observed in flexural toughness of the tested beams, revealing how the two terms, flexural toughness and residual flexural strength of steel fibre reinforced concrete materials are closely linked. The dominance of steel fibre 80/60 with 20mm maximum aggregate mix in the residual strength results as the mix exhibiting the highest residual strength of all the fibre reinforced concrete beams tested is in close uniformity with what with the results obtained in the flexural toughness of the beams. Also, the mixes containing 20 mm aggregate size irrespective of the fibre geometry are of higher residual flexural strength at both F_{R1} and F_{R4} demonstrating more effectiveness of the concrete mix at deformation under load. However, there is exceptional case in 50 kg/m^3 dosage at F_{R4} where 10 mm maximum aggregate size beam specimens exhibit higher residual flexural strength than the 20 mm maximum aggregate size beam specimens.

Besides, it was noticed that the highest value of residual strength at both F_{R1} and F_{R4} obtained from mixes containing fibre 80/60 was made possible at highest dosage of fibre 60 kg/m^3. It can be observed clearly, especially in residual flexural strength at CMOD 3.5 (F_{R4}) in Figure 5.17, the 20 mm maximum aggregate mixes have mix containing steel fibre 65/60 outperforming steel fibre 80/60 mixes until the last dosage of 60 kg/m^3 when mix containing fibre 80/60 overshoots the 65/60 fibre mixes. The effectiveness of aspect ratio of steel fibre 80/60 at highest dosage whereby more number of fibres are available at this dosage more than other fibres to bridge more

cracks leading to greater post-cracking strength could possibly be responsible for the obtained results.

5.5 Flexural performance of plain and fibre reinforced concrete slab

The same variables and concrete mix proportions were maintained for the series of experiments carried out on concrete square panel of 600 mm by 600 mm by 100 mm, apart from the fibre dosages being fixed at 50 kg/m³ for flexural investigation. Three replicate samples were made for each mix and were subjected to flexural testing at 28 days as described in section 4.7.4.2.

5.5.1 Load deflection curve of square panels

The load deflection curve of square panels cast using 10 mm maximum aggregate size and a steel fibre dosage of 50 kg/m^3 showing the effect of fibre length and aspect ratio is shown in Figure 5.18 while the same curve for those with 20 mm maximum coarse aggregate size is shown in Figure 5.19. The results were obtained as a typical test performed on three replicate panels for each fibre type/10 mm maximum aggregate size combination of 45/50, 65/60 and 80/60 type of steel fibres. The plain concrete square panels were also tested represented in Figure 5.18 and 5.19 as plain mix.

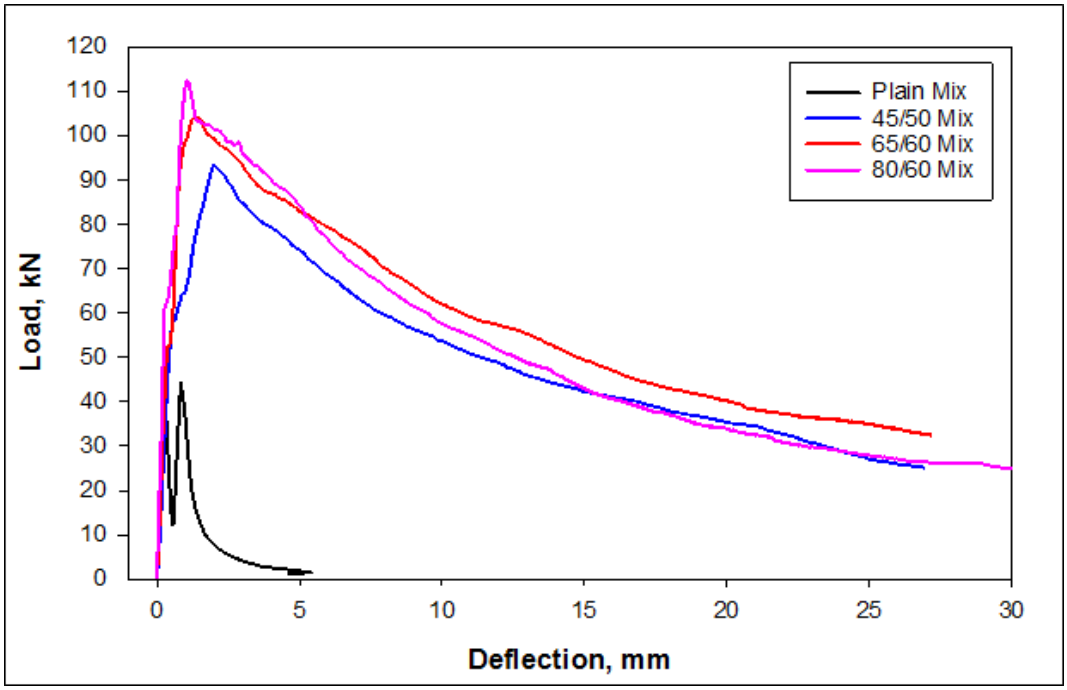

Figure 5.18: Load - deflection curve of concrete square panel with 10 mm maximum aggregate size

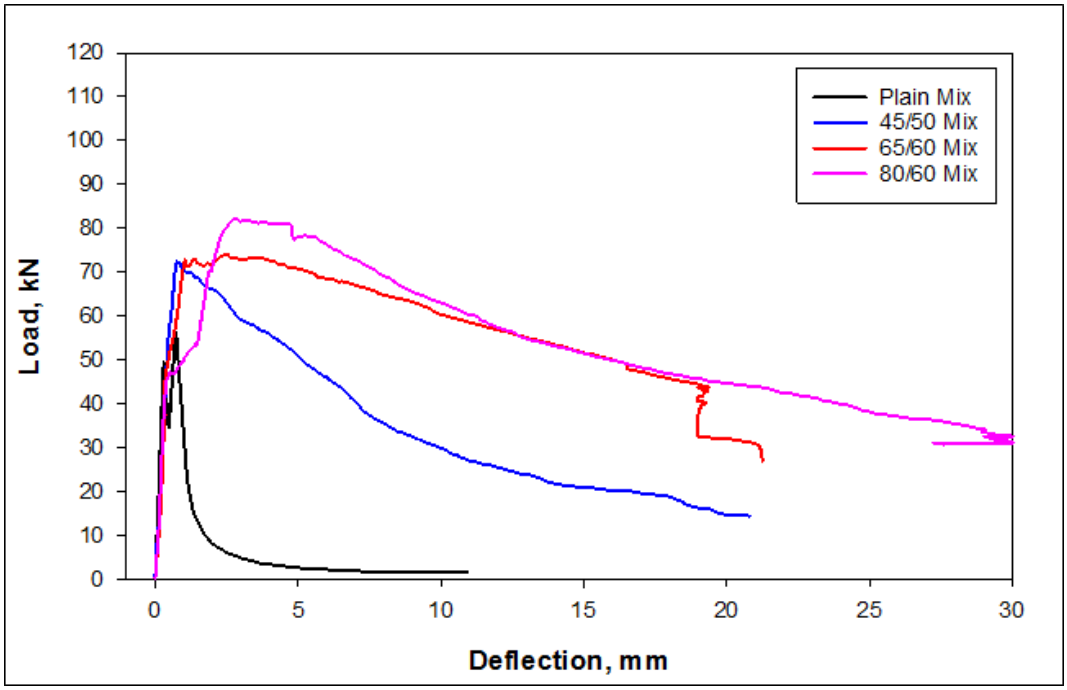

Figure 5.19: Load - deflection curve of concrete square panel with 20 mm maximum aggregate size

The results from the two Figures 5.18 and 5.19 show that the plain, unreinforced slabs failed immediately at the appearance of first crack exhibiting brittle nature of failure not withstanding any additional load. The inclusion of steel fibres in the concrete matrix made a significant difference in the failure pattern as the addition of steel fibres to the concrete slabs clearly improved the load carrying capacity of concrete. The steel fibre reinforced concrete slabs were still able to sustain additional load even after the first crack has been initiated by the imposed load. The slabs reinforced with steel fibres acted similarly in the same trend as the flexural performance of beams in terms of better performance of thinner steel fibres (of high aspect ratio), longer fibre outperforming the shorter ones and the post- cracking tendency of the fibre reinforced concrete. Meanwhile, the post cracking effect of inclusion of steel fibres can be seen in Figures 5.18 and 5.19 showing that after formation of the first crack, there was a strain hardening in the ascending part of the curve, revealing a high performance of steel reinforced concrete. This is as a result of bridging effects of steel fibres within the concrete matrix. It can also be noticed that the strain softening characteristics exhibited by the curves from slabs is different from the results obtained from beams. The decreasing criterion in slab is steeper than that of beam. The scatter of slab curves from the three replicates (provided in Appendix B) was relatively small compared to the results from beam.

However, it has been observed that mixture of 10 mm maximum coarse aggregate size were able to sustain more load than mixtures of 20 mm maximum coarse aggregate size, for all the fibre types. This is in sharp contrast to results obtained from flexural performance of beams in section 5.4.1 where better performance were exhibited by mixture of steel fibres and 20 mm maximum aggregate sizes in the typical curves. Figure 5.20 presents the mean of maximum load of slab specimen to summarise the load carrying capacity of the mixtures with both 10 mm and 20 mm maximum aggregate sizes.

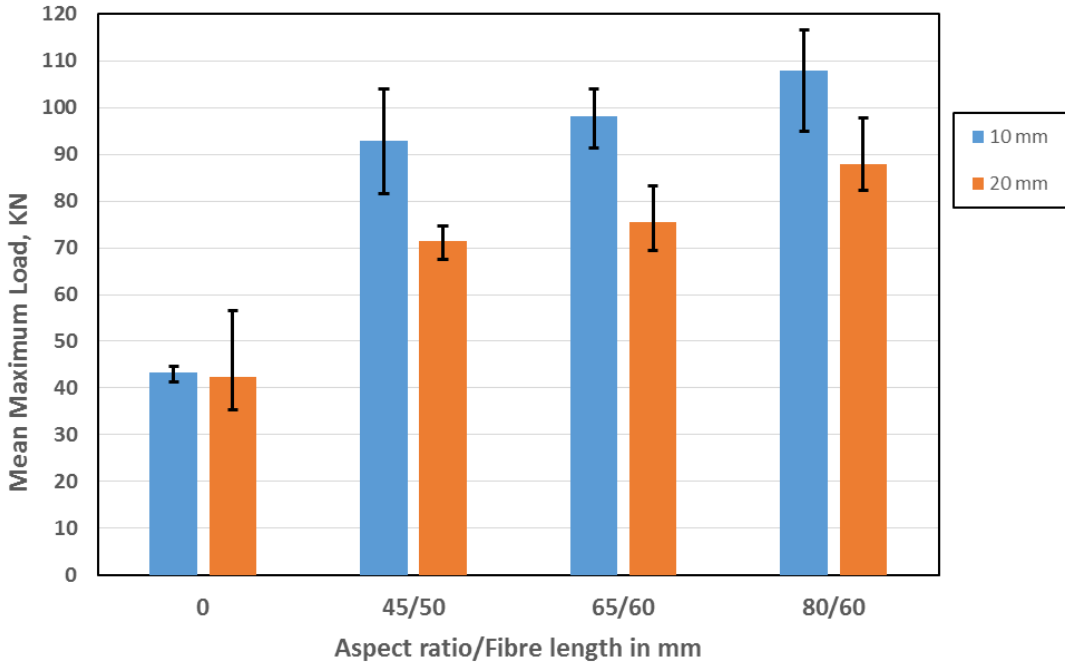

Figure 5.20: Mean of maximum load sustained by slab specimens

From the results presented in Figure 5.20, it can be seen that the mean maximum load sustained by mixture 80/60 + 10 mm has the highest failure load of 107.9 KN while the maximum load that could be sustained by the mixture of 20 mm maximum aggregate size with the same fibres is 88 kN, a difference of about 23 %.

5.5.2 Energy absorption of plain and steel fibre reinforced concrete slabs

The specimens of both the plain and steel fibre reinforced concrete slabs were tested for toughness characterization which is termed energy absorption as described in section 3.2.3.3. The main effect of inclusion of fibres is in characterization of energy absorption capacity of steel fibre reinforced concrete square slab specimens. The mean of energy absorption results of three replicates of square concrete slabs is presented as shown in Figure 5.21, displaying the energy absorption capacity of specimens made up of mixes containing different fibre geometry, 45/50, 65/60 and 80/60 of a single dosage of 60 kg/m^3 and two different maximum coarse aggregate sizes of 10 mm and 20 mm.

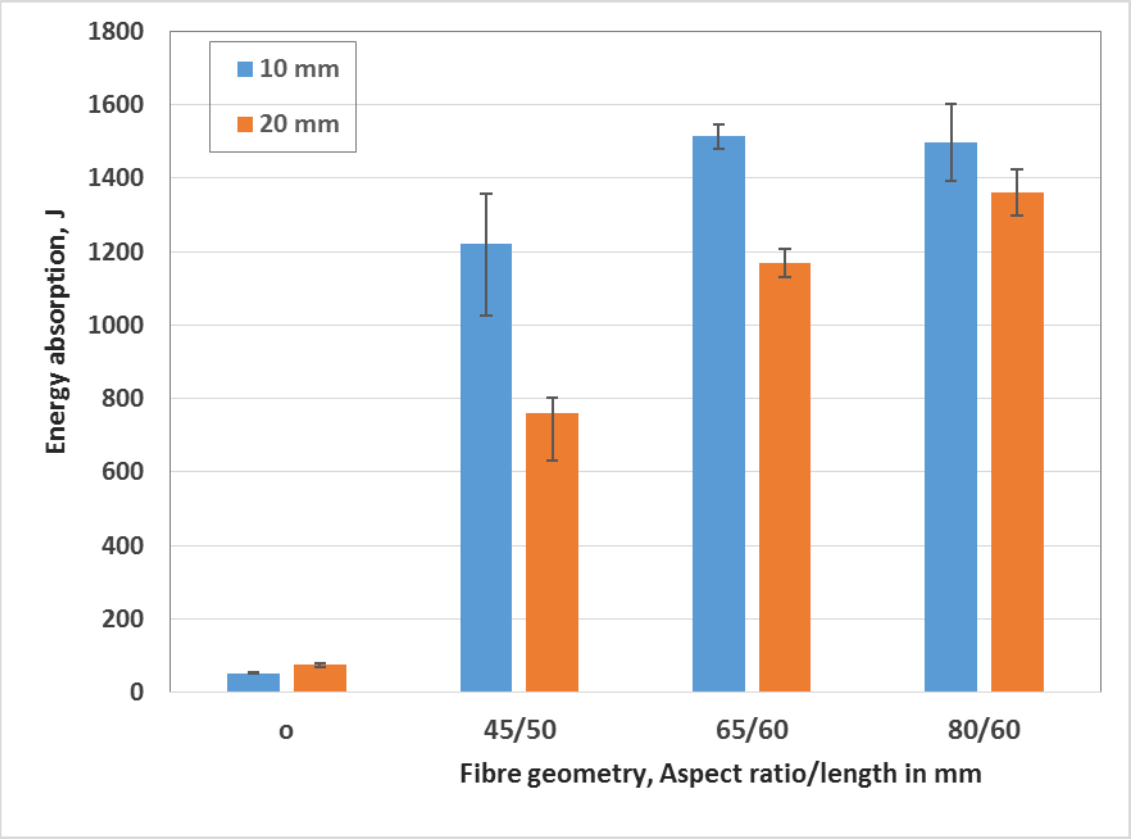

Figure 5.21: Energy absorption of plain and SFRC slabs of different fibre geometry

It can be observed that the results as presented in Figure 5.21 clearly reveal the ductility capacity of the tested concrete slabs. The plain concrete slabs which failed suddenly at cracking load without any warning of long deflection but exhibiting the brittle nature. Meanwhile, the 20 mm maximum aggregate size has higher value of energy absorption than the 10 mm maximum aggregate size mixes by a difference of almost 23 J, which is not the same trend after fibres have been added to the concrete. The effects of fibre inclusion in concrete can be apparently recognised from the results of energy absorption of slab specimens as there were substantial improvement from plain concrete to SFRC slabs. Energy absorption differences of close to 1500 J existed between the plain unreinforced concrete of 10 mm maximum aggregate size mix having value of roughly 53 J and the highest value of above 1500 J obtained from mix of same aggregate size with fibre 65/60 which translates to percentage increase of around 2750%. Similarly for the 20 mm maximum aggregate size mixes, energy

absorption differences of nearly 1300 J existed between plain concrete of value about 76 J and the highest value recorded for the aggregate size mix which is about 1360 J obtained from mix containing 80/60 type of steel fibres, indicating a percentage increase of nearly 1700%.

Consequently, the highest value of energy absorption results of all the slabs specimens tested was obtained from mix of 10 mm maximum coarse aggregate containing fibre 65/60 which was closely followed by mix of the same aggregate size containing fibre 80/60. The results therefore followed the same trends as other results for slab specimens which are in contrast to results from beam specimens. It can also be seen by comparing the results as presented in Figures 5.20 and 5.21 showing the mean of maximum load sustained by the slab specimens and that of energy absorption respectively, that the main effect of fibres in concrete slabs is better expressed in energy absorption. The improvement by fibre inclusion in concrete has a percentage increase of 150% in maximum load sustained by the slabs against about 2750% obtained in the case of energy absorption. This is a very wide margin. Also, as observed in the maximum load sustained, with mixes of fibre 45/50 + 10 mm having higher failure load than mixes of 80/60 + 20 mm, the result from energy absorption appears to contradict this. The longer length of fibre 80/60 is made more effective in the ductility tendency of the SFRC, bridging more micro-cracks, stronger pull out energy and therefore, showed a better energy absorption value than the shorter fibre of 45/50.

5.5.3 Crack behaviour of plain and steel fibre reinforced concrete slabs

The crack pattern of both the unreinforced plain concrete and steel fibre reinforced concrete slabs were visually examined and can be summarised to reflect the results as presented in sections 5.5.1 and 5.5.2. The slabs generally failed by the formation of radial cracks dividing the entire slab specimens into segments as described by Di Prisco et al. (2009) which characterises the mode of failure as predominantly flexural failure. Figures 5.22 and 5.23 show the crack pattern of unreinforced plain slab specimens.

Figure 5.22: Cracking on the surface of plain concrete slab at testing

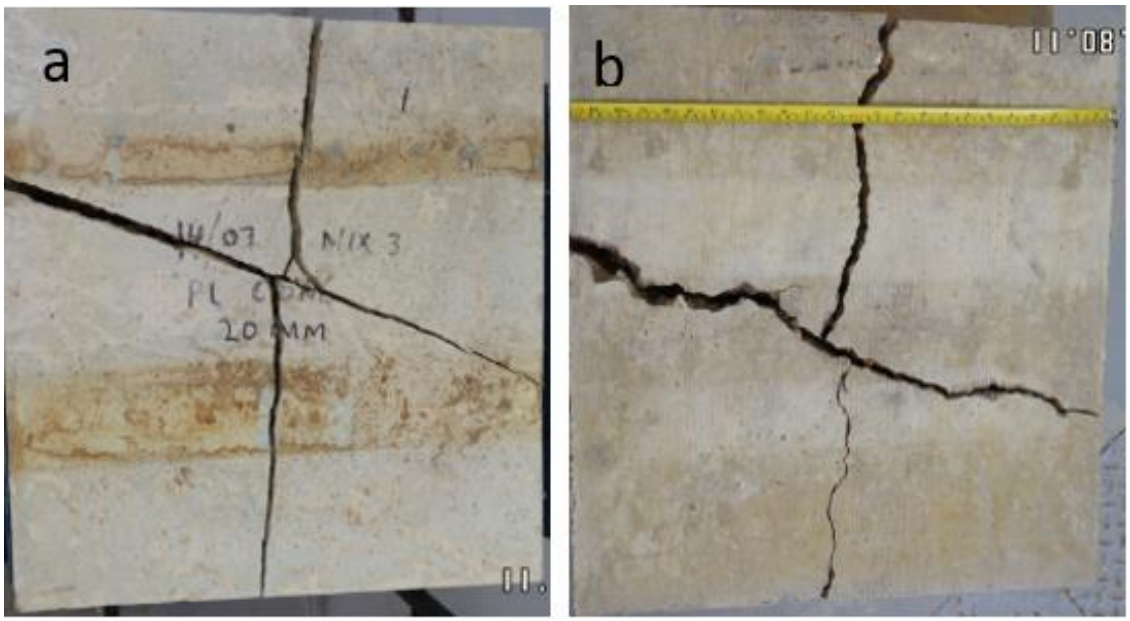

Figure 5.23: Cracks of plain concrete slab of 20 mm mix, (a) the slab surface where the load was applied and (b) the underside of the slab

The brittle nature of the unreinforced plain concrete slab was clearly demonstrated in the crack behaviour of the panels as revealed in the Figures 5.22 and 5.23. The crack appeared immediately at the surface of the slab at the cracking load without any warning whatsoever and displaying the brittle failure by separation of the specimen into four parts. It is apparent from the nature of the cracks that the unreinforced plain concrete did not distribute the load effectively before the first flexural crack occurred which continued to propagate speedily without any resistance until final failure. Figure 5.22 shows the sudden appearance of the crack at testing while Figure 5.23 (a) and (b) are the slab surface and bottom after the test. Figure 5.24 presents crack pattern of 10 mm maximum aggregate size slab

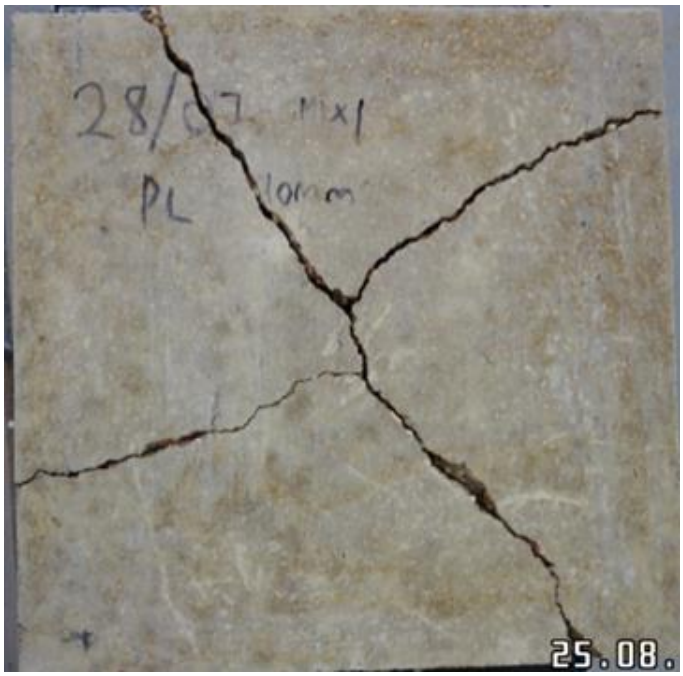

Figure 5.24: Cracks of plain concrete slab of 10 mm mix

Similarly, the crack pattern of the unreinforced plain concrete mixed with 10 mm maximum coarse aggregate size as shown in Figure 5.24 exhibit brittle nature as well, only that the pattern of the cracks seems to be a bit different in that the cracks are positioned closer to the edge of the panel in 10 mm maximum aggregate size slabs. The

crack pattern of unreinforced concrete slabs as shown in Figures 5.22, 5.23 and 5.24 revealed that there was no resistance to cracking propagation, this correlates to the results of low maximum load sustained and the low values of energy absorption obtained from the plain slabs which is responsible for braking into four pieces at ultimate strength while the fibre reinforced slabs maintained their integrity to a better deflection after ultimate strength as in line with previous study by Gopalaratnam and Gettu (1995).

The steel fibre reinforced slab specimens demonstrate different pattern of cracks which however differ from one to another depending on fibre geometry and the combined maximum aggregate size. Surface and side of steel fibre reinforced slab mixed with 20 mm maximum aggregate size containing fibre 45/50 is presented in Figure 5.25 while those for slabs of same aggregate size containing fibre 65/60 and 80/60 are presented in Figures 5.26and 5.27 respectively.

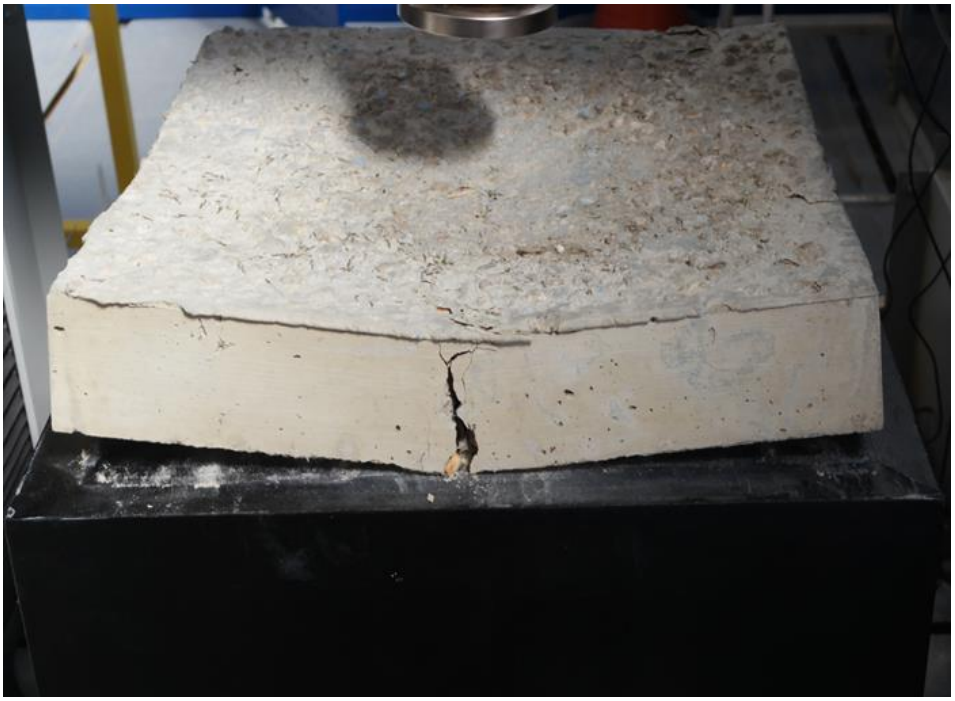

Figure 5.25: Mode of cracking on side and surface of slab 20 mm + 45/50 at testing position

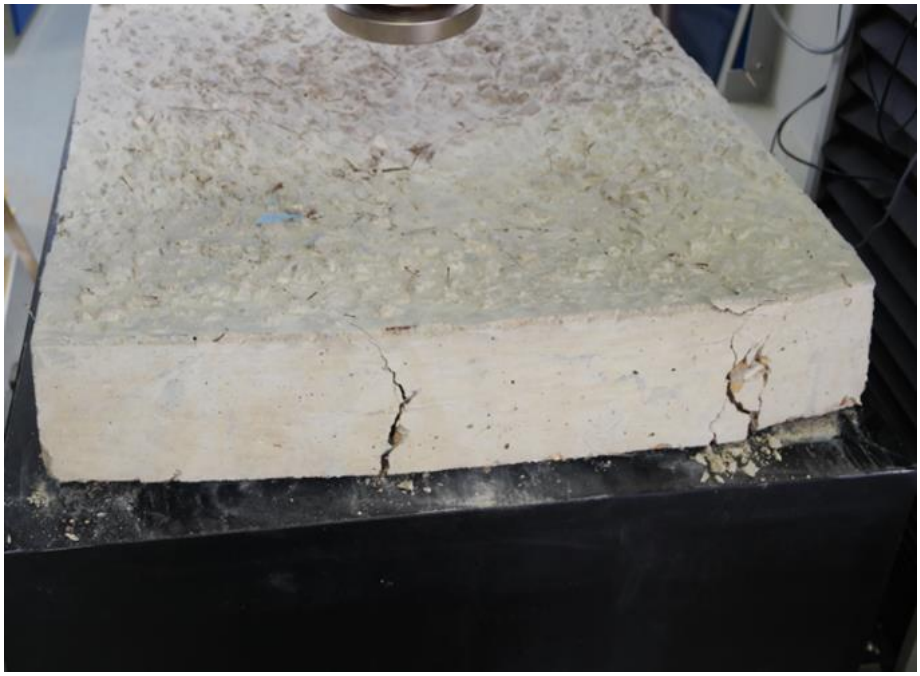

Figure 5.26: Mode of cracking on side and surface of slab 20 mm + 65/60 at testing position

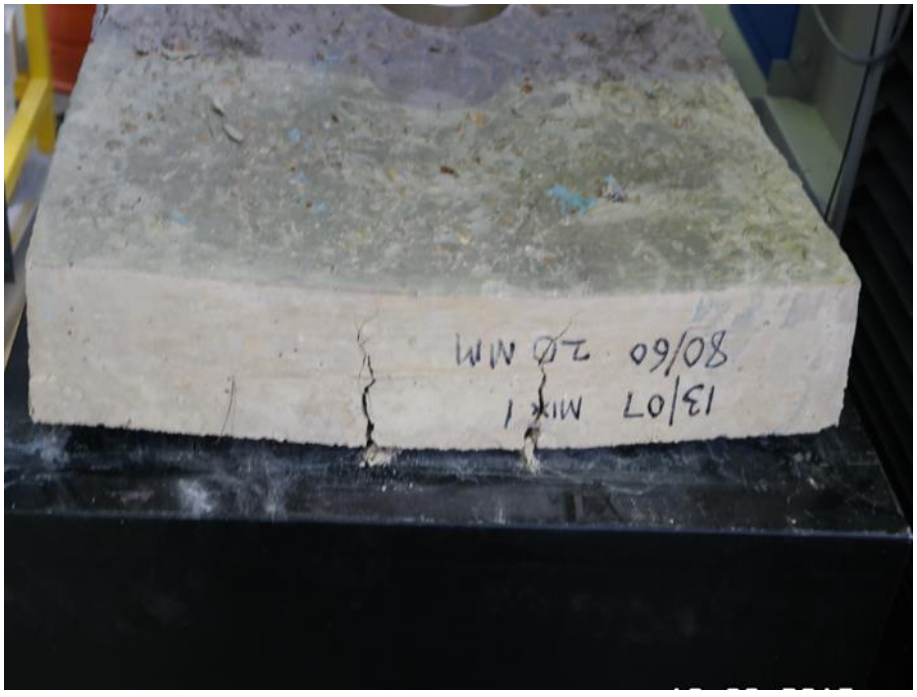

Figure 5.27: Mode of cracking on side and surface of slab 20 mm + 80/60 at testing position

The steel fibre reinforced concrete slabs, unlike the unreinforced plain concrete slabs failed exhibiting some restrains to cracking giving sufficient warning, experiencing appreciable deflection, showing more ductile behaviour and none experienced complete separation. It is clear that none of the steel fibre reinforced concrete slabs had the continuous cracks cutting across both surfaces of the slabs like the brittle plain concrete, the cracks were mainly on the underside of the slabs. Nevertheless, it can be observed from Figures 5.25, 5.26 and 5. 27 that the slab specimens of 20 mm + 45/50 had single main wide crack at the side which was noticed at other sides as well which is different from the cracking mode of the other two slab group, 20 mm + 65/60 and 20 mm + 80/60 which showed more and narrower cracks at the sides. This pattern can be said to show correlation with the results of the energy absorption and maximum load sustained by the slab specimens. It can be deduced that though, the 20 mm + 45/50 slab specimens contained steel fibres, the fibres of shorter length could not sustain higher cracking load because the fibres were easily pulled out of concrete matrix which affected the fibres' ability in bridging effectively the initiation of first crack formed along one slab axis as suggested by Barros et al. (2005). The reasons the cracks were mainly at one particular side could possibly be due to failure to distribute the load and engage other parts of the slab. The other specimen with longer fibres performed better with the fibres engaging in arresting the initiation of micro-cracks which resulted in dissipation of the load to produce more cracks at different areas of the slab with higher failure load and energy absorption.

The general crack pattern of slabs mixed with both 10 mm and 20 mm maximum aggregate size containing the two 60 mm long fibres, 65/60 and 80/60 are visually considered from the cracks displayed at the bottom of the slab specimens. Figure 5.28 shows the crack pattern of 10 mm maximum aggregate size with 65/60 and 80/60 fibres while slabs mixed with 20 mm maximum aggregate size containing fibre 65/60 and 80/60 are as shown in Figure 5.29.

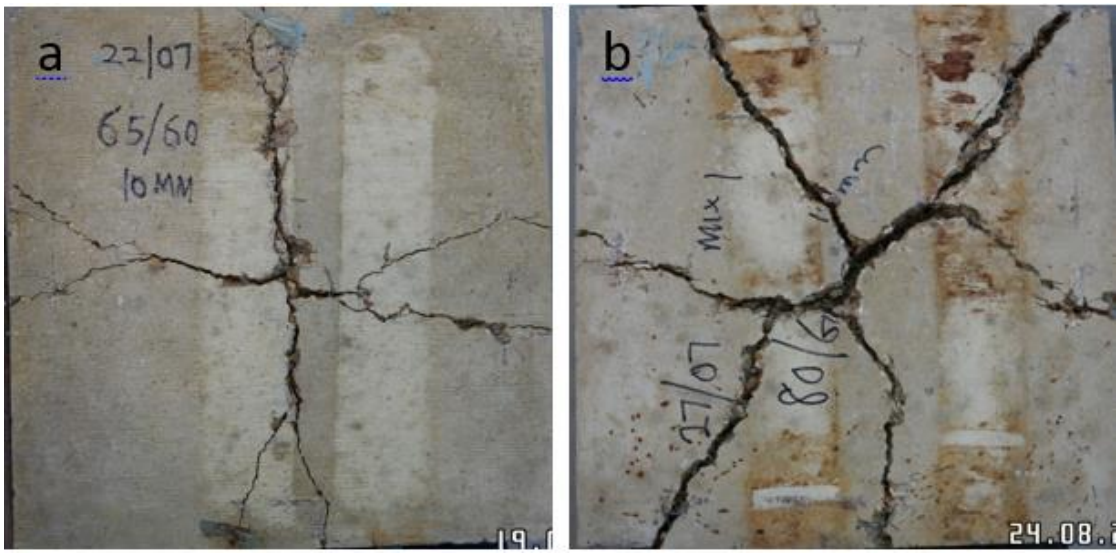

Figure 5.28: Crack pattern of slabs mixed with 10 mm aggregate size, (a) with 65/60, (b) with 80/60

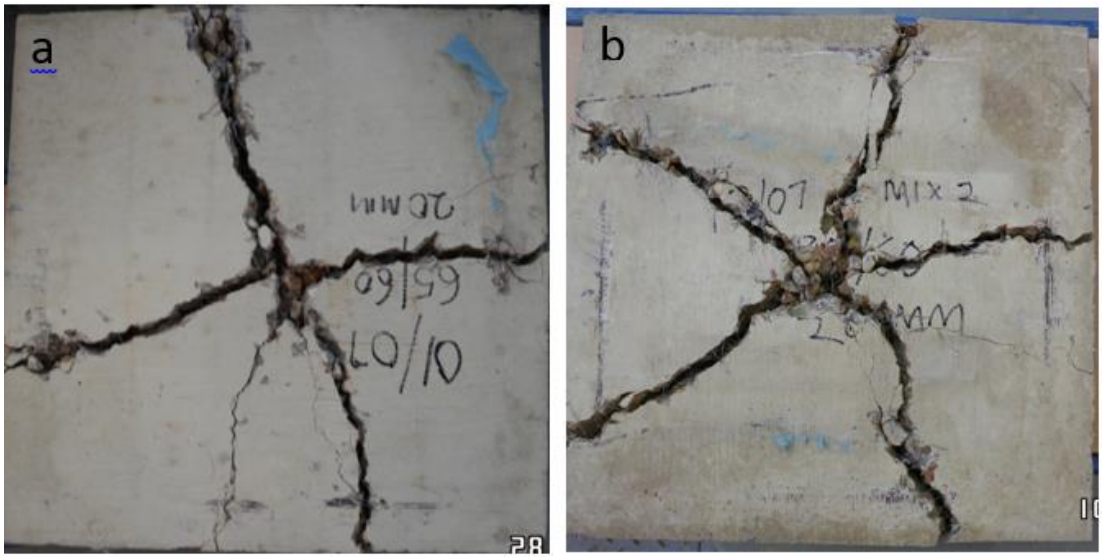

Figure 5.29: Crack pattern of slabs mixed with 20 mm aggregate size, (a) with 65/60, (b) with 80/60

It can be generally revealed from the crack behaviour of slabs as shown in Figures 5.28 and 5.29 that more and narrower cracks are formed when the maximum coarse aggregate size in the mix is 10 mm regardless of the fibre type, while the narrowness of the crack varies from slab to slab which has a direct and mutual connection with the

performance of the tested slabs in relation to the maximum load sustainable and energy absorption capacity. For example, the slab of mix 20 mm maximum aggregate containing fibre 65/60 as shown in Figure 5.29(a) has fewer but wider cracks than that in Figure 5.28(a) of the same fibre geometry. The same trend is seen repeating itself in Figures 5.28(b) and 5.29(b) with fibre 80/60. It can be noticed as well in Figure 5.28 when (a) is compared with (b) that the cracks of slab containing 65/60 is narrower than that of slab containing fibre 80/60.

From the results of maximum load sustained and the energy absorption capacity of slab specimens, it can be deduced that the slabs specimen with best performance are those with more but narrow cracks. This indicates significant increase in the ductility of the slab specimens with an increase in cracks demonstrating an effective bridging of crack and with increasing load, the fibres were able to transfer the additional stresses to the concrete matrix through bond stresses leading to additional cracks in the matrix according to suggestions by (Cengiz & Turanli, 2004; Salehian et al., 2014). The slab mixed with 10 mm maximum aggregate size containing fibre 65/60 had the highest energy absorption capacity which by indication, the most ductile specimen, which is in line with the cracking behaviour of the specimens which is the same trend with previous findings (Di Prisco et al., 2009; Fall et al., 2014; Sivakumar & Santhanam, 2007).

5.5.4 Comparison between flexural behaviour of SFRC beams and slabs

The flexural behaviour of normal and steel fibre reinforced concrete beams and slabs were compared to further analyse the possible effects of the specimens on the interaction of steel fibres and concrete matrix, especially, with the coarse aggregate in the mixes. The 50 kg/m^3 dosage of steel fibre in the mixtures of beam experimental procedure were selected for this comparison since slabs were tested only on the same dosage.

Considering Figure 5.13 which shows the flexural behaviour of steel fibre reinforced concrete beams as represented by maximum stress of the beams and Figure 5.20, the

maximum load sustained by the slabs before failure. The results revealed that for beam, concrete mixtures of both 10 mm and 20 mm maximum aggregate size performed relatively side by side with highest performance recorded for mixture containing steel fibre of aspect ratio (l/d) 80. However, in the case of slab, the trend observed was completely different from that of beam. The unreinforced concrete slabs had the mixture of 20 mm coarse aggregate maximum size outperforming the 10 mm maximum size but all other mixtures containing steel fibres had the 10 mm maximum aggregate size clearly outperforming the 20 mm maximum aggregate size.

The results as shown in Figures 5.13 and 5.20 indicate that the size of coarse aggregate in combination with the specimen dimension/geometry has an influence on the flexural performance of steel fibre reinforced concrete. Furthermore, in order to examine the post cracking strength behaviour of the beam specimens and the influence of maximum aggregates size and fibre geometry on the result outcome, the residual flexural strength at CMOD 0.5 (F_{R1}) and CMOD 3.5 (F_{R4}) as presented in Figures 5.16 and 5.17 respectively showing all the dosages of steel fibres in concrete were considered. The trend observed indicates that generally, most of the mixes containing 20 mm aggregate size irrespective of the fibre geometry are of higher residual flexural strength at both F_{R1} and F_{R4} demonstrating more effectiveness of the concrete mix at deformation under load. However, there is exceptional case in 50 kg/m^3 dosage at F_{R4} where 10 mm maximum aggregate size beam specimens exhibit higher residual flexural strength than the 20 mm maximum aggregate size beam specimens.

Meanwhile, steel fibre aspect ratio 80 and length 60 has the best performance of residual strength and at 20 mm aggregate mixes for both F_{R1} *and* F_{R4}. The different trend of flexural/strength behaviour revealed in slab tests where specimens with 10 mm maximum aggregate size distinctly performed better than their counterpart with 20 mm maximum aggregate could possibly be connected with the specimen dimension like the thickness which is 100 mm, the aggregate size and the interaction with fibre geometry.

The flexural behaviour demonstrated in beams and slabs whereby the mixes of 10 mm and 20 mm maximum aggregate sizes in beams behaved almost the same but varied widely in the case of slab can best be explained from the structural point of view. The differences in flexural capacity of the mixes after the inclusion of steel fibres in 10 mm and 20 mm maximum aggregate size could not be obvious in beams because of the nature of the test, the three – point loading. The notches introduced in the beams made the region of cracking a predetermined one and hence, tending towards an action of uniaxial state of stresses. In this regard, the heterogeneity of the materials consisting of steel fibres within the concrete matrix is less pronounced. The stresses in the failure surface of the beams are less affected by crack-bridging mechanism of the fibres and hence, the sensitivity to the aggregate size is little or of no effect.

However, in the case of slab flexural tests, there were more fracture surfaces and complete exhibition of bi-axial nature of bending. Here, the cracks within the slabs occurred freely in response to the loading and opened up at random, which initially started as micro-cracks at the week points and hard points interface zone. Again, it is evident that more cracks occurred within the slabs containing 10 mm maximum aggregate size than their 20 mm counterparts. This is because there were more points of interface zone in the 10 mm maximum aggregate mixtures caused by the smaller size of aggregates which in turn increased the number of week-hard points of interface. Therefore, there were full manifestations of action of bridging of cracks by steel fibres within the concrete matrix which boosted the sensitivity to the maximum aggregate size while the heterogeneity nature of the materials was highly pronounced. Consequently, the slabs containing mixes 10 mm maximum aggregate size outperformed their counterpart, 20 mm maximum aggregate size because the steel fibres were more positioned within the concrete matrix and this aided the probability of steel fibres to either stop or delay the propagation of cracks across the failure surfaces from micro to macro cracks which eventually results in failure.

The best flexural results recorded in both beams and slabs as being the mixtures containing steel fibres of aspect ratio (l/d) 80 however could be possibly be due to the fibre network and material property which favour fibres with aspect ratio 80 as stated in Table 4.3 in Section 4.5.4. By this indication, steel fibres 80/60, l/d 80 with 60 mm length have the highest presence in any mixture and have the greatest chance of bridging or arresting micro cracks as they are initiated than the other two types of fibres. For example, in mixes containing 50 kg/m^3, there are approximately 3117 of 80/60 steel fibres in a typical beam compared to 2164 of 65/60 and 1905 of 45/50 fibres in the same dosage and size of beam. This is an indication that there are more 80/60 fibres than other types of fibres. For example, in the mixes being considered, there are more 80/60 type of fibres than 65/60 fibres by 953 and then, by 1212 more than 45/50 type of fibres in a typical beam. It is therefore expected that the effect of 80/60 fibre would be felt more during the bridging of cracks within the concrete matrix more than the other types.

5.6 Harmonizing beam and slab results using yield line theory

The results from the 3-point bending test of the beam specimens as shown in section 5.4 and that of square slabs reported in sections 5.5.1 and 5.5.2 distinctively differ. That of the beams have been presented as flexural strength in MPa while the results of the slabs have been expressed in load capacity in kN. Therefore, the theoretical analysis presented here is making use of the flexural results obtained from the beams to predict the failure loads of the slabs using yield line analysis.

All laboratory test carried out in this study have been done as recommended by British standards covering each procedure of test. In the EN 14488-5:2006 standard followed in the mixing, manufacture and testing of the square slab, it was not specified that the corner uplift should be restrained during testing. The procedure as recommended by EN 14488-5 is the modified version of that presented in the Experts for Specialised Construction and Concrete System, EFNARC (British Standards Institute, 2002) which

has been designed primarily to produce energy absorption results for fallout of softer rocks or for stress induced damage absorption (Uotinen, 2011).

The yield-line theory used in this analysis is a usually used technique to determine the capacity of a reinforced concrete slab. It is an ultimate load analysis that establishes either the moments in a loaded slab at point of failure or the load at which an element will fail (Kennedy & Goodchild, 2004). Yield line is a crack in a reinforced concrete slab across which the reinforcing bars have yielded and along which plastic rotation occurs. The virtual work concept is adopted in this study where the plate is divided into yielding regions and virtual work is calculated for both the external loads and the internal energy dissipated. The conditions that must be adhered to is that the sum of the virtual works must be zero if equilibrium is not violated. The yield line pattern is derived from the position of the axes of rotation and ensuring conformity with certain rules as explained by Kennedy and Goodchild (2004). Example of the rule is that the yield line are straight and that they pass through intersection of axes of rotation ending at the slab boundary.

5.6.1 Yield-line pattern

The yield-line pattern were chosen following the conditions mentioned earlier above. Considering how the actual cracks were formed on the slabs at testing, a particular pattern as subjected by Uotinen *et al*. (2013) was adopted as shown in Figure 5.31. The dimension of the slab is 600 mm X 600 mm X 100 mm resting on a free continuous free support with internal dimension of 500 mm. Since the corner uplift was not restrained allowing the plate to rotate, the yield-line pattern adopted is parameterized to find a solution which corresponds to the least work (Uotinen *et al.*, 2013).

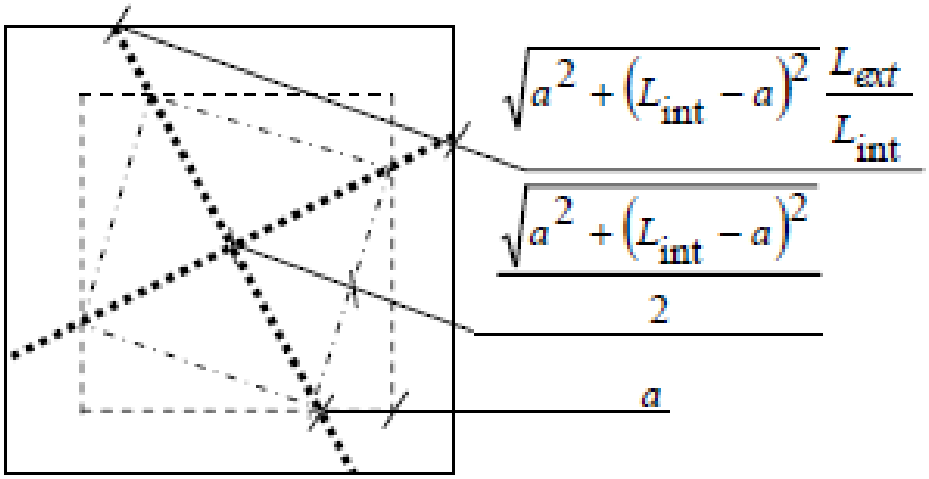

Fig. 5.31. Parameterized orthogonal cross yield-line pattern
(Uotinen *et al.*, 2013)

5.6.2 Virtual work

The virtual work method of yield-line analysis is simply that at failure, the energy expended by the applied loads on the slab must be equal to the energy dissipated by the resisting moments of the slab in rotating the yield lines. In other words, the external virtual work must be equal to the internal virtual work.

i.e. External Work (EW) = Internal Work (IW)

$$\sum (P\delta) = \sum (M_p L\theta) \qquad 5.1$$

Where

EW	=	external energy expended by loads moving
IW	=	internal energy dissipated by yield line rotating
P	=	load acting per unit area
δ	=	vertical displacement of the load at the centroid of slab region
M_p	=	plastic moment of resistance per unit length of the slab
L	=	length of a given yield line
θ	=	rotation of the region about its axis of rotation

The external virtual work is then calculated by taking the resultant of each load (which is a point load at this instance) multiplied by the vertical displacement travelled. The maximum displacement (δ) is normally assumed as unity. The total amount of external work is then expressed as:

$$EW = P\delta \quad (5.2)$$

From Figure 5.31 above, using parametrical representation, it can be shown according to Uotinen *et al*. (2013) that any orthogonal yield-line pattern will result in the same internal work as follows,

$$IW = 9.6M_p\delta \quad (5.3)$$

Therefore, for the parameterised orthogonal cross yield pattern, the sum of virtual work must be zero for any square slab. The virtual displacement being unity, failure load will be

$$P = 9.6M_p \quad (5.4)$$

The moment (M_p) in equation 5.4 is required and can be calculated adopting the basic approach for point loads as provided in the Concrete Society's Technical Report No. 34 on guide to design and construction of concrete floors (Cemex Mortars, 2016). The reports states that the moment per unit length at which the flexural tensile strength of concrete is reached is given by:

$$M_p = \frac{f_{ct}\, h^2}{6} \quad (5.5)$$

Where f_{ct} is the characteristic flexural strength of the plain concrete (MPa) and h is the slab thickness in mm. The Flexural tensile strength based on the 3 point bending test can be calculated as follows:

$$f_{ct} = \frac{3PL}{2bd^2} \quad (5.6)$$

Where *P* is maximum load on beam before failure. *L* is the test span, *b* is the section width while *d* is the section depth.

Therefore;

$$M_p = \frac{(3PL|2bd^2)h^2}{6}$$

Hence, Equation 5.4 becomes:

$$P = 9.6\frac{(3PL|2bd^2)h^2}{6}$$

Alternatively, Dupont and Vandewalle (2004) and Chotard et al. (2003) have determined yield line moment of round panel of thickness 75 mm which was based on the static equilibrium of bending moment of RILEM 3-point bending test. Therefore, the yield line moment M_p has been calculated as:

$$M_p = \frac{F_{ct}\ X\ I}{L} = \frac{\left(\frac{2}{3}f_{ct}b\frac{h}{2}\right)\ X\ \left(\frac{2}{3}h\right)}{\mathrm{L}} \qquad 5.7$$

Where

F_{ct} = flexural tensile strength in MPa

b = width of the notched section, b = 150 mm

h = depth of the notched section, h= 125 mm

L = span of prism specimen, L= 500 mm

I = 2h/3 = distance between F_{cc} and F_{ct} as shown by Le (2005) in Figure 5.32 below;

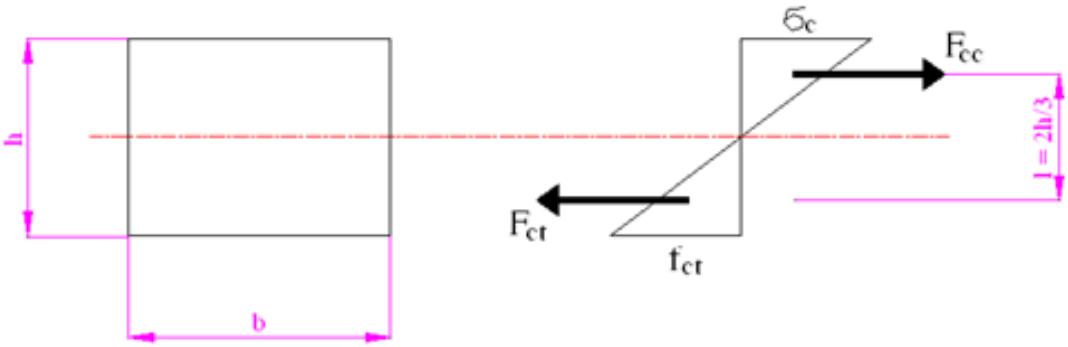

Fig 5.32. Stress distribution

The static equilibrium of stress of a specimen in flexure makes the Compressive stress to be equal to flexural tensile stress as in Figure 5.32.

5.6.3 Prediction of failure loads of slabs from flexural results of beams

In this investigation, flexural strength results of the beams containing 50 kg/m^3 of steel fibres 45/50, 65/60 and 80/60 at 3-point bending were used in predicting the failure loads of the slabs. The mixes containing both maximum coarse aggregate sizes of 10 mm and 20 mm have been considered. The maximum flexural strength attained at the beam tests were used for this analysis, bearing in mind the failure load of the slabs under consideration are all at the maximum point. For example, the beam containing steel fibres 45/50 with 20 mm maximum aggregate size produced a maximum flexural strength of 6.72 MPa at 3-point bending test, from the equations 5.7 and 5.4 above, the yield line moment M_p and the load, P can then be respectively calculated as follows;

The maximum flexural strength of beam 45/50 + 20 mm = 6.72 MPa

The beam is of 150 mm X 150 mm X 600 mm, span 500 mm and depth of notched section is 125 mm. The beam at flexure makes I = 2h/3.

The moment, M_p is

$$M_p = \frac{\left(\frac{2}{3} 6.72\ X\ 150 \frac{125}{2}\right) X \left(\frac{2}{3} 125\right)}{500} = 6999.72 \text{ Nmm/mm} = 7.0 \text{ kN m/m}$$

Therefore, the load, P = 9.6 M_p;

$P^{\text{estimated}}$ = 9.6 X 7.0 = 67.20 kN

The experimental value of the average failure load of three replicates slabs of mix containing steel fibres 45/50 + 20 mm is 71.56 kN.

Table 5.2 gives the details of both estimated and experimental values of the failure loads on the different mixes of the slabs. The values presented in Table 5.2 below for both used in the calculation of estimated and experimental loads are all the average of three replicates of the specimens employed in the study.

Table 5.2 : Prediction of failure loads of SFRC panels

Steel fibres configuration in mix	Aggregate size (mm)	Estimated failure load on slab (kN)	Experimental failure load from beams (kN)
45/50	10	62.30	92.94
65/60	10	73.60	98.09
80/60	10	75.00	107.92
45/50	20	67.20	71.56
65/60	20	73.90	75.57
80/60	20	70.40	88.00

From the predicted results in Table 5.2, the values of estimated failure load and experimental failure load of steel fibre reinforced square panels can be seen. The values are reasonably close when considering square panels of mixes containing 20 mm

maximum aggregate size, especially the mixes with steel fibres 45/50 and 65/60. On the other hand, the range of values of estimated and experimental loads for mixes containing 10 mm maximum aggregate size are a bit wide when comparison was made. This is due to the pattern and configuration of the specimens and experimental procedures as specified by the British Standards employed in this investigation. The results would have been different if the round panels were used as specified by other standards like ASTM (American Society for Testing and Materials). As earlier reported in section 5.5.3 of this chapter, the crack pattern of slabs containing 10 mm maximum aggregate size slightly defers from their 20 mm maximum aggregate size counterpart, this might be responsible for the differences in the failure load values. More so, the methods of harmonisation using the flexural strength results of beams to predict the failure loads of the slabs by yield line analysis does not take care of the different mechanisms of slab failures as yield line moment (M_p) is not a characteristic of structures but of materials.

Marti et al. (1999) in a study to harmonize test procedures for steel fibre reinforced concrete identified that the square slab tests are not straightforward to evaluate and that significant differences exist among the test procedures specified by different standards. The researchers then determined the moment per unit slab width considering different failure mechanisms resulting in different crack patterns. Two main crack patterns (four diagonal cracks and that of eight cracks) for square slabs were thus presented as follows;

$$M_p = \frac{F\ (b-a)}{8(b+2c)} \qquad 5.8$$

$$M_p = \frac{F\left(b-a\sqrt{2}\right)}{16\left(\sqrt{2}-1\right)(b-2c)} \qquad 5.9$$

Where

M_p = yield line moment

F = failure load of slab

b = span of the slab,

a = central inner square where cracks originates (taken as the rigid square load point)

c = the support edge

Equation 5.8 represents associated moment per unit slab with four crack pattern while equation 5.9 represents that with 8 crack pattern.

Interestingly, by applying equation 5.8 to the slab analysis under consideration and with the selected pattern of the four major cracks on most of the slabs tested, especially with those containing 20 mm aggregates, the equation agrees with that formulated by Uotinen *et al*. (2013), that is, equation 5.4. By substituting the values from the dimension of slab, b= 500, c= 50 and equating 'a' to be zero, equation 5.8 becomes;

$$P = 9.6M_p$$

However, equation 5.9 failed to take care of more cracks pattern experienced in some of the slabs in the sense that where more cracks have been noticed in the slab failure mechanism, it led to higher failure load in steel fibre reinforced concrete slab. This is due to the effective action of steel fibres in the mixes whereby the propagation of cracks was altered by the bridging mechanism of steel fibres resulting in dissipation of load to other stable parts of the slab manifesting in more cracks. This scenario played out more in square slabs containing 10 mm maximum aggregate size. However, if equation 5.9 is applied to this failure mechanism of slabs with more cracks, the values of failure loads would be reduced instead of increasing, which is the reflection of experimental failure loads. This also might be responsible for wide gap between estimated and experimental values in Table 5.2 mostly noted in slabs containing 10 mm maximum aggregate size.

CHAPTER 6

X-RAY COMPUTED TOMOGRAPHY IMAGING; RESULTS, DISCUSSION AND ANALYSIS

6.1 Introduction

In the previous chapters, compressive strength, flexural and post-cracking behaviour of different combinations of steel fibre dosages and maximum aggregate sizes including fibre geometry were determined. Different specimens were employed in carrying out the experimental tests to consider the effects of steel fibres and other selected variables on the mechanical properties of steel fibre reinforced concrete.

This chapter presents the procedures of using X-ray computed tomography (CT) imaging technique to investigate the distribution and orientation of steel fibres within the hardened concrete through scanning undertaken at University of Nottingham. The conversion of scanned images acquired from X-ray CT accomplished by employing the Insight Toolkit (ITK) software. The image processing was completed by an image analysis expert, Dr John Chiverton of the School of Engineering, University of Portsmouth. A complete description of the process used is given in this chapter to aid the reader's understanding of the subsequent outputs from his work. The chapter concludes with an analysis of the observed correlations between fibre distribution/orientation and mechanical performance of fibre reinforced concrete.

6.2 Preparation of SFRC cores from slab specimens

The square steel fibre reinforced concrete slabs of size 600 mm by 600 mm by 100 mm with dosage of 50 kg/m^3 of steel fibres after being tested for flexural and load bearing capacity were marked as shown in Figure 6.1 from which two core samples were

extracted. The cores were extracted from the areas randomly selected but in such a way that are far apart from each other to roughly represent the characterization of the slab.

Figure 6.1: Markings on slab showing where cores are to be extracted

One of the cores was made to be extracted close to the edge of slab (about 50 to 90 mm to the edge) while the other was made close to the centre of the slab as much as possible bur not too close so as not to be affected by the cracks in the centre of the slab. The cores were named ‘a’ and ‘b’ describing cores from same slab. For example, the two cores extracted from the slab in Figure 6.1 were tagged 3a and 3b with their other composition, the fibre types and aggregate size noted.

6.2.1 Extraction of cores

Extraction of cores from the slab was made possible by D-Drill Group using HILTI Diamond Coring Tool DD 350. The coring drill is an electric drill motor with a rated voltage of 110 V, rotational speed gear under no load ranging from 670 – 240 revolutions/minute and with 10 electronically switched gears. The drilling machine has a stand system for variety of core drilling applications with ‘Iron Boost’ for a quick performance with increased torque when drilling through rebar (HILTI, n.d.), and other

materials like steel fibre concrete. The tool was integrated with vacuum base while the coring bit of required diameter (100mm) was fixed before drilling operation as shown in Figure 6.2. The operation was a wet drill as water was supplied by hose during drilling process.

Figure 6.2: Extraction of SFRC cores by drilling machine

The drilling of the cores was easily operated since the depth of the cores at 100 mm was far less than the maximum drilling depth of the machine which is 500 mm. The core samples produced from the wet drilling process are as presented in Figure 6.3 which are 100 mm in diameter and of height 100 mm same as the thickness of slab from which they were extracted. The cores were extracted from the square steel fibre reinforced concrete slabs only and not from the plain (unreinforced) concrete slabs

since the objective was to investigate the distribution and orientation of steel fibres within the matrix of hardened concrete.

Figure 6.3: Core samples extracted from tested SFRC slab specimens

6.3 X-Ray CT scanning

After the extraction of the core samples from the tested slabs, the samples were taken for X-ray CT scan. The high resolution X-ray CT facility at University of Nottingham, Nottingham, UK was employed for this purpose to secure the best results. The X-ray Computed Tomography facility at Central Engineering Stores, Faculty of Engineering, University of Nottingham, United Kingdom employed in this research work. The high-resolution X-ray facility at University of Nottingham uses a dual-spot 350-kV X-ray source, with spot sizes of 0.4 and 1.0 mm. The small spot has a maximum load of 720 W, and the large spot has a maximum load of 1485 W (TEXASGeosciences, 2015).

X-ray computed tomography (CT) is a novel and rapidly evolving technology of proven value ideally suited for a wide range of geological investigations which is a non-destructive method for producing images which correspond closely to serial sections

through an object (Ketcham & Carlson, 2001). X-ray CT was originally developed for medical applications but has now been applied as a tool for investigating the properties of concrete as well as geological materials. CT scanning technology can reveal the internal meso/microstructure of materials and the reason why it has been applied in this research is to investigate the distribution and orientation of steel fibres within the matrix of hardened steel fibre reinforced concrete. TEXASGeosciences (2015) reported that because industrial CT systems image (captures) only non-living objects, they can be designed to take advantage of the fact that the items being studied do not move and are not harmed by X-rays. Therefore, the use of higher-energy X-rays, which are more effective at penetrating dense materials is made possible with longer exposure times, increasing the signal-to-noise ratio to compensate for the loss in signal from the diminished output and efficiency of the source and detectors. There is also the possibility of using finer and more densely packed X-ray detectors which also increases resolution at a cost in X-ray output.

6.3.1 CT Scanning technique

The process of scanning the core samples have been partly described in chapter 4 of this thesis. Furthermore, the volume CT (Computed Tomography) employed in this investigation uses X-rays source and detectors to digitally cut the core sample open to reveal the internal details. The cutting of the sample then produces CT images which are presented in a format called ‘slices’ with a corresponding thickness of the steel fibre reinforced concrete core which is being scanned. Also, unlike a typical digital image which is composed of pixels, a CT slice image is composed of voxels meaning volume elements. The recommended and most efficient geometry to scan in CT scanning system is a cylinder because of the full scan field of CT which is a cylinder, a stack of circular fields of view (TEXASGeosciences, 2015). Therefore, in the case of the 100 mm height steel fibre reinforced concrete cores, the scans are taken 1 mm apart and the voxels have dimensions of 0.0652 mm in x and y, and 0.4 mm in z axis. This produced 90 slices per core.

The X-ray CT scan equipment at University of Nottingham used in scanning the core samples drilled from tested steel fibre reinforced concrete slabs are presented in Figures 6.4 and 6.5 showing the core sample with the equipment set up and the equipment with the computer system attached respectively. The computer system is used during the reconstruction which is the mathematical process of converting sinograms into two-dimensional slice images. The computer system is used to determine the range of CT numbers or CT values to which the raw intensity data in the sinogram are converted to. The systems use a 16-bit scale, which has been reported to allow values ranging from 0 to 65535 which correspond to the grayscale in the image files created or exported by the systems (TEXASGeosciences, 2015).

Figure 6.4: Core sample with X-ray CT facility ready for scanning

The steel fibre reinforced concrete cores subjected to CT scan is of different components ranging from aggregates, cement matrix and fibres. However, CT has been

described as being appropriate for the inspection of a range of components that are non-invasive and are unlimited by the complexity of internal and external surfaces, since high-energy CT system can penetrate large objects fabricated from wide variety of materials (Chotard et al., 2003).

Computed Tomography creates two-dimensional or three-dimensional imagery of the internal structure of the solid objects that usually reflect relative X-ray attenuation, which is primarily a function of the X-ray energy and the density and atomic number of the material being scanned (Ketcham & Iturrino, 2005). Steel fibre reinforced concrete cores is a high density material which is being scanned by high resolution CT scan facility, these parameters are those that successful imaging are depended on.

Figure 6.5: X-ray CT equipment with attached computer system for data processing

6.3.2 Acquisition of CT images

The most important components in X-ray CT scanning process that determine the clarity of the output images are the X-ray source, attenuation and detectors. The X-ray source according to Ketcham and Carlson (2001) is however dependent on size of the focal spot, the spectrum of X-ray energies generated, and the X-ray intensity while the focal-spot size partially defines the potential spatial resolution of a CT system by determining the number of possible source-detector paths that can intersect a given point in the object being scanned. Furthermore, the penetrating power of X-rays and their expected attenuation when they pass through the material comprising different density are determined by the energy spectrum. On the part of X-ray intensity, TEXASGeosciences (2015) states that X-ray intensity directly affects the signal-to-noise ratio and thus image clarity and that higher intensities improve the underlying counting statistics, but often require a larger focal spot.

6.3.2.1 X-Ray Attenuation and detectors

The remarkable characteristic of X-Ray CT that makes it possible for imaging of the internal structure of the steel fibre reinforced concrete cores is their penetrating ability. When the radiation is directed to the cores, some of the photons are absorbed or scattered while others completely penetrate the cores. The penetration of any object therefore depends on energy of the individual photons and the density, atomic number and thickness of the object being scanned, therefore, increasing photon energy generally decreases the probability of attenuation and increases penetration (Sprawls, n.d.).

According to TEXASGeosciences (2015), the attenuation of the X-rays signals passing through the object being scanned is by scattering and absorption, and followed the basic equation for attenuation of a monoenergetic beam through a homogeneous material which is Beer's Law:

$$I = I_0 \, exp[-\mu \, x] \tag{6.1}$$

where I and I_0 are the final and the initial intensities respectively, μ is the linear attenuation coefficient (linear absorption coefficient) for the material being scanned and having a unit of 1/length, x corresponds to the length of the X-ray path through the material. Equation 6.1 only applies to a perfectly homogeneous material, in this present case however, the tested material, steel fibre reinforced concrete core is composed of a number of different materials, hence, the equation becomes

$$I = I_0 \, exp\left[\sum_i (-\mu_i x_i)\right] \tag{6.2}$$

Where I represents a single material with attenuation coefficient μ_i over a linear extent x_i.

The detectors influence image quality through their quantity, size and efficiency in detecting the energy spectrum generated by the X-ray source while the number of detectors determines the amount of data that can be gathered simultaneously (Ketcham & Carlson, 2001). The detector used to capture attenuated flat fan-shaped beam in this research work consisted of a single line array of over 3000 light sensitive diodes.

6.3.2.2 CT images

The steel fibre reinforced core was positioned on the manipulator, after the scanner had been calibrated and optimized, the X-rays were acquired as they pass through a calibration material over a 360° rotation. The manipulator was responsible for the rotation and vertical movement of the core sample. The movement of core sample was done after each scan had been completed in order to get set for the next scan. As the core specimen rotates, the X-ray source at discrete intervals emits rays which pass through the core and are collected by the detector. Halverson et al. (2005) reported that as the sample is rotated inside the X-ray fan beam, the rays collected as shadow at each interval (views) is numerically processed and translated into a two-dimensional cross-section slice, and by measuring several of these cross-sections at small intervals,

they can be stacked upon another to form a three-dimensional digital representation of variations in sample density.

Finally, the images are then stored in 'Tagged Image File' TIF format as seen in Figure 6.6, showing typically images in form of 'slices' from steel fibre reinforced concrete core extracted from slab containing 20 mm maximum aggregate size and steel fibre 45/50, representing aspect ratio 45 and fibre length 50 mm. Figure 6.6 a, b and c correspond to slices 3, 53 and 89 respectively which are slices picked from top, middle and bottom of the core comprising of 90 slices. From the horizontal slices obtained by X-ray CT scan through the 100 mm core at different heights, direct observation can be carried out as fibres can be clearly seen within the concrete matrix in the images.

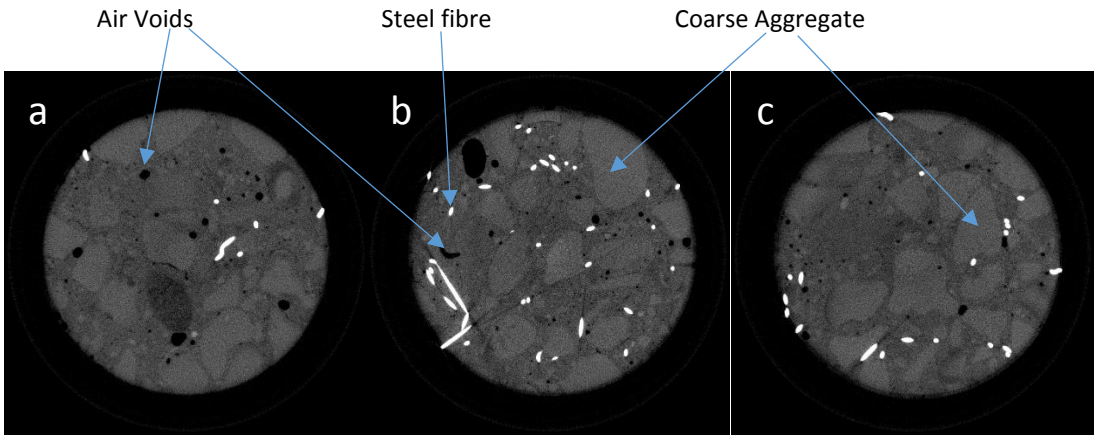

Figure 6.6: Volumetric X-ray CT image slices from different height of a typical core sample of 45/50 + 20 mm

The fibres show up as white elements all over the surface of the round horizontal slices of 100 mm diameter as seen in Figure 6.6 a, b and c. The shape of a fibre on these images provides information about their orientation relative to the plane of the images. Fibres lying close to parallel show as short or long line, in distinctive white colour (very high density of steel fibre at advantage) while fibres lying perpendicular to the plane of the image (i.e. parallel to the axis of the core) show as dots or circles. Air

voids in Figure 6.6 are shown in black because of their very low density while the coarse aggregate of better density can be clearly seen in the slices as well.

Figure 6.7 (a, b, and c) shows the slices from different height of a typical core sample of fibre 45/50 containing 10 mm maximum coarse aggregate size. Figure 6.7 a, b and c correspond to slices at top, middle and bottom of the core respectively.

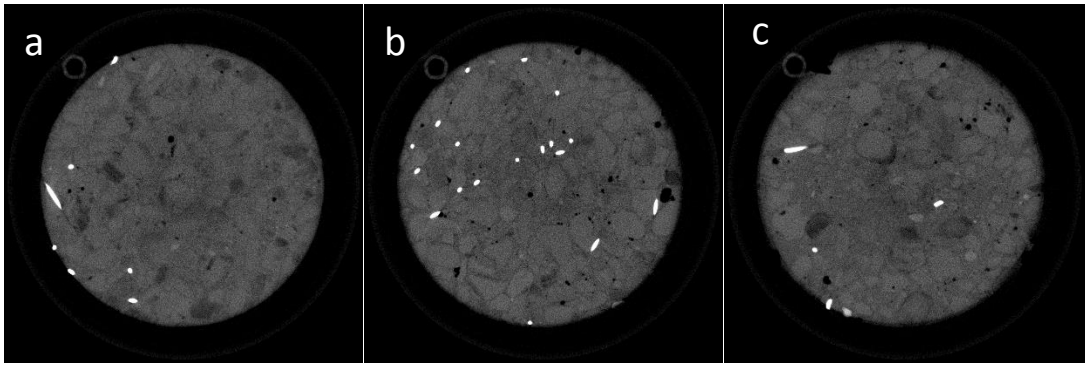

Figure 6.7: Volumetric X-ray CT image slices from different height of a typical core sample of 45/50 + 10 mm

Cores of the same fibres but with different maximum coarse aggregate sizes were selected for the visual inspection to give insight into the nature of fibre distribution between the two mixes as revealed in the shown slices. The slices in both Figures 6.6 and 6.7 were from the same heights at the top, middle and bottom of the core. By visualising the position of fibres in the slices, it can be observed that the distribution of steel fibres in the concrete matrix followed the same trend in both Figures 6.6 and 6.7, the fibres were fairly distributed at the middle of the cores than at the top and bottom. Figures 6.8 and 6.9 show more image slices from different heights of different cores from mixes containing both 10 mm and 20 mm maximum coarse aggregate sizes. The number on each slice denotes the slice number as regarding the height of the core from slice 01 to slice 90 representing top to bottom. The 10 mm or 20 mm stands for the maximum aggregate size of the mixture that produced the core.

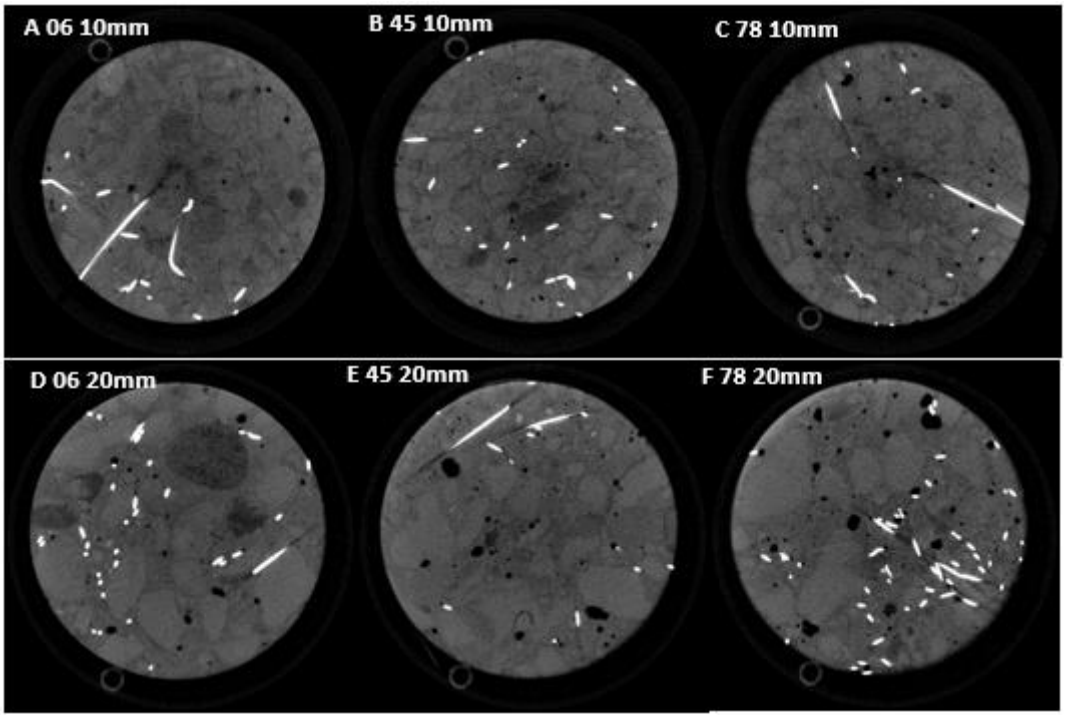

Figure 6.8: Volumetric X-ray CT image slices from different height of typical core samples of fibre 65/60 with 10 mm and 20 mm mixes

Visual inspection of the image slices reveals that the coarse aggregates in slices with 20 mm aggregate size are distinctively recognised in the image than the counterparts in 10 mm maximum aggregate size cores.

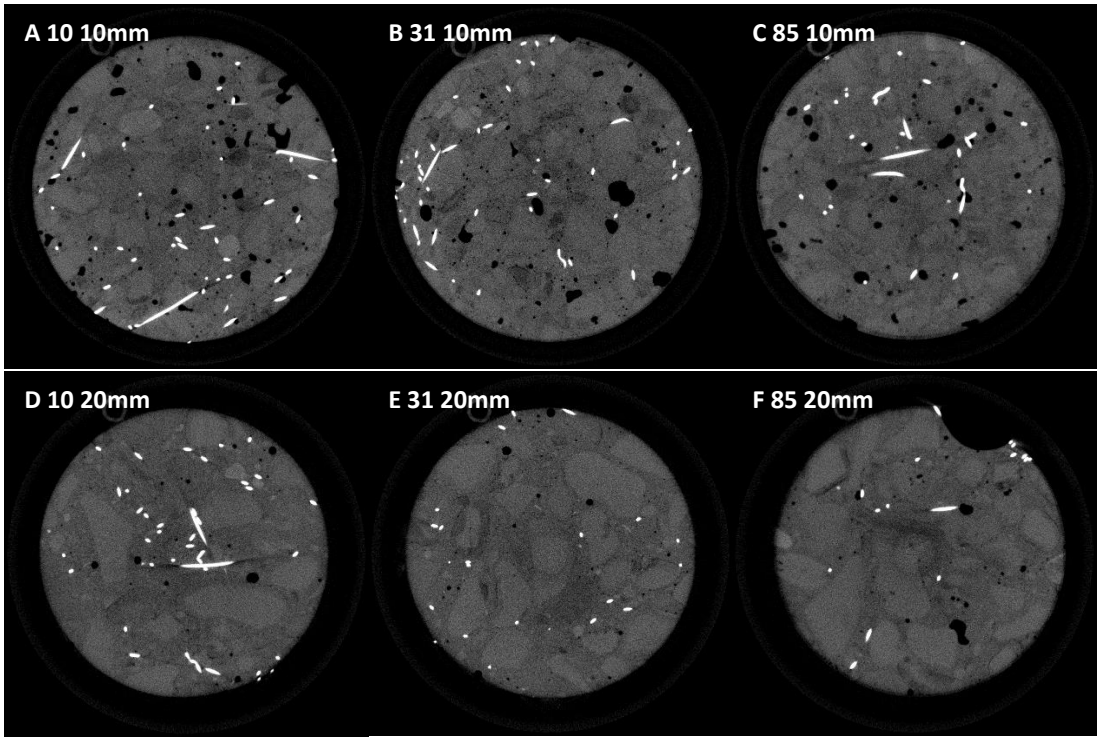

Figure 6.9: Volumetric X-ray CT image slices from different height of typical core samples of fibre 80/60 with 10 mm and 20 mm mixes

It can be observed from Figure 6.9 that the distribution of steel fibres within the concrete matrix seems better in slices from 10 mm maximum aggregate size than what is obtainable in slices from 20 mm maximum aggregate size cores. The spaces without the whitish appearance of steel fibres are more in slices D, E and F compared to their counterparts in A, B and C. However, there are more air voids noticed in image slices of 10 mm maximum aggregate size.

The 3D view shown in Figure 6.10 was achieved by the analysis carried out on a typical core combining all the slices together. Figure 6.10 (a) was to visualise the positioning of the fibres within the SFRC core to ensure that the data was loading correctly into an appropriate 3D volume with a short video to demonstrate how the volume appears in 3D. Figure 6.10 (b and c) presents the animations of the fibre positioning within the matrix at two different axis. The images shown in the figure are the analysis performed

on the first 30 slices, it was done on 30 slices at a time before combining them to make a whole.

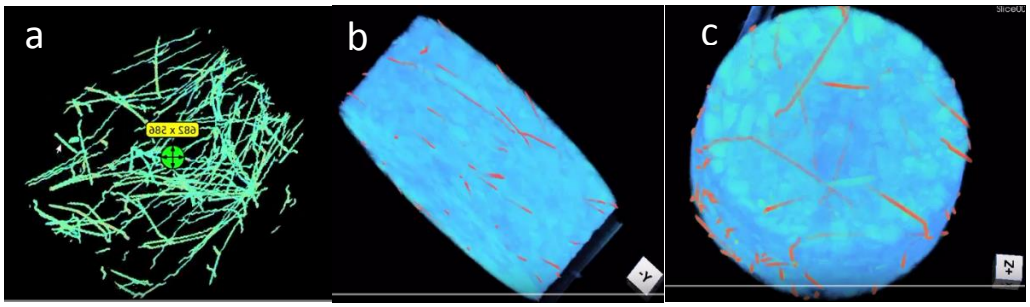

Figure 6.10: Analysis of CT image slices. (a) 3D volume view, (b) animation viewed at –Y axis and (c) animation viewed at +Z axis.

6.4 Image processing

The volumetric images that were acquired from CT scan presented in horizontal slices at different heights through the 100 mm diameter and 100 mm height core require further analysis to develop a technique that will allow quantification of distribution and orientation of the fibres within each image slice and within the whole core. This process of quantification would enable an investigation of the correlation between the distribution and orientation of fibres within concrete and the mechanical properties of the resulting steel fibre reinforced concrete such as load bearing capacity, residual flexural strength and energy absorption.

There have been a number of techniques adopted by various researchers for determining the distribution and orientation of fibres in fibre reinforced composites, namely: X-ray computed tomography (CT) scan (Barnett et al., 2010; Ponikiewski et al., 2014; Suuronen et al., 2013), magnetic method (Ferrara et al., 2012), ultrasound and quantitative acoustic emission technique(Reinhardt et al., 2001), image analysis technique (Abrishambaf et al., 2013) and electrical resistivity method (Barnett et al., 2010; Lataste et al., 2011). The X-ray CT method was adopted for this research work

while open source medical image processing C++ libraries, The Insight Toolkit (ITK), (Yoo et al., 2002) was used by an image analysis expert, Dr John Chiverton to process the images from CT scan.

6.4.1 Image analysis software

The Insight Toolkit (ITK) is an open-source software toolkit for performing registration and segmentation. Segmentation is the process of identifying and classifying data found in a digitally sampled representation, which is an image acquired from such instrumentation as CT scanners, ITK employs leading-edge segmentation and registration algorithms in two, three, and more dimensions (The ITK software, n.d.). The software, ITK is implemented in C++. ITK is a useful collection of software functions that are able to perform quite a wide range of algorithms on imaging data, such as aligning two different image data, thresholding and many others.

In combination with ITK software for this research work are other software like Visualisation Toolkit (VTK) and VolView. VTK is also an open source software system mainly used for 3D computer graphics, image processing and visualization of volumetric imaging data using software programs written by users of the library. VolView on the other hand is not a library but an application for viewing image data and similar. VolView does not require any programming.

6.4.2 Outline of image processing technique

The systematic step-by-step procedure in analysing the volumetric images acquired from CT scan is presented in the flow diagram in Figure 6.11. The flow chart summarised the technique adopted in the analysis of the CT scan image for the quantification of distribution and orientation of fibres within concrete matrix. This procedure includes binarization of image data, thinning and skeletonization technique, application of distance transform, histogram and entropy computation. The

distribution orientation of steel fibres in the concrete were then accomplished by application of statistical tools.

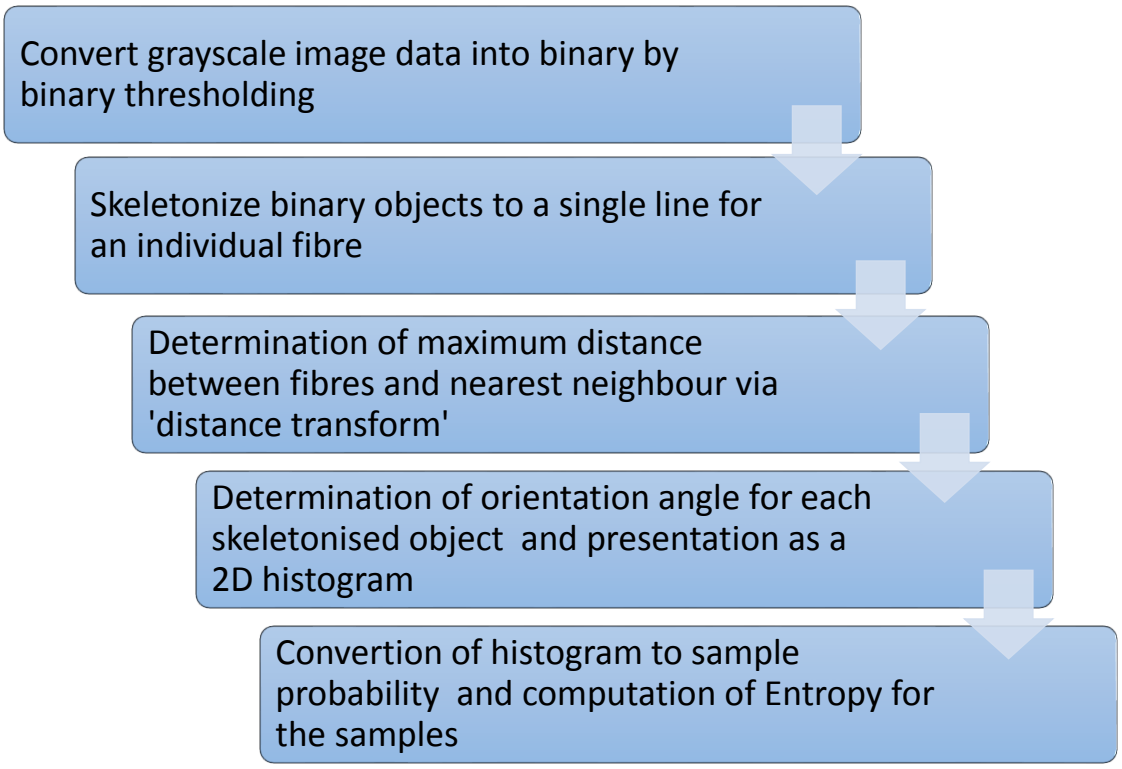

Figure 6.11: Flow diagram of image technique

6.4.3 Binary thresholding

This is the operation of converting a grayscale image that may vary in value to an image consisting of only two values. Here, the filter produces an output image whose pixels are one of two values, outside value or inside value depending on whether the corresponding image data pixels has a value above upper threshold or below lower threshold, if the value is above, it is set to upper threshold and if below, it is set to lower threshold while values equal to either threshold is regarded to be between the thresholds.

This is useful because the steel fibres have high intensity and if thresholding the image data, then it is deciding where the fibre material is or is not. Mathematically:

$$\text{Output (xi)} = \begin{cases} Inside\ Value\ if\ Lower\ Threshold \leq xi \leq Upper\ Threshold \\ Outside\ Value \qquad otherwise \end{cases} \tag{6.3}$$

Here, the filter is templated on the input image type and the output image type while both images are expected to have the same number of dimensions. The output of this filter is binary and follow this trend; InsideValue if the pixel value falls inside the threshold window, or OutsideValue otherwise. Figures 6.12, 6.13 and 6.14 show examples of images of both original slice image and image using the Binary threshold image filter.

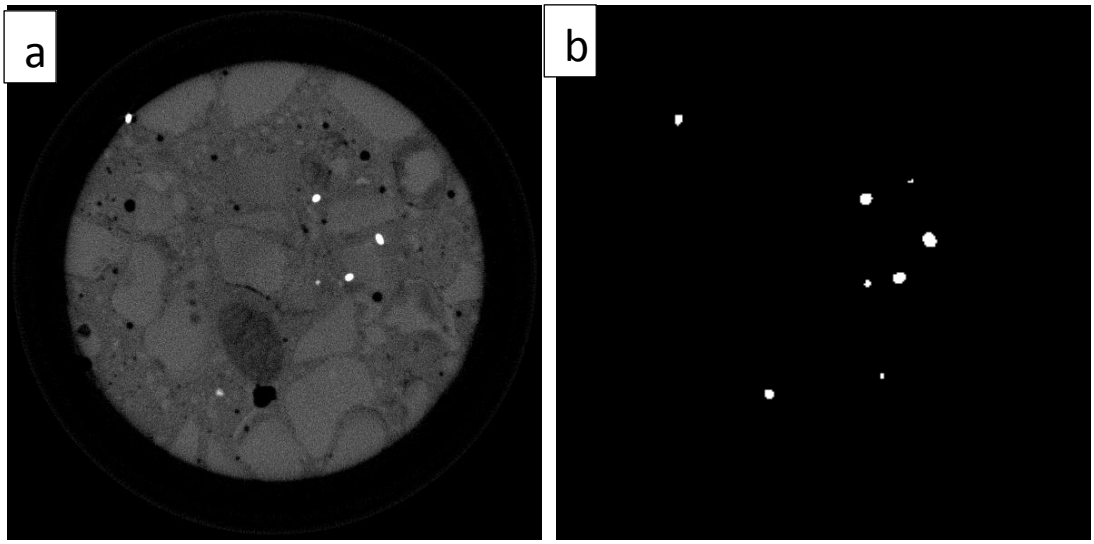

Figure 6.12: Conversion of grayscale image of slice 01 of core from slab 45/50, (a) original slice image and (b) image after conversion

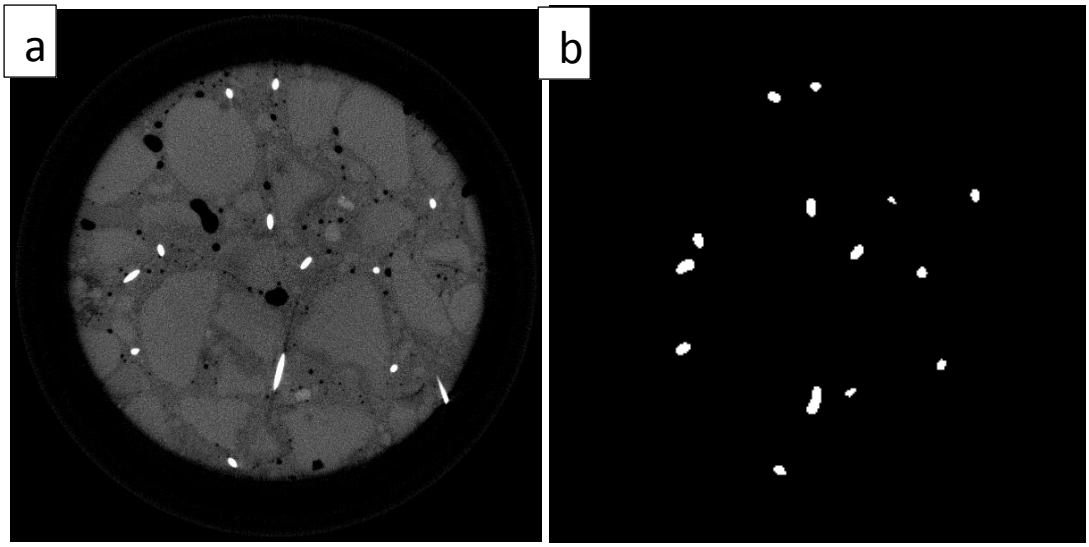

Figure 6.13: Conversion of grayscale image of slice 20 of core from slab 45/50, (a) original slice image and (b) image after conversion

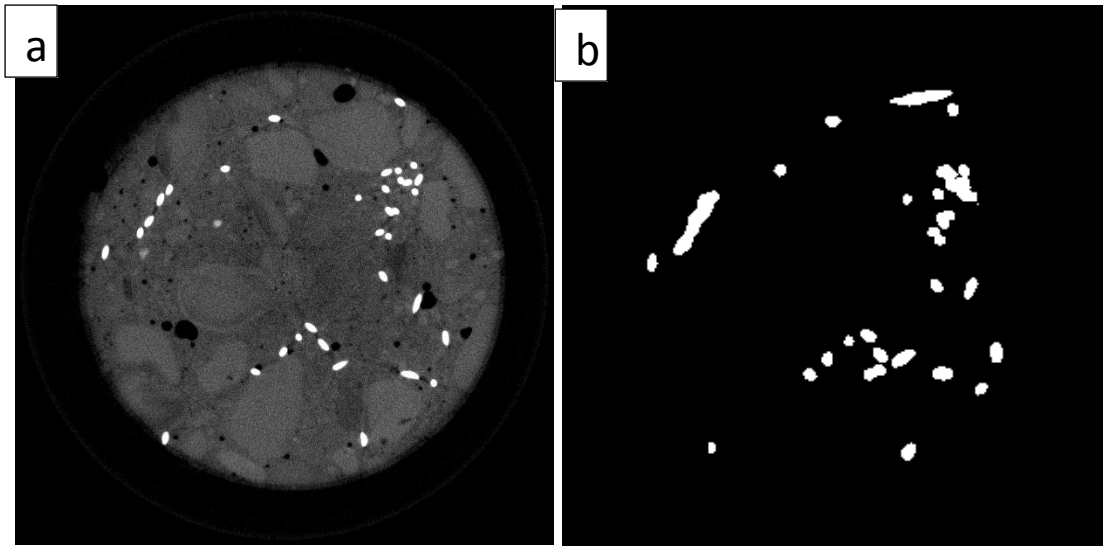

Figure 6.14: Conversion of grayscale image of slice77 of core from slab 45/50, (a) original slice image and (b) image after conversion

From Figures 6.12, 6.13 and 6.14, the resulting images as shown in 'b' part of the figures are the output after the convention by Binary threshold image filter to clearly single out the steel fibres in the volumetric images. The correlation between 'a' and

'b' part of the figures can be noticed visually, though in some cases, it is picking up extra things or combining several fibres into one.

6.4.4 Skeletonization of binary objects

This is the process that reduces the fibres down to a single pixel/voxel width in diameter while still preserving the shape and topology of the original object. This process directly followed after deciding where fibre material is located for which voxel/pixel. The reason for doing this is because it reduces the number of points that need to be processed by the computer later and it is also helpful in making a decision on the overall direction that a fibre is pointing.

The technique used here to reduce fibres down to a single line is "Thinning", an iterative object reduction technique that removes a layer of points from the outside of each fibre until there is only one pixel thin fibre left. According to Palagyi (n.d.), some beneficial properties thinning include

- Preservation of topology of the original object
- Preservation of the shape by extracting feature suitable for object recognition
- It forces the "skeleton" to be in the middle of the object, and
- It produces one pixel/vowel width "skeleton"

After thinning the direction for each fibre is estimated using an estimation algorithm that is capable of estimating the parameters for a straight line in 3D.

6.4.5 Probability and orientation

Probability distribution is a useful tool that is often considered for all the fibres in a volume it helps understand how fibres are distributed within a volume or sub-volume. Often, the full orientation of fibres is not needed and it may be preferred to somehow summarize the distribution of the fibres in terms of how randomly they are distributed.

For each fibre *i* in the volume, the discrete angle indices are calculated with

$$\begin{cases} n_i = cos^{-1}\,(z)\frac{N}{\pi}; \\ m_i = tan^{-1}\left(\frac{y}{x}\right)\frac{M}{2\pi}, \end{cases} \tag{6.4}$$

where N and M are the number of values in which the angles are divided so that the orientation distribution is discretized. Then the probabilities of fibre direction;

$$\hat{P}(n_i, m_i) = \frac{f(n,m)}{\sum_{\forall n} f(n_i m_{i)}} \tag{6.5}$$

Where $$p(n,m) \cong \hat{p}(n,m) \tag{6.6}$$

i.e. the probabilities *p(n, m)* are approximated by the sample probabilities $\hat{p}(n,m)$ which were calculated from histogram *f(n, m)* of the fibre directions, discretized using equation (6.4).

A point estimate to measure the degree of randomness used here is Shannon's Entropy, given by

$$H = \sum_{n,m} P(n,m) log_2 \left(\frac{1}{p(n,m)}\right) \tag{6.7}$$

For fibre detection, the directionality of steel fibres in volumetric data may be corrupted because of the thickness of the steel fibre in relation to the interplane thickness in the acquired X-ray microtomography (XμT) data. Nevertheless steel fibres are detected here using a combination of thresholding and interpolation between detected points. An example output of the fibre detection process is shown in Figure 6.15.

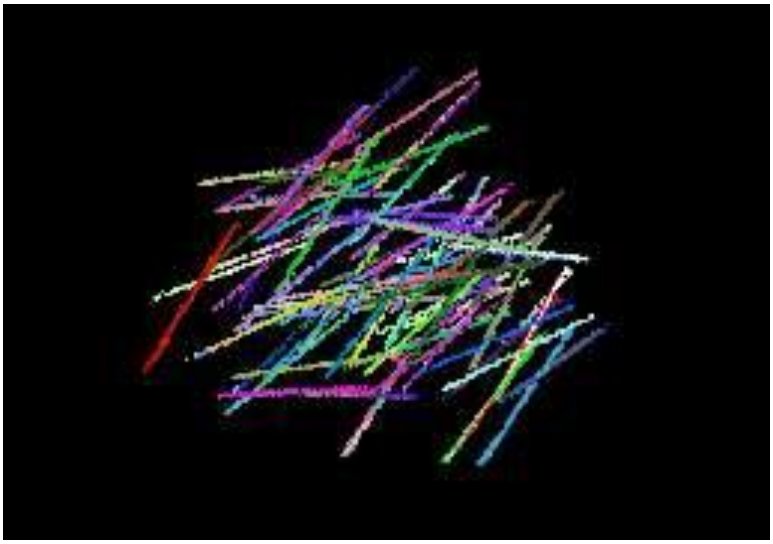

Figure 6.15: Example output of the clustering algorithm used to label individual

6.4.5.1 Volume rendering images of steel fibres in the cores

The 3D rendering images showing the actual volumetric positioning of steel fibres after combining all the 90 slices together to make a whole core of 100 mm height are presented in Figures 6.16 – 6. 18. Two typical cores were randomly selected from a mix proportion of same fibre type and aggregate size while cores of the same fibre type but of different aggregate sizes were compared in each Figure presented below. For clarity, Figure 6.16 shows the cores from mixes containing fibres 45/50 while cores 'A' and 'B' are of maximum aggregate size 10 mm, and 'C' and 'D' are of the same fibre type but of maximum aggregate size of 20 mm. The typical cores randomly selected represent the general appearance of images from the mixture while the two cores from a mixture were selected from deferent slab specimens of the same mix.

The 3D images of concrete cores extracted from slabs containing steel fibres 45/50 as shown in Figure 6.16 reveals that most of the steel fibres are positioned horizontally in the slab and randomly distributed.

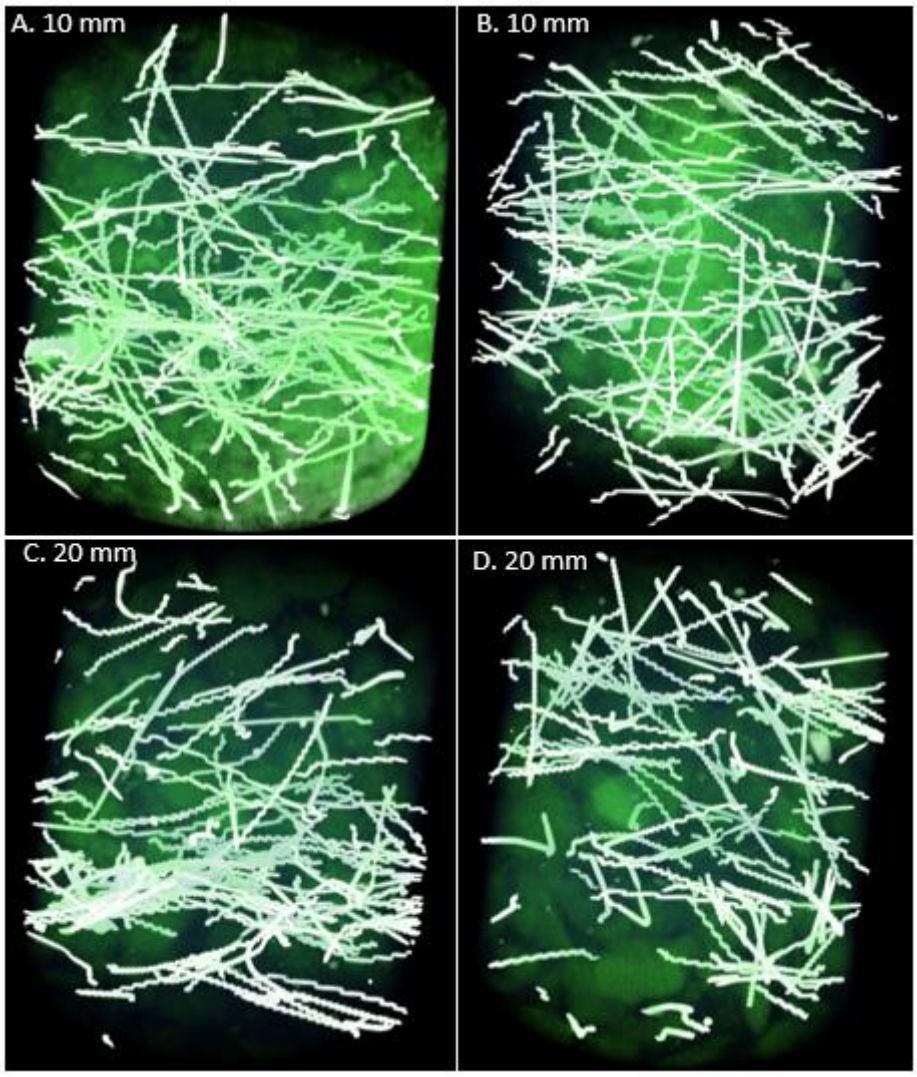

Figure 6.16: 3D rendering images of 45/50 fibres in typical core samples of 10 mm and 20 mm maximum aggregate sizes

Though, some of the fibres are seen in vertical or near vertical position within the cores, there seems to be better distribution of fibres in Figure 6.16 A and B which are cores from 10 mm maximum aggregate size than their counterpart in 'C' and 'D' which are extracted from slabs containing 20 mm maximum aggregate size. The fibres in all the cores as presented in Figure 6.16 (A – D) when compared with the cores in Figures 6.17 and 6.18 can be seen to generally have least presence of fibres which seems more pronounced in cores of 20 mm maximum aggregate size, 'C' and 'D'. The smallest number of steel fibres observed in all the cores of mixes containing fibre 45/50 is anticipated since by calculation, 5,071 of the type of steel fibres are expected to be in

a 600 mm by 600 mm by 100 mm slab considering the properties of steel fibre used in the study as described in section 4.5.4.

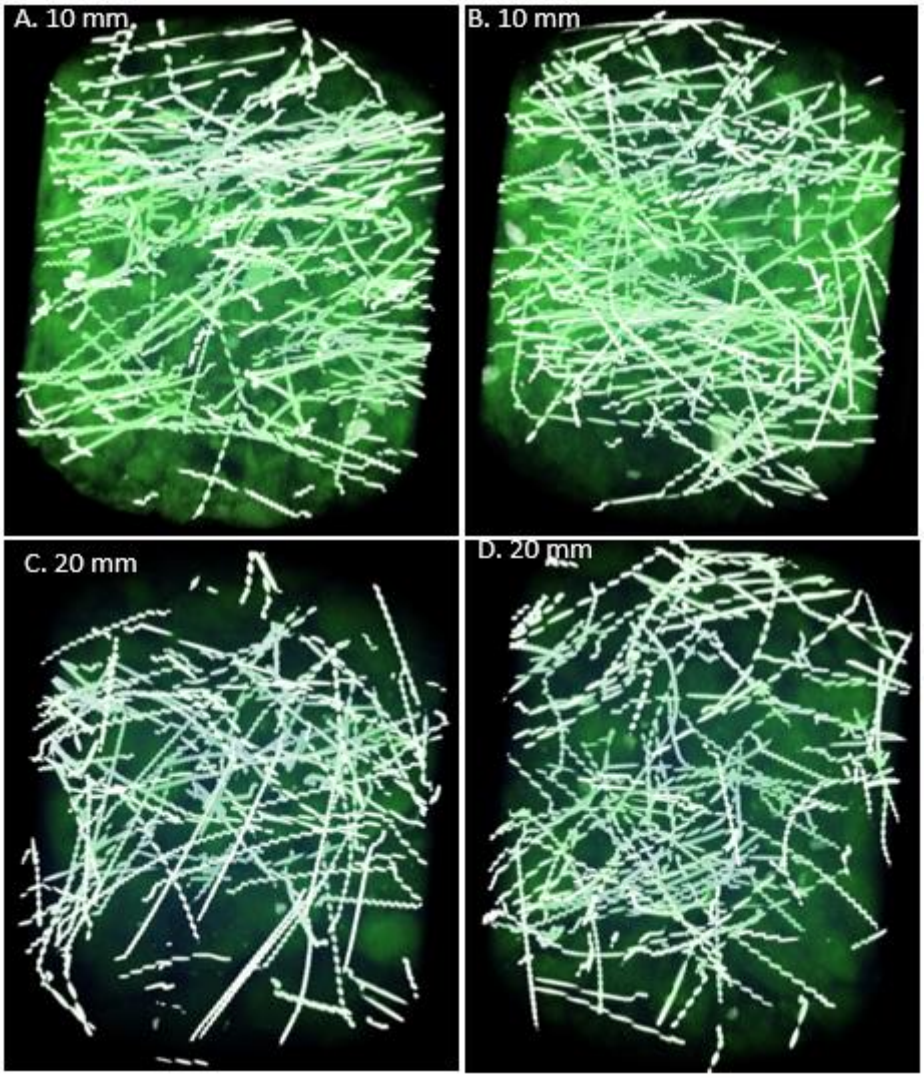

Figure 6.17: 3D rendering images of 65/60 fibres in typical core samples of 10 mm and 20 mm maximum aggregate sizes

Figure 6.17 shows the 3D rendering images of fibres in the cores extracted from slabs containing steel fibres 65/60 with 'A' and 'B' representing the cores from 10 mm maximum aggregate size mixes while 'C' and 'D' are those from mixes of 20 mm maximum aggregate size. It can be observed that majority of the fibres are horizontally positioned as seen in Figure 6.16 while steel fibres in the cores 'A' and 'B' from mixes

of 10 mm maximum aggregate size exhibit a better distribution, more randomly situated around the whole core and show more presence than their counterparts in cores 'C' and 'D' from slabs containing 20 mm maximum aggregate size. Few of the fibres can also be seen in vertical or near vertical positions as well. It can also be noted that all the cores in Figure 6.17 revealed more appearance of steel fibres than the cores in Figure 6.16, which is expected. By estimation, the number of 65/60 type of steel fibres expected to be in each slab is 5,761 which is higher than the number of fibres of type 45/50 in a slab presented in Figure 6.16 by 690 fibres.

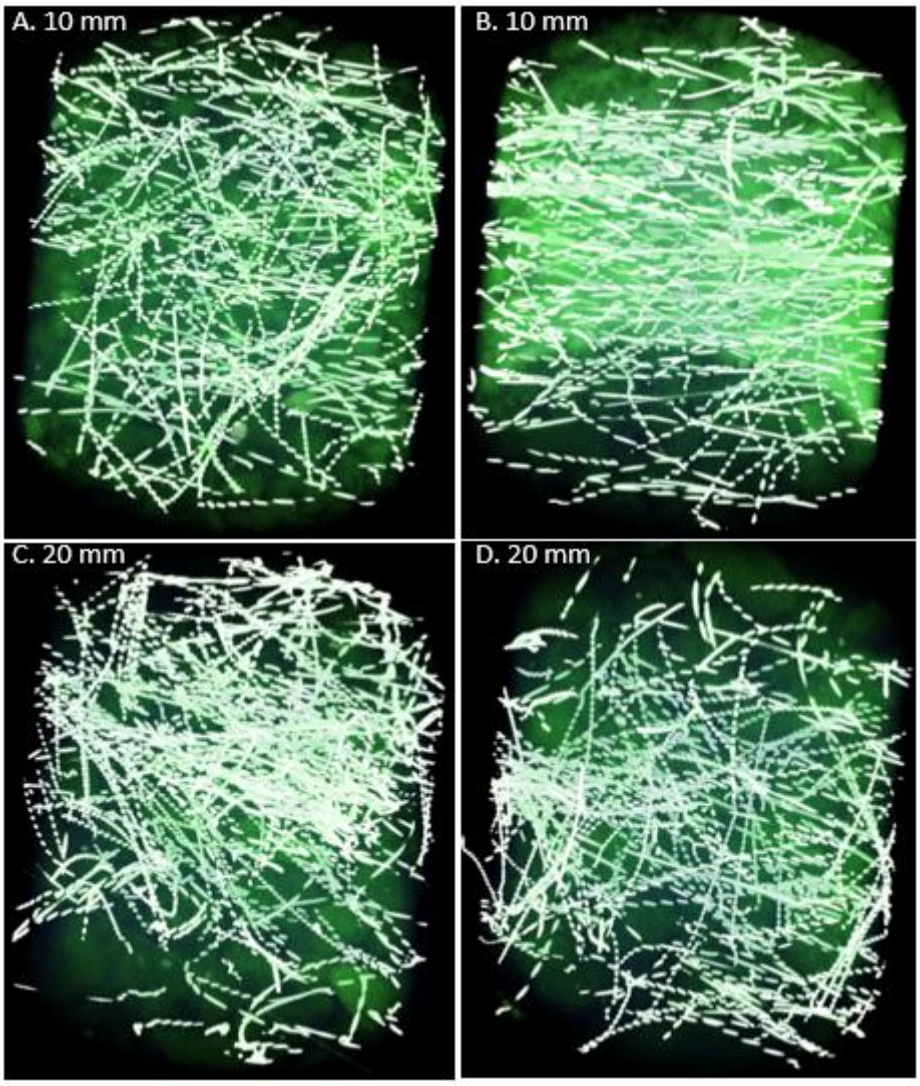

Figure 6.18: 3D rendering images of 80/60 fibres in typical core samples of 10 mm and 20 mm maximum aggregate sizes

In Figure 6.18, the images of cores presented are those extracted from slabs containing steel fibres of 80/60 type. The 'A' and 'B' cores are the cores from slabs mixes of 10 mm maximum aggregate size while 'C' and 'D' cores are those from slabs of mixes containing 20 mm maximum aggregate size. The same trend of horizontal positioning of larger percentage of steel fibres like in other rendering images in Figures 6.16 and 6.17 is noticed in Figure 6.18 as well with few of the steel fibres aligning vertically. Also, like in the other images as well, the cores extracted from slabs containing 10 mm maximum aggregate size in Figure 6.18 (A and B) are of better random distribution and better orientation than their 20 mm maximum aggregate size counterparts in Figure 6.18 (C and D). The steel fibres of type 80/60 are the thinnest of all the fibres used in this study and therefore estimated to give the highest number of fibres in a slab, reasons why all the cores from slabs containing fibres 80/60 revealed maximum appearance of steel fibres of all the rendering images of steel fibres in the cores presented in this section. By calculation, about 8,297 80/60 fibres are expected to be in each of the slabs which is higher than the estimated number of fibres of type 45/50 in a slab and that of fibre type 65/60 in a slab by 3226 and 2536 fibres respectively.

Consequently, it can be established from the volume renderings of the fibres in the cores, that the fibres are generally aligned horizontally within the slabs used in this study. This may not be too far from the fact that the thickness of the slab specimens is 100 mm. It is also evident from the core images that the slab mixes with 10 mm maximum aggregate size will exhibit a better performance in post-cracking behaviour than the slabs containing 20 mm maximum aggregate size. This is because, all the core images of 10 mm maximum aggregate size had the steel fibres well distributed and positioned with more number of fibres seen all over the cores than revealed in 20 mm aggregate size cores. The more the presence of steel fibres in the slab, the more the probability of availability of fibres to bridge the micro-crack as they form, which will in turn improve the load carrying capacity of the steel fibre reinforced concrete slab.

6.4.6 Orientation estimation

According to Eberhardt and Clarke (2001), orientation of an individual fibre may be defined in terms of two angles θ and φ because of the number of fibres involved, therefore, specifying the orientation of each individual fibre will be practically difficult to achieve. Therefore, a probability distribution is often considered for all the fibres in a volume using probability function, $\psi(\theta, \phi)$, and the probability that a fibre will be oriented between the angle θ_1 and $\theta_1 + d\theta$, ϕ_1 and $\phi_1 + d\phi$ is defined by;

$$\mathrm{P}(\theta_1 \leq \theta \leq \theta_1 + d\theta, \phi_1 \leq \phi \leq \phi_1 + d\phi) = \psi(\theta_1, \phi_1) sin\theta_1 d\theta d\phi \qquad (6.8)$$

Hence, the orientation of each fibre in this research work was determined in terms of a spherical coordinate system, consisting of two angles, theta (θ) and phi (φ) and a length. Since the steel fibres are quite numerous and may thus complicate the fibre detection process, the accurate estimation is dependent on accurate estimation of the underlying probability distribution(s) $\hat{p}_k$.

$$\lim_{k \to \infty} \widehat{p_k} \to p_k \qquad (6.9)$$

which requires a large sample size to accurately estimate the probabilities $\hat{p}_k$. Obviously, this is impractical from a computational point of view. However the stochastic nature of the fibre detection process provides an opportunity to repeat the fibre detection process over a number of iterations which can provide somewhat dependent re-sampling of the fibre volume.

Estimation of orientation experimentally utilised both simulated data and real X-ray microtomography (XμT) data of steel fibre cores. The benefit of simulating XμT data is because it enables parameters to be precisely controlled such as the orientation distribution and distancing of the simulated steel fibres, the inter slice thickness, noise levels and it is also possible to have precise knowledge about the location of the simulated fibres. The fibres were randomly located in the imaging data by adopting the method suggested by Weisstein (2016) in obtaining points on the surface of unit sphere such that any small area on the sphere is expected to contain the same number of points, if U and V are chosen to be random variants on (0,1). Then,

$$\begin{cases} \theta = 2\pi u \\ \phi = \cos^{-1}(2v - 1) \end{cases} \quad (6.10)$$

where u and v are sampled from uniform distributions in (0,1). The real XμT data are the scans of 100mm core samples of steel fibre reinforced concrete square panels as described in section 6.2.1.

6.4.6.1 Conversion of Vector from Cartesian to spherical coordinate

After estimating the straight line associated with each fibre, orientation angle for each skeletonized object was determined by converting vectors from Cartesian to spherical coordinate. A spherical coordinate system is a system for three dimensional space which specifies the position of a point by three coordinate numbers; the length which is the radial distance of the point from a fixed origin, the azimuthal angle in the x-y plane from the x axis with $0 \leq \theta \leq 2\pi$ and the polar angle also called the Zenith angle which is measured from a fixed zenith direction (Weisstein, 2016).

The Cartesian coordinates (x, y, z) are related to the spherical coordinates (r, θ, ϕ) by the followings;

$$r = \sqrt{x^2 + y^2 + z^2} \quad (6.11)$$

$$\theta = tan^{-1}\left(\frac{y}{x}\right) \quad (6.12)$$

$$\phi = cos^{-1}\left(\frac{z}{r}\right) \quad (6.13)$$

Inversely, in terms of Cartesian coordinates, the following equations apply;

$$X = r\ cos\ \theta\ sin\ \phi \quad (6.14)$$

$$Y = r\ sin\ \theta\ sin\ \phi \quad (6.15)$$

$$Z = r\ cos\ \phi \quad (6.16)$$

Figures 6.19 and 6.20 show the spherical coordinate system and changing coordinate system illustrating both rectangular (Cartesian coordinates) and spherical coordinates.

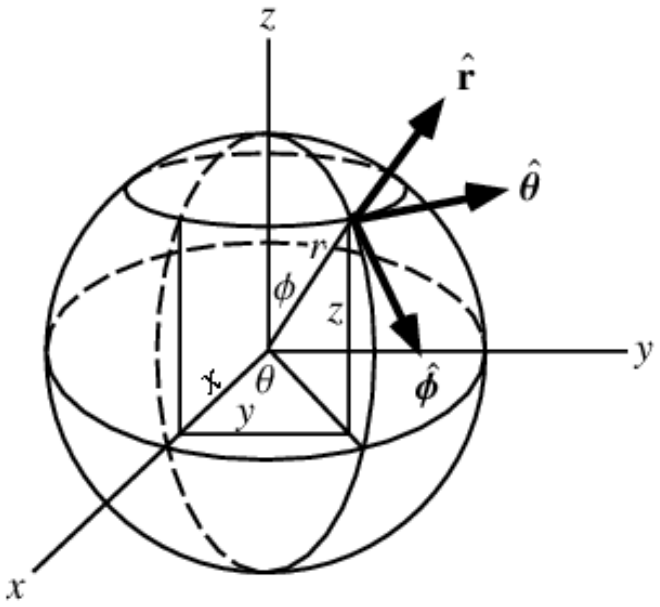

Figure 6.19: Spherical coordinate system
(Weisstein, 2016)

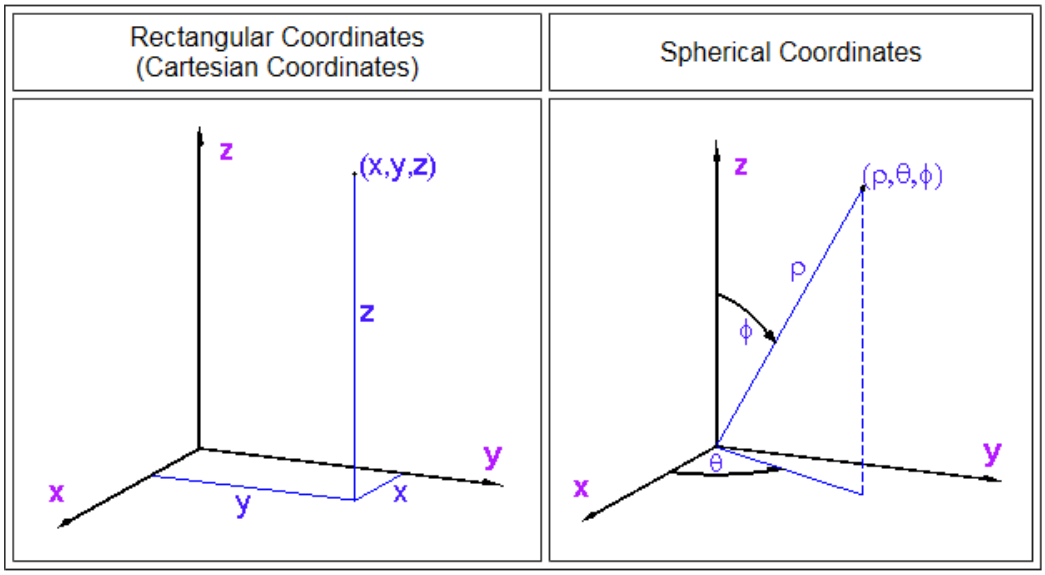

Figure 6.20: Conversion of coordinate system from Cartesian to spherical
(Math.byu.edu, 2016)

From the conversion, it was then possible to determine the orientation of the fibres in terms of spherical coordinate system with 'θ', the inplane angle describing the direction of the fibres within a single scanned slice and 'ϕ', the interplane angle describing the direction of the fibre across slices.

6.5 Analysis of outcome of imaging techniques

The outcome of imaging processing by Insight Toolkit software is analysed in this section in terms of distribution and orientation of fibres within the concrete.

6.5.1 Fibre distribution

Figure 6.21 shows how the average nearest neighbour distance of fibres varies with height within the core for both 10 mm and 20 mm maximum aggregate sizes. It is computed via a 'distance transform' that computes and transforms for every pixel in the data the closest object. Then for every slice, for all pixels in that slice, the maximum distance in that slice is found. The transform here is computed in 3D so it quantifies the fibre non-occupancy space across all 3 dimensions and provides an idea as to if there is a big gap or not in a particular slice.

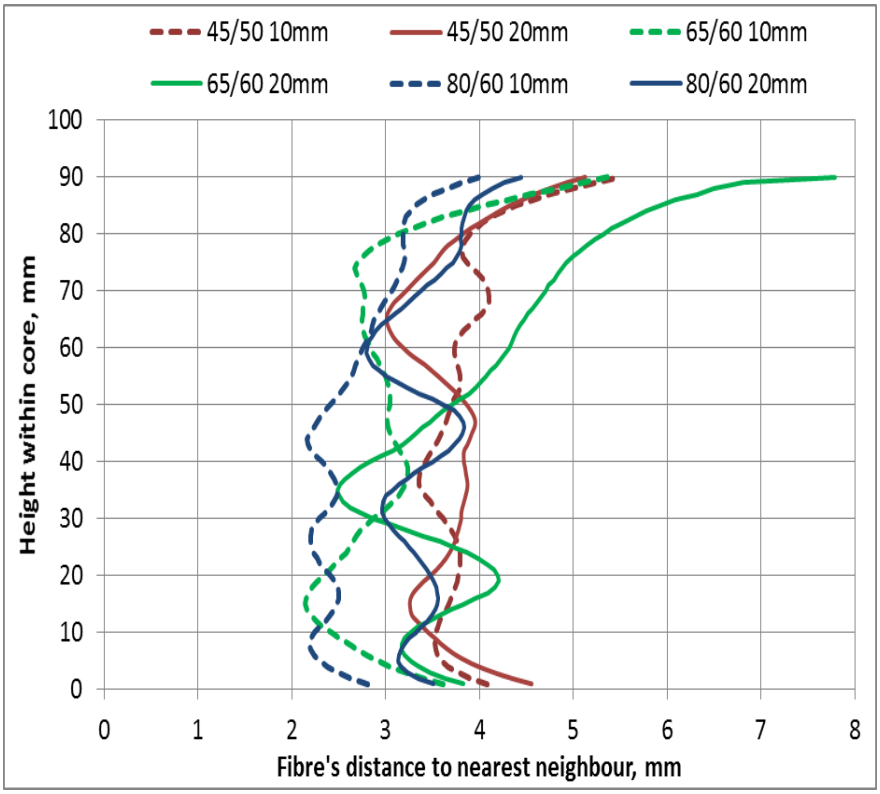

Figure 6.21: Plot of variation in mean nearest neighbour distance with height in the core

The plot therefore provides information on fibre distribution in each core. All results from the plot in figure 6.21 show lower nearest neighbour distances in the middle of the core height, suggesting generally that fibres are more closely distributed at the middle than in the bottom and top surface areas.

Cores extracted from slabs of both 10 mm and 20 mm maximum aggregate size with the same fibre geometry were also compared in the results of distribution of fibres within cores to further evaluate how the fibres are distributed within mixes with main aim of examining the effect of matrix and fibre combination on steel fibre distribution within steel fibre reinforced concrete. Figures 6.22, 6.23 and 6.24 present the plots of variation in mean nearest neighbour distance with height in the cores of mixes of 10 mm and 20 mm maximum coarse aggregate size containing steel fibres 45/50, 65/60 and 80/60 respectively. Two cores each named 'A' and 'B' were selected from different slabs of the same mix of the three replicates which normally produced six cores. It has been observed that cores extracted from the same mixes exhibit very similar behaviour

in the pattern of fibre distribution as seen in the following Figures. For example, core A (10 mm) and core B (10 mm) extracted from the same slab can be seen in Figure 6.22 as showing the same pattern of result. Also, core A (20 mm) and core B (20 mm) extracted from the same slab can be seen in Figure 6.22 as well with widely varied pattern of distribution in a similar form.

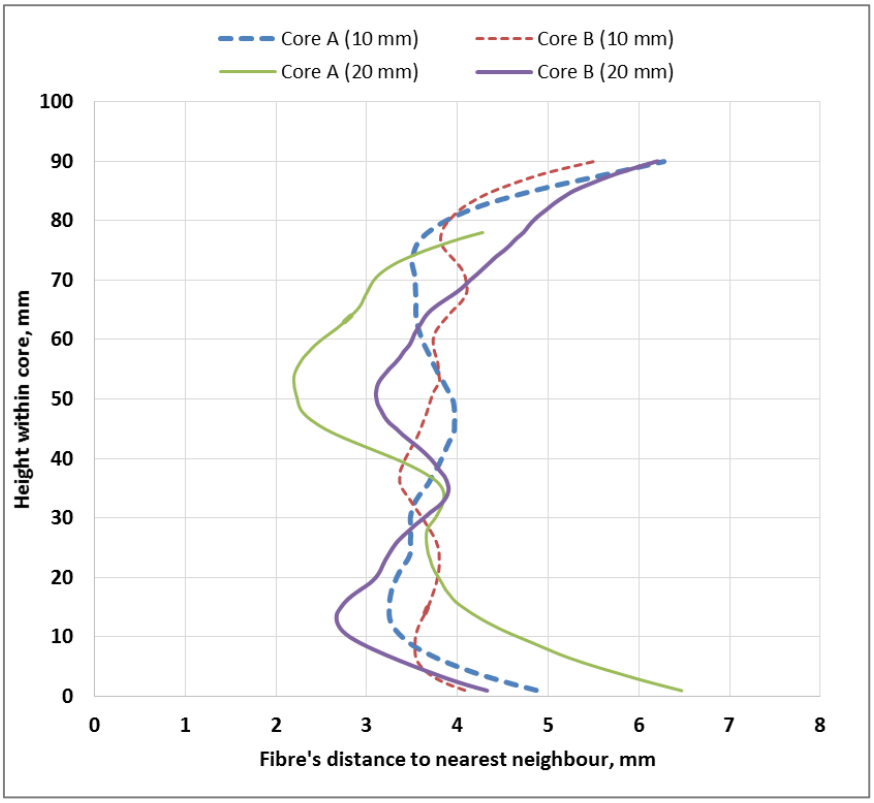

Figure 6.22: Distribution of fibres within cores of 10 mm and 20 mm maximum aggregate size containing fibre 45/50

From the above Figure 6.22, the distribution of steel fibres as revealed in the results show that mixes of 10 mm maximum aggregate size in combination with steel fibre 45/50 are more evenly distributed than 20 mm maximum aggregate size mixes. The 10 mm maximum aggregate size cores containing fibre 45/50 are represented in the Figure with dotted line curves showing close resemblance in the pattern of distribution. On the other hand, 20 mm maximum aggregate size cores with same fibre geometry of

45/50 show varied and inconsistent pattern of distribution as revealed in the results represented by the continuous curves of Figure 6.22. However, for both types of cores, they were more closely distributed at the middle of cores than at the bottom and surface of the cores.

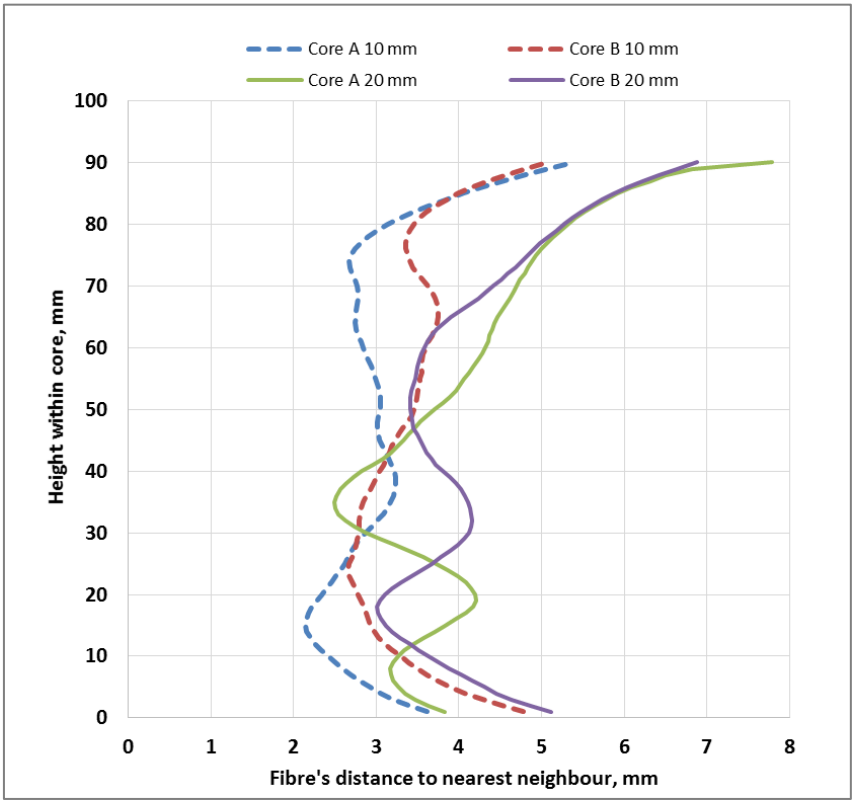

Figure 6.23: Distribution of fibres within cores of 10 mm and 20 mm maximum aggregate size containing fibre 65/60

The distribution of fibres in cores of steel fibre reinforced concrete containing fibre type of 65/60 with 10 mm and 20 mm maximum aggregate size are as shown in Figure 6.23. The results revealed the same trend as the result in Figure 6.22. However, the distribution of fibres in Figure 6.23 with steel fibres 65/60 showed a lower nearest neighbour distance with larger percentage of the curves when compared with cores of mixes of 45/50. Also, mixes of 10 mm maximum aggregate size are more closely distributed in the results as the two cores are closely related and of lower nearest

neighbour distance within the height of the core except for few spread at the bottom of the cores.

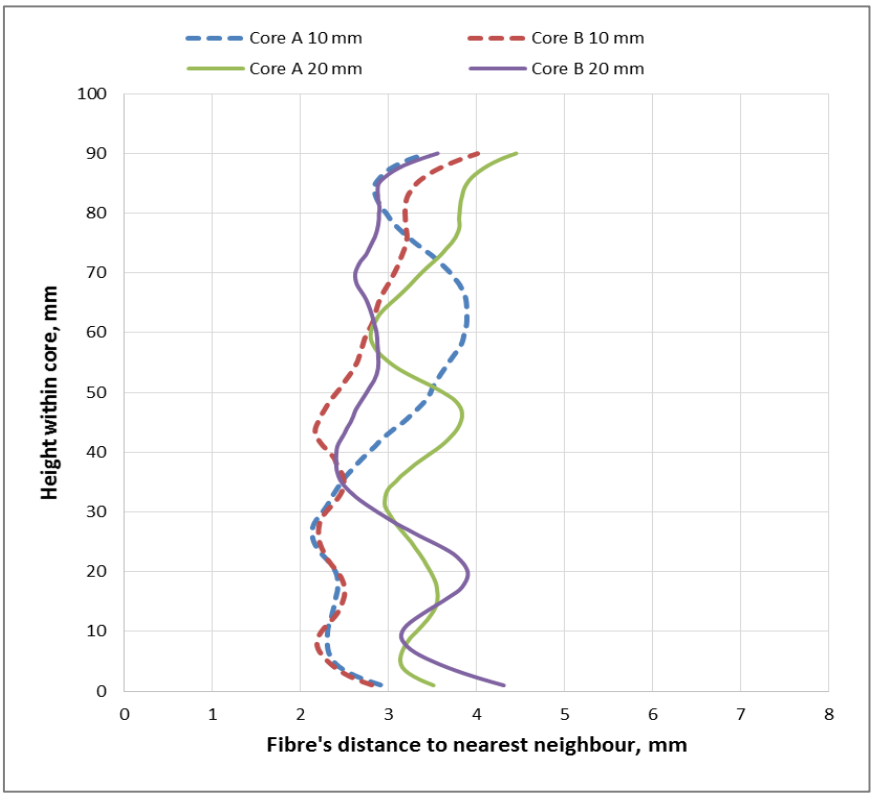

Figure 6.24: Distribution of fibres within cores of 10 mm and 20 mm maximum aggregate size containing fibre 80/60

The results of the variation in mean nearest neighbour distance with height in the cores of concrete mixes of 10 and 20 mm maximum aggregate size with steel fibre of 80/60 as presented in Figure 6.24 clearly show the closest nearest neighbour distance of fibre within the concrete matrix of all the mixes under consideration. Cores from both mixes of 10 mm and 20 mm aggregate size exhibit the lowest nearest neighbour distance which is an indication that fibres are closely distributed within the concrete matrix. Besides, the concrete mix containing steel fibres 80/60 shows an even distribution of steel fibres within the core heights unlike other steel fibre reinforced concrete cores where the spread of fibres at bottom and top surface are wide.

However, from Figure 6.24, it can be deduced that the cores of mixes containing 10 mm maximum aggregate size with fibre 80/60 produced the lowest nearest neighbour distance of all the mixes tested. This suggests that the best fibre distribution within the concrete matrix occurred in the mix of 10 mm aggregate size and 80/60 steel fibres. The nearest neighbour distance of 10 mm maximum aggregate size with fibre 80/60 is lower than that of 20 mm maximum aggregate size with the same fibre.

6.5.2 Fibre orientation

The point estimate was calculated for real steel fibre reinforced concrete and some comparisons were performed, the results of which can be seen in Figures 6.25 and 6.26. The term entropy used in quantifying the orientation of fibre within concrete matrix is the estimation of degree of randomness of steel fibres considering the angles of inclination in relation to the Cartesian coordinates as described in section 6.4.6. The data were generated for each core after running the fibre orientation estimation process several times to reduce the variation within the cores. The entropy values of maximum, minimum and mean values for each core were then evaluated.

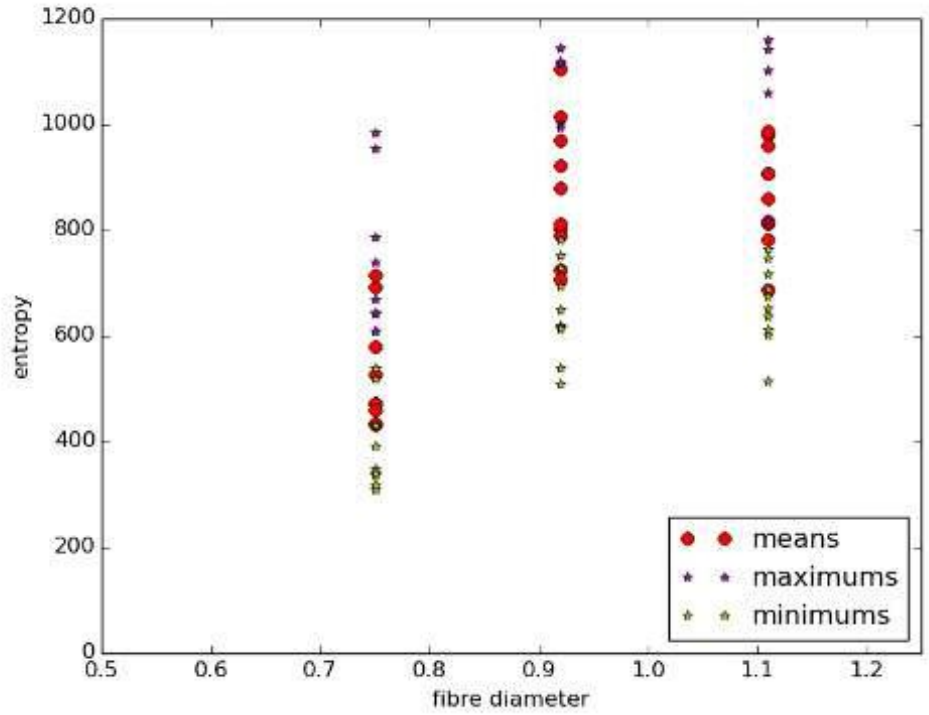

Figure 6.25: Results of applying point estimate calculations to real steel fibre reinforced concrete (fibre diameter in mm)

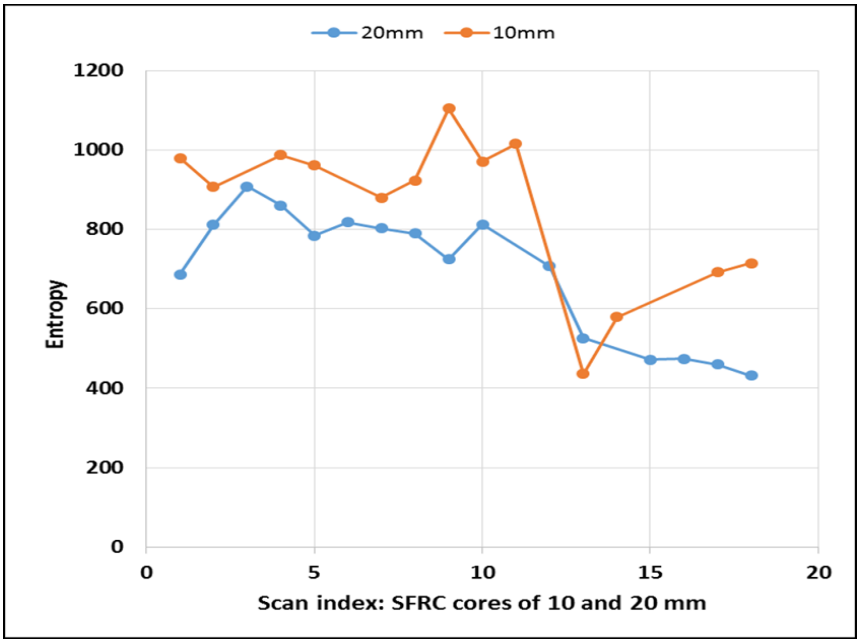

Figure 6.26: Results of comparison of entropy between 10 mm and 20 mm aggregate SFRC cores

After thinning, the thinned fibre data are converted to individual voxel points from which straight lines are fitted using a robust statistical estimation process. Each fitted line can represent an individual fibre. The estimation of randomness of the orientation of the fibres given in terms of entropy are presented in Figures 6.25 and 6.26 above.

In Figure 6.25 the values of entropy against the fibre diameter in mm as presented shows that concrete cores containing fibre 65/60 exhibit the highest estimated randomness of orientation. The performance here shows the possibility of fibres within the cores to be randomly distributed as seen in Figure 6.24 and non-randomly oriented as revealed in Figure 6.25. This scenario seems to be responsible for the performance of mixes containing steel fibres 80/60.

However, the results presented in Figure 6.26 show the cores of 10 mm maximum aggregate size regardless of the fibre types outperforming cores of 20 mm maximum aggregate in the estimation of randomness of orientations. This is an indication that 10 mm maximum aggregate size suitably mixed and interacted well with the steel fibres for good positioning within the concrete matrix. This in turn increases the ability of the steel fibres to bridge and arrest initiation of cracks effectively.

Figure 6.27 show the mean value of entropy of cores of different fibre aspect ratio and length. The maxima entropy values of typical core from the replicates were selected for the analysis.

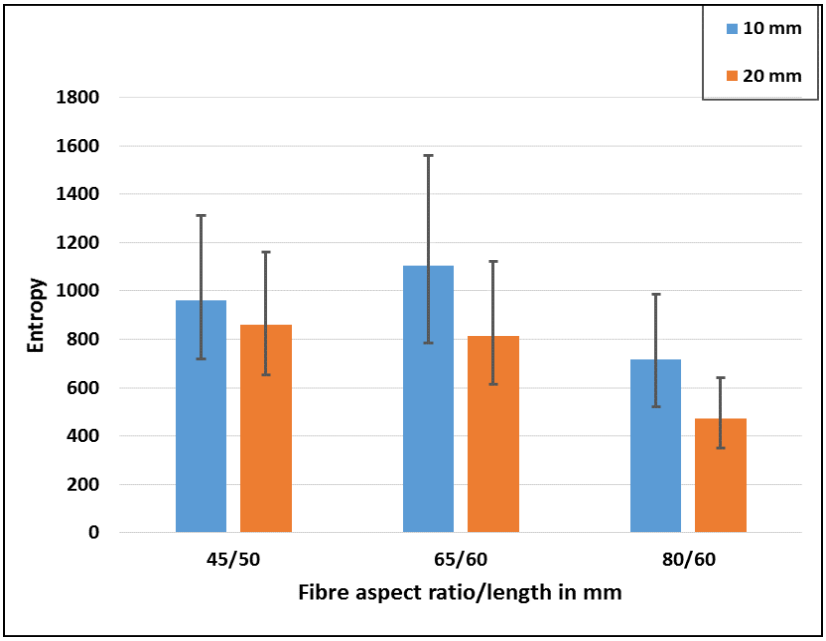

Figure 6.27: Results of comparison of entropy between 10 mm and 20 mm aggregate SFRC cores of different fibre aspect ratio and length

It can be deduced that the results follow the same trend of the results presented earlier in Figure 6.25. The cores with 10 mm maximum aggregate size exhibited the highest value of entropy for orientation randomness while the highest value of entropy was displayed by mix of 12 mm maximum aggregate size and one of the long fibres, 65/60.

6.5.2.1 Entropy values at maximum

Entropy is a function of the orientation angle which quantifies the values of orientation of the whole system of fibres and not just for individual ones. Entropy, according to Shannon (2001) can be calculated as:

$$H = \sum_{i=1}^{n} P_i \log P_i \tag{6.17}$$

Where:

H is the entropy, P_i is the probability of a system being in cell of its phase space and sum is calculated over all the angles of the fibres.

Basically, entropy (H) is a maximum when all the probabilities are equal. This means, entropy is maximised if probability that fibre orientation is uniform. Here, it can be said that if all the steel fibres in a core are distributed at angles with equal frequency, then the entropy for that core will be at a maximum. Also, if some fibres are concentrated in a particular direction, then the H will not be at a maximum. This theory is applicable when determining how the fibres are randomly orientated and distributed within the matrix.

6.5.2.2 Entropy values of in-plane angles of steel fibres

The general orientation of steel fibres in the slabs have been found to be generally horizontal while few fibres are vertical or almost vertical in longitudinal position within the slab as shown in the 3-D view of the core samples presented in Figures 6.16 – 6.18. The entropy values for simulations of the core samples indicating the in-plane angles of steel fibres where the angle in a plane has been constrained to within the range 0 – 5 degrees whilst varying the other angle from 5 to 180 in steps of 5 degrees. On the other hand, considering the orientation of fibres in terms of spherical coordinate system (Section 6.4.6.1), entropy values of angle θ ranging from 5 to 180 degrees have been found while φ is constrained to a range of 0 – 5°. The outcome of the simulation is presented in Figure 6.28. This shows the range of entropy values where the fibres are distributed within a plane.

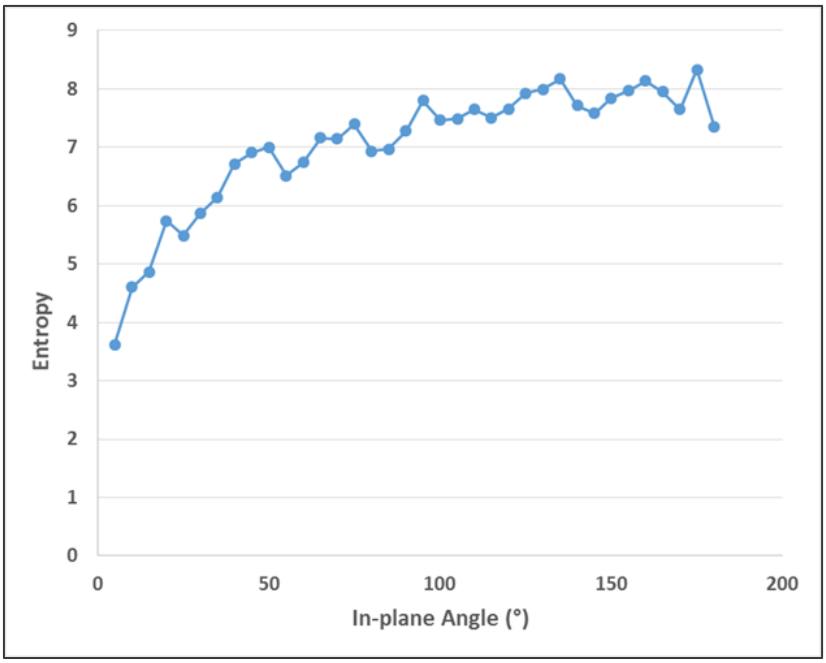

Figure 6.28: Entropy values against in-plane angles of steel fibres within the core samples

The results presented in Figure 6.28 reveals the value of entropy regarding the positioning or horizontal distribution of steel fibres within a plane and from a relative point. The results of the simulation show that the fibres are generally well distributed within the concrete matrix and in this study, mostly in horizontal position in the slab specimen. The entropy values range from 3.62 to 8.32 with lowest and highest entropy value recorded against fibres at angles 5° and 175° respectively. The relative high values of entropy at some angles of fibres like from 135°, 160° and 175° is an indication that the fibres are positioned and distributed at these angles with equal frequency while those at angles with lower values of entropy are positioned and distributed in a direction.

6.6 Correlation between X-ray CT imaging data and mechanical performance

In stating the objectives of this PhD study, it was itemised that the correlation between distribution and orientation of steel fibres within concrete matrix, investigated through

X-ray CT imaging techniques on core samples and the mechanical performance of the same composite materials accessed through laboratory testing would be carried out. The outcomes of the correlation are as given below;

Workability of steel fibre reinforced concrete is generally affected negatively by the inclusion of steel fibres when tested by slump test. The compressive strength was only marginally affected by the addition of steel fibres and the main differences were noticed in varying the dosage of steel fibres so the cores for X-ray CT test were extracted from a single dosage mixture of slabs. Therefore, the outcome of workability and compressive tests were not considered in the study of correlation between mechanical performance and the distribution and orientation results.

The flexural properties of steel fibre reinforced concrete specimens such as flexural strength and flexural toughness are those considered for the correlation analysis.

The results of slab flexural properties in section 5.5 clearly showed mixes of 10 mm maximum aggregate size significantly outperforming that of 20 mm maximum aggregate size, regardless of steel fibre types. Figures 5.20 and 5.21 of maximum load sustained and energy absorption of slab specimens testified to this. Results of distribution of steel fibres in section 6.4.5 where closest nearest neighbour distance of fibres within the matrix indicating close distribution of steel fibres were observed in 10 mm maximum aggregate size than that of 20 mm maximum aggregate size affirmed this.

Better performance in mechanical laboratory tests performed on slab specimens of 10 mm maximum aggregate size mixes than its counterpart, 20 mm maximum aggregate size can also be seen displayed in the result of fibre orientation in section 6.4.7. Figure 6.26 showed that 10 mm maximum aggregate size had the higher estimation of randomness of orientation of steel fibres within the steel fibres reinforced concrete cores in most cores assessed by estimation of randomness of orientation process. This must have equally been responsible for demonstration of superior flexural capacity of all the mixes containing 10 mm maximum aggregate size by prompt bridging of cracks within the concrete matrix. The results of mechanical properties showing higher

performance of 10 mm aggregate size therefore have good correlation to the image analysis results displaying the same trend. It can be deduced that with 10 mm maximum aggregate size, fibres are more evenly distributed and more randomly orientated which equally resulted in superior mechanical performance. There is a strong probability of well distributed fibres in 10 mm aggregate size bridging more cracks efficiently.

There have been observations of excellent performance of mixes containing fibre aspect ratio (l/d) of 80 in almost all the mechanical performance tests carried out of both beam and slab specimens. This can be clearly seen as being demonstrated in sections 5.4.1 and 5.4.1. Steel fibre reinforced concrete specimens containing steel fibre 80 aspect ratio outperformed all other specimens containing 45 and 65 aspect ratio as revealed in Figures 5.13 and 5.20. The image analysis outcome corroborated the excellent mechanical performance of fibre aspect ratio 80 as seen in the distribution of fibre results in section 6.4.5. It has been revealed that the higher the aspect ratio, the better the distribution of fibres within the concrete matrix as observed in Figures 6.22, 6.23 and 6.24. The closest average nearest neighbour distance of fibres within the cores analysed was recorded at fibre aspect ratio 80, even for both 10 mm and 20 mm maximum aggregate sizes. The fibres (80/60) however seem less randomly orientated from the imaging result. From fibre networking in Table 4.3, fibre 80/60 has the highest number of fibre / kg than any other, which might be responsible for the randomness result. However, considering being the highest number in a mix, there is possibility of interacting more than others.

The length of steel fibres investigated in this research work are 50 mm and 60 mm. Though, fibres of 60 mm length combined with two other aspect ratio of 65 and 80, the mechanical performance of longer fibres in all the tests carried out has been noted to give superior results. Some of the results had specimens comprising fibres of 60 mm and aspect ratio 80 or with aspect ratio 65 performing side by side especially in Figures 5.12, 5.13 and 5.14, which is an indication of advantage of higher fibre length in the performance. The relationship of fibre length and good mechanical performance is also observed in the X-ray CT image analysis where fibres with higher length resulted in

close and even nearest neighbour distance and high estimation of randomness of orientation. Such can be seen as presented in Figures 6.23 and 6.24 showing low nearest neighbour distance, indication of good distribution of steel fibres in cores containing both fibres of 60 mm than the result fibre distribution presented on Figure 6.22 for cores containing fibre of length 50 mm.

In summary, the mechanical performance of steel fibre reinforced concrete is a direct reflection of the distribution and orientation of steel fibres within the concrete matrix. This is so as the main function of fibres to provide multi-directional reinforcement within the concrete matrix may be inefficient when the fibres are not well distributed to be available where they (fibres) are needed in arresting the cracks, or when not perfectly oriented to bridge the crack at initiation stage. The 3D rendering images in Figures 6.16 to 6.18 clearly showing the distribution and orientation of steel fibres within the hardened concrete confirms the above statement.

6.6.1 Importance of image analysis to the study

The X-ray Computed Topography with the image analysis tool was employed in this research work to examine the internal positioning of steel fibres within the hardened steel fibre reinforced concrete. The main findings of this analysis as expressed in this chapter are; the visual inspection of the positioning of steel fibres as they were revealed through the 3D images which helped in gaining better understanding of the arrangement of steel fibres within the hardened concrete, the quantitative measure of the distribution (via distance transform) and orientation (via principle of entropy) of steel fibres within the concrete matrix, and the outcome of the image analysis used to study the correlation between the mechanical performance and distribution and orientation of steel fibre within the concrete matrix.

The X-ray Computed Topography and the analysis of the volumetric images from X-ray CT have been used in this research work as a tool for validation and confirmation, to corroborate the outcome of laboratory experiments on effects of research variables on mechanical properties of SFRC. Therefore, better understanding of how the chosen

variables affect the internal positioning of steel fibres within the concrete with the effects on mechanical properties of the resulting steel fibre reinforced concrete was made possible by X-ray CT and image analysis.

CHAPTER 7

CONCLUSIONS AND RECOMMENDATIONS

7.1 Introduction

This chapter presents the summary of the investigation that has been carried out in this project. Comparison between summary data of X-ray CT imaging and mechanical performance of the research specimens are presented, the most significant contributions and findings of the research and recommendations for future research work are also provided in this chapter.

7.2 Conclusions

The research work presented in this thesis focused on investigating the key factors affecting distribution and orientation of fibres within the steel fibre reinforced concrete and ensuing effects of the positioning of fibres on mechanical properties of the composite material. The variables considered to influence how steel fibres interact with concrete matrix were selected and various stages of laboratory experiments and image analysis technique employed in the study. Each of the objectives set out to meet in section 1.2 have been practically met and the following summary of conclusions drawn based on findings of the experimental works are presented.

The inclusion of steel fibres in concrete had a negative effect on the workability of the concrete mixture as checked by the slump test. The workability of steel fibre reinforced concrete reduced as the fibre dosage increases with worst results observed at the highest dosage of 60 kg/m^3 steel fibre in concrete.

The density of plain concrete and steel fibre reinforced concrete mixes measured through 100 mm cubes revealed that there was increase in density as the fibre dosage increases in the mixture. Also, mixtures of 20 mm maximum aggregate size generally

recorded higher values of density than their 10 mm maximum aggregate size counterparts which reflected in plain unreinforced concrete as well. In plain concrete without fibres, there was a difference of 47 kg/m^3 in the density values of 10 mm maximum aggregate size and that of 20 mm maximum aggregate size. This shows that, though, compaction period was short, there was a better compaction for 20 mm maximum aggregate size than 10 mm, which probably triggered an increase in air content of 10 mm aggregate size mixture.

Fibre effects on compressive strength is slightly pronounced, with optimum compressive strength noticed at fibre dosage of 50 kg/m^3 and with fibre of 80 l/d ratio. The maximum increase in compressive strength brought about by the inclusion of steel fibres in 10 mm maximum aggregate size mixtures is about 5 MPa, translating to about 9% increase while that of 20 mm maximum aggregate size mixtures recorded the maximum increase of about 8 MPa, which is 14 % increase. Compressive strength increases with increase in fibre dosage until optimum compressive strength was achieved at 50 kg/m^3 fibre dosage for both 10 mm and 20 mm maximum coarse aggregate sizes after which it declined.

Addition of steel fibres to concrete remarkably improves the strength of steel fibre reinforced concrete beams when compared to plain concrete as there were up to 83% increase in maximum stress reached for concrete mix containing fibre aspect ratio (l/d) 80 with maximum coarse aggregate size of 20 mm. The best performance in terms of strength was recorded for mixture containing steel fibres at higher fibre dosages of 50 kg/m^3 and 60 kg/m^3.

The influence and effectiveness of steel fibres in concrete are distinctively noticed at higher dosages of fibres. There was a significant improvement of ultimate flexural strength attained at higher dosage of fibres in concrete (50 kg/m^3 and 60 kg/m^3), which resulted in better post-cracking tendency with composite exhibiting strain hardening behaviour with stresses increasing even after first crack. This is attributed to more availability of steel fibres within the concrete matrix leading to a better distribution of

steel fibres within the concrete as a result of adequate dosage of fibres providing effective multi-directional reinforcement within the concrete matrix.

The significance of fibre length was clearly identified from the findings of experimental investigation carried out, as the specimens containing shorter fibre length of 50 mm exhibited the least strength when compared to the results from other specimens containing steel fibre of length 60 mm. This trend is seen in both maximum coarse aggregate sizes of 10 mm and 20 mm, and in all dosages of fibres.

The post cracking tendency of the steel fibre reinforced concrete beams is affected by the fibre length, most of the results from beams containing steel fibres of 50 mm length had the first cracking value as the highest flexural value achieved, whereas, results from specimens containing steel fibres of 60 mm length show better post-cracking capability with strain hardening behaviour. Good post-cracking behaviour of all the steel fibre reinforced concrete specimens was also noticed at higher dosages of steel fibres and at highest fibre aspect ratio of 80.

By means of overall consideration of various experimental tests carried out in the first phase of this research work, especially from the fresh steel fibre reinforced concrete to compressive strength and flexural properties of the specimens, it can be concluded that 50 kg/m^3 is the optimum steel fibre dosage for the range of fibre type employed in this research. This is because optimum performance was generally achieved at this dosage and where higher fibre dosage of 60 kg/m^3 performed better in some instances, the difference was not significant.

The outcome of the experimental investigations on the flexural performance of square slab specimens manufactured at fibre dosage of 50 kg/m^3 revealed that addition of steel fibres to the concrete matrix of slabs significantly improved the failure pattern and load carrying capacity of the concrete composite. Unreinforced slabs failed immediately at the appearance of first crack exhibiting brittle nature of failure and not withstanding any additional load. Also, better performance of thinner steel fibres (of high aspect ratio) was noticed and longer fibre outperforming the shorter ones.

The experimental findings on the two sizes of 10 mm and 20 mm maximum coarse aggregates employed in this research conclude that, in general, 10 mm maximum coarse aggregate size performed better than 20 mm maximum aggregate size. Though, there were instances where beam specimens containing mixes of 20 mm maximum aggregate size performed better than 10 mm maximum aggregate specimens in beam tests, the results of investigation carried out on slab specimens substantiated the superiority of 10 mm maximum aggregate mixes when combined with steel fibres over the 20 mm maximum aggregate size. This could be as a result of heterogeneity of SFRC being less pronounced in beam testing with predetermined region of cracking initiated by the notches in the beams, However, in the slab testing, there were more fracture surfaces and hence, complete exhibition of bi-axial nature of bending where the heterogeneity of the material manifested with the sensitivity of aggregate size effectively revealed.

Consequently, when crack patterns are viewed visually, more cracks are formed in the slab when the maximum aggregate size is 10 mm regardless of the fibre type. This correlates with a higher load bearing capacity. The cracks in steel fibre reinforced concrete slabs with 20 mm maximum size aggregates were fewer but wider with lower load bearing capacity while the unreinforced concrete slabs exhibited brittle failure. This is due to the fact that smaller aggregate in the matrix led to more week-hard points interface zone, generating more cracks and possibly more bridging exercise in the slabs containing 10 mm maximum aggregate size.

The experimental results obtained from the beams tested in flexure were harmonized with the results of slabs using yield line theory. From the theoretical and experimental results of the exercise, the values obtained were reasonably close in the case of mixtures of 20 mm maximum aggregate size while the values for 10 mm maximum aggregates size varied widely. It is therefore concluded that the yield line analysis does not take care of the failure pattern of more cracks experienced in slabs containing 10 mm maximum aggregate size.

Through the analysis of the laboratory experimental investigations carried out on beams and slabs and the results of post-cracking ability of steel fibre reinforced concrete assessed by toughness characterization, which is energy absorption in slabs, flexural toughness and residual strength in beams, it is concluded that the influence of steel fibre inclusion in concrete is more significant in toughness characterization of the composite as the ductility parameter of the material is appropriately measured.

By visualising the position of fibres in the X-ray volumetric slices and relating this to the outcome of the image analysis software, the distribution of steel fibres in the concrete matrix followed the same trend. It is concluded that generally, fibres are fairly and more closely distributed at the middle of the cores than in the bottom and top surface areas.

The results of X-ray CT image analysis by The Insight Toolkit (ITK) software correlate well with the mechanical performance results. Mixes of 10 mm maximum coarse aggregate size with steel fibre of highest aspect ratio and of longer length exhibited the closest fibre distribution measured by the nearest neighbour distance of fibres within the concrete matrix. However, the mixes containing steel fibres of aspect ratio 65 but of 10 mm maximum aggregate size and length 60 mm demonstrated the highest value of estimation of orientation randomness of fibres within the matrix.

The 3D images of volumetric renderings of the fibres in the cores revealed that fibres are generally aligned in horizontal position within the slab specimens employed in this study. From the comparison of the results of image analysis and the laboratory experimental results, it is concluded that the more the fibres are positioned horizontally, the higher the load bearing capacity of the slab specimens. Also, it was established that slab containing 10 mm maximum aggregate size had more fibres horizontally positioned which resulted in the higher load bearing capacity.

The study has revealed a clear relationship between the geometry of steel fibre and maximum aggregate size, establishing the fibre-aggregate interaction effects on post-cracking capacity of SFRC. Also, the study has quantitatively measured the distribution

and orientation of steel fibre within the concrete and the correlation between the internal mechanism and the mechanical properties of SFRC established.

7.3 Recommendation for future work

Based on the results of this research work that have been presented, it is evident that inclusion of steel fibres in concrete significantly improves the performance of concrete with enhancement of its structural integrity. Also, it is clear that there are factors as investigated in this research work that affect the mechanical properties of steel fibre reinforced concrete by affecting the way the fibres are distributed and oriented within the concrete matrix. Therefore, there are areas which this research work has presented to be of significant advantage by incorporating steel fibres in concrete. The ideas for future works should be to explore more of these areas already identified for additional understanding of internal mechanism of the interaction between fibre and concrete matrix for greater benefit. The following suggestions for future work have been given:

- Investigation of how the workability of steel fibre reinforced concrete at higher dosage can be improved through different mix designs that will allow a good interaction between steel fibres and concrete matrix at fresh state.
- Application of modelling and simulation tools using appropriate software to model both the rheology of fresh steel fibre reinforced concrete and the hardened form of the materials. This will involve complete monitor of the composite material from fresh stage to hardened stage while laboratory experimental procedures are simultaneously engaged to confirm and revalidate the numerical modelling outcome.
- Determination of effects of specimen dimensions on internal arrangement and positioning of steel fibres within the concrete matrix. This should involve maximum sizes of coarse aggregate and geometry of steel fibres as variables. The effects of different specimen dimensions on how steel fibres interact with concrete matrix be studied as well.

- Investigation into new generation hooked end steel fibres with improved anchorage system and strength to be carried out to study if distribution and orientation are enhanced by the additional anchorage system or not. The investigation should consider how loose and glued steel fibres interact with concrete matrix and establish which of the two types enhance good distribution.
- The development and use of techniques to provide an external approach to control the distribution and orientation of steel fibre in concrete at stage of production.

LIST OF REFERENCES

Abrishambaf, A., Barros, J. A., & Cunha, V. M. (2013). Relation between fibre distribution and post-cracking behaviour in steel fibre reinforced self-compacting concrete panels. *Cement and Concrete Research, 51*, 57-66.

Abrishambaf, A., Barros, J. A., & Cunha, V. M. (2014). *Mechanical performance of fibre reinforced concrete: the role of fibre distribution and orientation*. Paper presented at the XIV Portuguese Conference on Fracture.

Akcay, B., & Tasdemir, M. A. (2012). Mechanical behaviour and fibre dispersion of hybrid steel fibre reinforced self-compacting concrete. *Construction and Building Materials, 28*(1), 287-293.

Akubueze, E., Ezeanyanaso, C., Orekoya, E., Akinboade, D., Oni, F., Muniru, S., & Igwe, C. (2014). Kenaf fiber (Hibiscus cannabinus L.): a viable alternative to jute fiber (Corchorus genus) for agro-sack production in Nigeria. *World J Agric Sci, 10*(6), 308-331.

Alani, A. M., Aboutalebi, M., & King, M. J. (2013). Influence of fibre content on crack propagation rate in fibre-reinforced concrete beams. *International Journal of Civil, Architectural Science and Engineering, 7*(9), 117-123.

American Concrete Institute. (2002). ACI 544.1-R96 (Reapproved 2002) State-of-the Art Report on Fiber Reinforced Concrete.

Anderson, T. L. (2005). *Fracture mechanics: fundamentals and applications*: CRC press.

Aydın, S., & Baradan, B. (2013). The effect of fiber properties on high performance alkali-activated slag/silica fume mortars. *Composites Part B: Engineering, 45*(1), 63-69.

Balendran, R., Zhou, F., Nadeem, A., & Leung, A. (2002). Influence of steel fibres on strength and ductility of normal and lightweight high strength concrete. *Building and Environment, 37*(12), 1361-1367.

Barnett, S. J., Lataste, J.-F., Parry, T., Millard, S. G., & Soutsos, M. N. (2010). Assessment of fibre orientation in ultra high performance fibre reinforced concrete and its effect on flexural strength. *Materials and Structures, 43*(7), 1009-1023.

Barros, J. A., Cunha, V. M., Ribeiro, A. F., & Antunes, J. (2005). Post-cracking behaviour of steel fibre reinforced concrete. *Materials and Structures, 38*(1), 47-56.

Bayramov, F., Taşdemir, C., & Taşdemir, M. (2004). Optimisation of steel fibre reinforced concretes by means of statistical response surface method. *Cement and concrete composites, 26*(6), 665-675.

Bekaert NV. (2013) Technical Presentation; Reinforcing the future. *New and ultimate Dramix range*. London.

Bencardino, F., Rizzuti, L., Spadea, G., & Swamy, R. N. (2008). Stress-strain behavior of steel fiber-reinforced concrete in compression. *Journal of Materials in Civil Engineering, 20*(3), 255-263.

Bencardino, F., Rizzuti, L., Spadea, G., & Swamy, R. N. (2013). Implications of test methodology on post-cracking and fracture behaviour of Steel Fibre Reinforced Concrete. *Composites Part B: Engineering, 46*, 31-38.

Boulekbache, B., Hamrat, M., Chemrouk, M., & Amziane, S. (2010). Flowability of fibre-reinforced concrete and its effect on the mechanical properties of the material. *Construction and Building Materials, 24*(9), 1664-1671.

Brandt, A. M. (2008). Fibre reinforced cement-based (FRC) composites after over 40 years of development in building and civil engineering. *Composite structures, 86*(1), 3-9.

British Standards Institute. (1990). BS 1377-2: Methods of test for soils for civil rngineering purposes- Classification tests. London: BSI.

British Standards Institute. (2002). Mixing Water for Concrete. Specification for Sampling, Testing and Assessing the Suitability of Water, Including Water Recovered from Processes in the Concrete Industry, as Mixing Water in Concrete. London: BSI.

British Standards Institute. (2005). BS EN 14651:Test method for metallic fibre concrete. Measuring the flexural tensile strength (limit of proportionality (LOP), residual). London: BSI.

British Standards Institute. (2006a). BS EN 14488-5:Testing sprayed concrete. Determination of energy absorption capacity of fibre reinforced slab specimens *Part 5*. London: BSI.

British Standards Institute. (2006b). BS EN 14488 Testing sprayed concrete *Part 3: Flexural strengths (first peak, ultimate and residual) of fibre reinforced beam specimens*. London: BSI.

British Standards Institute. (2009a). BS EN 934-2: Admixtures for concrete, mortar and grout *Concrete admixtures- Definitions, requirements, xonformity, marking and labelling*. London: BSI.

British Standards Institute. (2009b). BS EN 12350-2,“Testing fresh concrete-Part 2: Slump test”. London: BSI.

British Standards Institute. (2009c). BS EN 12390-3: Testing hardened concrete *Compressive strength of test specimens*. London: BSI.

British Standards Institute. (2009d). BS EN 12390-7:2009 Testing hardened concrete *Density of hardened concrete*. London: BSI.

British Standards Institute. (2011). BS EN 197-1: Composition, Specifications and Conformity Criteria for Common Cements *Part I:* . London: BSI.

Caggiano, A., Cremona, M., Faella, C., Lima, C., & Martinelli, E. (2012). Fracture behavior of concrete beams reinforced with mixed long/short steel fibers. *Construction and Building Materials, 37*, 832-840.

Castro, J., & Naaman, A. E. (1981). *Cement mortar reinforced with natural fibers.* Paper presented at the Journal Proceedings.

Cemex Mortars. (2016). Educational guide to cementitious materials *Expert in Concrete*. Surrey, U.K.

Cengiz, O., & Turanli, L. (2004). Comparative evaluation of steel mesh, steel fibre and high-performance polypropylene fibre reinforced shotcrete in panel test. *Cement and Concrete Research, 34*(8), 1357-1364. doi: http://dx.doi.org/10.1016/j.cemconres.2003.12.024

Chotard, T., Boncoeur-Martel, M., Smith, A., Dupuy, J., & Gault, C. (2003). Application of X-ray computed tomography to characterise the early hydration of calcium aluminate cement. *Cement and concrete composites, 25*(1), 145-152.

Claydon, J. F. (2015). Structural Analysis. *Online.* from http://www.jfccivilengineer.com/index.htm

Concrete Foundations Association. (2005). Concrete cracking. *Foundations*. http://www.cfawalls.org/foundations/cracking.htm

ConcreteNetwork.com. (n.d.). Timeline of concrete and cement history. Retrieved [Accessed], 2016, from http://www.concretenetwork.com/concrete-history/

Condit, C. W. (1968). The first reinforced-concrete skyscraper: The Ingalls Building in Cincinnati and its place in structural history. *Technology and Culture, 9*(1), 1-33.

Di Prisco, M., Plizzari, G., & Vandewalle, L. (2009). Fibre reinforced concrete: new design perspectives. *Materials and Structures, 42*(9), 1261-1281.

Ding, Y., Zhang, Y., & Thomas, A. (2009). The investigation on strength and flexural toughness of fibre cocktail reinforced self-compacting high performance concrete. *Construction and Building Materials, 23*(1), 448-452. doi: http://dx.doi.org/10.1016/j.conbuildmat.2007.11.006

directindustry.com. (2016). Direct Industry Retrieved [Accessed], 2016, from http://www.directindustry.com/prod/testing-feuerherdt-bluhm/product-118703-1731749.html

Dobbins, A. (2012). Twintec Advisory Paper 4 : 'Jointless' SFRC External Yards. *Twintec technical article*, 4. Retrieved from www.twintec.co.uk website:

Domone, P., & Illston, J. (2010). *Construction materials: their nature and behaviour* (4th ed.): CRC Press.

Dupont, D., & Vandewalle, L. (2004). *Comparison between the round plate test and the RILEM 3-point bending test.* Paper presented at the 6th RILEM symposium on fibre-reinforced concrete (FRC), Varenna, Italy.

Düzgün, O. A., Gül, R., & Aydin, A. C. (2005). Effect of steel fibers on the mechanical properties of natural lightweight aggregate concrete. *Materials Letters, 59*(27), 3357-3363.

Eberhardt, C., & Clarke, A. (2001). Fibre-orientation measurements in short-glass-fibre composites. Part I: automated, high-angular-resolution measurement by confocal microscopy. *Composites Science and Technology, 61*(10), 1389-1400.

Eddy, D. (2008). UK's biggest-ever SFRC flooring project. *Concrete, 42*(2), 24.

Eddy, D. (2012). Twintec Advisory Paper 2: Steel Fibre Reinforced Concrete (SFRC). *Twintec technical article,* (2). doi:www.twintec.co.uk

Elices, M., & Rocco, C. (2008). Effect of aggregate size on the fracture and mechanical properties of a simple concrete. *Engineering Fracture Mechanics, 75*(13), 3839-3851.

Ezeldin, A. S., & Balaguru, P. N. (1992). Normal-and high-strength fiber-reinforced concrete under compression. *Journal of Materials in Civil Engineering, 4*(4), 415-429.

Fall, D., Shu, J., Rempling, R., Lundgren, K., & Zandi, K. (2014). Two-way slabs: Experimental investigation of load redistributions in steel fibre reinforced concrete. *Engineering Structures, 80*, 61-74.

FAO. (2016). The Future Fibres, Food and Agriculture Organization of United Nations,. Retrieved [Accessed], 2016, from http://www.fao.org/economic/futurefibres/fibres/jute/en/

Ferrara, L., Faifer, M., & Toscani, S. (2012). A magnetic method for non destructive monitoring of fiber dispersion and orientation in steel fiber reinforced cementitious composites—part 1: method calibration. *Materials and Structures, 45*(4), 575-589.

Ferrara, L., & Meda, A. (2006). Relationships between fibre distribution, workability and the mechanical properties of SFRC applied to precast roof elements. *Materials and Structures, 39*(4), 411-420.

Gao, J., Sun, W., & Morino, K. (1997). Mechanical properties of steel fiber-reinforced, high-strength, lightweight concrete. *Cement and concrete composites, 19*(4), 307-313.

García-Taengua, E., Arango, S., Martí-Vargas, J., & Serna, P. (2014). Flexural creep of steel fiber reinforced concrete in the cracked state. *Construction and Building Materials, 65*, 321-329.

Gettu, R., García-Álvarez, V. O., & Aguado, A. (1998). Effect of aging on the fracture characteristics and brittleness of a high-strength concrete. *Cement and Concrete Research, 28*(3), 349-355.

Giaccio, G., & Zerbino, R. (1998). Failure mechanism of concrete: combined effects of coarse aggregates and strength level. *Advanced Cement Based Materials, 7*(2), 41-48.

Gopalaratnam, V. S., & Gettu, R. (1995). On the characterization of flexural toughness in fiber reinforced concretes. *Cement and concrete composites, 17*(3), 239-254.

Graeff, A. G., Pilakoutas, K., Neocleous, K., & Peres, M. V. N. (2012). Fatigue resistance and cracking mechanism of concrete pavements reinforced with recycled steel fibres recovered from post-consumer tyres. *Engineering Structures, 45*, 385-395.

Guo, L.-P., Sun, W., Zheng, K.-R., Chen, H.-J., & Liu, B. (2007). Study on the flexural fatigue performance and fractal mechanism of concrete with high proportions of ground granulated blast-furnace slag. *Cement and Concrete Research, 37*(2), 242-250.

Habel, K., & Gauvreau, P. (2008). Response of ultra-high performance fiber reinforced concrete (UHPFRC) to impact and static loading. *Cement and concrete composites, 30*(10), 938-946.

Halverson, C., White, D. J., & Gray, J. (2005). *Application of x-ray CT scanning to characterize geomaterials used in transportation construction.* Paper presented at the Proc. Mid-Continent Transp. Res. Symp., Ames, IA. Aug.

Hannant, D. (2002). Fibres in concrete: a perspective. *Concrete, 36*(8), 40-43.

Hannant, D. J. (2003). Fibre-reinforced concrete. In J. S. C. Newman, B (Ed.), *Advanced Concrete Technology*. Burlington, USA.

Henager, C. H. (1981). Steel fibrous shotcrete: a summary of the state-of-the-art. *Concrete International: Design and Construction, 3*(1), 55-58.

HILTI. (n.d.). DD 350-CA Diamond coring tool. Accessed 2016, from https://www.hilti.co.uk/diamond-coring/diamond-drilling-tools/r3411829#

Holschemacher, K., Mueller, T., & Ribakov, Y. (2010). Effect of steel fibres on mechanical properties of high-strength concrete. *Materials & Design, 31*(5), 2604-2615.

Huang, C., & Zhao, G. (1995). Properties of steel fibre reinforced concrete containing larger coarse aggregate. *Cement and concrete composites, 17*(3), 199-206.

Illston, J., & Dinwoodie, J. (1994). *Construction materials: their nature and behaviour* (Second ed.). London: E & FN Spon.

Jackson, M. D., Moon, J., Gotti, E., Taylor, R., Chae, S. R., Kunz, M., . . . Levitz, P. (2013). Material and elastic properties of Al-tobermorite in ancient Roman seawater concrete. *Journal of the American Ceramic Society, 96*(8), 2598-2606.

Jensen, B. (2013). Declaration of performance. *Aalboug White Portland cement CEM 1.* [Accessed] 2015, from http://www.aalborgwhite.com/media/pdf_files/aalborg_white

Kang, S.-T., & Kim, J.-K. (2012). Investigation on the flexural behavior of UHPCC considering the effect of fiber orientation distribution. *Construction and Building Materials, 28*(1), 57-65.

Kayvani, K. (2014). Design of high-rise buildings: past, present and future.

Kazemi, S., & Lubell, A. S. (2012). Influence of specimen size and fiber content on mechanical properties of ultra-high-performance fiber-reinforced concrete. *ACI Materials Journal, 109*(6).

Kennedy, G., & Goodchild, C. (2004). *Practical yield line design*. Surrey UK: The concrete centre.

Ketcham, R. A., & Carlson, W. D. (2001). Acquisition, optimization and interpretation of X-ray computed tomographic imagery: applications to the geosciences. *Computers & Geosciences, 27*(4), 381-400.

Ketcham, R. A., & Iturrino, G. J. (2005). Nondestructive high-resolution visualization and measurement of anisotropic effective porosity in complex lithologies using high-resolution X-ray computed tomography. *Journal of Hydrology, 302*(1), 92-106.

Kim, J. J., Kim, D. J., Kang, S. T., & Lee, J. H. (2012). Influence of sand to coarse aggregate ratio on the interfacial bond strength of steel fibers in concrete for nuclear power plant. *Nuclear Engineering and Design, 252*(0), 1-10. doi: http://dx.doi.org/10.1016/j.nucengdes.2012.07.004

Köksal, F., Şahin, Y., Gencel, O., & Yiğit, İ. (2013). Fracture energy-based optimisation of steel fibre reinforced concretes. *Engineering Fracture Mechanics, 107*, 29-37.

Kolluru, S. V., O'Neil, E. F., Popovics, J. S., & Shah, S. P. (2000). Crack propagation in flexural fatigue of concrete. *Journal of Engineering Mechanics, 126*(9), 891-898.

Lataste, J.-F., Barnett, S. J., Parry, T., & Soutsos, M. N. (2011). Study of fibre distribution and orientations in UHPFRC by electrical resistivity and mechanical tests. *European Journal of Environmental and Civil Engineering, 15*(4), 533-544.

Li, H., Zhang, M.-h., & Ou, J.-p. (2007). Flexural fatigue performance of concrete containing nano-particles for pavement. *International Journal of Fatigue, 29*(7), 1292-1301.

Marti, P., Pfyl, T., Sigrist, V., & Tomaz, U. (1999). Harmonized Test Procedures for Steel Fiber-Reinforced Concrete. *ACI Materials Journal, 96*(6), 676-685.

Math.byu.edu. (2016). Changing coordinate systems. Retrieved 24th August 2016, 2016, from https://math.byu.edu/~math302/content/learningmod/coordinates/rectsphere.html

Michels, J., Christen, R., & Waldmann, D. (2013). Experimental and numerical investigation on postcracking behavior of steel fiber reinforced concrete. *Engineering Fracture Mechanics, 98*, 326-349.

Miller Waste Mills. (2016). Sisal fibers. Retrieved [Accessed], 2016, from http://www.millerwastemills.com/

Mindess, S. (2007). *Thirty years of fibre reinforced concrete research at the University of British Columbia.* Paper presented at the Proceedings of first international conference on sustainable construction materials and technologies, Conventry.

Mohammadi, Y., Singh, S., & Kaushik, S. (2008). Properties of steel fibrous concrete containing mixed fibres in fresh and hardened state. *Construction and Building Materials, 22*(5), 956-965.

Naaman, A. E. (2003). Engineered steel fibers with optimal properties for reinforcement of cement composites. *Journal of Advanced Concrete Technology, 1*(3), 241-252.

Neville, A. M. (1995). *Properties of Concrete* (Fourth ed.). Essex, England: Longman Group Limited.

Neville, A. M., & Brooks, J. J. (1987). *Concrete technology*. Essex, England: Longman Group.

Oh, B. H. (1992). Flexural analysis of reinforced concrete beams containing steel fibers. *Journal of Structural Engineering, 118*(10), 2821-2835.

Oh, B. H., Kim, J. C., & Choi, Y. C. (2007). Fracture behavior of concrete members reinforced with structural synthetic fibers. *Engineering Fracture Mechanics, 74*(1), 243-257.

Okafor, F. O. (1988). Palm kernel shell as a lightweight aggregate for concrete. *Cement and Concrete Research, 18*(6), 901-910.

Pająk, M., & Ponikiewski, T. (2013). Flexural behavior of self-compacting concrete reinforced with different types of steel fibers. *Construction and Building Materials, 47*, 397-408.

Palagyi, K. (n.d.). 3D Thinning algorithms and its medical applications. *Skeletonization.* 2016, from http://www.inf.u-szeged.hu/~palagyi

Ponikiewski, T., Katzer, J., Bugdol, M., & Rudzki, M. (2014). Determination of 3D porosity in steel fibre reinforced SCC beams using X-ray computed tomography. *Construction and Building Materials, 68*, 333-340.

Portland Cement Association. (1991). *SP039T - MIT Fiber reinforced concrete*. Illinois USA: Portland Cement Assn.

Pujadas, P., Blanco, A., Cavalaro, S., de la Fuente, A., & Aguado, A. (2014). Fibre distribution in macro-plastic fibre reinforced concrete slab-panels. *Construction and Building Materials, 64*, 496-503.

Pujadas, P., Blanco, A., de la Fuente, A., & Aguado, A. (2012). Cracking behavior of FRC slabs with traditional reinforcement. *Materials and Structures, 45*(5), 707-725.

Ramakrishnan, V., Tolmare, N. S., & Brik, V. B. (1998). Performance evaluation of 3-D basalt fiber reinforced concrete & basalt rod reinforced concrete: Transportation Research Board of National Research Council, US.

Reinhardt, H., Grosse, C., & Weiler, B. (2001). Material characterization of steel fiber reinforced concrete using neutron CT, ultrasound and quantitative acoustic emission techniques. *NDT. net, 6*(5), 1-12.

Rossi, P., Ulm, F.-J., & Hachi, F. (1996). Compressive behavior of concrete: physical mechanisms and modeling. *Journal of Engineering Mechanics, 122*(11), 1038-1043.

Roumaldi, J., & Batson, G. B. (1963). *Mechanics of crack arrest in concrete.* Paper presented at the American Society of Civil Engineers.

Sable, K. S., & Rathi, M. K. (2012). Effect of Different Type of Steel Fiber and Aspect Ratio on Mechanical Properties of Self Compacted Concrete. *International Journal of Engineering and Innovative Technology (IJEIT) Volume, 2*, 184-188.

Salau, M. A., Adegbite, I., & Ikponmwosa, E. E. (2012). Characteristic strength of concrete column reinforced with bamboo strips. *Journal of Sustainable Development, 5*(1), 133.

Salehian, H., Barros, J. A., & Taheri, M. (2014). Evaluation of the influence of post-cracking response of steel fibre reinforced concrete (SFRC) on load carrying capacity of SFRC panels. *Construction and Building Materials, 73*, 289-304.

Sebaibi, N., Benzerzour, M., & Abriak, N. E. (2014). Influence of the distribution and orientation of fibres in a reinforced concrete with waste fibres and powders. *Construction and Building Materials, 65*, 254-263.

Shah, S. P. (1981). Fiber reinforced concretes. *ACI journal,* 36-43.

Shannon, C. E. (2001). A mathematical theory of communication. *ACM SIGMOBILE Mobile Computing and Communications Review, 5*(1), 3-55.

Sivakumar, A., & Santhanam, M. (2007). Mechanical properties of high strength concrete reinforced with metallic and non-metallic fibres. *Cement and concrete composites, 29*(8), 603-608.

Slater, E., Moni, M., & Alam, M. S. (2012). Predicting the shear strength of steel fiber reinforced concrete beams. *Construction and Building Materials, 26*(1), 423-436.

Sorelli, L. G., Meda, A., & Plizzari, G. A. (2006). Steel fiber concrete slabs on ground: a structural matter. *ACI structural journal, 103*(4).

Soulioti, D., Barkoula, N., Paipetis, A., & Matikas, T. (2011). Effects of Fibre Geometry and Volume Fraction on the Flexural Behaviour of Steel-Fibre Reinforced Concrete. *Strain, 47*(s1), e535-e541.

Soutsos, M., Le, T., & Lampropoulos, A. (2012). Flexural performance of fibre reinforced concrete made with steel and synthetic fibres. *Construction and Building Materials, 36*, 704-710.

Sprawls, P. (n.d.). The Physical Principles of Medical Imaging. *Radiation Penetration.* [Accessed] 2016, from http://www.sprawls.org/ppmi2/RADPEN/

Suuronen, J.-P., Kallonen, A., Eik, M., Puttonen, J., Serimaa, R., & Herrmann, H. (2013). Analysis of short fibres orientation in steel fibre-reinforced concrete (SFRC) by X-ray tomography. *Journal of Materials Science, 48*(3), 1358-1367.

Taylor, M., Lydon, F., & Barr, B. (1997). Toughness measurements on steel fibre-reinforced high strength concrete. *Cement and concrete composites, 19*(4), 329-340.

TEXASGeosciences. (2015). University of Texas High-Resolution X-ray Computed Tomography Facility. [Accessed] from http://www.ctlab.geo.utexas.edu/

The Concrete Society. (2007). Guidance for the design of stell-fibre-reinforced concrete. Camberley, Surrey.

The ITK software. (n.d.). The Insight Segmentation and Registration Toolkit. [Accessed] 2016, from https://itk.org/ITK/project/about.html

Thomas, J., & Jennings, H. (n.d.). The Science of Concrete. *Online.* Retrieved

from http://iti.northwestern.edu/cement/monograph/Monograph2_2_5.html

Tradekorea.com. (2008). Crimped steel fibre. Retrieved Accessed on 15 June 2016, from http://www.tradekorea.com/product/detail/P262700/crimped-steel-fiber.html

Udoeyo, F. F., Anyanwu, C. I., Brooks, R., & Udo-Inyang, P. (2011). Properties of Palm Nut Fiber–Reinforced Cement Composite Containing Pulverized Kernel Shell as Supplementary Material. *Journal of Materials in Civil Engineering, 23*(4), 378-384.

Uotinen, L. (2011). *Design of shotcrete rock reinforcement in hard rock according to Eurocode.* Paper presented at the Proceeding of: Seminar on Geoengineering, Espoo, Finland.

Uotinen, L., Salo, O., & Rinne, M. (2013). *Design of sprayed concrete as hard rock reinforcement using yield-line theory.* Paper presented at the ISRM SINOROCK 2013.

Uzomaka, O. J. (1976). Characteristics of akwara as a reinforcing fibre. *Magazine of Concrete Research, 28*(96), 162-167.

Vallarasu Manoharan, S., & Anandan, S. (2014). Steel Fibre Reinforcing Characteristics on the Size Reduction of Fly Ash Based Concrete. *Advances in Civil Engineering, 2014*.

Van Chanh, N. (2004). *Steel fiber reinforced concrete.* Paper presented at the Faculty of Civil Engineering Ho chi minh City university of Technology. Seminar Material.

Vandewalle, L., Nemegeer, D., Balazs, L., Barr, B., Barros, J., Bartos, P., . . . Di Prisco, M. (2003). RILEM TC162-TDF: test and design methods for steel fibre reinforced concrete: sigma-epsilon design method (final recommendation). *Materials and Structures, 36*(262), 560-567.

Veenendaal, D., West, M., & Block, P. (2011). History and overview of fabric formwork: using fabrics for concrete casting. *Structural Concrete, 12*(3), 164-177.

Wang, H., & Wang, L. (2013). Experimental study on static and dynamic mechanical properties of steel fiber reinforced lightweight aggregate concrete. *Construction and Building Materials, 38*, 1146-1151.

Weisstein, E. W. (2016). "Sphere Point Picking." From MathWorld--A Wolfram Web Resource. {Accessed} 2016, from http://mathworld.wolfram.com/SpherePointPicking.html

Yazıcı, Ş., & Arel, H. Ş. (2013). The effect of steel fiber on the bond between concrete and deformed steel bar in SFRCs. *Construction and Building Materials, 40*, 299-305.

Yazıcı, Ş., İnan, G., & Tabak, V. (2007). Effect of aspect ratio and volume fraction of steel fiber on the mechanical properties of SFRC. *Construction and Building Materials, 21*(6), 1250-1253.

Yoo, T. S., Ackerman, M. J., Lorensen, W. E., Schroeder, W., Chalana, V., Aylward, S., . . . Whitaker, R. (2002). Engineering and algorithm design for an image processing API: a technical report on ITK-the insight toolkit. *Studies in health technology and informatics*, 586-592.

Zhang, Y.-y., Harries, K. A., & Yuan, W.-c. (2013). Experimental and numerical investigation of the seismic performance of hollow rectangular bridge piers constructed with and without steel fiber reinforced concrete. *Engineering Structures, 48*, 255-265.

Zhou, F., Barr, B., & Lydon, F. (1995). Fracture properties of high strength concrete with varying silica fume content and aggregates. *Cement and Concrete Research, 25*(3), 543-552.

Zollo, R. F. (1997). Fiber-reinforced concrete: an overview after 30 years of development. *Cement and concrete composites, 19*(2), 107-122. doi: http://dx.doi.org/10.1016/S0958-9465(96)00046-7

APPENDICES

Appendix A: Results showing three replicates of 3-point loading of beam

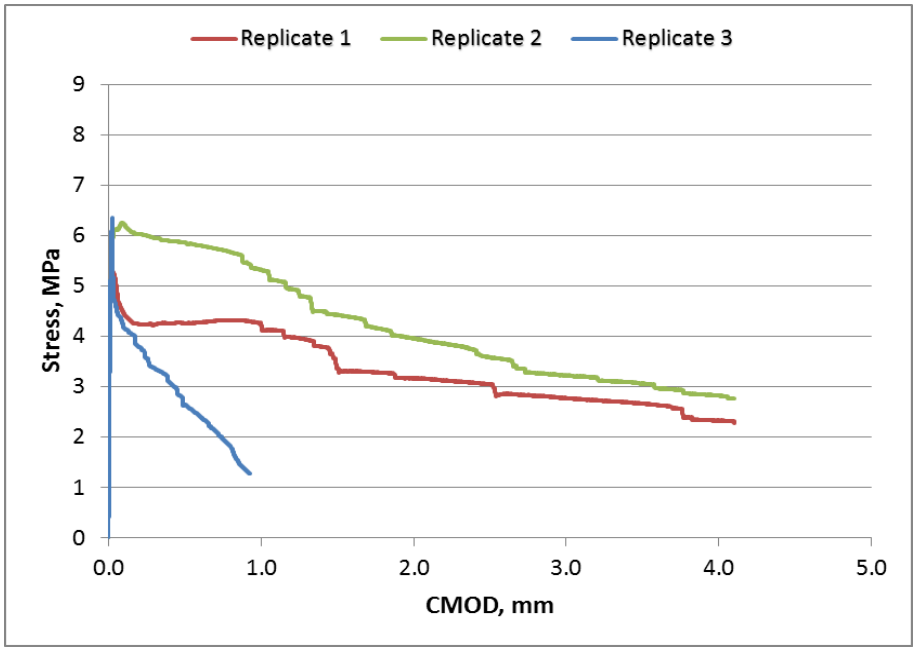

Flexural curves of SFRC of 25 kg/m^3 dosage of 80/60 + 10 mm concrete beams (Fault with extensometer attached during replicate 3 test)

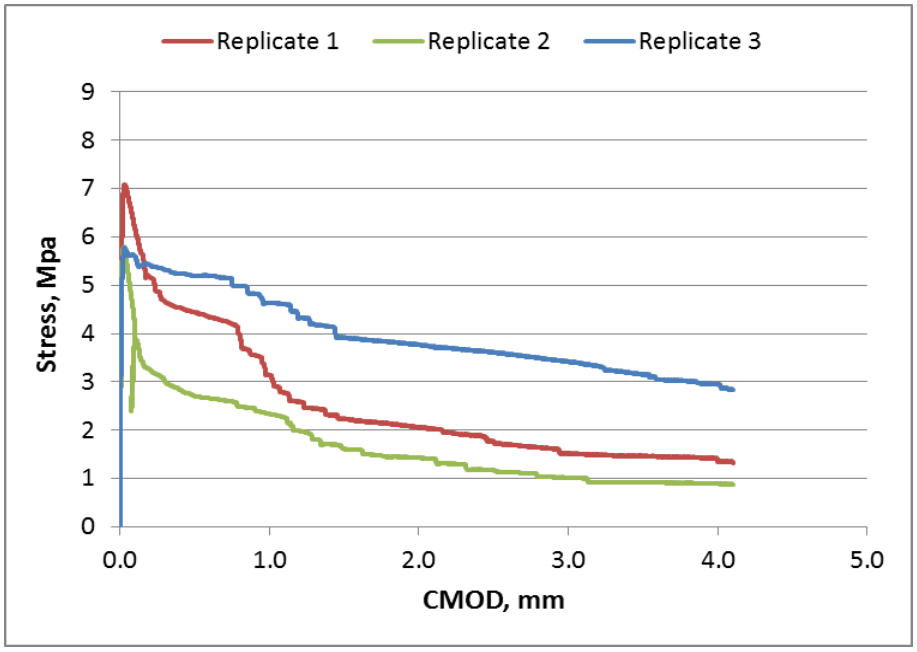

Flexural curves of SFRC of 25 kg/m^3 dosage of 80/60 + 20 mm concrete beams

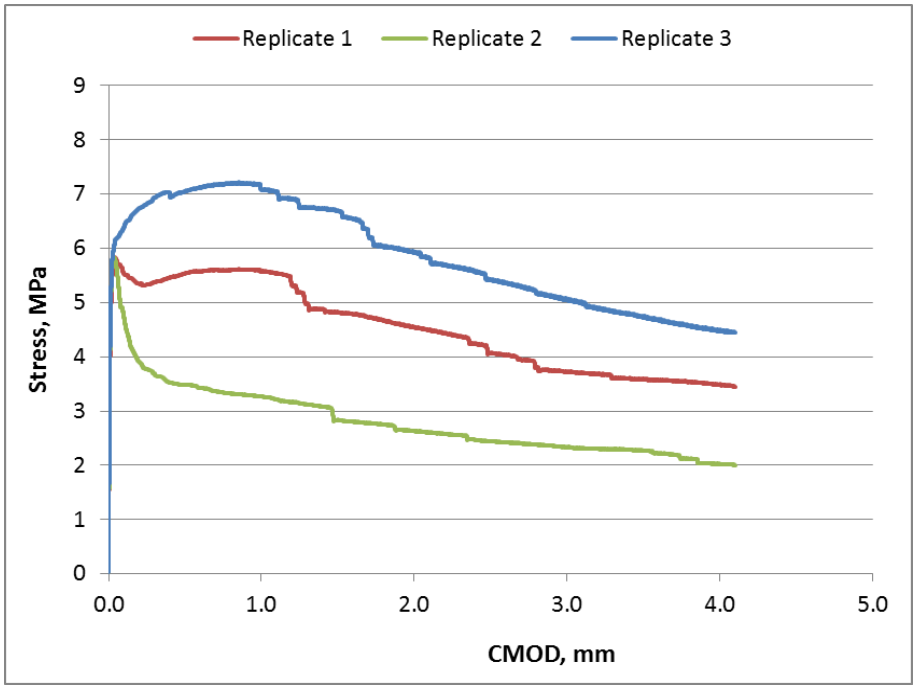

Flexural curves of SFRC of 40 kg/m^3 dosage of 80/60 + 10 mm concrete beams

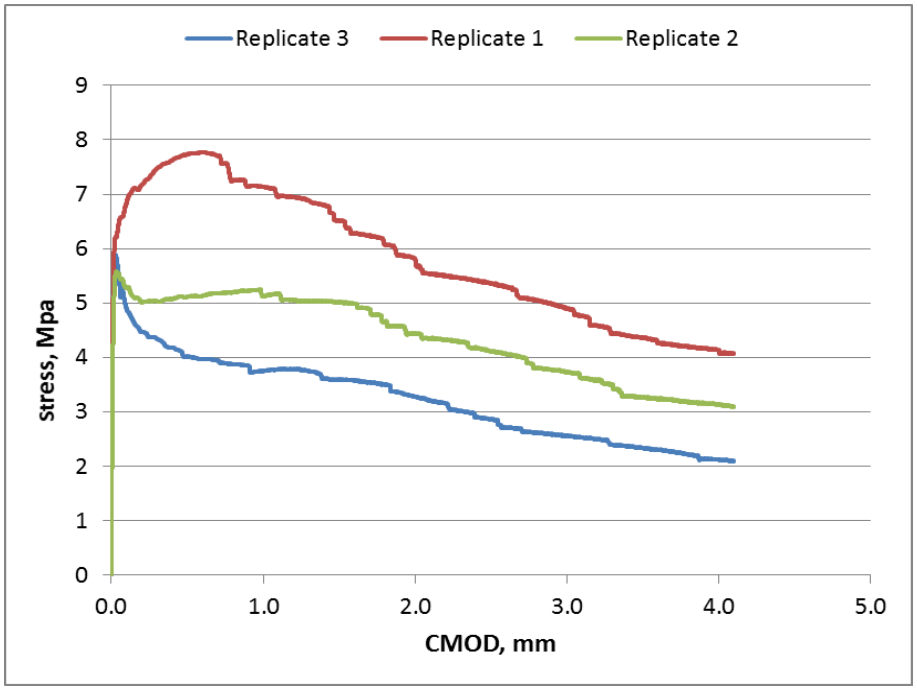

Flexural curves of SFRC of 40 kg/m^3 dosage of 80/60 + 20 mm concrete beams

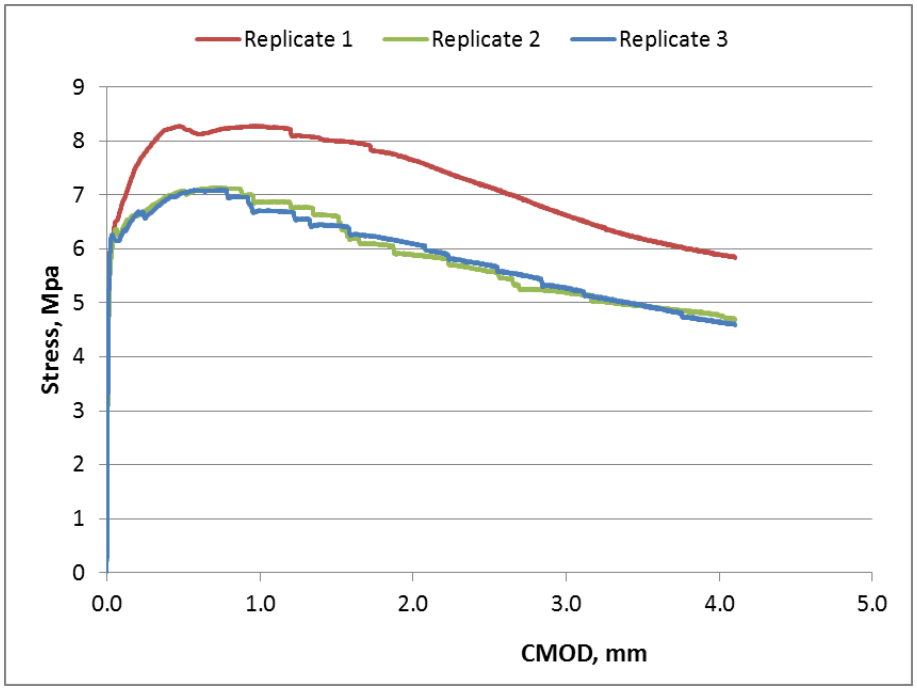

Flexural curves of SFRC of 50 kg/m^3 dosage of 80/60 + 10 mm concrete beams

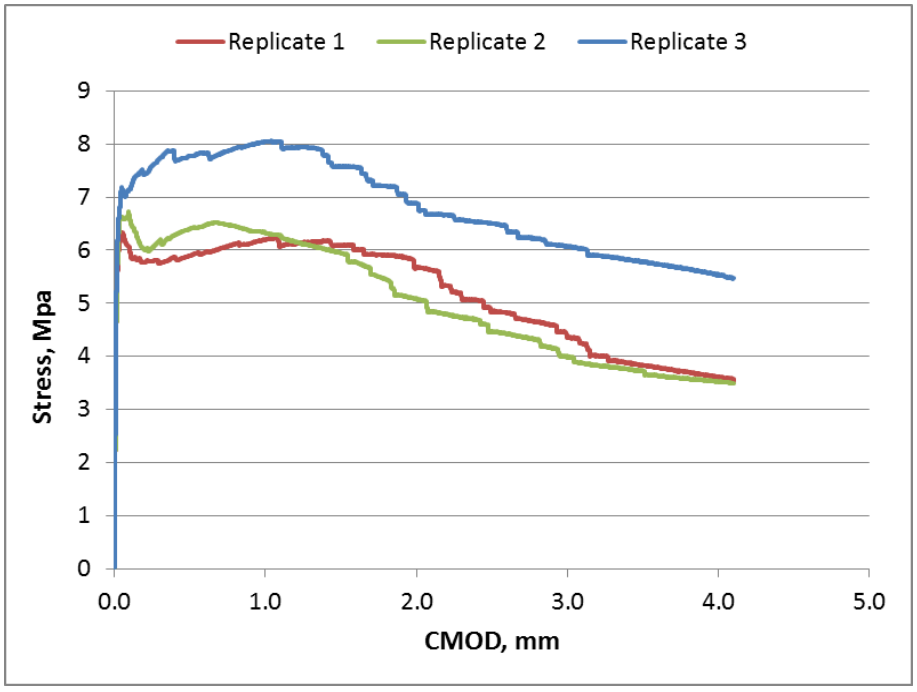

Flexural curves of SFRC of 50 kg/m^3 dosage of 80/60 + 20 mm concrete beams

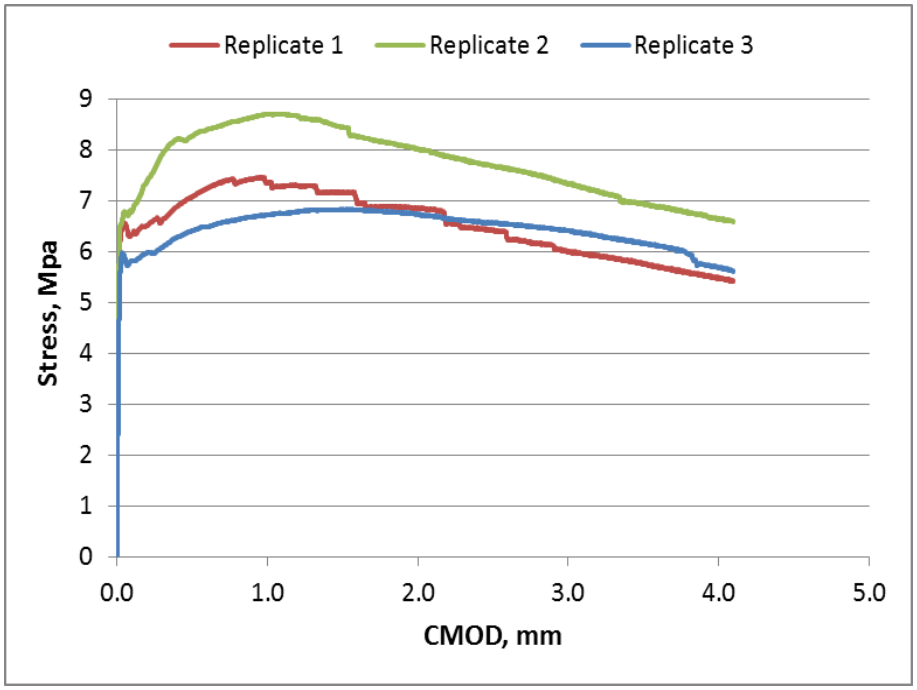

Flexural curves of SFRC of 60 kg/m^3 dosage of 80/60 + 10 mm concrete beams

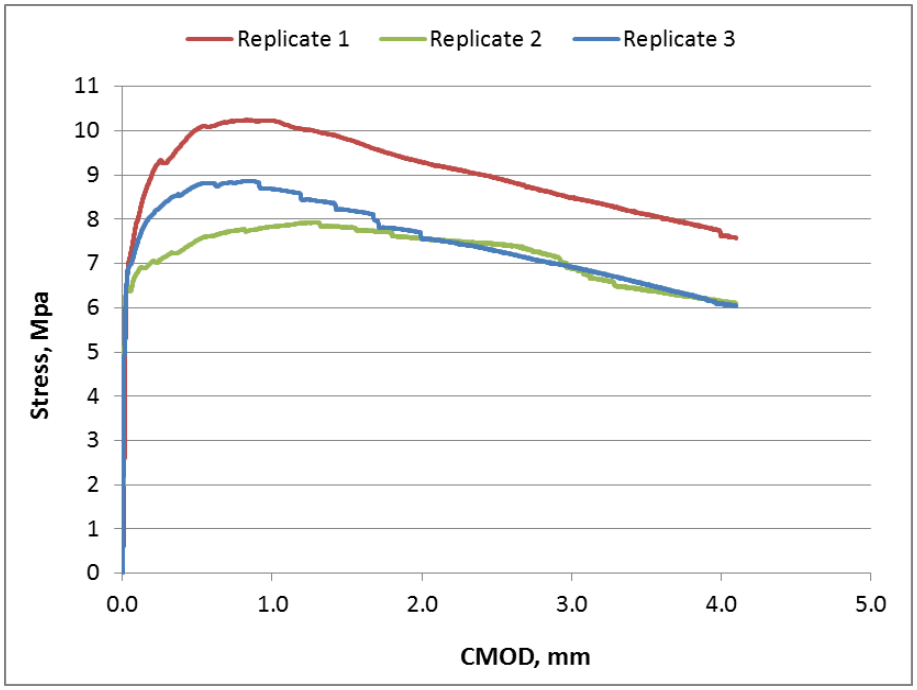

Flexural curves of SFRC of 60 kg/m^3 dosage of 80/60 + 20 mm concrete beams

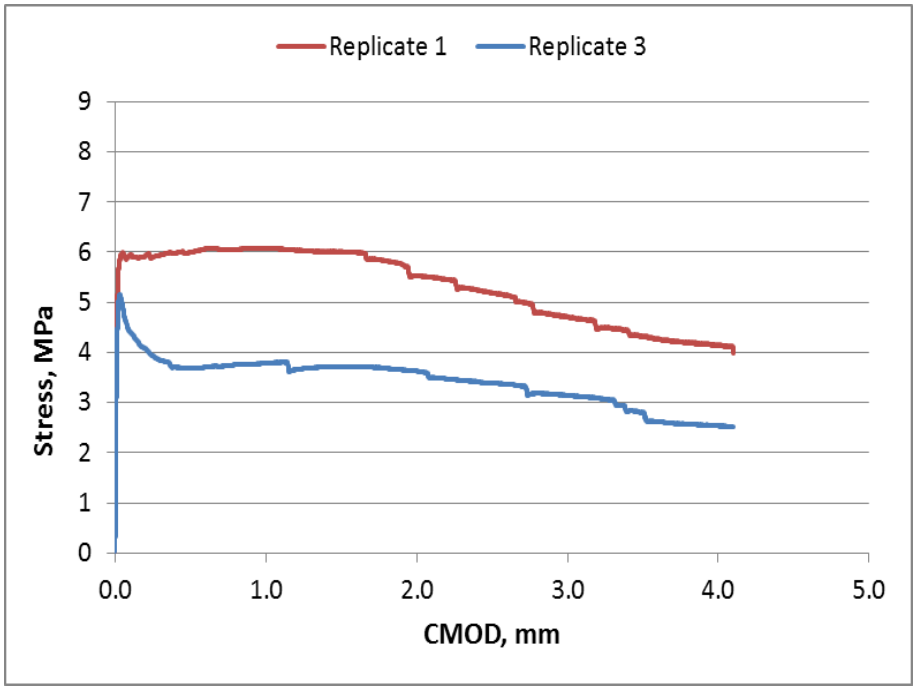

Flexural curves of SFRC of 25 kg/m^3 dosage of 65/60 + 10 mm concrete beams (Error detected with readings during test of replicate 2)

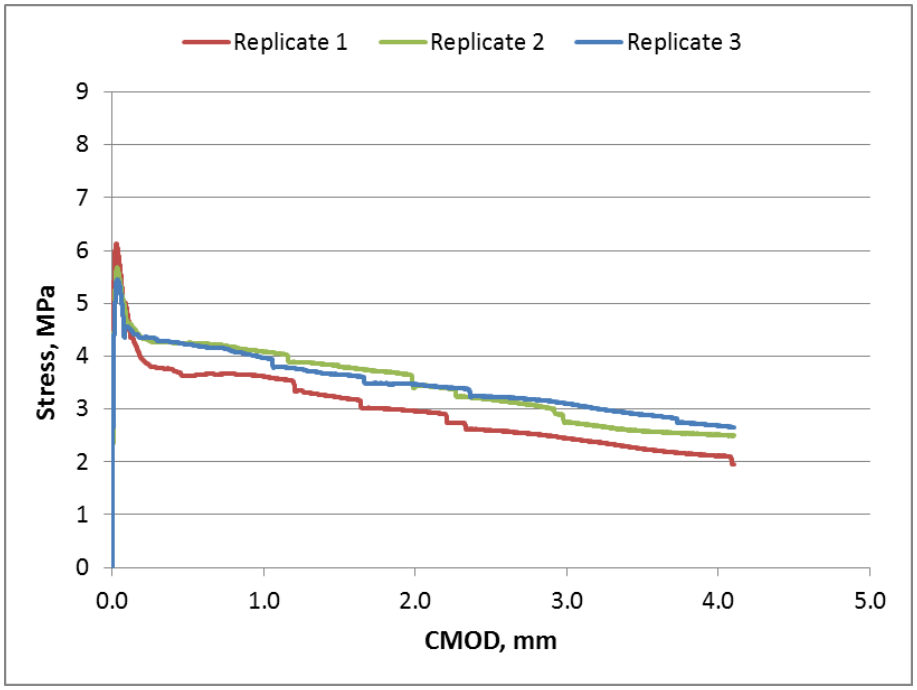

Flexural curves of SFRC of 25 kg/m^3 dosage of 65/60 + 20 mm concrete beams

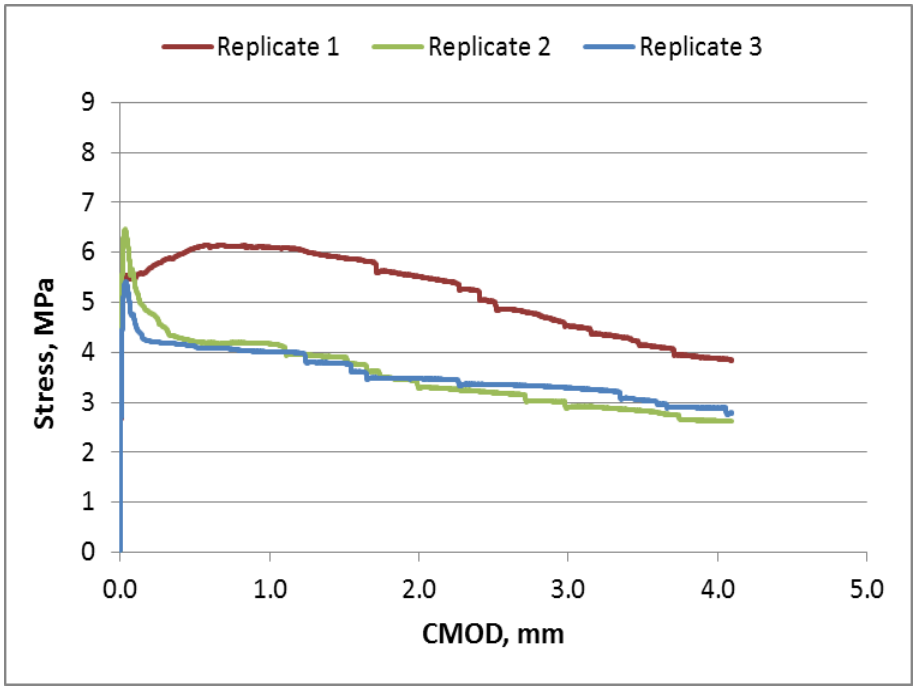

Flexural curves of SFRC of 40 kg/m^3 dosage of 65/60 + 10 mm concrete beams

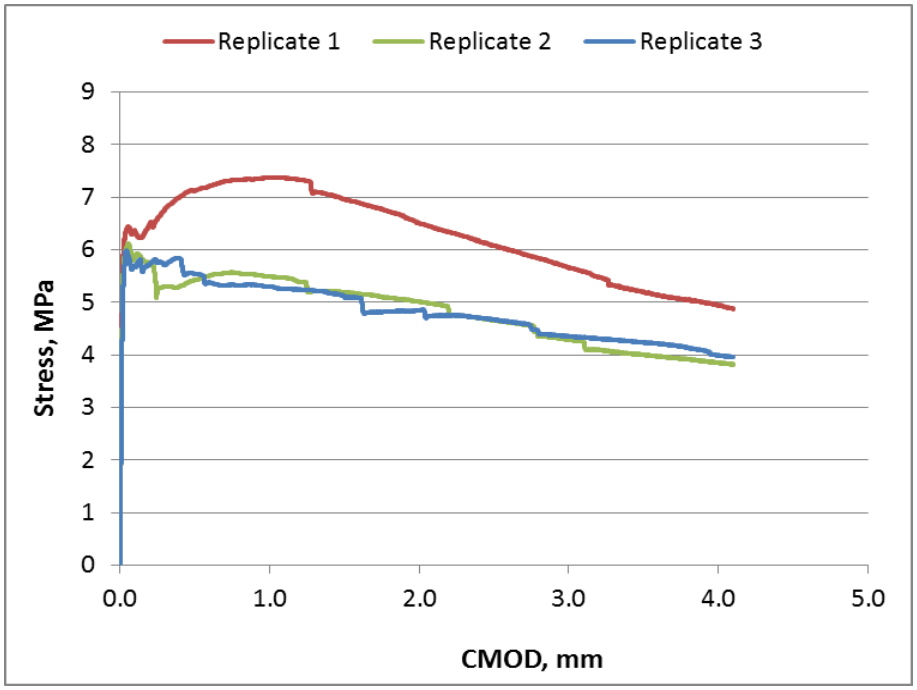

Flexural curves of SFRC of 40 kg/m^3 dosage of 65/60 + 20 mm concrete beams

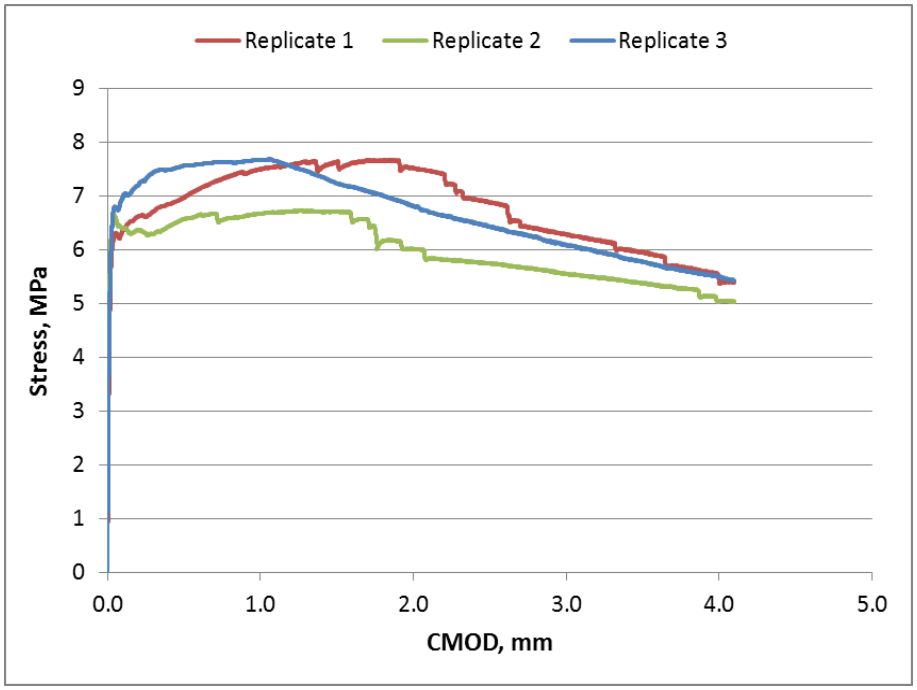

Flexural curves of SFRC of 50 kg/m^3 dosage of 65/60 + 10 mm concrete beams

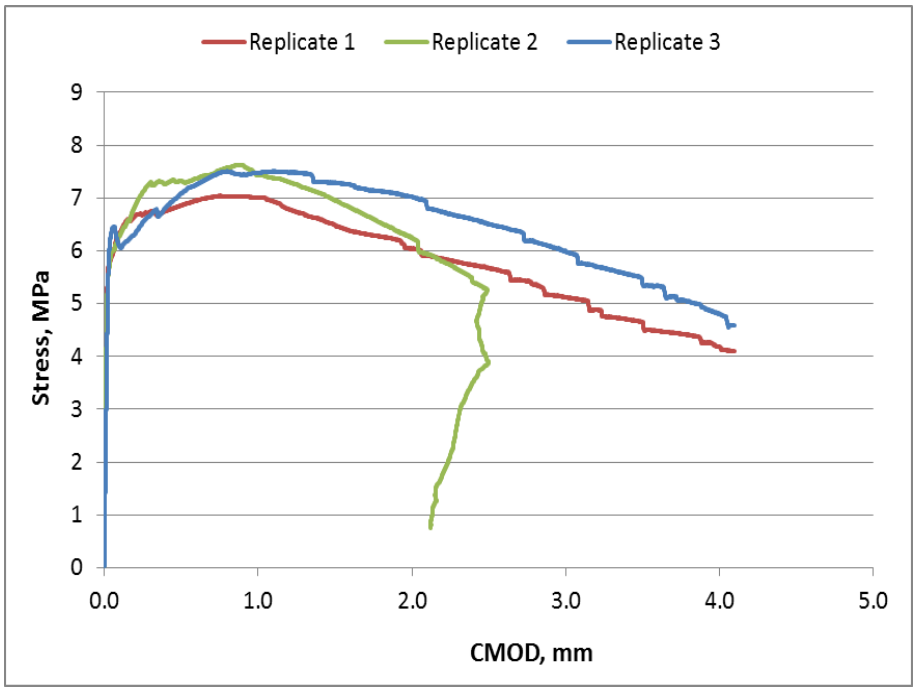

Flexural curves of SFRC of 50 kg/m^3 dosage of 65/60 + 20 mm concrete beams

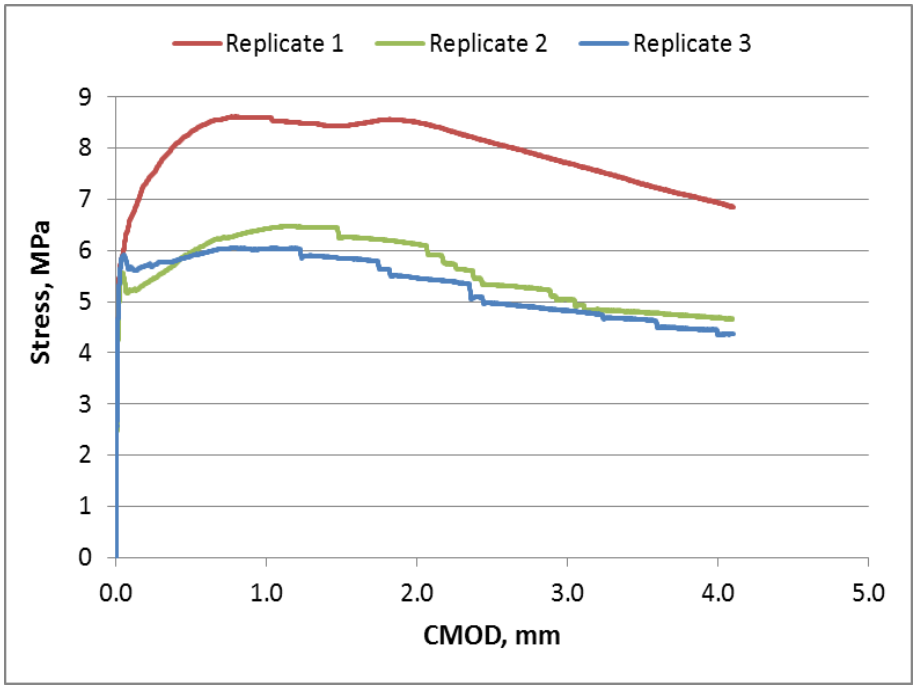

Flexural curves of SFRC of 60 kg/m^3 dosage of 65/60 + 10 mm concrete beams

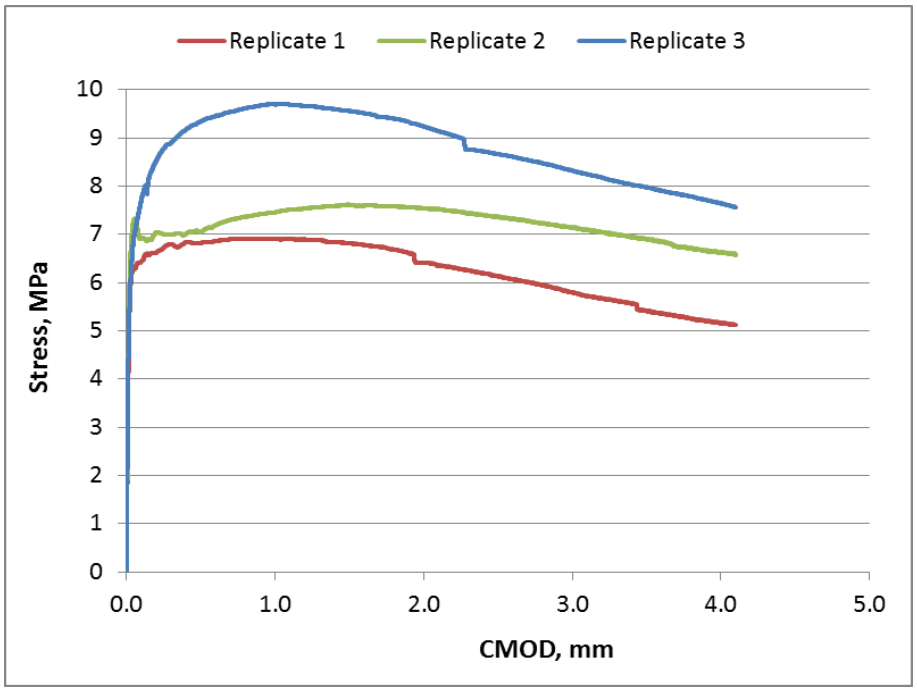

Flexural curves of SFRC of 60 kg/m^3 dosage of 65/60 + 20 mm concrete beams

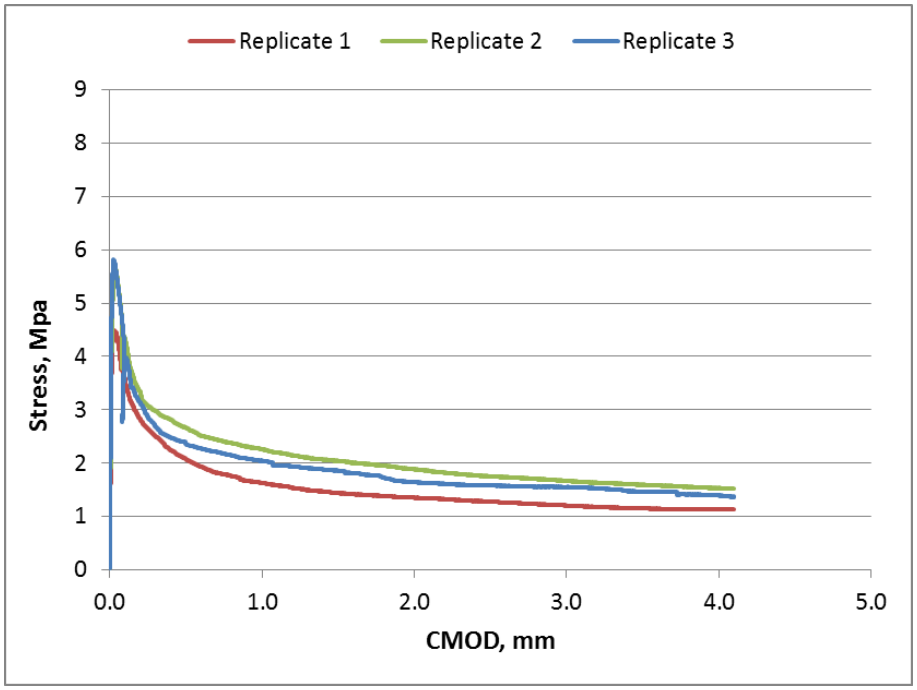

Flexural curves of SFRC of 25 kg/m^3 dosage of 45/50 + 10 mm concrete beams

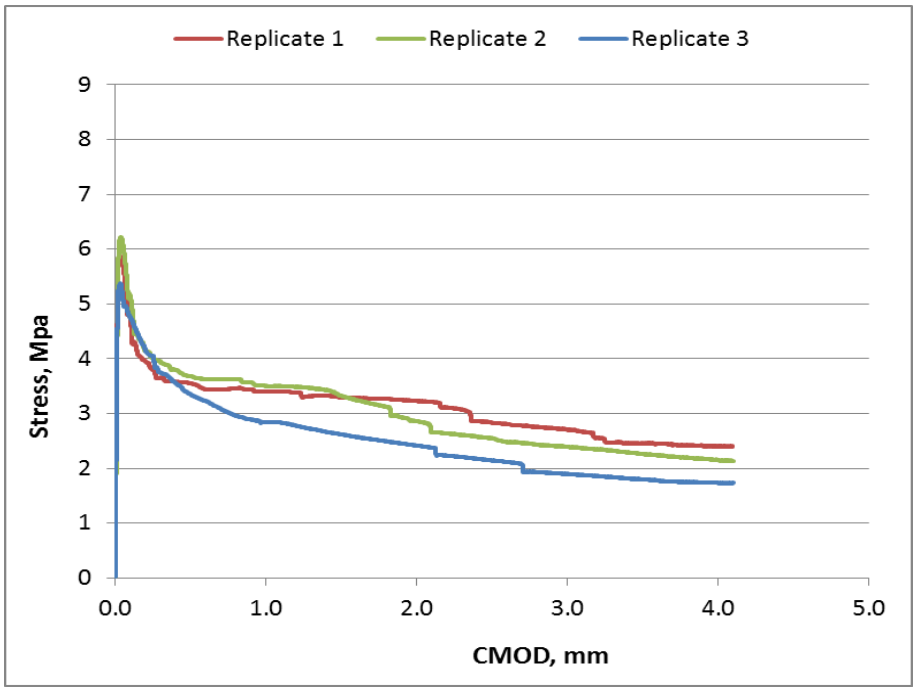

Flexural curves of SFRC of 25 kg/m^3 dosage of 45/50 + 20 mm concrete beams

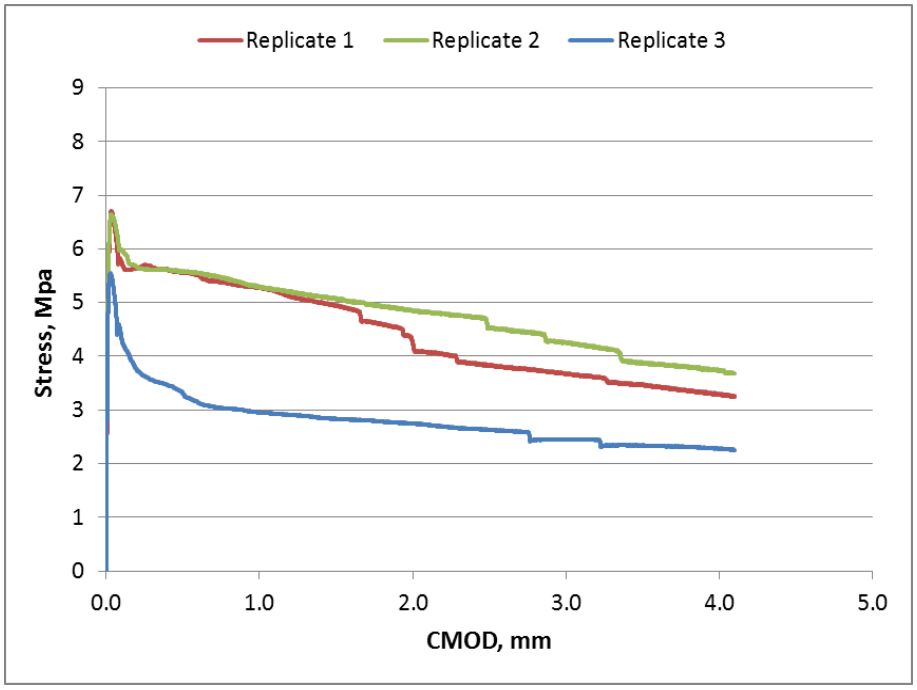

Flexural curves of SFRC of 40 kg/m^3 dosage of 45/50 + 10 mm concrete beams

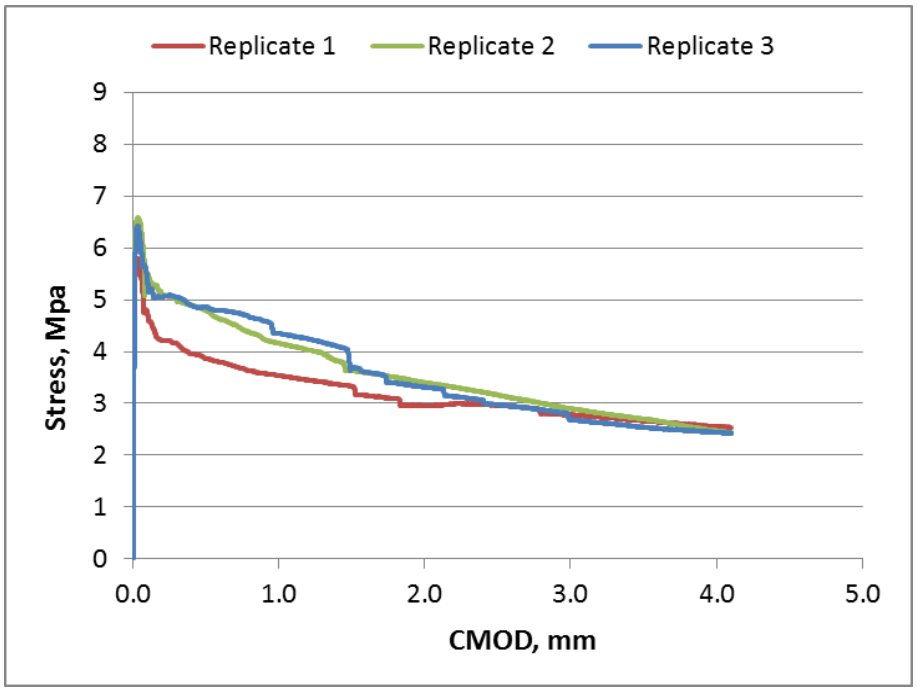

Flexural curves of SFRC of 40 kg/m^3 dosage of 45/50 + 20 mm concrete beams

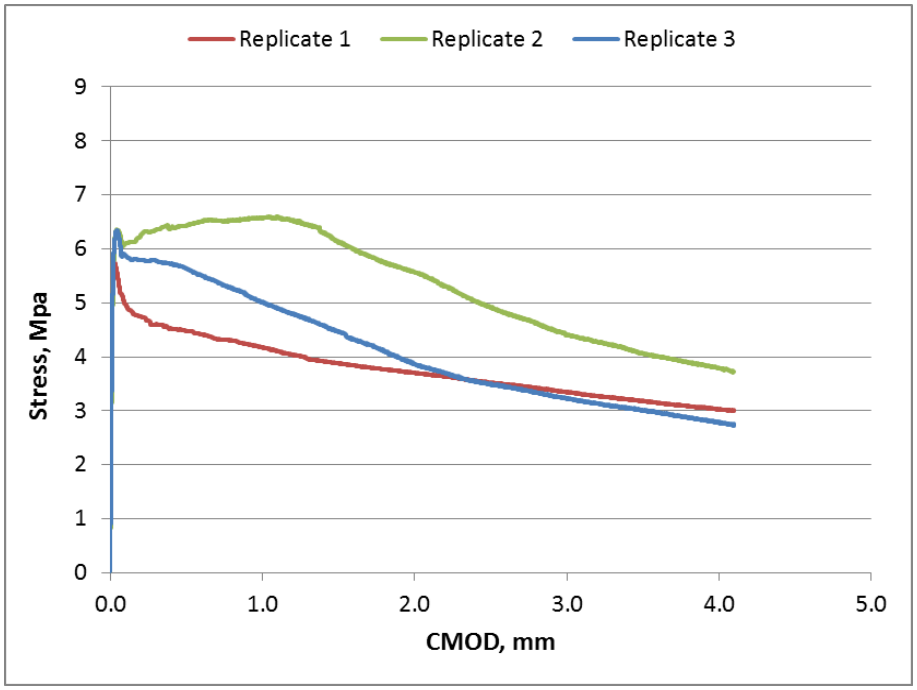

Flexural curves of SFRC of 50 kg/m^3 dosage of 45/50 + 10 mm concrete beams

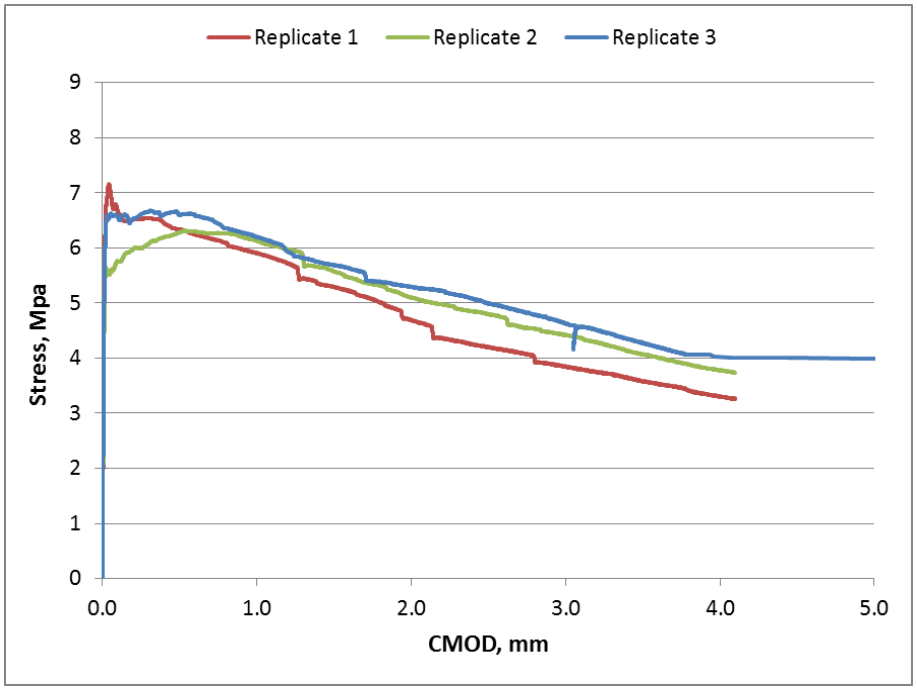

Flexural curves of SFRC of 50 kg/m^3 dosage of 45/50 + 20 mm concrete beams

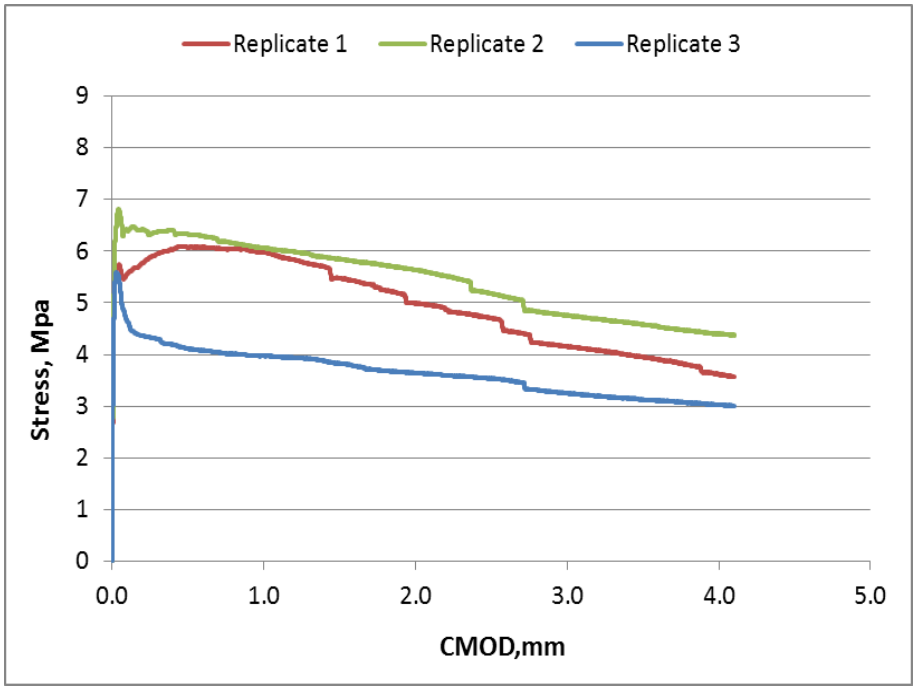

Flexural curves of SFRC of 60 kg/m^3 dosage of 45/50 + 10 mm concrete beams

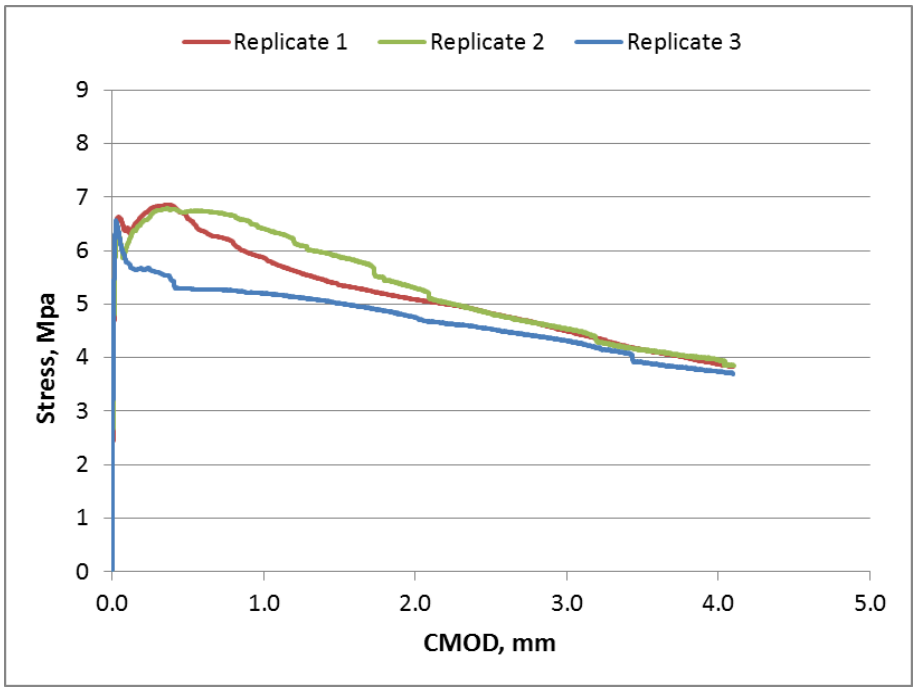

Flexural curves of SFRC of 60 kg/m^3 dosage of 45/50 + 20 mm concrete beams

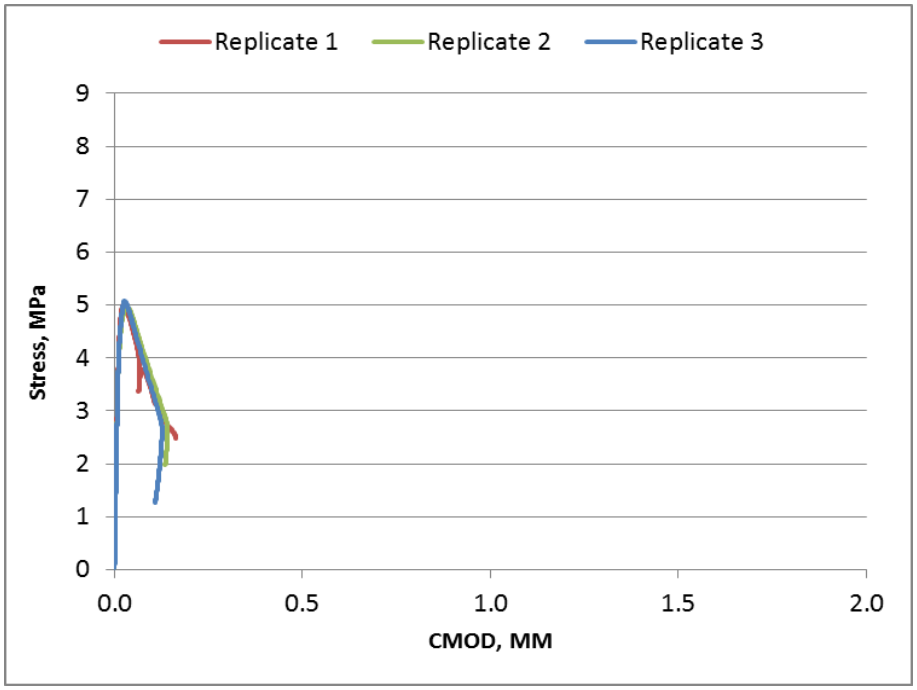

Flexural curves of plain unreinforced concrete beams, 10 mm

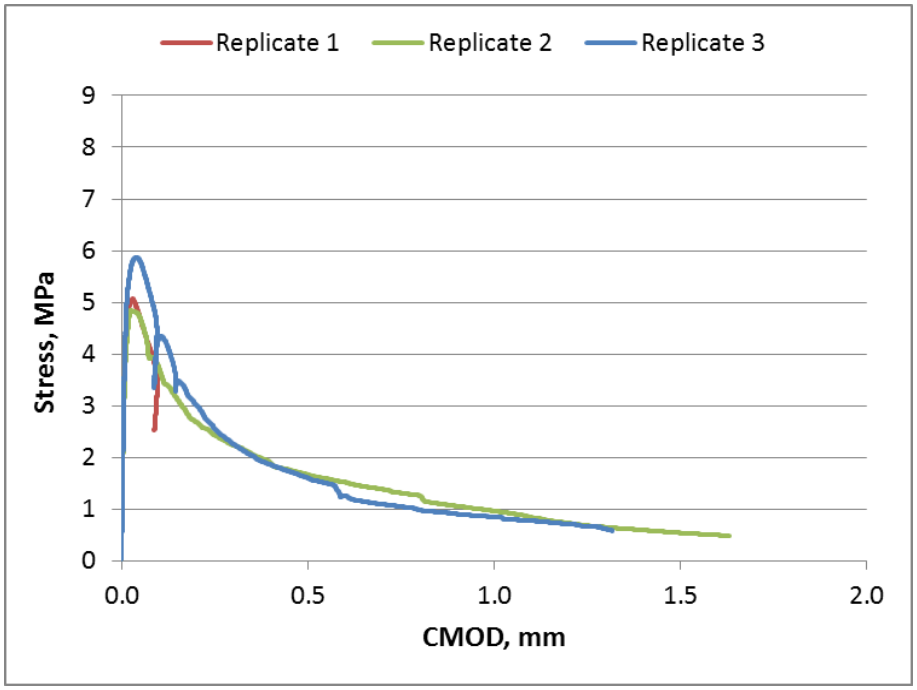

Flexural curves of plain unreinforced concrete beams, 20 mm

Appendix B: Results showing three replicates of slab flexural tests (failure load)

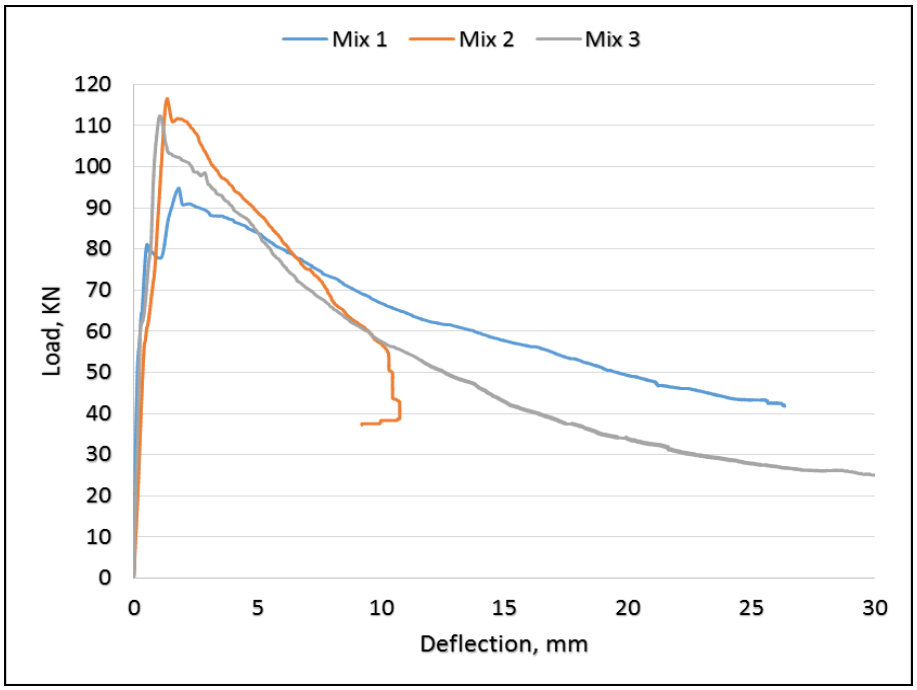

Load - deflection curve of concrete square panel, 65/60 + 10 mm

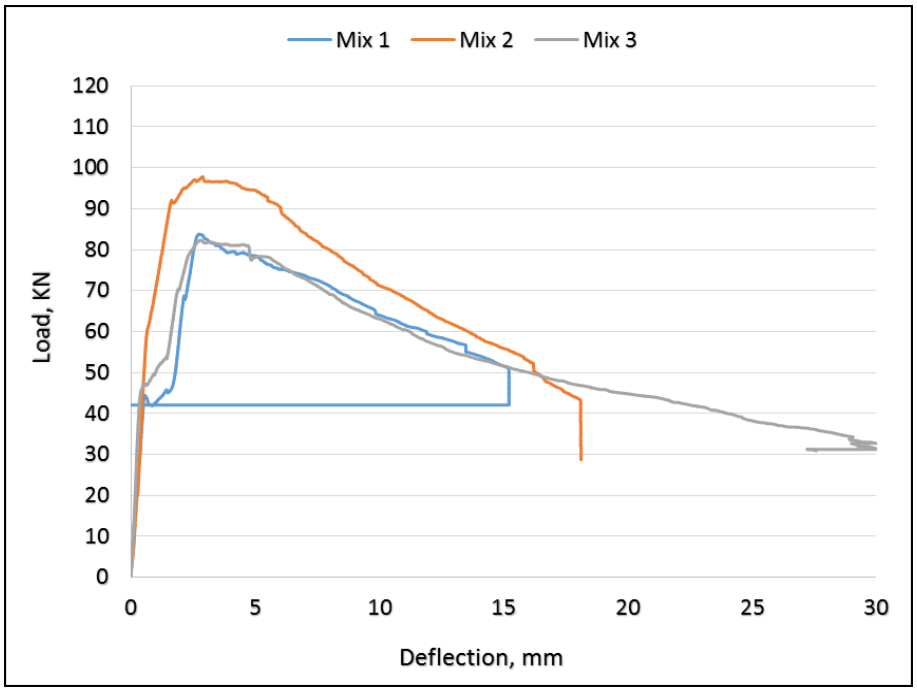

Load - deflection curve of concrete square panel, 65/60 + 10 mm

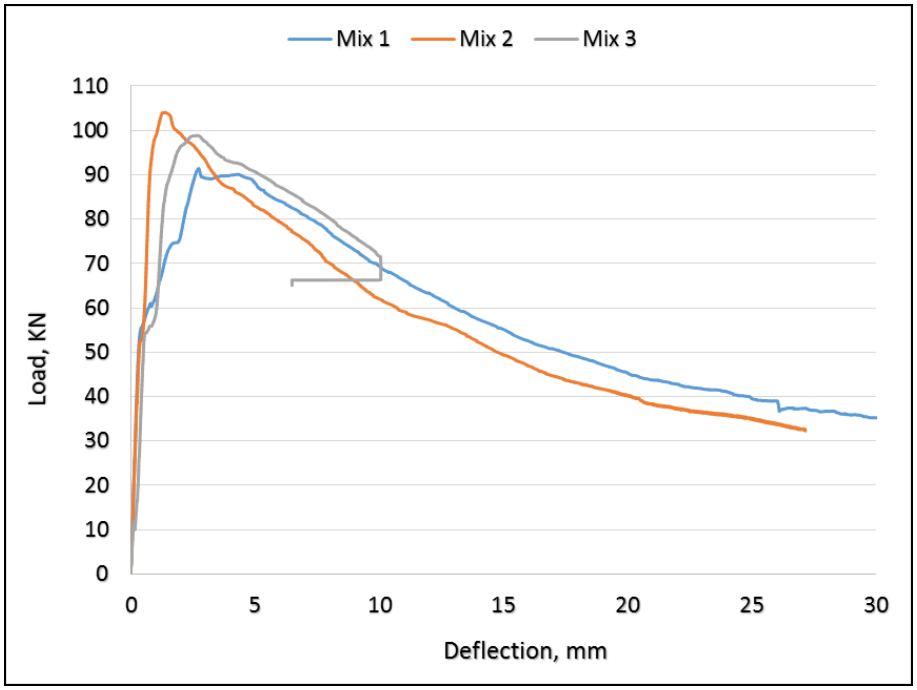

Load - deflection curve of concrete square panel, 65/60 + 10 mm

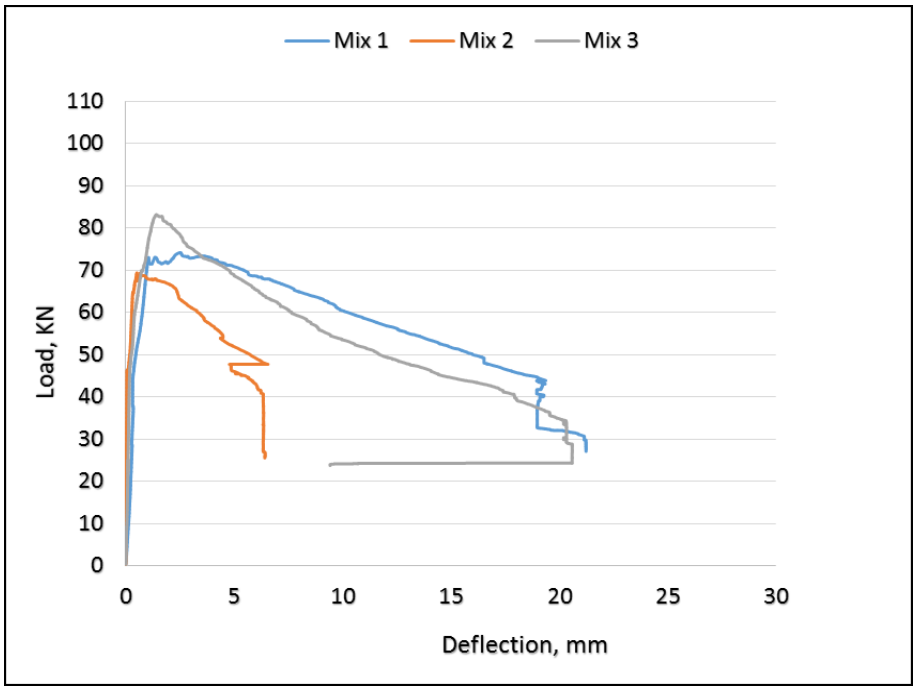

Load - deflection curve of concrete square panel, 65/60 + 20 mm

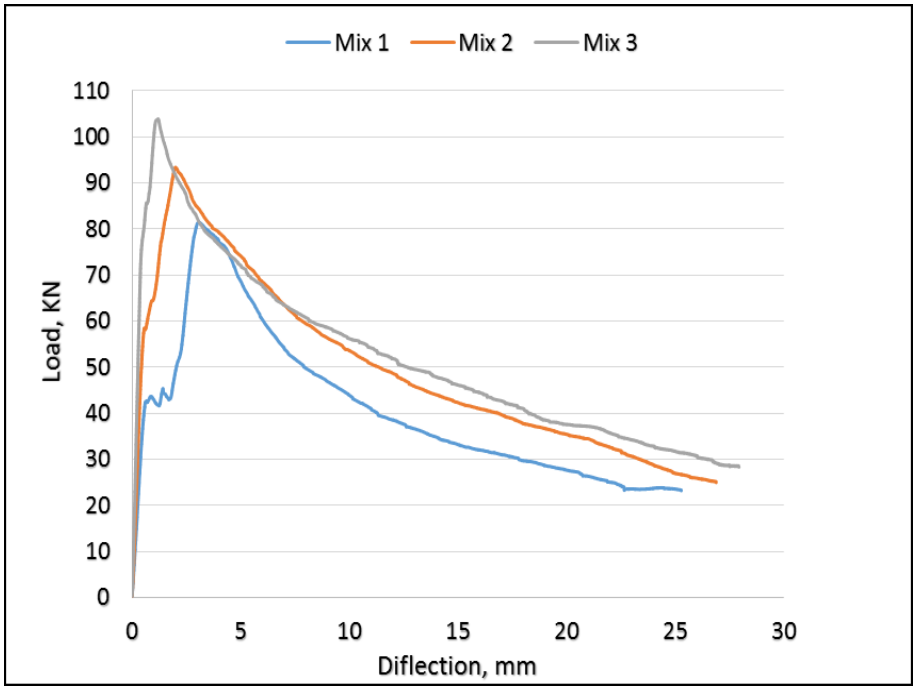

Load - deflection curve of concrete square panel, 45/50 + 10 mm

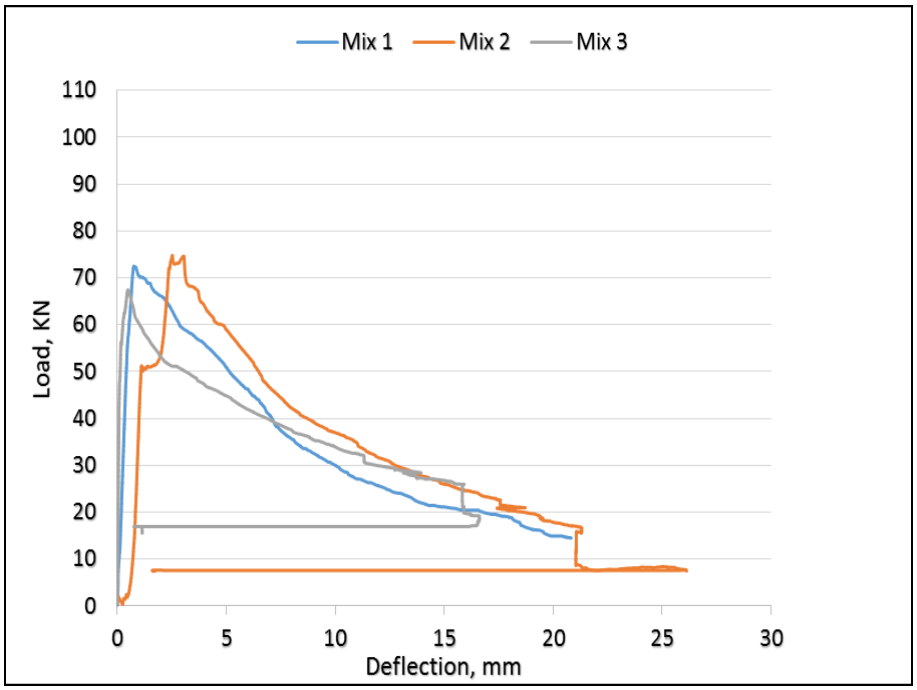

Load - deflection curve of concrete square panel, 45/50 + 20 mm

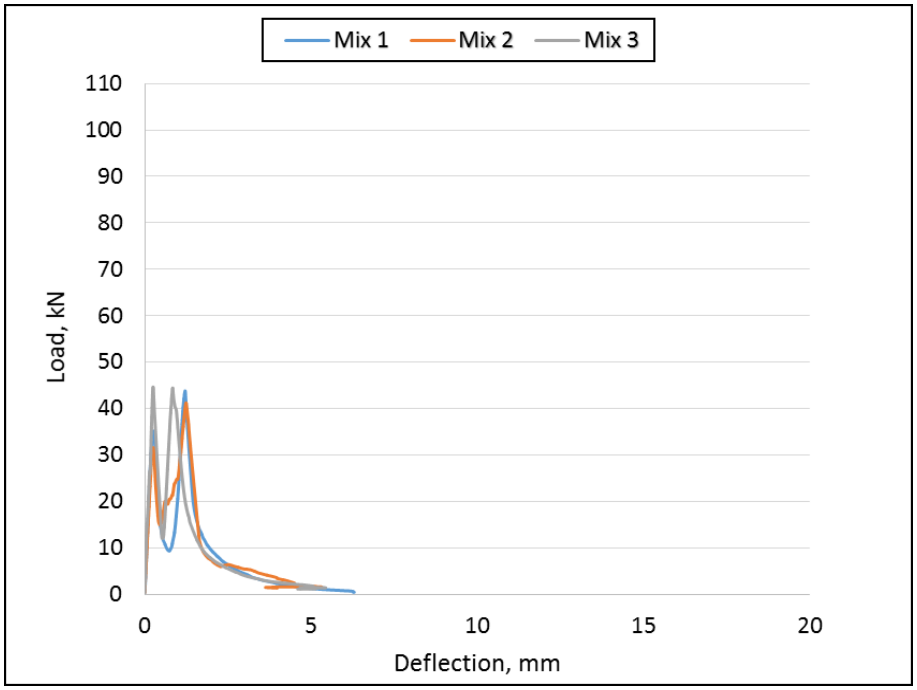

Load - deflection curve of plain unreinforced concrete square panel, 10 mm

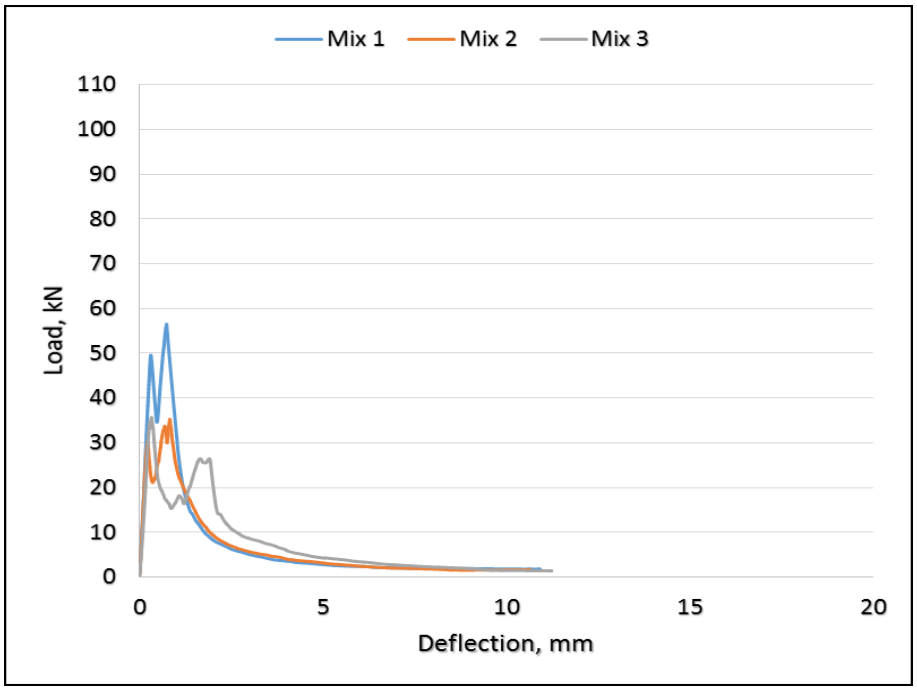

Load - deflection curve of plain unreinforced concrete square panel, 20 mm

Appendix C: Anderson-Darling Normality test carried out on data

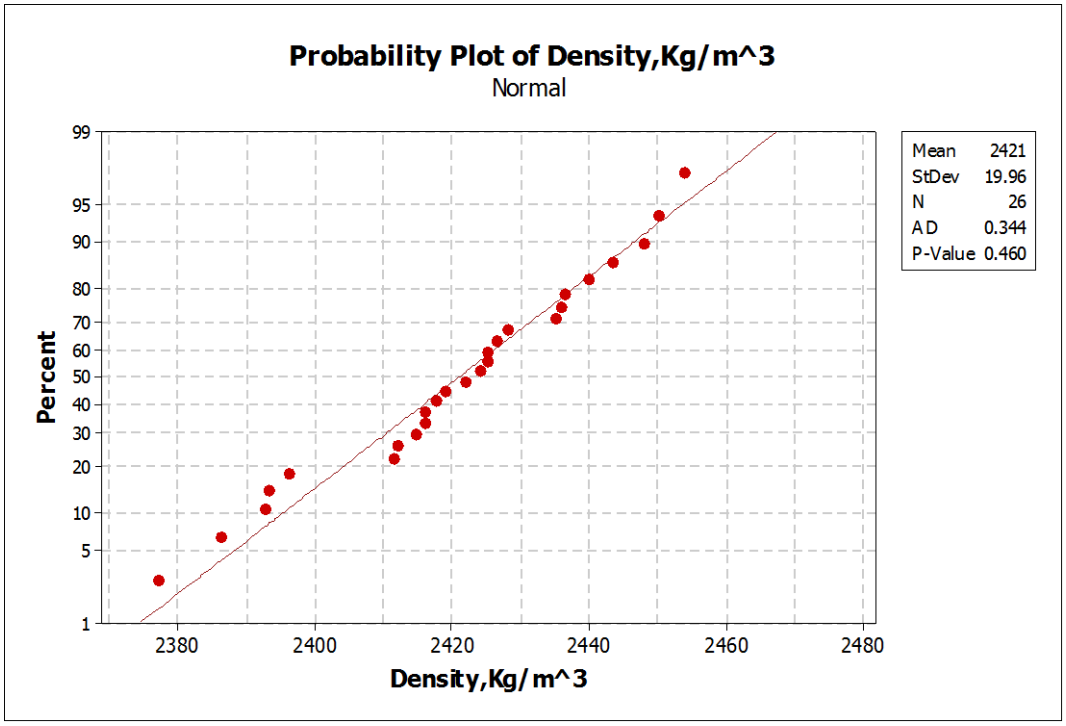

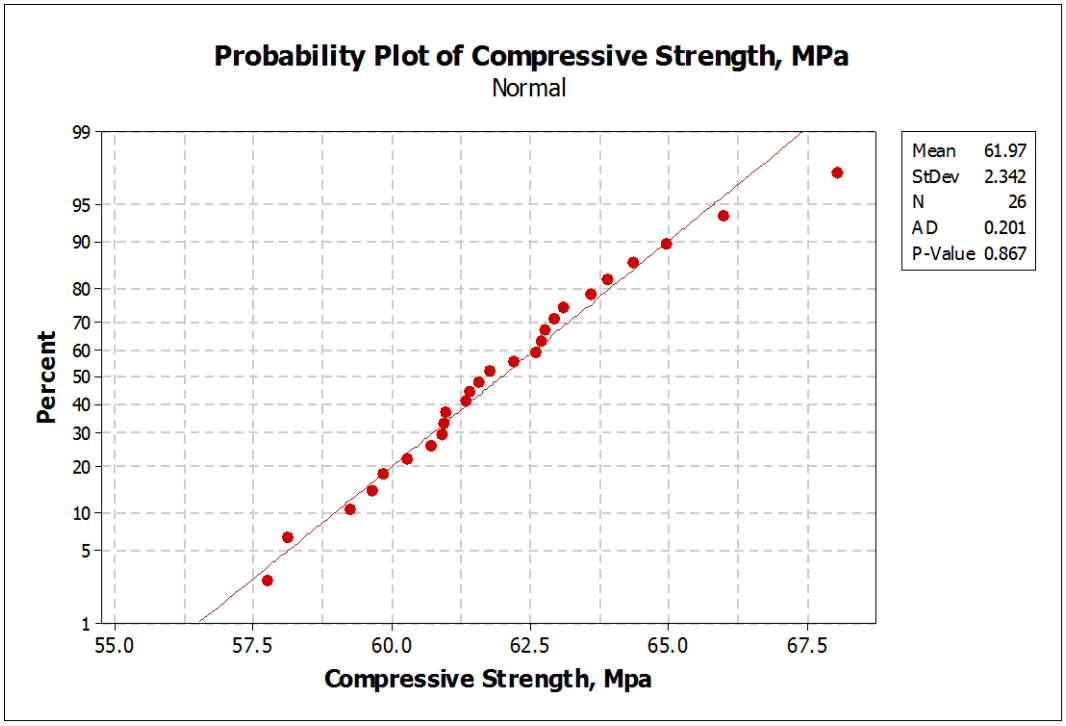

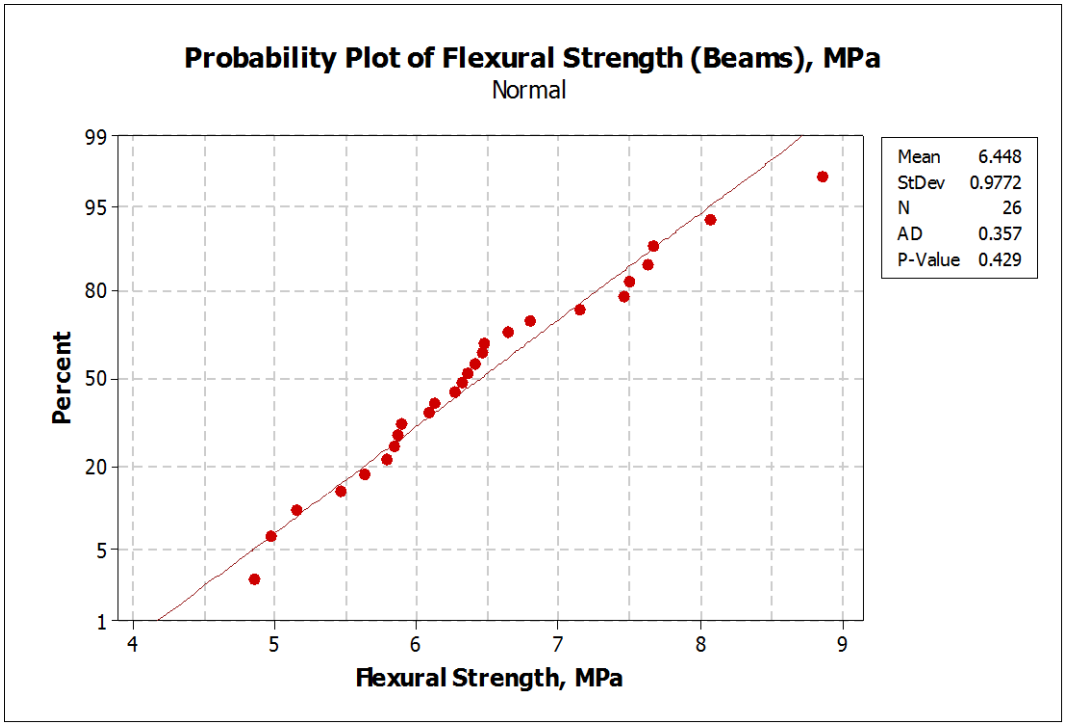
Probability Plot of Flexural Strength (Beams), MPa
Normal
Percent
99
95
80
50
20
5
1
4
5
6
7
8
9
Flexural Strength, MPa
Mean 6.448
StDev 0.9772
N 26
AD 0.357
P-Value 0.429

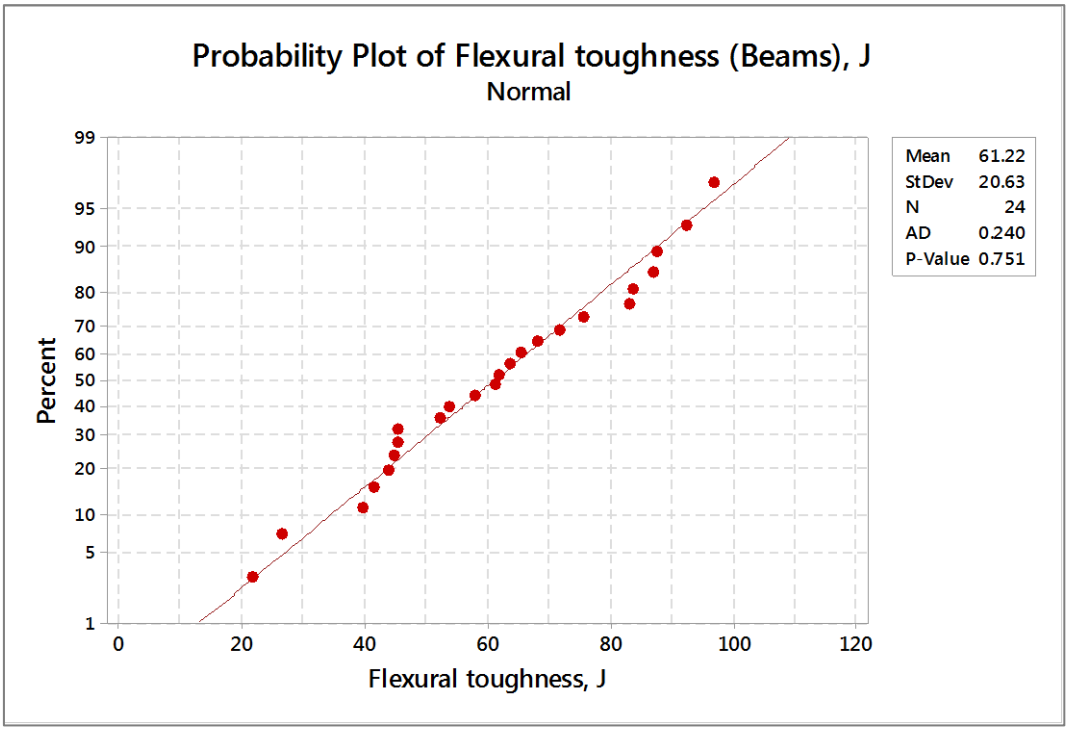
Probability Plot of Flexural toughness (Beams), J
Normal
Percent
99
95
90
80
70
60
50
40
30
20
10
5
1
0
20
40
60
80
100
120
Flexural toughness, J
Mean 61.22
StDev 20.63
N 24
AD 0.240
P-Value 0.751

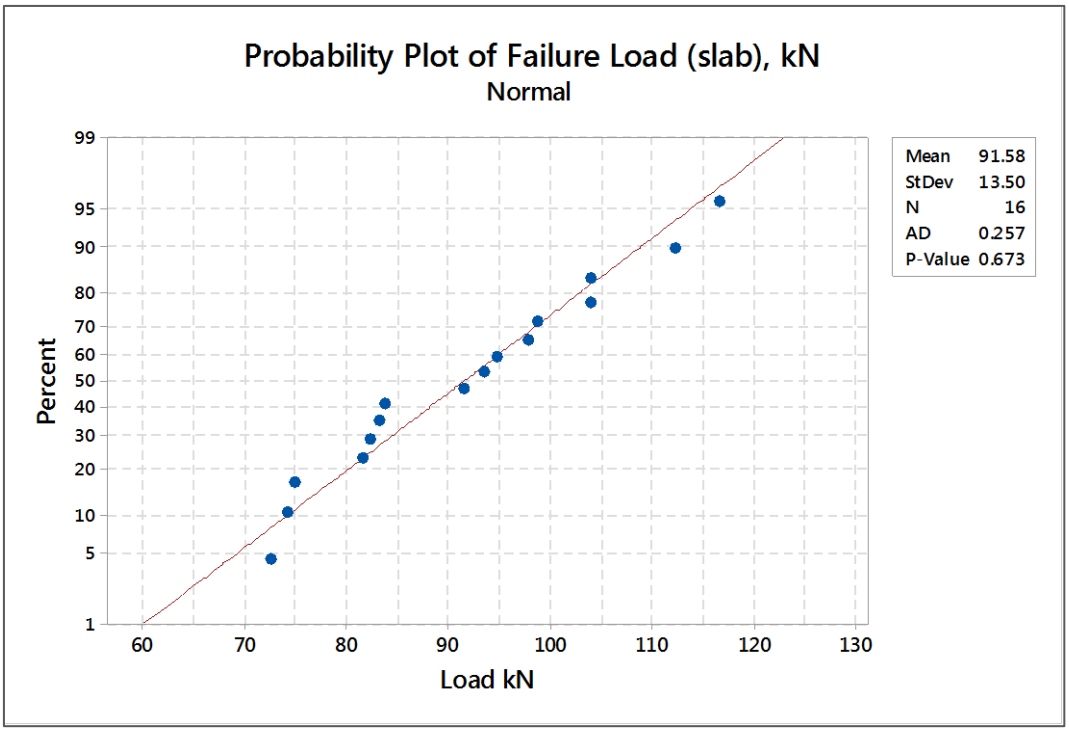
Probability Plot of Failure Load (slab), kN
Normal
Percent
99
95
90
80
70
60
50
40
30
20
10
5
1
60
70
80
90
100
110
120
130
Load kN
Mean 91.58
StDev 13.50
N 16
AD 0.257
P-Value 0.673

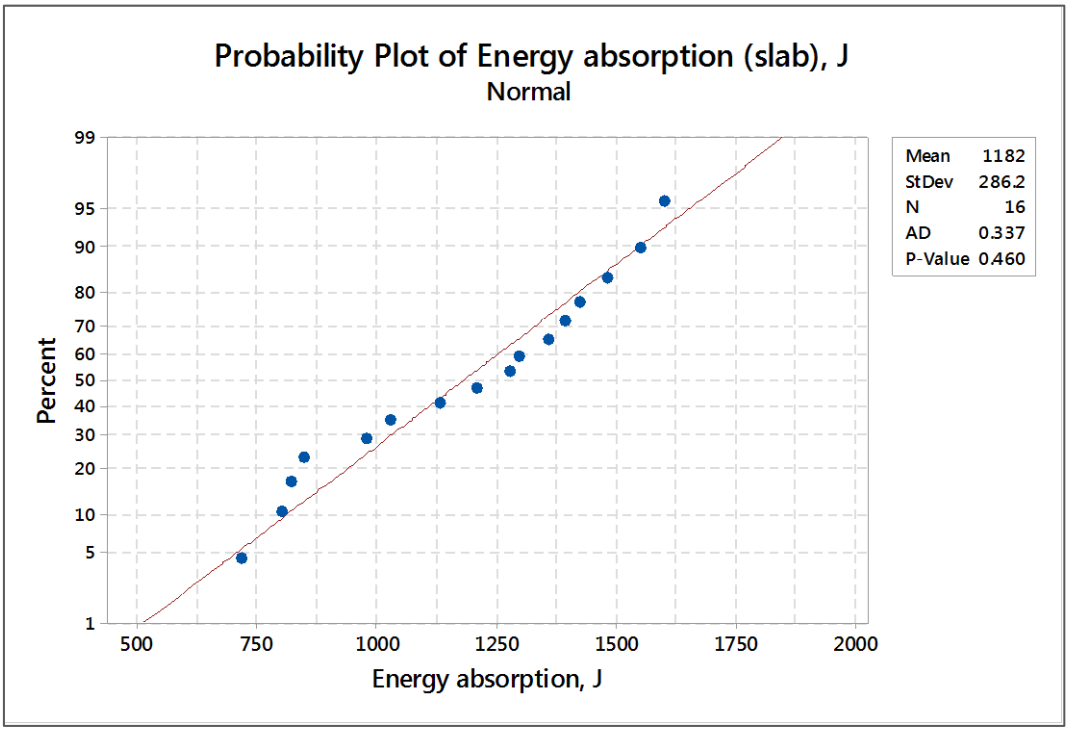
Probability Plot of Energy absorption (slab), J
Normal
Percent
99
95
90
80
70
60
50
40
30
20
10
5
1
500
750
1000
1250
1500
1750
2000
Energy absorption, J
Mean 1182
StDev 286.2
N 16
AD 0.337
P-Value 0.460